MOLECULAR CONTROL OF GENOME ARCHITECTURE

IVANA HERRERA

A thesis submitted to the University of Ottawa in partial fulfillment of the PhD program in Cellular and Molecular Medicine

University of Ottawa

Faculty of Medicine

Department of Cellular and Molecular Medicine

ABSTRACT

Heterochromatin (HC) tethering at the nuclear lamina (NL) is observed in almost every cell, and mutations in tethering proteins lead to a variety of diseases called laminopathies that have been the subject of intense study. Nonetheless, the importance of HC tethering for genome regulation and/or other cellular functions is not fully understood. Unlike most cells, murine rod photoreceptors have an inverted organization, in which euchromatin (EC) is localized to the nuclear periphery, and HC is untethered. Using rods as a model system devoid of any tethering proteins, two players were identified as crucial in HC tethering. The lamin B receptor (Lbr) is sufficient for HC tethering and is expressed during development, but Lbr levels decline upon rod photoreceptor differentiation. A second tether is the intermediate filament lamin A (LA), which is not normally expressed in murine rods. In my first published data chapter, I found that LA ectopically upregulates and reorganizes the genome during rod degeneration. Using ATAC-seq to examine genome accessibility, we showed that LA and Lbr tethering proteins both lead to marked increases in genome accessibility at regions associated with stress-responsive genes. However scRNA-seq on LA- and Lbr-expressing rods revealed relatively minor stress-responsive gene transcription. Together, our data reveal that HC tethers have a global effect on genome accessibility and suggest that HC tethering primes the photoreceptor genome to respond to stress.

In my next data chapter, I performed experiments designed to understand why LA upregulates during degeneration. Along with Jasmine Levesque , we found that in the *rd1* model of retinitis pigmentosa, LA upregulation correlates with markers of DNA damage. Moreover, functional manipulations suggest that LA upregulation promotes rod photoreceptor survival. Together, these data imply that LA may upregulate as an adaptive response to DNA damage.

Next, to better understand the logic of HC tethering, I performed experiments designed to elucidate the tethering mechanism. I performed a structure/function study of LA-dependent HC tethering. More than 400 different *LMNA* gene mutations are associated with laminopathic disease. Studies have previously linked mutations to reduction of HC, abnormal nuclear morphology and DNA damage, but most experiments have been performed in conventionally organized cell types – many of which express wild-type LA/C and Lbr. It has therefore been difficult to determine whether genome disorganization is directly caused by specific LA mutations, or is a consequence of other pathological mechanisms. I expressed a panel of mutant LA constructs in rod photoreceptors to determine how mutations affect tethering competence. I identified protein domains necessary for HC tethering within the LA C-terminus and IG-fold domain. Moreover, progeroid and non-progeroid laminopathic disease mutations exhibited a complete loss of tethering competence. However, defarnesylating these laminopathic mutants partially restored HC tethering. My results suggest that the LA C-terminus is necessary and sufficient for HC tethering, in part, due to the requirement for C-terminal processing.

In my final data chapter, since LA does not have an obvious chromatin binding domain, we evaluated the hypothesis that partner proteins act as a bridge between chromatin and LA. Using rod photoreceptors as a model for tethering sufficiency, I ectopically expressed a set of LA-interacting proteins. However, my results suggest that these partner proteins could not act in trans to restore tethering to versions of LA that were tethering-incompetent. Together with proteomic experiments profiling LA and molecular modelling, our results suggest that LA does not depend on known partner proteins to interact with HC, but interacts directly with nucleosomes. Our findings might impact the field of human disease genomics and provide insight into mechanisms regulating genome organization.

Table of Contents

List of Figures

Chapter 1.

Chapter 3.

List of Abbreviations

ATAC-seq Assay for transposase-accessible chromatin with sequencing

BAF/BANF1 Barrier-To-Autointegration Factor

cHC Constitutive heterochromatin

CTCF CCCTC-binding factor

DCM Dilated cardiomyopathy

DDR DNA damage repair

EC Euchromatin

EMD Emerin

EDMD Emery-Dreifuss muscular dystrophy

fHC Facultative heterochromatin

FPLD Familial partial lipodystrophy

HC Heterochromatin

HGPS Hutchinson-Gilford progeria syndrome

LA Lamin A

LAD Lamina associated domain

LB1 Lamin B1

LBR Lamin B-receptor

LC Lamin C

NL Nuclear lamina

NGPS Nestor-Guillermo Progeria Syndrome

PRR14 Proline-rich protein 14

RBBP4 Retinoblastoma-binding protein 4

RD Restrictive dermopathy

scRNA-Seq Single-cell RNA-sequencing

Acknowledgements

Thank you to all the people who continue to love and support me and have patience with me, from my Supervisor Dr. Mattar, Co-Supervisor Dr. Stanford, TAC Committee (Dr. Picketts, Dr. Tesson, Dr. Tsilfidis); Mattar, Stanford and Picketts lab members,

to my husband and my family –

standing with me in faith. I am grateful for every day.

I dedicate this thesis to my parents who sacrificed everything for me,

Rest in peace.

Chapter 1. Introduction

1.1. Higher order genome architecture

The genetic material of every cell is hierarchically organized. Different levels of three-dimensional (3D) DNA organization in the nucleus contribute to gene regulation. The hierarchical structure of the genome is necessary for allowing cell-type specific gene expression programs to play out at the right point in development, and to regulate various physiological processes. Therefore, higher order genome organization is crucial for different biological functions, and its impairment can lead to deregulation of gene expression.

The building blocks of chromatin are called nucleosomes. Each nucleosome consists of a core histone protein octamer, made of H3-H4 histone tetramer and two H2A-H2B histone heterodimers, encircled by 146 base pairs (bp) of DNA.

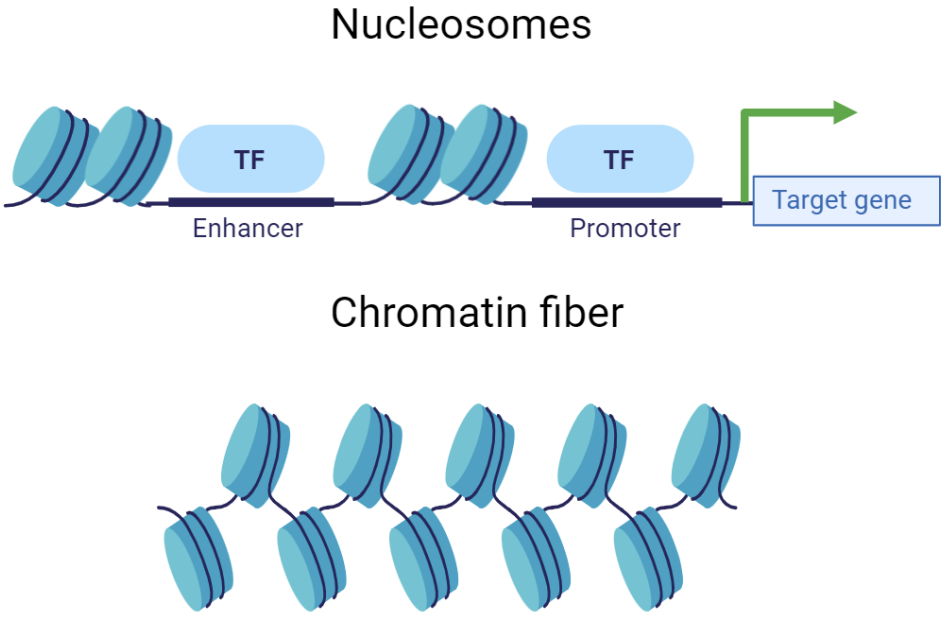

Figure 1.1. Nucleosomes – basic units of chromatin.

DNA (dark blue) encircles the nucleosome. Nucleosome (light blue) compaction forms the chromatin fiber.

Negatively charged DNA and highly basic histones form a stable complex with five- to ten-fold compaction. The amino-terminal histone tails are susceptible to post-translational modifications which regulate chromatin accessibility and ultimately gene expression. For example, acetylation and phosphorylation lower the charge of the histone core and loosen its association with DNA, enabling transcriptional factors (TFs) to regulate gene transcription [1,2,3] (Figure 1.1). In a similar manner, the methylation or monoubiquitination of some tail residues strengthens the nucleosome contacts and promotes compaction of chromatin. Alternatively, nucleosomes can be evicted or slid by ATP-dependent nucleosome remodelers[4]. Between each nucleosome is a 10-80 bp linker DNA. H1 linker histones can be recruited to the linker DNA and support further folding of the chromatin fiber[5] with a diameter of 5–24 nm and a fifty-fold compaction that suppresses gene expression[6].

The chromatin fiber also self-interacts to form chromatin loops, which mediate short to medium range interactions between promoters and enhancers[7]. At the largest scale, self-interacting genomic regions associate into topologically associating domains (TADs) ranging to several hundred kilobases (kb) in size, as detected by Hi-C[8]. TADs form through an ATP-dependent loop extrusion mechanism driven by cohesin[9], defined at the boundaries by the architectural chromatin protein CTCF[10]. Finally, major units of the genome are chromosomes. During interphase, decondensed chromosomes occupy specific territories within the nucleus[11] (Figure 1.2).

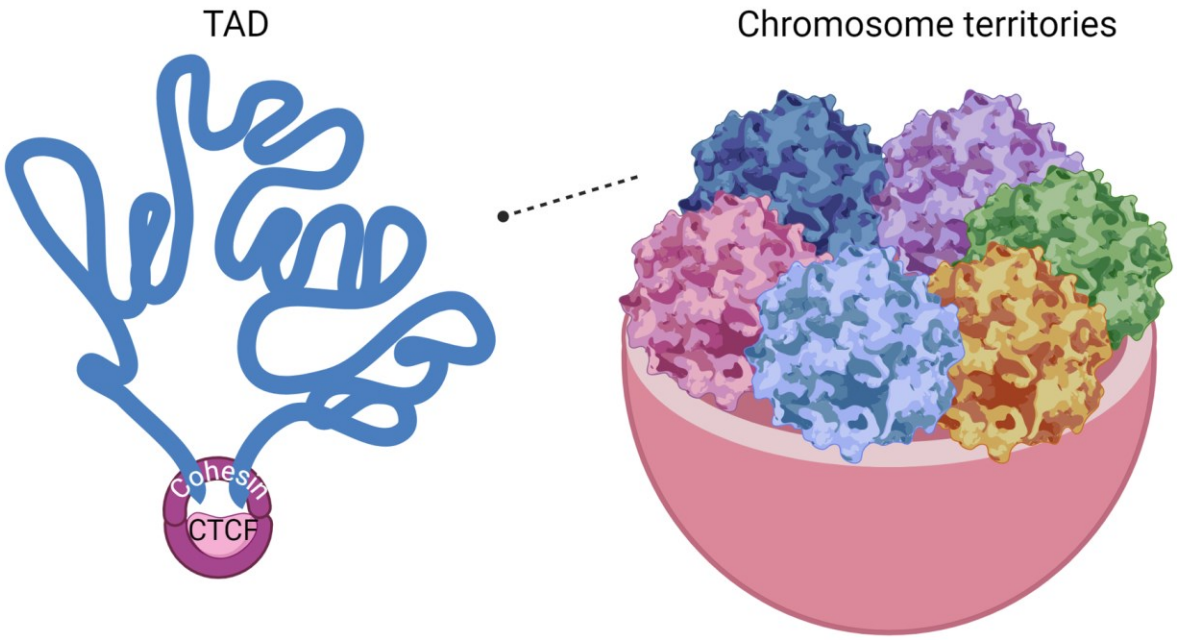

Figure 1.2. The organization of the eukaryotic genome.

Chromatin fiber folds into topologically associating domains (TADs). The DNA of each chromosome occupies a distinct chromosome territory (different colors).

1.2. Functional units of chromatin organization

The logic of genome regulation may be determined to a large extent by the intricate spatial organization of chromatin within the nucleus. Chromatin types tend to be segregated into different compartments; gene poor condensed heterochromatin (HC), and gene rich decondensed euchromatin (EC)[12]. EC is characterized mostly by histone acetylation (eg. H3K9ac, H3K14ac, H3K27ac) which loosens the association between the nucleosome and the DNA. Some types of histone methylation can also be euchromatic (eg. H3K4me3, H3K36me3)[13]. HC is further classified into stable constitutive HC (cHC), enriched in centromeres and telomeres[14], and facultative HC (fHC) that is able to decondense in response

to developmental or environmental signals[15]. cHC is typically demarcated by the presence of H3K9me3, a histone modification deposited by the histone methyltransferase (HMT) Suppressor of variegation 3–9 homologue (Suv39h), and H3K9me2 deposited by G9A (also known as euchromatic histone-lysine N-methyltransferase 2; EHMT2) and G9A-like protein (GLP; also known as EHMT1) in mammals[16,17]. Methylation of H3K9 provides the foundation for association with the heterochromatin protein HP1 in mammals[18,19,20]. fHC is marked by the presence of the H3K27me3, deposited by Polycomb repressive complex 2 (PRC2)[21].

Further insight into compartmentalization of the genome was provided by using chromosome conformation capture techniques such as Hi-C, which enabled researchers to get a glimpse into chromosomal looping configurations and TAD structures. It was noted that chromosomes additionally organize in A and B compartments, which correlate with high and low transcriptional activity, respectively[22].

1.3. Nuclear lamina

A driving force for chromatin segregation is homotypic association between heterochromatic domains, facilitated by binding to scaffolding structures like the nucleolus and the nuclear lamina (NL)[23]. In most cell types, transcriptionally inactive genes tend to locate at the nuclear periphery, and active genes mostly reside in the nuclear interior[24]. The nuclear envelope (NE) is a system that consists of an inner nuclear membrane (INM) and an outer nuclear membrane (ONM). The inner and outer nuclear membrane represent a boundary between the nucleus and the cytoplasm in eukaryotic cells. The nucleus of most metazoans contains NL, a network of

intermediate filament proteins called lamins as well as their partner proteins, that are located beneath the INM (Figure 1.3.)

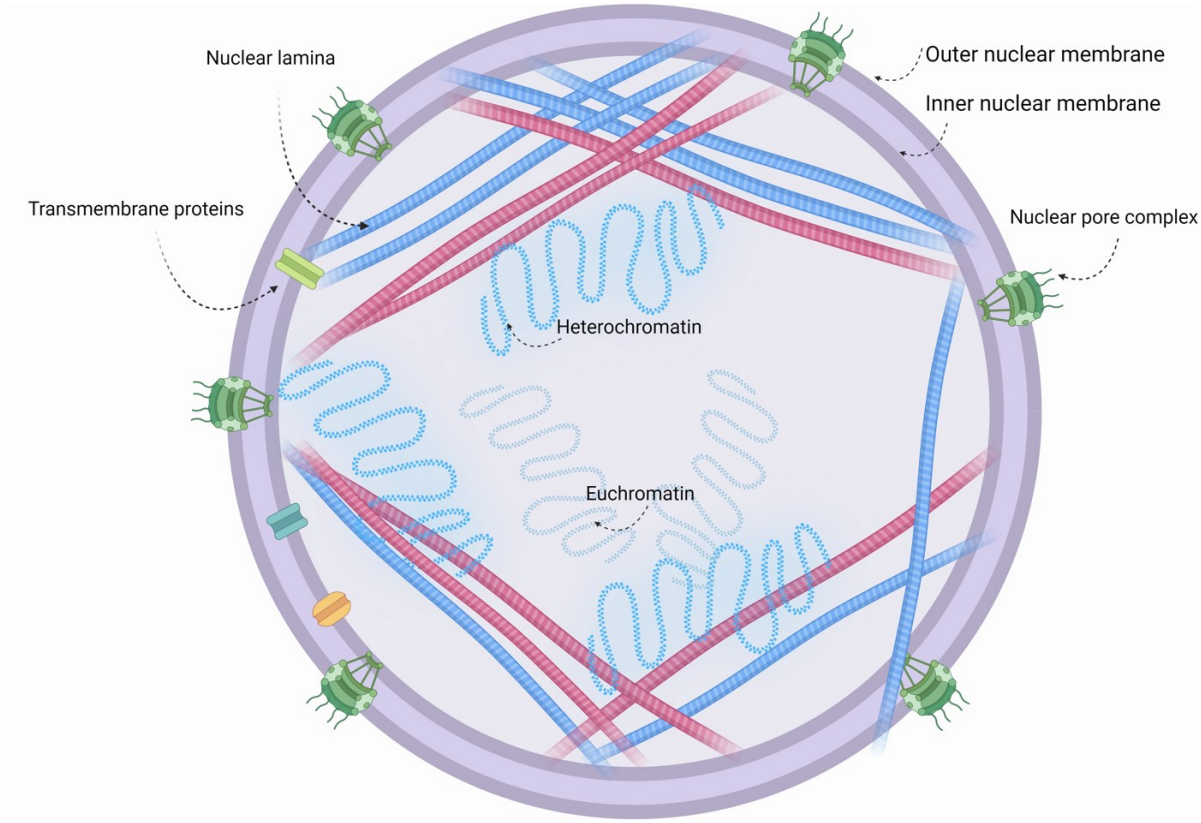

Figure 1.3. Nuclear envelope membrane system and the nuclear lamina.

Nuclear envelope is a system made of inner and outer nuclear membrane. The nuclear lamina, which consists of the lamin intermediate filament proteins and associated inner nuclear membrane proteins, is located on the interior of the inner nuclear membrane.

1.3.1. Lamina associated domains

The identification of genomic regions associated with the NL was made possible via the development of the DNA adenine methyltransferase identification (DamID) technique using lamin B1 (LB1)[25]. Lamina associated domains (LADs) have been shown to be dynamically

reorganized in response to developmental changes in gene regulation, and are newly established in every cell after fertilization[25]. LADs have a characteristic genomic signature, consisting of gene poor regions, that tend to be rich in repetitive elements, A/T content, H3K9me2/3 and H2K27me3 histone modifications[26] (Figure 1.4). 35–40% of the mammalian genome is bound to the NL in LADs[27]. In terms of gene regulation, research shows that the NL actively promotes the compaction and repression of chromatin in LADs[28,29].

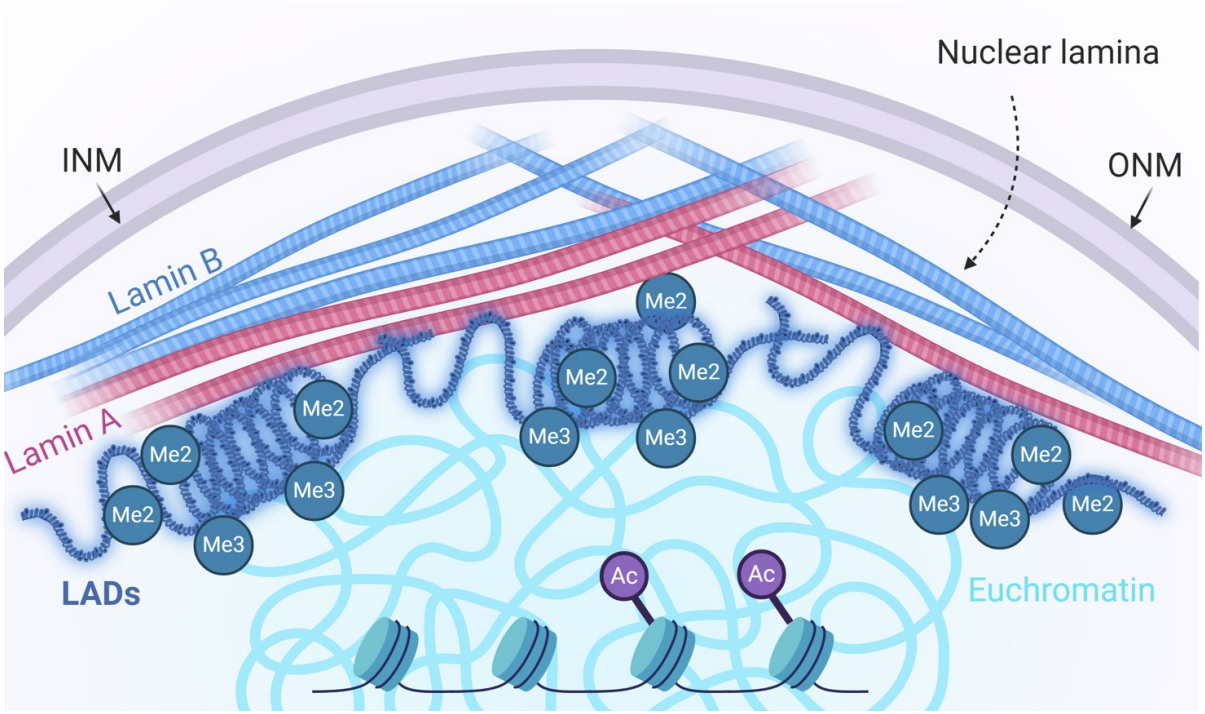

Figure 1.4. Lamina associated domains.

Lamina associated domains are gene poor regions, rich in the repressive histone modifications H3K9me2/3 and H2K27me3. Euchromatin is rich in acetylated histones.

However, heterochromatic repression can be achieved without the NL[23]. LADs which show stability and consistency within different cell types are called constitutive LADs (cLADs), while LADs which are present in specific types of cells are called facultative LADs

(fLADs)[30,31]. Single-cell DamID has shown that contacts with the NL involve continuous stretches of chromatin up to several Mb in length[32]. Although H3K9me3 is associated with cHC, H3K9me2 is the mark most associated with LADs and required for nuclear peripheral localization of chromatin[33,34]. The fHC mark H3K27me3 is also enriched at LAD boundaries of some cell types[35].

1.3.2. Lamin structure

In vertebrates, lamins are classified as A or B type. The A-type lamins, lamins A (LA) and C (LC) are alternative splice forms transcribed from the *LMNA* gene and are expressed in most differentiated cells[36] (Figure 1.5). B-type lamins, lamin B1 (LB1) and lamin B2 (LB2) are encoded by *LMNB1* and *LMNB2* genes, respectively, and ubiquitously expressed (Figure 1.5). Thus, A- and B-type lamins display unique expression patterns and have different assembly properties, suggesting they have independent functions[37,38].

Based on sequence homology, nuclear lamins are classified as type V intermediate filament proteins[39]. Lamins consist of a central coiled coil rod domain composed of four α-helical subdomains (coils 1A, 1B, 2A, 2B) that are separated by flexible linker regions. The rod domain is flanked by an N-terminal head domain and a C-terminal tail domain containing lamin-specific motifs. The C-terminal domain includes a nuclear localization signal (NLS), an immunoglobulin IG-fold, and a C-terminal CaaX (C, cysteine; a, aliphatic amino acid; X, any amino acid) that is present in lamins A, B1, and B2, but not LC[39] (Figure 1.5). The rod domain contains highly conserved elements that are essential for lamin filament assembly[40,41]. The IG-fold domain is known as an interaction hub that serves as an anchor site for numerous partner proteins[42,43].

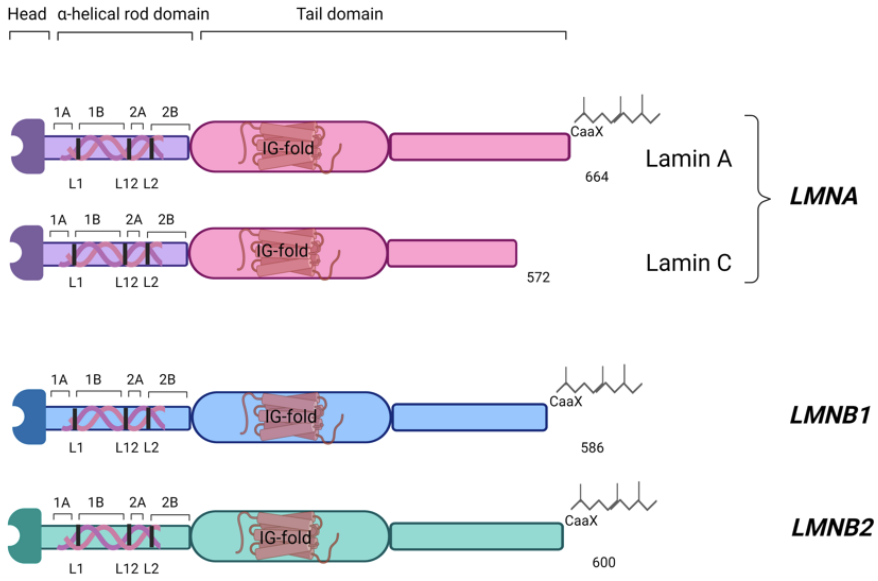

Figure 1.5. Lamin domain organization and protein structure.

Nuclear lamins are characterized by an N-terminal head domain; a central coiled coil rod domain (α-helical coils 1A, 1B, 2A, and 2B) with flexible linker regions (L1, L12, L2), a C-terminal tail domain with the globular immunoglobulin (IG)-fold, and a CAAX box, which undergoes farnesylation in lamin A, and lamin B1/B2.

1.3.3. Lamin sequence homology

Lamins are highly conserved. All invertebrate lamins show the same overall sequence organization typical for vertebrate lamins and resemble the B-type lamins in terms of overall protein size. The LA sequences of mammalian species are very similar, with 97–98% homology between mouse, dog, pig, and human[44]. Lamins B1 and B2 are also highly homologous, with human and mouse LB1 sharing 95.92% amino acid homology, LB2 sharing 81.51% homology, LA sharing 96.40% homology, and LC sharing 97.21% homology. Human LA and LB1 exhibit high sequence homology, as they share 62% sequences in short coil 2 (rod), and 51% in globular IG-fold (tail) domain[45], with overall 56.70% homology (Figure

1.6). However, the structure of LA differs from all other lamins, since the LA C-terminal tail domain is longer than that of the B-type lamins, and is divergent at the level of the amino acid sequence (Figure 1.6). These extra amino acid residues are encoded by a single exon.

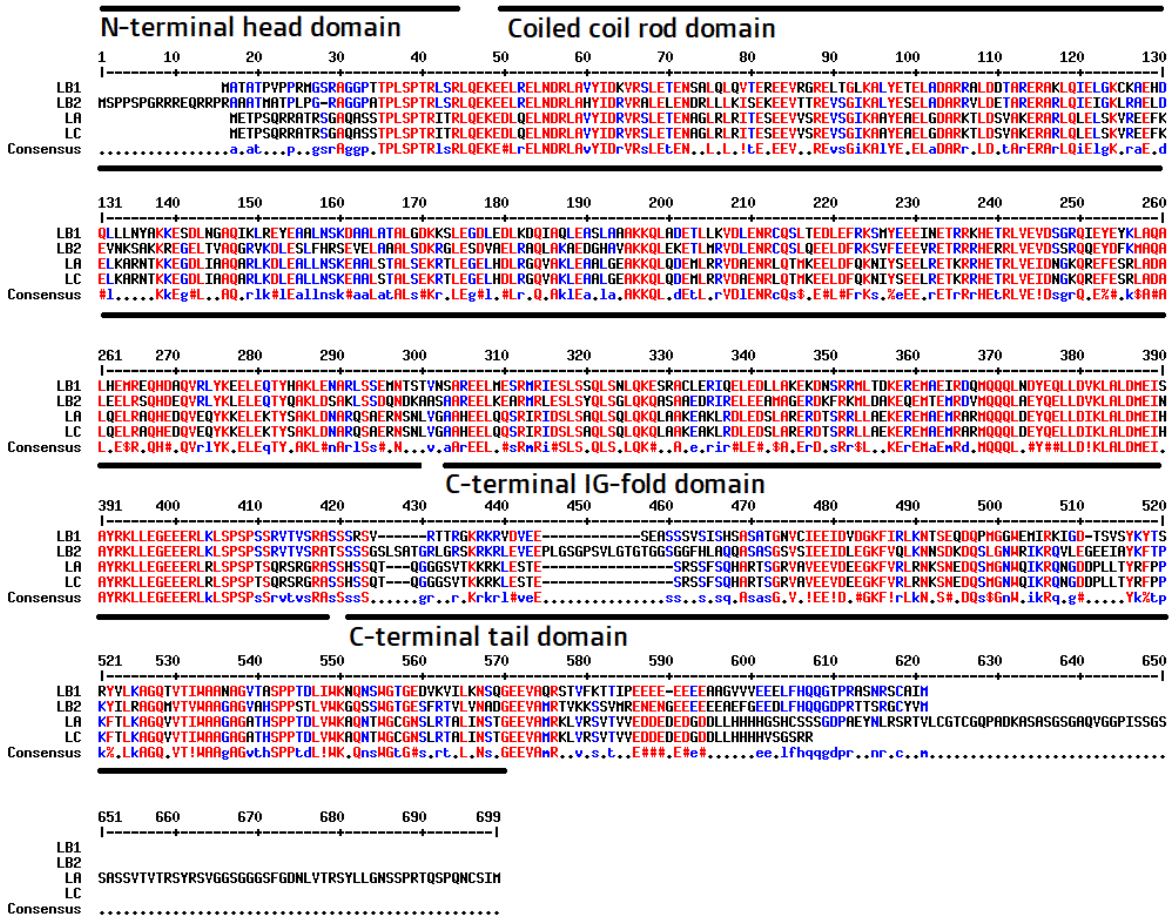

Figure 1.6. Alignment between human B- and A-type lamins. Multiple sequence alignment of the human lamin B1, lamin B2, lamin A, lamin C. Highly conserved amino acids are shown in red, less conserved in blue.

The first 566 or 568 residues of two main somatic isoforms LA and LC are identical in human and mice, respectively[46] and have identical sequences at the N-terminal head, rod and C-terminal IG-fold domains. LC has six unique C-terminal residues (567 – 572), whereas LA has a unique extended tail domain (567 – 664) that undergoes four post-translational modification

steps to achieve its final mature length of 646 or 647 residues, in humans and mice, respectively[47].

1.3.4. Post-translational modifications of lamins

Lamins undergo post-translational modifications (PTMs) via phosphorylation, farnesylation, myristoylation, ubiquitination, acetylation, sumoylation and proteolytic cleavage[48].

Lamins generally share a C-terminal CaaX motif, where "C" represents Cysteine, "aa" are two aliphatic amino acids and "X" is some other terminal amino acid[49]. Each group of lamins has different amino acids in the C-terminal tail sequence (e.g. CSIM, CAIM and CYLM in human LA, LB1 and LB2, respectively). LA also has a signal RSYLLG for proteolytic cleavage by protease ZMPSTE24 (Face1), which also cleaves off the terminal aaX sequence after fatty acid modification[50]. The C-terminus of lamins A, B1, and B2, but not LC, contains this C-terminal CaaX motif.

Post-translational modifications of A- and B-type lamins starts with the addition of the farnesyl (isoprenyl) group to the C-terminal CaaX Cysteine residue[51]. The farnesyl group is extremely hydrophobic and supports interactions with the lipid inner nuclear membrane. The zinc metalloprotease ZMPSTE24 and the endopeptidase Rce1 recognize the Cysteine farnesyl group and proteolytically remove -aaX from prelamin A and LB, respectively. The farnesylated Cysteine therefore remains exposed and is then methylated by isoprenyl carboxymethyltransferase. Finally, ZMPSTE24 again cleaves prelamin A at Leucine 647 to produce mature LA with only 646 residues (Figure 1.7A). Therefore, the C-terminal farnesylation is ultimately removed from mature LA protein. Although they share the polymerization mechanism with A-type lamins (Figure 1.7B), B-type lamins remain

permanently farnesylated (Figure 1.7C), and thus, they are anchored at the inner nuclear membrane[52] (Figure 1.7D). Although primarily located at the NL, A-type lamins have been found to localize to the nucleoplasm[53,54]. A-type lamins are thus more dynamic than B-type lamins[53].

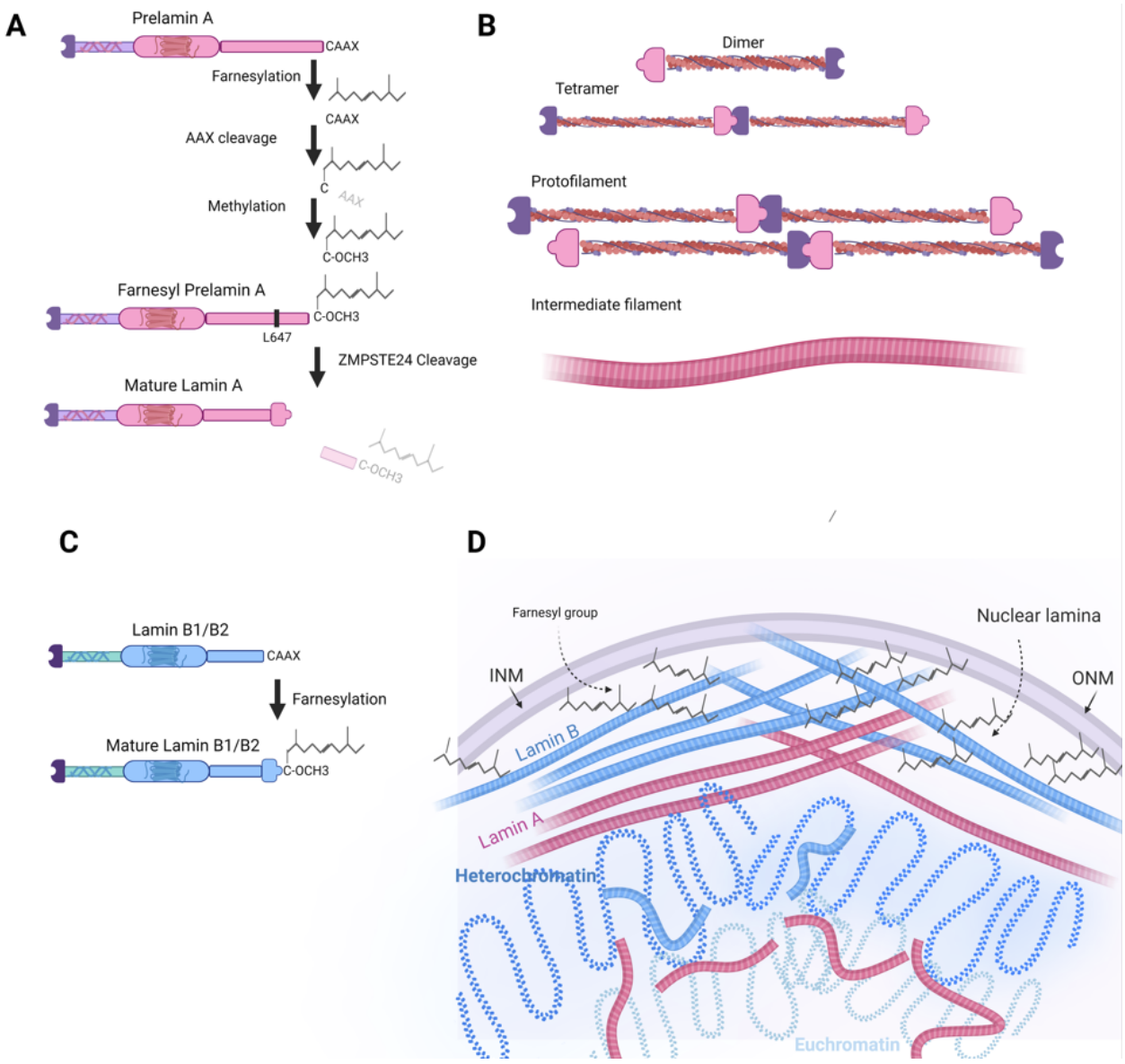

Figure 1.7. Schematic model of lamin polymers and processing.

A. Prelamin A goes through several post-translational modifications before becoming mature lamin A. Farnesylation of the Lamin A C-terminal Cysteine is necessary for recognition by

ZMPSTE24 zinc metallopeptidase which catalyzes its cleavage at Leucine 647. Mature lamin A is defarnesylated and can freely interact with chromatin within the nucleus.

B. Lamin A and B monomers associate in a head-to-head fashion into parallel dimers, mainly through the α-helical rod coiled coil domain. Dimers associate in a head-to-tail fashion into polymers. Lamin polymers associate in an anti-parallel manner into lamin protofilaments. Protofilaments associate laterally into a lamin intermediate filament.

C. B-type lamins remain permanently farnesylated at the C-terminal tail.

D. B-type lamins are anchored at the inner nuclear membrane through a hydrophobic farnesyl group, while A-type lamins are located interior to B-type lamins.

1.3.5. Polymerization of lamins

A- and B-type lamins polymerize to form the NL in interphase cells. Previous super-resolution microscopy studies indicated that A- and B- type lamins form separate intermediate filament networks which interact with each other[55,56,57]. Consequently, the loss of one lamin isoform can impact the structural organization of the other isoform filamentous network. For example, the loss of either LA/C or LB1 in mouse embryonic fibroblasts (MEFs) changed the structural organization of the remaining NL filaments. Loss of LB2 had minimal effect on the structure of the remaining lamin filaments in the NL network[53].

The first phase of lamin polymerization begins with parallel joining of two lamin monomers through their α-helical rod domain, which is abundant in hydrophobic and charged residues. It was previously shown that prelamin A, LA, LB1 and LC are able to associate into homo- and hetero-dimers *in vitro*[58,59]. Lamin dimers form a polymer through head-to-tail association between highly conserved rod domain segments[60]. Interestingly, the amino-terminal head, the shortest lamin domain, is essential for the head-to-tail polymerization *in vitro* and for

intermediate filament formation *in vivo*[61]. Lamin polymers join in an anti-parallel manner into a lamin protofilament (Figure 1.8B). Interestingly, lamins are the most bendable of all known intracellular filament systems[57,62.] Typically, A-type lamins are positioned on the interior of the B-type lamin network[63] (Figure 1.7D).

1.3.6. Lamin interacting proteins

Besides the A- and B-type lamins, the NL is formed through the interlinking of lamins with many structurally and functionally distinct inner nuclear membrane proteins, including the Linker of Nucleoskeleton and Cytoskeleton (LINC) complex, Lamin B Receptor (Lbr), LAP2 (thymopoietin or lamina-associated polypeptide 2), emerin, LEMD2 (NET25), MAN1 (LEMD3), and many others[64,65] (Figure 1.8). By using different proteomics-based studies, researchers have discovered more than thirty direct, and up to a hundred indirect partners of lamins and other lamina proteins[64,65].

LBR - a nuclear multipass transmembrane protein, is an essential molecular tether for HC at the NE[66]. Studies have characterized LBR's[67] mechanism of binding peripheral H3K9me2/3 HC through HP1, and direct interaction with the H4K20me3 histone modification[68]. Specifically, the nucleoplasmic N-terminal chromatin-binding Tudor domain of LBR, associates with the B-type lamins and HP1 chromatin proteins[69], while the C-terminal domain, domain, which is localized in between the inner and outer nuclear membrane, functions as a sterol C14 reductase, making LBR one of the major proteins required for cholesterol synthesis in human cells[70].

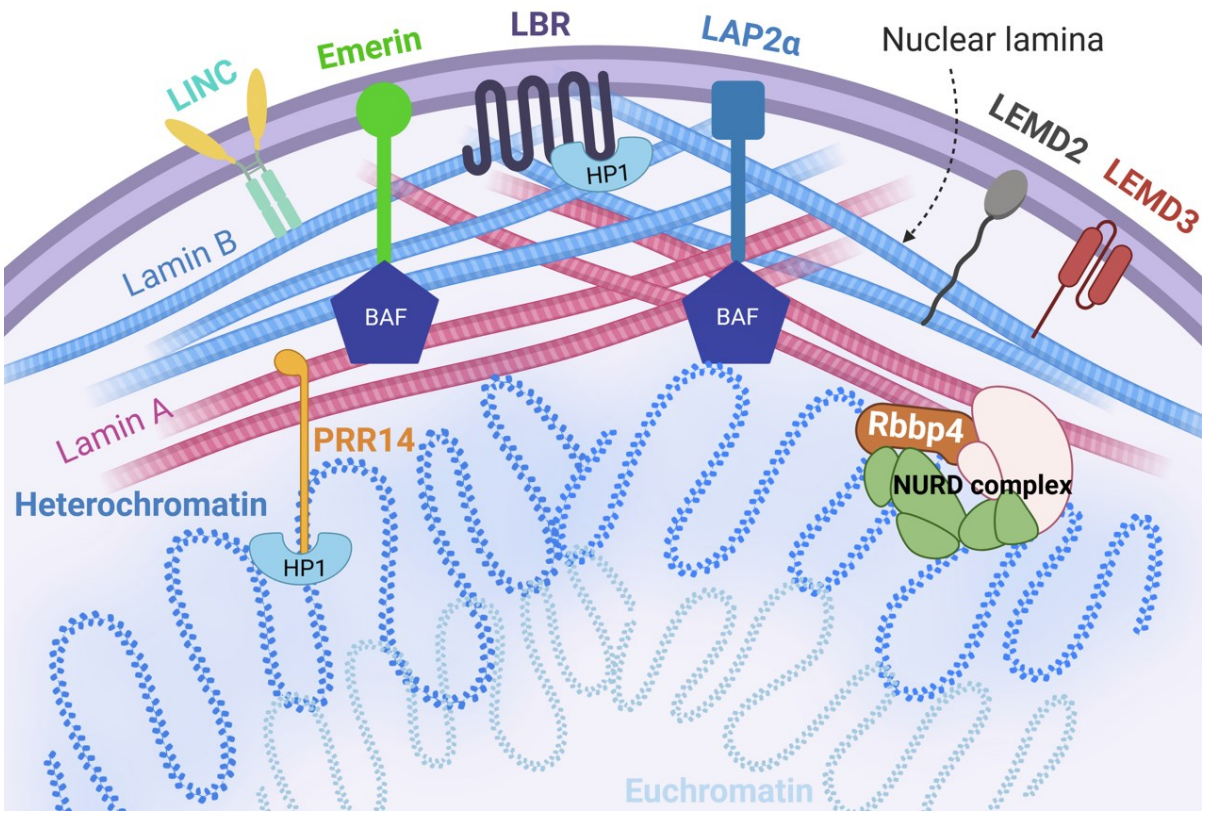

Figure 1.8. Inner nuclear membrane proteins.

Inner nuclear membrane proteins, TMPO (LAP2α), Emerin, LEMD and LBR, interact directly with the nuclear lamins. Emerin, TMPO (LAP2α), LEMD2 and LEMD3 contain a LEM domain which interacts with BAF (barrier-to-autointegration factor), a chromatin-binding protein. The nuclear lamina forms a network underneath the inner nuclear membrane, where A- type lamins (pink) are positioned interior to B-type lamins (blue) and form separate, filamentous networks.

This enzymatic activity is also very important for controlling the size of the endoplasmic reticulum, which is contiguous with the ONM[71]. Solovei et al. identified LBR as one of the key players in genome organization, sufficient for tethering of the HC to the NL. The absence of both LBR and LA/C led to loss of peripheral HC[66]. B-type lamins seem to be dispensable for HC tethering since absence of LB1 and LB2 in murine cells doesn't affect HC distribution

at the nuclear periphery[72], and because cells can lack HC tethering despite expressing B-type lamins.

The molecular mechanism of LA/C tethering is still not elucidated. A variety of studies have shown that lamins can bind DNA *in vitro* [73,74,75], but these studies show that A and B -type lamins bind DNA with equivalent affinity, suggesting that these results may not relate to *in vivo* HC tethering. Interestingly, LA/C was found to be required for HC tethering in some tissues by Solovei, et al. using mouse knockouts[66]. However, Solovei et al. transgenically expressed LC in mouse rods but found that it was not sufficient for HC tethering, suggesting that LA/C needs a mediator for HC binding[66]. Unlike *Lbr*, lamins do not encode a conventional DNA or chromatin binding domain. However, a number of interacting partners have been proposed to bridge chromatin to the lamina cytoskeleton. Thus, an adapter protein may be required for LA/C-mediated HC tethering in rods. Below, we review the leading candidates.

LEMD proteins (emerin, LAP2, LEMD2, LEMD3) are integral membrane proteins at the inner nuclear membrane. They are known to bind lamins and the DNA-bridging protein BAF (Banf1) through the LEM domain[76,77,78]. The structural inter-dependence of lamins, LEM-domain proteins and BAF was revealed by downregulating each of the complex components in *C. elegans*. If any component was missing, the other two couldn't properly assemble[79,80]. However, *C. elegans* encodes only a single lamin. The *Lmn-1* gene appears to be most homologous to B-type lamins[80], suggesting that these results may not reflect how these proteins assemble with LA/C. A variety of LEMD adapters, which are potential candidates for LA/C and HC interaction, were tested by Solovei in detail[66]. Solovei et al. reported that the absence of LA/C is correlated with the lack of LEMD proteins (emerin, LEMD2, LEMD3) in different tissues[66]. This, along with a reported insufficiency of transgenic LC to reverse the

nuclear inversion[66], suggested that LA/C might bind HC indirectly through LEMD adapter proteins. However, studies in rod photoreceptors suggest that LEMD proteins are not sufficient for HC tethering – both individually and when co-expressed with LC[66,81].

There are other potential candidates that could function as intermediates between LA and HC. Like Lbr, rods express low levels of BAF, PRR14 and RBBP4.

BAF is a small (89 amino acid) chromatin protein that localizes to the nucleus, at the NE and in the cytoplasm. BAF dimerizes and binds to LEMD proteins and the IG-fold domain of LA/C[82], while each individual subunit can bind dsDNA[83]. It was shown that without LA, BAF remains in the cytoplasm, and LA accumulation induces BAF nuclear translocation[84].

Interestingly, PRR14 is a nucleocytoplasmic protein that simultaneously binds HC and the NL. It contains a NL targeting domain and a domain that binds HP1α, which is known to bind H3K9me2/3. PRR14 requires LA/C for its localization at the NL. Depletion of PRR14 causes a wrinkled NL morphology and partial loss of H3K9me3 at the nuclear periphery[85].

Finally, retinoblastoma-binding protein 4 (RBBP4) is a protein crucial for chromatin remodeling and transcriptional regulation [86, 87]. RBBP4 is a member of H3K27 methyltransferase polycomb repressive complex PRC2 and has additionally been reported to interact with the histone acetyltransferase activator p300/CREB [88]. The Nucleosome Remodeling and Deacetylase complex (NuRD) contains RBBP4 and its homolog RBBP7[89,90]. Based on data that is available, it is ultimately unclear which candidate, if any, would be the key one for tethering HC.

In summary, a large number of chromatin-binding proteins have been shown to interact with LA/C, and these proteins are excellent candidates that could be required for lamin -dependent

HC tethering. However, the Misteli lab recently showed that a domain spanning the IG-fold and C-terminus of LA could bind directly to histone H3 *in vitro*, and exhibited a preference for certain heterochromatic modifications including H3K9me2[91]. Intriguingly, the equivalent domain within LC was incapable of interacting with histones. These data suggest that LA might specifically and directly bind to heterochromatic nucleosomes, but this model had not previously been tested in an intact cellular system.

1.4. Multifunctionality of lamins

Lamins are highly multifunctional proteins that play roles in nuclear assembly, nucleo-cytoskeletal coupling, nuclear stability, nuclear migration, chromatin organization, gene silencing, DNA replication, transcriptional regulation and DNA damage repair[78,54 92 , 93]. Traditionally, genetics has been a key method with which to study protein function in living cells. However, most of the *LMNA* mutations observed in humans are heterozygous[94], meaning that cells express wild-type LA (and/or LC) along with the mutated protein. This enables a compensation for the mutated allele, which makes it challenging to understand how *LMNA* mutations affect HC tethering. It has therefore been difficult to determine the exact role of LA in genome organization and pathological mechanisms of disease. Knockout and conditional knockout models have provided a way around this conundrum, but functional redundancy with LBR and other lamina proteins nonetheless make it complicated to dissect the contributions of individual lamin genes to HC tethering and other cellular functions. It is important to emphasize that it remains unclear that all tethers of HC have been identified to-date. In certain cell types, proteins other than lamins and LBR might be sufficient to tether HC, perhaps providing additional layers of functional compensation.

1.4.1. Developmental and tissue-specific expression of Lamin A

All mammalian cells express at least one B-type lamin throughout development, while high levels of LB1 and LB2 are found in embryonic stem cells (ESCs). LBR is important in dividing stem and progenitor cells[95,96]. By contrast, A-type lamins are absent from embryonic cells, and are usually expressed only after cells commit to a differentiation program. A-type lamin expression is not essential for murine development as mice that lack LA/C appear to be normal at birth. This might be due to functional compensation since LBR is often expressed in cells that lack LA/C[66]. However, *LMNA* absence leads to postnatal death in knockout mice[97]. In humans, complete loss of *LMNA* may lead to preterm lethality[98].

Interestingly, besides developmental regulation, LA/C expression has a cell-type-specific dimension. For example, in neurons of the central nervous system (CNS), the translation of LA, but not LC, is prevented by the microRNA miR-9[99]. However, B-type lamins are required for normal development of the CNS[100,101].

1.4.2. Lamin A/C and DNA damage response

LA has both direct and indirect influences on the regulation of DNA damage response (DDR). The ATM, ATR and DNA-PK kinases are main regulators of DNA repair pathway, and they directly detect broken DNA ends. The DNA repair pathway starts with ATM phosphorylation of H2A.X Ser-139 residue as an initial response to a DNA break, amplifying the DNA damage response signaling[102].

One of the key proteins in chromatin based DNA damage response cascade is 53BP1, which is crucial in regulating the balance between DNA repair pathways[103,104], and promoting the local enrichment of proteins required for non-homologous end joining[104]. LA/C binds 53BP1,

protecting it from degradation and maintaining its availability for rapid recruitment during DNA repair[105]. There is a significant decrease in 53BP1 levels at radiation-induced DNA breaks in LA/C deficient cells[106]. LA is also involved in SIRT6-dependent recruitment of the DNA-PK catalytic subunit to chromatin in response to DNA damage, additionally enhancing SIRT6 deacetylase activity[107]. LA/C was shown to bind RAD51, another regulator of the DNA damage response, protecting it from degradation[108].

After irradiation, DNA repair in EC proceeds faster than DNA repair in HC, which follows later. Heterochromatic ATM –dependent DDR is activated through phosphorylation of KAP-1 (KRAB-associated protein 1), which was shown to be critical for the 53BP1-associated DNA damage response[109]. Interestingly, DNA double-strand break repair is inefficient in rod photoreceptors, which correlates with low level of KAP1 expression and phosphorylation, as well as LA/C absence[110,111].

Lmna-null fibroblasts have a marked increase of chromosome breaks with γ-H2AX foci, which are signs of unrepaired DNA[112,113]. Increased DNA damage during aging can coincide with loss of LA/C[114,115] and accumulation of progerin, a mis-spliced mutant version of LA missing 50 C-terminal amino acid residues. Accordingly, LA increase in centenarian cells favored recruitment of DNA repair machinery[116].

PARP1 is a protein with a role in non-homologous end joining, homologous recombination and base excision repair pathways. As a response to DNA breaks, PARP1 covalently attaches adenosine di-phosphate (ADP)-ribose chains to itself and other proteins, which signals the recruitment of DNA repair proteins[117]. LA/C interactor SIRT6 activates PARP1 as part of the DNA damage response[107]. Overall, evidence for LA/C involvement in DNA damage repair

remains compelling, although whether LA/C modifies DNA repair by scaffolding chromatin and repair proteins together remains less clear.

1.4.3. Role of lamins in chromatin organization and gene regulation

In addition to acting as a mechanical support for the nucleus, the NL serves as an anchor for HC. Tethering of HC to the NL plays a crucial role in establishing interphase chromosome topology and the overall genome spatial organization, which is known to contribute to nuclear stiffness[118]. It is reported that chromatin by itself can provide a resistance force to prevent deformation[119,120,121,122,123], while lamins can resist more extensive nuclear deformations[110,124]. The specific contribution of each lamin isoform to LAD organization is still unclear. Different DamID studies suggest that LB1, LB2 and LA can interact with the same LADs, however, with different frequency[125]. In contrast, it is possible that certain LAD regions are uniquely associated with LA/C or LB1[126].

Depletion of all lamins in *Drosophila*[28] or mammals[29] alters the state of chromatin organization and affects gene activation or repression patterns. When lamins are absent in *Drosophila* cell lines, HC tethering is reduced[28]. However, Lbr expression in those cell lines is persistent, thus the role of lamins in HC tethering mechanism in this study is not clarified. In murine embryonic stem cells, absence of lamins produces a partial loss of LADs[29], similarly to what is reported in cells where LA/C is mutated[127,128]. The loss of lamins in *Drosophila*[28] is not only associated with the reduction of HC tethering at the nuclear periphery, but also repositioning to the nuclear interior and condensation[28]. This might suggest that HC tethering at the NL anchors the HC, and simultaneously promotes stretching of the chromosomes in the nuclear interior. Additionally, artificial tethering of the internal genome regions to the nuclear periphery led to their repression[129,130]. Although the absence of A-type lamins in differentiated cells was proved

to be sufficient to disrupt peripheral HC organization, despite the presence of B-type lamins[66], some studies have reported that B-type lamins[131] and even LC[132] are required to maintain LADs and tether HC. Given all the research on this topic, the molecular mechanisms by which chromatin interacts with the nuclear periphery are still poorly understood.

1.5. Lamina-related diseases

Discovered in 1994, the *EMD* gene that codes for LEM domain protein emerin, was the first to be associated with a laminopathic disease, namely X-linked Emery-Dreifuss Muscular Dystrophy (EDMD)[133]. Over the few decades, mutations in other genes encoding proteins of the inner/outer nuclear membrane or the NL were found to be responsible for several diseases collectively called nuclear envelopathies. Most of envelopathies are caused by mutations in *LMNA* and are called primary laminopathies, with diverse clinical phenotypes and overlapping symptoms, ranging from cardiac and skeletal myopathies to lipodystrophy, peripheral neuropathy, and premature aging or Hutchinson-Gilford progeria syndrome (HGPS)[134]. More than 400 mutations in *LMNA* have been identified as causative of diseases[135]. The secondary laminopathies are caused by mutations in the gene encoding the enzyme ZMPSTE24, which results in an incomplete post-translational processing of prelamin A[136]. Surprisingly, most laminopathies are tissue-specific, affecting the skeletal muscle, heart, peripheral nerves, bone(s) or adipose tissue, although lamins are ubiquitously expressed[137]. *LMNA* mutations in a single residue can result in different diseases, affecting different tissues[138]. This may suggest that specific LA mutations could be responsible for disrupted interactions between tissue-specific transcription factors[64]. This is specifically true for transcription factors Oct1[139] and

SREBP1 [140], which are important regulators of adipogenesis, cholesterol and fatty acid synthesis.

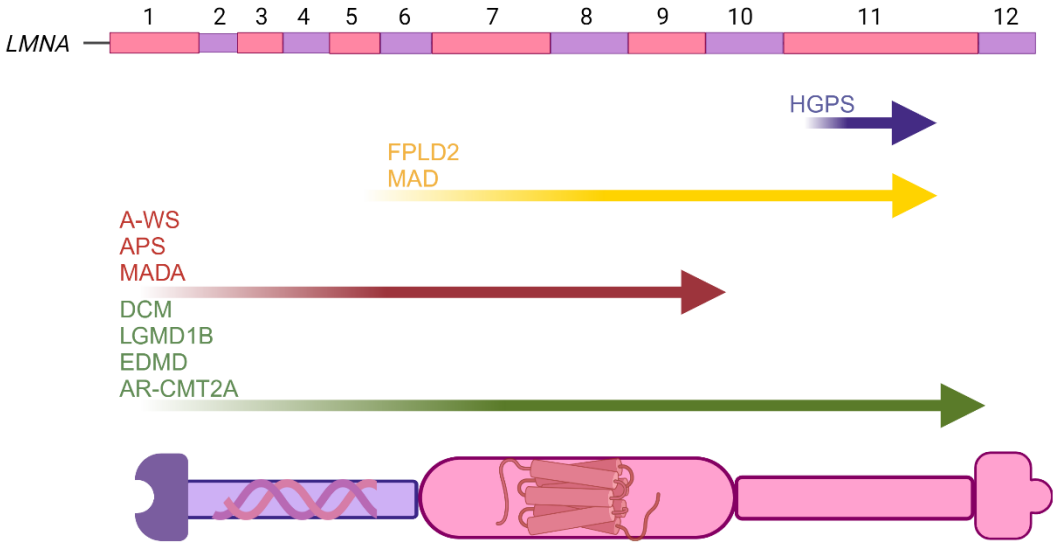

Figure 1.9. The structure of the human *LMNA* gene. Various mutations identified correlate to pathologies that cause progeroid syndromes (blue, red) and/or segmental diseases affecting connective tissues (green, yellow). MAD, mandibualoacral dysplasia. APS, atypical progeroid syndrome. A-WS, atypical Werner syndrome. HGPS, Hutchinson–Gilford progeria syndrome. EDMD, Emery–Dreifuss muscular dystrophy. DCM, dilated cardiomyopathy. EDMD2 (LGMD1B), AR-CMT2A, Autosomal recessive Charcot-Marie-Tooth disease type 2A, Limb-girdle muscular dystrophy 1B. FPLD2, Dunnigan familial partial lipodystrophy 2[141].

These are processes impaired in lipodystrophy and many other lamin-linked diseases. *LMNA* has 12 exons encoding 664 amino acids (Figure 1.9). The first 10 exons, encoding 566 amino acids of LA/C, are identical in LC and prelamin A, the precursor to mature LA.

Duplication of the *LMNB1* gene is associated with autosomal dominant leukodystrophy associated with demyelination of neurons, while mutations in *LMNB2* gene produce an acquired partial lipodystrophy disease phenotype[142].

Genetic mutations in *LBR* are also linked to Pelger-Huet anomaly and Greenberg skeletal dysplasia, which share common problems in cholesterol biosynthesis due to loss of LBR sterol C14 reductase activity. Pelger-Huet anomaly is a benign autosomal dominant laminopathic blood disorder, characterized by distorted nuclear organization of white blood cells (neutrophils and eosinophils). In contrast, Greenberg dysplasia is a lethal, autosomal recessive, prenatal bone disorder[143]. Taken together, these disorders point to the potential importance of HC tethering, but the multi-functional roles of lamina genes leave open the possibility that disease pathology is primarily driven by other cellular mechanisms.

1.5.1. Lamin A in premature and normal aging

Progeroid laminopathies may arise due to mutations in different genes. Progeroid syndromes caused by *LMNA* mutations include HGPS, Atypical Progeria Syndrome (APS), type A Mandibuloacral Dysplasia (MADA), Atypical-Werner's Syndrome (A-WS) and Restrictive dermopathy (RD)[144]. HGPS, A-WS, RD and APS are mostly associated with heterozygous dominant *LMNA* mutations[145], while MADA is characterized by recessive *LMNA* mutations[146]. Type B Mandibuloacral Dysplasia (MADB) is a consequence of heterozygous and homozygous *ZMPSTE24* mutations[147]. Diseases with a MAD phenotype are usually associated with *LMNA* mutations which abrogate the ZMPSTE24 cleavage site[148]. Complete loss of *ZMPSTE24* gene function due to homozygous mutation cause a severe developmental disease which results in perinatal death (RD)[149,150]. Interestingly, there are several additional

progeroid syndromes caused by mutations in genes which are a part of DNA repair pathways[151], suggesting convergence between the NL, DNA repair and lifespan.

Among the premature aging traits such as aged appearance, short stature caused by growth abnormalities and lack of subcutaneous fat, progeroid laminopathies are characterized by symptoms shared with other age-related disorders such as osteoporosis, atherosclerosis and cardiovascular defects, which are the most frequent cause of death, along with strokes[152].

One of the most notable progeroid laminopathies is Hutchinson-Guilford Progeria syndrome (HGPS). Children affected with progeria suffer a slower growth rate and in childhood their appearance resembles that of old age. HGPS is characterized by baldness, accelerated skin aging and a small face and jaw relative to head size. HGPS patients suffer from stiffness of joints, hip dislocations and severe cardiovascular disease. In HGPS, a partially processed LA isoform lacking 50 amino acids (LA Δ50), called progerin, accumulates at the NL. Progerin is a product of a single nucleotide *de novo* mutation c.1824C>T (Gly608Gly) which generates a cryptic splice site in exon 11. The cryptic splice site results in a deletion of 150 base pairs in pre-mRNA, that correspond to 50 amino acid residues from C-terminal domain of LA protein (LA Δ50, 606 – 656), including the second ZMPSTE24 recognition site (L647). Therefore, progerin cannot be cleaved by ZMPSTE24 and remains farnesylated at the C-terminal Cysteine[153,154,155] (Figure 1.10). The mutation is heterozygous dominant.

The transition from prelamin A to mature LA is a process that happens very fast under physiological conditions[156]. As farnesylated progerin accumulates in progeroid cells, its pathogenic effects manifest as abnormal nuclear morphology [157, 158, 129], chromatin disorganization[159] and aberrant transcription[160]. Loss of peripheral HC and generally altered

nuclear architecture with mislocalized NE proteins is a signature of HGPS[158], MAD[159] and other progeroid disorders.

The accumulation of damaged DNA seems to be another feature of progeria, with HGPS[161], MADA[162] and RD nuclei[163] exhibiting increased DNA damage and impaired repair. In most progeroid laminopathies, LA mutations can directly affect intermolecular interactions and/or protein stability[164].

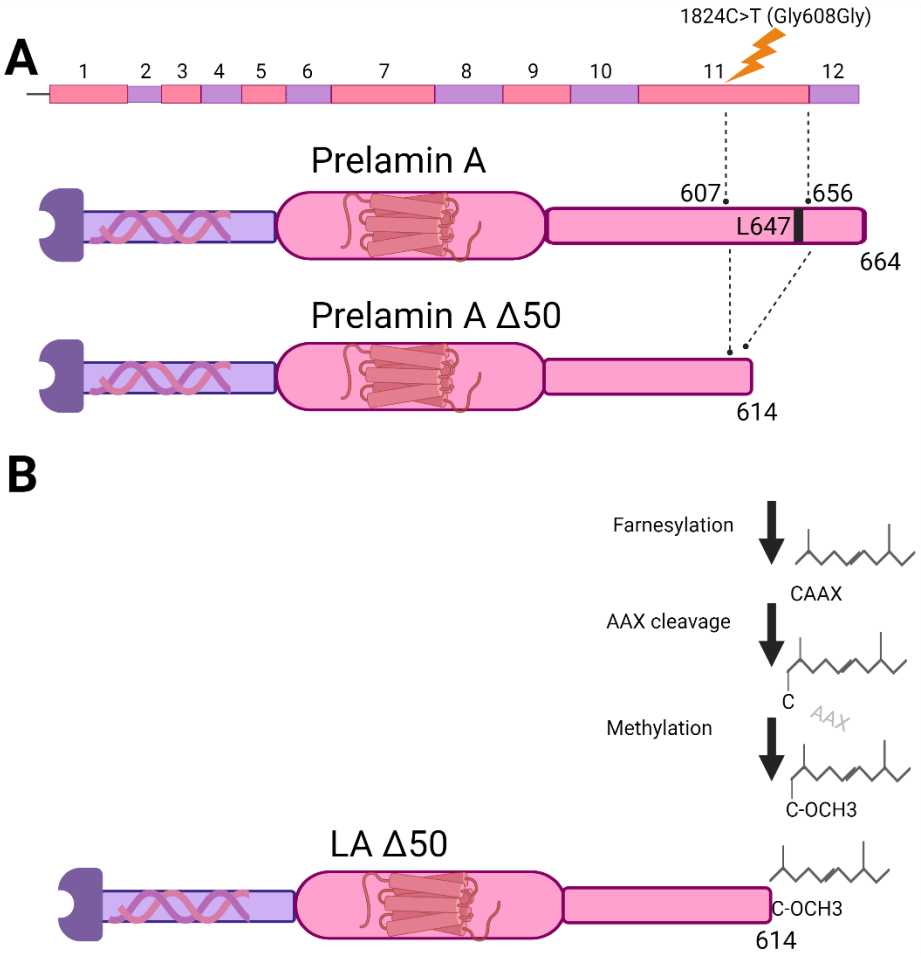

Figure 1.10. Comparison of Lamin A and Progerin (LA Δ 50) structures. A. Lamin C is encoded by exons 1 to 10, while Lamin A is encoded by exons 1 to 12. A dominant *de novo* c.1824C>T (Gly608Gly) mutation activates a cryptic premature splice donor, excluding 150 nucleotides from exon 11. This event leads to the production of mutant Lamin A (prelamin A

Δ50) lacking 50 residues (aa 607 - 656) from the C terminus of pre-lamin A. The second proteolytic cleavage site (L647) involved in prelamin A processing is missing. **B.** Pre-lamin A Δ50 is farnesylated and carboxymethylated at the Cysteine residue of the CAAX box, identically to pre-lamin A processing (for details, see Fig. 1.7A). As the Zmpste24 (L647) cleavage site is missing in the mutant pre-lamin A Δ50, the mature Lamin A Δ50 (LA Δ50, progerin) is permanently farnesylated and carboxymethylated.

In addition to HGPS, progerin protein can be found in normal aging cells where lamin transcript splicing is not as efficient[165]. Premature and normatively aged cells both lose methylation at Lysine of H3K9 and H3K27 heterochromatic histone marks. In those cells, genome organization is significantly impaired and HC structures at the nuclear periphery are disrupted[166,156], with a notable loss[29] and epigenetic deregulation of LADs[167]. Important heterochromatic proteins like HP1 are downregulated[168,128] and there is a noted loss of repression at genome regions that are normally heterochromatic[169]. In the same time, LA interaction with SIRT1/6 and HDAC2 deacetylases is diminished in aging cells[170,171,107]. Accordingly, several NuRD complex components are lost in premature and normally aged cells[172], along with DNA damage accumulation[162]. LB1 was found to have a role in aging, specifically in the formation of the senescence-associated heterochromatin foci which serve to repress proliferation of damaged cells[173]. However, LB1 is downregulated during physiological[174,175] and premature aging[169,176], promoting neurodegeneration[177]. LA- and LB-networks diverge in laminopathic cells[178], which could explain LB1 dysfunction during aging.

1.6. Retina and rod photoreceptors as a model system

The retina is an innermost part of the eye and a crucial visual processing component of the central nervous system (CNS) that consists of seven different cell types[179]. They are rod and

cone photoreceptors, retinal ganglion cells (RGCs), bipolar cells, horizontal cells, amacrine cells, and Müller glia[180] (Figure 1.11). The retinas of humans (but not mice) contain a high acuity region within the central retina called the macula or fovea. This structure is made up of mostly cone photoreceptors which are responsible for color vision, while the peripheral retina is thinner and is composed of mostly rods which mediate vision in low light conditions. The outer segments of rod and cone photoreceptors contain all the components required for phototransduction. The retina is supported by the retinal pigment epithelium (RPE)[181].

1.6.1. Rod photoreceptors in phototransduction cascade

Rods are depolarized at rest, and must constantly expend energy to maintain ionic homeostasis. Along with the photopigment Rhodopsin, which is encoded by the gene *Rho*, the outer segment contains the cationic cyclic guanosine monophosphate (cGMP)-gated channels, which control the flow of sodium (Na^+) and calcium (Ca^{2+}) ions into the outer segment. In the dark, cGMP levels are high, so Na^+ and Ca^{2+} flow in to the outer segment through the channel. This dark current keeps rods depolarized at about -40 mV, leading to glutamate release at the synapse. Although glutamate is usually an excitatory neurotransmitter, it binds a metabotropic glutamate receptor called mGluR6 expressed by some postsynaptic bipolar cells, which can invert the signal to turn it into an inhibitory signal[182]. In this way, glutamate release can prevent the excitation of downstream neurons in the dark.

Photoreceptors are energetically expensive to maintain. Na^+K^+-ATPase and Na^+K+-Ca^{2+} exchangers pump the excess Na^+ and Ca^{2+} ions out of the cells and maintain ionic homeostasis, but at a high cost. A single rod consumes about four times more ATP in darkness than in light[183]. Rod photoreceptors are able to respond even to single photons of light[184]. Light activation of Rhodopsin starts a chain of reactions that lead to hyperpolarization of the

photoreceptor's membrane potential. Upon light stimulation, the covalently bound 11-cis retinal isomerizes to the all-trans form, enabling Rhodopsin to activate transducin (G protein). Activated transducin excites a third protein, cGMP phosphodiesterase (PDE), which hydrolyzes cGMP to 5′-noncyclic GMP.

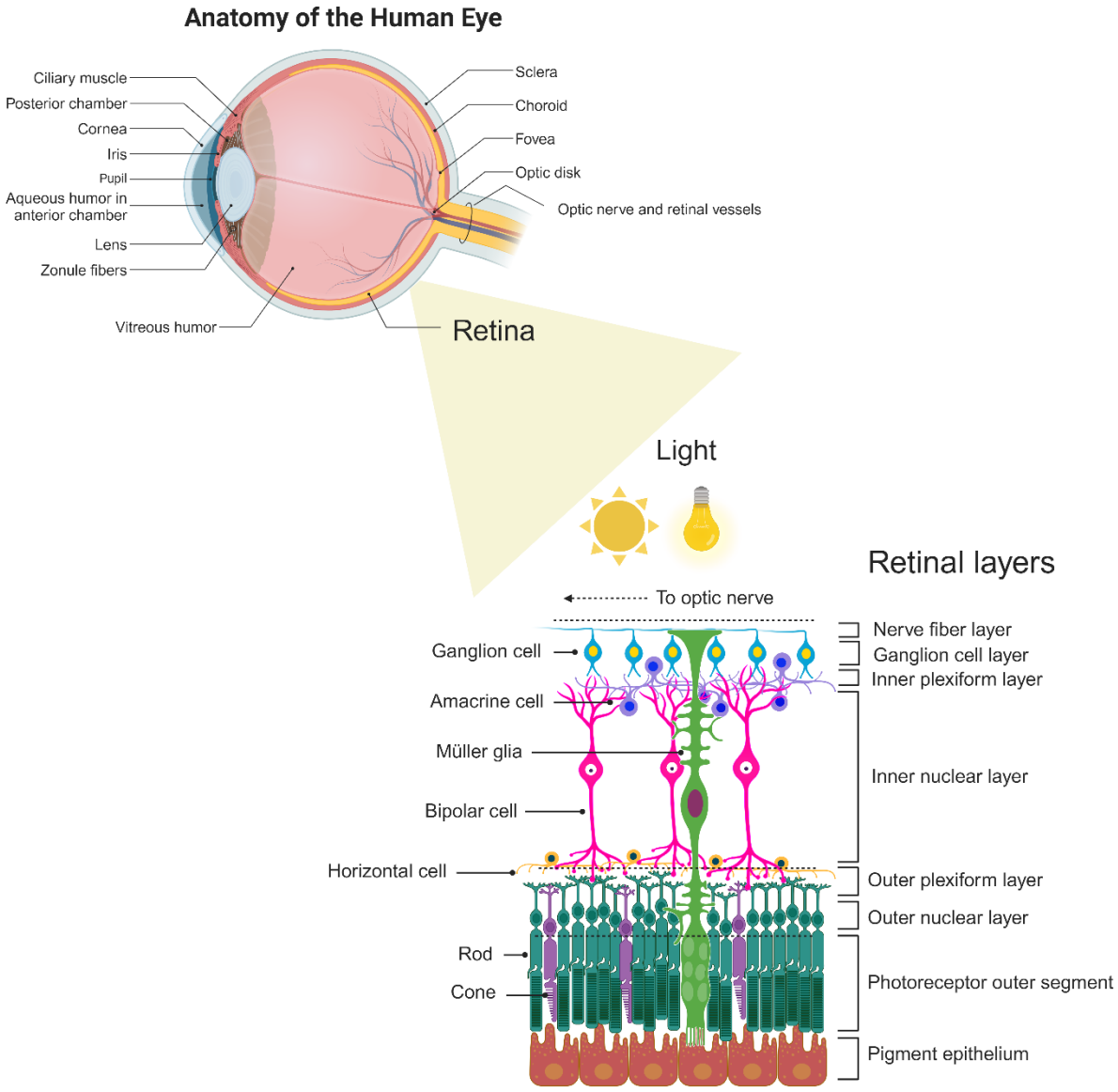

Figure 1.11. Retinal neurons.

Retinal layers: nerve fiber layer; ganglion cell layer encompassing retinal ganglion cells and displaced amacrine cells; inner plexiform layer containing synaptic connections; inner nuclear layer made of cell bodies of bipolar cells, horizontal cells, amacrine cells and Müller glia; outer plexiform layer containing ribbon synapses; outer nuclear layer containing the cell bodies of rod and cone photoreceptors and photoreceptor layer consisting of the inner segments and outer segments of rods and cones.

The decrease in cGMP closes the channels, which stops entry of Na^+ and Ca^{2+} and hyperpolarizes the rod[185]. While the physiology of rod photoreceptors makes them exquisitely sensitive to light, the high metabolic costs associated with this physiology make rod photoreceptors vulnerable to oxidative stress and degeneration.

1.6.2. Retinal degeneration

Retinal tissue is extremely sensitive to genetic and environmental changes. Retinal tissue surpasses any tissue in the human body by its level of metabolic activity and oxygen consumption[181]. Interestingly, photoreceptors are the most susceptible cell type in humans to genetic diseases[186]. Gene regulation may contribute to this vulnerability. Photoreceptors must maintain a high-level expression of at least 50 genes that specifically cause retinal degeneration when compromised [187, 188]. Among genetic causes of blindness, retinitis pigmentosa is among the most common[189]. Genetic studies have identified at least 80 disease-causing genes, and it starts with the loss of night vision by accelerated degeneration of rod photoreceptors[190]. This is accompanied by the secondary loss of cone photoreceptors, since rods and cones depend on each other for survival[191]. There is evidence that photoreceptor degeneration is accompanied by higher order reorganization of the genome. Defects in key rod transcription factors, such as Crx and Nr2e3, or their co-factors, result in photoreceptor degeneration [66,192,193,194,195,196,197,198,199]. Genome organization[66,193,199,200] and chromosome

looping[201] were shown to be significantly affected on a global level when these transcriptional regulators were mutated.

1.6.3. *Rd1* model

The *rd1* mouse model of retinal degeneration was first described in the early 1920s[202]. In *rd1* animals, the gene encoding for the beta subunit of the rod photoreceptor-specific cGMP phosphodiesterase-6 B (*PDE6B*) is mutated[203], causing PDE6 dysfunction, accumulation of cGMP and rod cell death, followed by secondary cone photoreceptor cell loss[204,205]. Similar mutations have been linked to human retinitis pigmentosa[206]. Nowadays, the *rd1* model is used to study the pathogenesis of retinal degeneration and to discover potential therapeutic pathways. Although rods degenerate rapidly in the *rd1* model, this model also provides an opportunity to study genome organization changes in rod photoreceptors during retinal degeneration.

1.6.4. The unique inverted organization of rod photoreceptors

The majority of eukaryotic nuclei, including cone photoreceptors, exhibit a conventional pattern of chromatin distribution, with HC tethered at the nuclear periphery and the nucleoli, whereas EC is situated in the nuclear interior between the heterochromatic domains. According to computer modeling and Hi-C data, the tendency of heterochromatic regions to interact with each other seems to be essential for the separation of the EC and HC, whereas interactions of the chromatin with the NL are necessary to build the conventional nuclear architecture[23].

Unlike cones, the nuclei of rod photoreceptors found in nocturnal mammals are a unique example of an inverted nuclear architecture. Rod nuclei actually function as microlenses that help prevent photon scattering in the retina, which affects vision in low light conditions[207].

Behavioral and physiological studies revealed that inverted rod nuclei enhance contrast sensitivity and general optical quality in mice[208]. Mature mouse rod nuclei are highly spherical with an approximately 5 μm diameter, and consist of three concentric chromatin classes (Figure 1.12). A decade ago, studies on the peculiar rod photoreceptor genome organization were intensifying. Solovei et al. used DNA fluorescence in situ hybridization (FISH) to define the central dense domain of constitutive HC surrounded by a more decondensed region of HC[208], while Kizilyaprak et al. used immunogold electron microscopy [209] to study rod photoreceptor distinct chromatin domains. Finally, the Solovei lab used confocal microscopy to examine the distribution of specific chromatin marks to reveal the cellular organization of of the epigenome in inverted and conventional mouse retinal nuclei[210], making a distinction between central pericentromeric satellite and surrounding "LINE-rich" HC.

The center of the rod nucleus is formed by the single condensed chromocenter (cHC), encircled by a shell of fHC, whereas EC outlines the periphery. Rod genome inversion occurs during postnatal differentiation of rod photoreceptors (P1 – P28), through remodeling of the conventional nuclear architecture. HC first segregates from the nuclear periphery and it concentrates around chromocenters, which fuse together (P21) and eventually form a single chromocenter at P28 (Figure 1.12). Kizilyaprak et al. also showed that HC increases markedly over this time period, occupying a much larger fraction of the total nuclear volume[210].

Combining aforementioned techniques and chromatin modeling, Aldiri et al. and Norrie et al. described rod nuclear chromatin organization using genome-wide methods as well as DNA FISH, and found that some retinal progenitor genes that are localized to EC during development, become sequestered and repressed by polycomb during rod maturation, and relocalize within the outer shell of HC enriched for H3K27me3 known as "LINE-rich" or

"facultative" (fHC)[211, 212]. Norrie et al. reported that the number of TADs is markedly increased as rod photoreceptors differentiate and the central HC condenses[213,213.]

Interestingly, rods are characterized with a uniquely closed global chromatin landscape in comparison to cones and other cell types[214]. The unique organization of the rod nucleus has been suggested to arise due to the lack of HC tethering. Previous studies have shown that mature rod cells completely lack LA/C expression, and Lbr expression drops below a functional threshold[66,215].

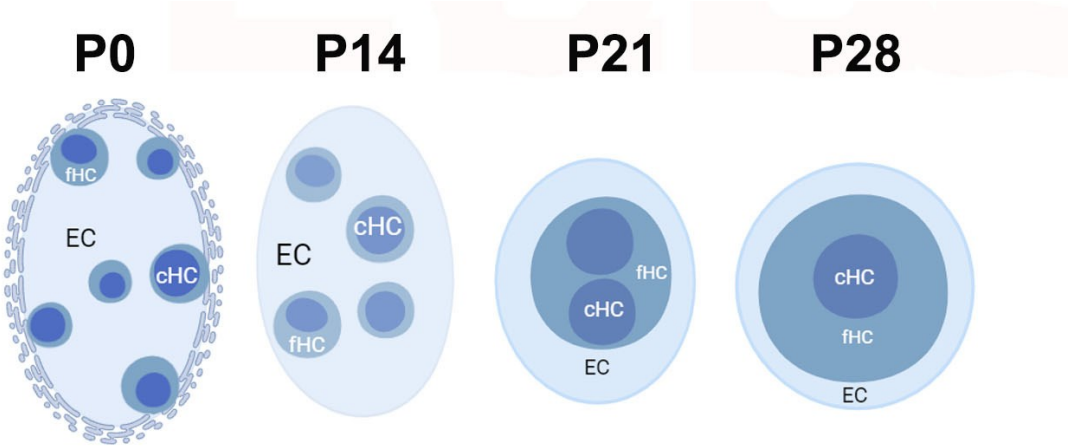

Figure 1.12. Stages of rod genome inversion. From conventionally organized postnatal P0 to P28 mature reorganized and remodeled inverted rod nuclei. EC = euchromatin, fHC = facultative heterochromatin, cHC = constitutive heterochromatin.

Therefore, NL of murine rod photoreceptors is structured by B-type lamins only. Solovei et al. showed that in various tissues, knocking out LA/C or Lbr leads to rod-like nuclei[66].

In rods, the single central chromocenter displays enrichment of H4K20me3 and H3K9me3 methylated histones. The surrounding ring of fHC is accordingly enriched in H3K27me3[210]. It

has been suggested that prior the inversion, *de novo* methylated H3K9me3 histones relocate from the nuclear periphery to the center of the nucleus, while H3K9me2 marked histones remain at the periphery, even at euchromatic regions in rods[34]. This might suggest that spatial inversion of chromatin in rods is accompanied with epigenetic relabeling. However, Eberhart et al. (Solovei lab) showed that H3K9me2 is not enriched at the nuclear periphery in rod photoreceptors, but localizes to the LINE-rich fHC[211]. Moreover, they generated G9A knockout rods, and showed loss of H3K9me2, validating their reported staining pattern. In these rods, although H3K9me2 was ablated early in development, the rate of chromatin inversion in rod photoreceptors was not accelerated. Thus, it is somewhat difficult to reconcile these two studies.

The mouse retina provides an advantageous model system with which to study dynamic changes in genome organization and the functions of specific molecular chromatin tethers. Specifically, rod photoreceptors provide a clean read-out system since they don't express any tethering proteins in the adult stage, and the process of chromatin inversion can be studied in rod photoreceptors using confocal microscopy[211]. Additionally, sorted rods have been investigated at the transcriptomic and epigenomic level, at mature stages[216], and during differentiation[217]. While these studies provide a strong groundwork for understanding of rod photoreceptor dynamic genome organization, molecular determinants of the higher order genome organization are still poorly understood.

1.7. Significance of the thesis

1. In our previously published research, we discovered LA is sufficient for tethering of the HC to the nuclear lamina and for restoring conventional nuclear architecture[218]. We hypothesized that LA might contribute to degeneration-associated nuclear reorganization. We examined *rd1* mice, the most studied mouse model of retinitis pigmentosa caused by *Pde6b* gene mutation. At the onset of degeneration, we found that LA/C significantly upregulates in rod photoreceptors, and reorganizes the genome. Together, our data reveal that the HC tethers LA and LBR have a global effect on genome accessibility, and suggest that tethering primes the photoreceptor genome to respond to stress[219].

2. Photoreceptor cells are highly susceptible to degeneration. Retinitis pigmentosa and in age-related macular degeneration are among the most common forms of neurodegeneration. However, the mechanisms of photoreceptor cell death and pathophysiology of retinal diseases are not fully understood. Not many molecular markers can be used to distinguish between early and later stages of rod photoreceptor cell death. We previously showed that LA upregulated at the onset of rod photoreceptor degeneration in the *rd1* mouse model of retinitis pigmentosa[220]. These data suggest that LA might be a marker of early degeneration and cell death. Here, we show that LA upregulation correlates with the DNA damage response. Our data suggest that

LA transiently marks an early phase of the cell death process, while phosphorylated (p)KAP1 marks rods throughout degeneration. We found that LA depletion accelerated cell death, whereas LA overexpression prolonged survival. Together, these data suggest that LA upregulation forestalls degeneration and facilitates the DNA damage response.

3. The potential importance of LA in genome organization is suggested by more than 400 different *LMNA* gene mutations associated with laminopathic disease. We reasoned that ectopically expressing laminopathic mutants in mouse rods might allow the interaction between mutant LA proteins and HC to be analyzed systematically. We hypothesized that laminopathic mutations would disrupt the interaction between LA and HC. By expressing C-terminal progeroid and non-progeroid IG-fold LA mutants in rod photoreceptors, we discovered that both sets of laminopathic mutants disrupt tethering, thus shedding light on the molecular mechanisms underlying HC tethering and IG-fold dependent stability of the protein. These data suggest that specific progeroid and non-progeroid laminopathic disease mutations exhibit a complete loss of tethering, indicating that this may play a role in disease pathology.

Since LA, B-type lamins and LC proteins only diverge at the C-terminus, our data implicate the LA C-terminus is necessary for HC tethering. While the LA C-terminus might therefore be sufficient to interact with HC, an alternative hypothesis is that C-terminal processing is required in order for LA to be competent to tether HC. To distinguish between these possibilities, we ectopically expressed a panel of LA constructs in rods. We found that the C-terminus of LA was sufficient to tether HC. However, we also found evidence that C-terminal processing is required to allow LA to tether HC. In particular, mutation analysis suggests that the LA C-terminus must be defarnesylated in order to be tethering-competent.

Progeroid mutants affected nuclear morphology more strongly versus wild-type LA, excessively elongating the nuclei and causing nuclear distortion. Overall, we find that defarnesylated progeroid mutants that partially tether HC, have a reduced effect on nuclear shape, reversing the nuclear phenotypes of progeroid cells and preventing nuclear distortion.

4. Although the tethering of HC to the nuclear lamina is a well-described phenomenon, the molecular mechanisms mediating this process remain poorly understood. While our experiments provided evidence that LA can tether HC by directly interacting with nucleosomes, these findings do not exclude the idea that A-type lamins might need additional co-factors. Since LA does not contain a conventional chromatin interaction domain, we hypothesized that it might need to interact with partner proteins in order to tether HC. We explored the tethering ability of several LA binding partners, which were proposed to participate in LA-dependent tethering, according to previous literature. We hypothesized that BAF (BANF1), RBBP4, PRR14 or LEMD proteins might be important for the function of LA-tethering complex. We tested this in rod photoreceptors, but found that none exhibited tethering activity – either when expressed alone, or in combination with a tethering incompetent version of LA. Moreover, LA mutations that reduced or abolished BAF binding retained tethering competence. Since all of these partner proteins appeared to be dispensable for LA- mediated HC tethering, we used proteomics to find the most enriched proteins in LA tethering complex. The results suggest that LA interacts with H2 and H4 nucleosomes directly rather than through additional partner proteins. PARP1 was also found to be enriched in the tethering-competent LA complex, suggesting that LA might also interact with damaged DNA.

Along with molecular modelling, my studies reveal the importance of the LA C-terminus in HC tethering. My work also suggests that rod photoreceptors upregulate LA in response to

DNA damage, and that the consequent increase in HC tethering can help to counteract retinal degeneration.

Chapter 2. Methods

2.1. Animals

Animal work was conducted according to the guidelines of the Canadian Council on Animal Care and the Animal Care and Veterinary Service at uOttawa using ethical protocols OHRI-2856, OHRI-2867, OHRI-3949 and OHRI-4029. CD1 mice were obtained from Charles River Laboratories. *C57BL/6J* and *rd1* (C57BL/6J-*Pde6b*$^{rd1\text{-}2J}$/J; strain# 004766) mice were obtained from Jackson Laboratories and maintained as homozygous stocks.

2.2. DNA constructs

pCIG2 and pCIG2 Lamin A were previously described[219,220]. A pCIG2 Lbr plasmid was generated by PCR amplifying Lbr from pMSCV-Flag-Lbr, generously provided by Peter Gaines[221] in order to remove the Flag tag.

Primers were Lbr XhoI F: 5'-CACACTCGAGATGCCAAGTAGGAAGTTTGTTG-3' and Lbr EcoRI R: 5'- CACAGAATTCTCAGTAAATGTAGGGGAATATG-3'. To mark rod photoreceptors, we utilized pRho-DsRed generously provided by Connie Cepko (Addgene #11156)[222]. Stable cell lines were generated using pBABE-puro-GFP-wt-lamin A (Addgene #17662) and pBABE-puro-GFP-Progerin (Addgene #17663) plasmids, generously shared by the Tom Misteli lab[223]. For the purpose of ectopic overexpression of NL proteins in rod

photoreceptors, we cloned several constructs. For the pCIG LA C-terminus (LA 540-646), we used pCIG LA vector and the primers were Mm Lmna C-term EcoRI F:

5'- GTGTGAATTCCACTGGAGAAGAAGTGG CCA TG-3' and Mm Lmna C-term EcoRI R: 5'- GTGTGATATCTTACATGATGCTGCAGTTCTGGG-3'. We cloned pCIG LA 646-Stop using pCIG LA vector and LmnA 1646 R primer: 5'-GAGAAGATCTTTAGTAGGAGC GGGTGACCAGATTGTCC-3', which replaces Leucine 647 with a stop codon. We cloned pCIG LA L647R using pCIG LA vector and Gibson Assembly protocol[224] using L647R-F: 5'GGTCACCCGCTCCTACCGCCTGGGCAACTCCAGCCCCCGAACCCAG-3' and L647R-R: 5'-GCGGTAGGAGCGGGTGACCAGATTG-3' primers. pCIG RBBP4 was amplified from cDNA using primer sets Rbbp4 EcoRI F: 5'- GAGAGAATTCAT GGCTGACAAGGAAGCGGC-3' and Rbbp4 PstI R: 5'-CTCTCTGCAGCTAGGACCCTTGTCCCTCTGG-3'.

Recombinant protein construct pIRES2-EGFP Hs Lamin BA was synthesized by Bio Basic (Markham, Ontario) by fusing the N-terminal LB1 domain and LA C-terminal domain (AA 534 to 664). We cloned pRho LA via directional cloning, by excising an LA open reading frame via Eco RI and PmlI restriction endonucleases. We subcloned LA coding sequence into Rho2.2 promoter pRho-DsRed plasmid, generously provided by Connie Cepko (Addgene #11156)[223].

Several modified plasmids were purchased: pBABE-puro-GFP-wt-lamin A (Addgene #17662), EGFP-BAF-L58R (Addgene #101776), EGFP-BAF (Addgene #101772), pLPC-L647RLaminA-CS (Addgene #69062), pLPC-Progerin-CS (Addgene #69064), Lemd2 (Myc-DDK-tagged, Origene MR203621), Lemd3 (Myc-DDK-tagged, Origene MR221903) and pCMV6 Prr14 (Myc-DDK-tagged, Origene MR205081). GFP-Lbr was generously provided

by Irina Solovei and Heinrich Leonhardt[71]. pCLE Lamin C was generated by inserting the Lamin C sequence into the pCle gateway retroviral vector. The Lamin C gateway donor plasmid was purchased from DNASU (HsCD00295844).

mCherry-LaminB1-10 was purchased (Addgene #55069). mCherry was removed and Lamin B1 coding sequence was cloned into pCIG2 vector to generate pCIG LB1.

pcmvTAG2A-FLAG-Lamin A, LA mutants with reduced affinity for BAF (R435C, K542N, A529V, R527H) and IG-fold mutants (R453W, R482W) were generously shared by Zinn-Justine lab[82]. We removed the Flag-tag from LA R435C, K542N, A529V, R527H, R453W, R482W mutants by using PCR amplification with Lamin A primers using constructs as templates. We also removed the GFP-tag from pBABE-puro-GFP-progerin (Addgene #17663).

2.3. DsiRNA constructs

TriFECTa RNAi Kit was purchased from Integrated DNA Technologies. Three small interfering double-stranded RNA (DsiRNA) constructs were predesigned to specifically suppress the expression of Lamin A. With minimal light exposure, DsiRNA duplexes were resuspended in nuclease-free water to make a 100 μM solution. All three Lamin A targeting DsiRNAs were pooled together. P0 rd1 pups were transfected with Lamin A DsiRNAs along with pCIG2 vector expressing EGFP, using electroporation. Non-targeting negative DsiRNA control was applied in another group of P0 rd1 mice. Transfected rd1 retinas were harvested at P16.

2.4. Electroporation

In vivo retinal electroporations were performed as described previously[219,223]. Briefly, P0 pups were anesthetized on ice, and an incision was made into the eyelid to expose the orbit of the eye. Plasmid DNA (2 µg/µl) was mixed with Fast Green dye and injected subretinally, using a Femtojet microinjector (Eppendorf) and pulled borosilicate needles (Drummond). Pups were placed into an incubator to re-warm, and then replaced into the home cage.

2.5. Short PFA fixation

After 42 days (six weeks), when rods are mature/inverted, retinas were harvested and dissected. Using curved and straight forceps, a tear was made on the dorsal side of the eyes. Retinas were carefully dissected away from the lens under the microscope. Retinas were examined for EGFP transfection signal using Zeiss Discovery Stereo microscope with LED illumination and filter cubes that could visualize EGFP fluorescence. Retinas were short-fixed in 4% paraformaldehyde (PFA), permeated in 20% sucrose overnight and cryo-sectioned using a Thermo Shandon cryostat.

2.6. Immunohistochemistry and microscopy

Retinas were processed for immunohistochemistry (IHC) as previously described[219,225]. We used the following primary antibodies: Nr2e3 (PNR: R&D Systems PP-H7223-00), lamin A (Fortis A303-433A), and Lamin A/C (Harald Herrmann Lab), Lbr (Monika Zwerger and Heinrich Leonhardt). H3K9me3 (Diagenode C15410056), H3K27me3 (Epigentek A-4039-025), H3K9me2 (Active motif 39240), gammaH2A.X (Bethyl Laboratories (A300-081-T), Anti-Myc tag (Abcam ab32), Lamin B1 (Abcam ab16048), Rbbp4 (Fortis A301-206A), BAF (Santa Cruz Biotechnology sc-166324), Nab2 (Proteintech 19601-1-AP), KAP1 pS824 (Bethyl Laboratories A300-767A-T). Hoechst 33342 (Tocris NB5117) and Alexa Fluor-568-

conjugated peanut agglutin (Molecular Probes L32458) were applied along with the primary antibodies. Fluorescently-conjugated secondary antibodies were applied to match the appropriate species of the primary antibodies.

Images were acquired using Zeiss LSM880 or LSM900 confocal microscopes with Airyscan detectors. All images presented in the paper are from individual Z-planes, and all level transformations were linear. Images were processed using Zen (Zeiss), Fiji (ImageJ), and Adobe Photoshop (Adobe) software.

2.7. Nuclear morphometric analysis

We applied Hoechst staining to visualize changes in genome organization with Zeiss LSM880 or 900 confocal microscope using fixed settings to capture single 8-bit Airyscan Z planes. This permits high-resolution analysis of rod HC, while allowing transfected cells to be identified via the EGFP marker. As a control we used an empty pCIG2 vector expressing GFP. Using ImageJ (Fiji)[226], a detailed morphometric analysis of transfected nuclei was performed manually as described previously[219,220]. Based on the Hoechst signal intensity, transfected nuclei were quantified and analyzed. The "Freehand Selection" tool was first used to measure mean pixel intensity of each selected nucleus. Then, perimeters were traced along the margin of the visible Hoechst signal using the "Freehand Line" tool, and the mean pixel intensity at the nuclear perimeter was measured. This measurement was divided by the mean pixel intensity of the entire nucleus in order to normalize against cell-to-cell or image-to-image variations in intensity. For the chromocenter midpoint/lamina measure, the distance between the centroid of each chromocenter within a given nucleus and the nuclear periphery was measured (non-cumulatively) using the "Straight Line" tool. Plot profiles for the perimeter intensity were generated using the "Freehand Line" tool in concert with the "Plot Profiles"

feature in ImageJ. Plot profiles for transect intensity measurements were performed using "Straight Line" tool with the "Plot Profiles" feature. Cumulative plot profile intensity values were plotted in Graphpad Prism (Graphpad Inc.). We were able to quantitate nuclear perimeter, area, nuclear distortion (perimeter/area ratio), facultative and constitutive HC, EC area and intensity, proportion and number of chromocenters per nuclei, as well as peripheral HC intensity as a measure of tethering activity.

2.8. Statistics

Statistical analyses for count and measurement data were performed using Microsoft Excel and GraphPad Prism 8 software. n-values refer to biological replicates (independent experiments, animals, or cells as indicated in the text and figure legends). All error bars are mean ± SEM. After comparing the variance within the group means using one-way ANOVA, tethering values were compared with the control using Tukey's post-hoc test. The analysis was performed on 30 cells (technical replicates) per retina (biological replicate), using three independently transfected CD1 retinas per construct (ie. n=3; 90 cells total) and completed for all constructs.

2.9. Flow cytometry

Adult retinas were dissected and placed in StemPro Accutase (Gibco) for 30 minutes at 37 °C. Cells were triturated manually, incubated with Dapi as a viability marker, and then sorted by the OHRI Flow Cytometry and Cell Sorting Facility using a Beckman Coulter MoFlo XDP.

2.10. Cell culture and western blot

Cell culture and western blotting were performed as previously described[219,226]. See above for immunocytochemistry antibody information. Stable cell lines expressing pBABE-puro-GFP-wt-lamin A**,** pBABE-puro-GFP-Progerin, or a vector control plasmids were generated by transfecting 293 cells with plasmids and selecting with puromycin (Bio Basic). 293 cells were transfected using lipofectamine 2000, with plasmid to lipofectamine ratio 1:2. Cells were harvested 36-48h after transfection. For optimal cell adhesion, coverslips were washed with 1% acid alcohol for 5 minutes and dried for 10 minutes. Coverslips were coated with 0.01% poly-L-Lysin in Dulbecco's phosphate-buffered saline for 5 minutes and dried. Coverslips were used in the cell culture dish and imaged.

HEK293 polyclonal TRex cell immunoprecipitation for western blot and mass-spectrometry

HEK-293 cells (control or stably transfected) were grown up to 80% confluency. Cell plates (100mm) were gently rinsed (twice) with 1x PBS. Cells were gently scraped and pipetted into 1.5 ml Eppendorf tube. Cells were centrifuged for 5 minutes at 1100 rpm, 4 °C, and the remaining PBS was removed. Cells were resuspended in 500 µl of cold RIPA buffer (on ice) containing proteinase inhibitors (430 ul RIPA, 70 µl 7x proteinase inhibitors, 1mM PMSF, 1 mM EDTA, 1 mM EGTA, 10 µg/ml DNAse). Samples were sonicated (on ice) at 10% amplitude with a cycle of 8 seconds on and 40 seconds off (3x). Cell debris was pelleted for 30 minutes at 13000 rpm, 4 °C. Supernatant was collected into tubes (input, IgG control, IP). 25 µl (5% of the lysate) was collected in the input tube for western blot). The rest of the supernatant was equally split between IgG control and IP tube. 20 µl of Protein A magnetic beads (Cell Signaling Technology 73778L) were washed with RIPA buffer and added in both the IP and IgG control tubes (for MS). 2 µg of the primary antibody was added in appropriate tubes (10 µl of Lamin A Bethyl anti rabbit (200 µg/ml) per sample and 2 µl of rabbit IgG (1

µg/ml) per sample). Tubes were rotated overnight at 4 °C. 7 µl of 4x sample loading buffer was added to the input tube and boiled at 95 °C for 5 minutes. Next day, beads were transferred to a new set of tubes and then pelleted using a magnetic rack. They were replenished with 500 µl of RIPA buffer after each pelleting (3x) and pipetted up and down. Once the beads were pelleted, 500 µl of 50 mM pH 7.8 ammonium bicarbonate was added to each tube. Beads were washed by pipetting up and down, and ammonium bicarbonate wash cycles were repeated two more times. After the washes, beads were transferred to a new set of tubes. Ammonium bicarbonate washes were repeated two more times. Beads were resuspended with 100 µl of 50 mM ammonium bicarbonate and 1 µg of MS-grade Trypsin (Thermo Scientific, PI90057) was added. Beads were incubated at 37 °C, rotating overnight. The next day, another 1 µg of MS-grade Trypsin was added to the each tube and incubated at 37 °C while rotating for 3 hours. Samples were transferred to new tubes. Beads were washed twice with 100 µl of HPLC-graded ddH20. Beads were pelleted using the centrifuge. A total of 300 µl of peptide solution per sample was acidified by adding 12 µl of 50% formic acid to each tube. Samples were lyophilized using a speed vac on medium heat for 2 hours. Samples were resuspended in 5% formic acid and submitted for mass spectrometry (MS). MS was performed at the Ottawa Hospital Research Institute Proteomics Core Facility (Ottawa, Canada). Peptide samples were concentrated using a Vacufuge (Eppendorf) and with ZipTips (Millipore Sigma). LC-MS/MS was performed using a Dionex Ultimate 3000 RLSC nano HPLC (Thermo Scientific) and Orbitrap Fusion Lumos mass spectrometer (Thermo Scientific). Peptide mass/spectral fingerprinting was performed using MASCOT software version 2.7.0 (Matrix Science, UK). Observed spectra were matched against human sequences from SwissProt (version 2021-02) against an in-house-curated database of common contaminants. The results were exported to Scaffold 5.0.1 (Proteome Software, USA). Identification of significantly enriched proteins was

performed using Graphpad Prism 8 via the Holm-Sidak method, with alpha = 0.05. Gene Ontology analysis was performed using ShinyGO 0.76 [227] (http://bioinformatics.sdstate.edu/go76/) using "Cellular Process" and "Cellular Component". Data were visualized and clustered using Morpheus [228] (https://software.broadinstitute.org/morpheus).

2.11. ATAC-seq

ATAC-seq data were generated following Buenrostro et al.[229]. Briefly, 50,000 flow-sorted cells were lysed in cold lysis buffer (10 mM Tris-Cl, pH 7.4, 10 mM NaCl, 3 mM MgCl2 and 0.1% IGEPAL CA-630). Lysed nuclei were tagmented using 6.5 µl of TDE1 transposase from the Nextera DNA Flex Library kit (Illumina). Samples were purified using Zymo-Spin IC columns (Zymo), and libraries constructed according to the Nextera workflow. Libraries were cleaned up using the AMPure XP kit (Beckman Coulter). Paired end (PE) 150 sequencing was performed using the NextSeq 500 platform to a read-depth of 25-35 million reads per sample.

2.12. Multi-seq

After flow cytometric sorting, cells were barcoded with 'anchor' and 'co-anchor' lipid-modified oligonucleotides generously provided by the Zev Gartner lab [230]. Barcode oligonucleotides were purchased from Integrated DNA Technologies as follows. Barcode 1: F: 5′-CCTTGGCACCCGAGAATTCCAGGAGAAGAAAAAAAAAAAAAAAAAAA

AAAAAAAAA-3′; Barcode 2: F: 5′- CCTTGGCACCCGAGAATTCCACCACAATGAGA

AAAAAAAAAAAAAAAAAAAAAAAAAAAA-3′; Barcode 3: F: 5′- CCTTGGCACC

CGAGAATTCCATGAGACCTAAAAAAAAAAAAAAAAAAAAAAAAAAAA-3′.

Each replicate was incubated with barcode oligonucleotides for 10 minutes. Cells were pelleted and washed 3 times with PBS. Replicates were pooled and processed in a single 10X Genomics Chromium run. Gene expression libraries were sequenced to an average depth of 369,327 reads per cell. Expression library FASTQs were processed using CellRanger (10X Genomics).

2.13. Bioinformatics – ATAC-seq

ATAC-seq Fastq files were processed via Fastq Groomer[231] and Trimmomatic[232], and then mapped to the mm10 genome using Bowtie2[233]. Summit and narrowpeak calling was performed with Macs2[234], and we used GREAT[235] for peak-to-gene annotation. GO terms analysis was performed using Panther[236,237] followed by ReViGO[238]. ATAC-seq gene metaplots were generated using Seqplots[239].

Sorted rod and double-sorted green cone ATAC-seq data and narrowpeak files (mm10) were obtained from Hughes et al.[215] (GSE83312). Ctcf ChIP-seq data (ENCSR343RKY) generated by the Bing Ren lab[240] were obtained from the ENCODE Consortium[241,242]. Additional ChIP-seq and cut&run-seq datasets were obtained from the Jeremy Nathans lab[217] (GSE72550), or the Epstein/Poleshko labs[34] (GSE180006).

For comparison with compartment data generated by Falk et al.[23] and Ctcf ChIP-seq data from ENCODE, ATAC-seq data were re-mapped to the mm9 genome as per above, except that we used Cutadapt for adapter trimming.

Footprinting analysis was performed using TOBIAS[243]. As per the guidelines, we merged peak files together: lamin A with control; Lbr with control. Bindetect was performed using 220 mammalian transcription factor motifs selected from the TRANSFAC database.

2.14. Bioinformatics – RNA-seq

RNA-seq data from sorted rod photoreceptors from P10 *Rd1* mice were obtained from Jiang et al.[244] (GSE183117). Figure 5.2 (Chapter 5) presents the bioinformatic data published in the original paper. To visualize *Lmna* transcription and splicing, we re-mapped the data to the mm9 genome using Galaxy[245]. Fastq files were processed via Fastq Groomer[232] and Trimmomatic[233], and then mapped to the mm9 genome using RNA Star[246]. Genome visualization and sashimi plots were generated using IGV[247]. Heatmaps were generated using Morpheus (https://software.broadinstitute.org/Morpheus). We quantitated differential transcripts using FeatureCounts[248] and DeSeq2[249].

2.15. Bioinformatics – scRNA-seq

Fastq files were aligned to the mm10 genome using CellRanger version 6.1.2 (Cell Ranger software, 10x Genomics). Output files were filtered and analyzed using Scanpy version 1.9.1[250] in Python (Python Core Team n.d.). Genes detected in less than 3 cells were removed from the analysis. Low-quality cells (less than 200 genes detected, more than 2500 genes detected or more than 18% of mitochondrial genes) were also excluded. Scrublet version 0.2.2 was used to detect doublets[251]. Replicates were demultiplexed with using the MULTI-seq workflow[231]. To annotate cell types, we trained a deep learning model grounded on previously published retinal single cell expression data[252] using scDeepSort version 1.0[253]. Mitochondrial gene regression and initial gene expression analysis was performed using scVI-tools version 0.19.0[254]. Differential gene expression analyses were performed using MAST version 1.24.0[255]. Data integration was carried out on PostgreSQL version 14.3 (PostgreSQL Core Team n.d.) and Python's library Pandas version 1.5.2 (Pandas Core Team n.d.).

Chapter 3. Lamin A upregulation reorganizes the genome during rod photoreceptor degeneration

Cell Death & Disease, 14, Article number: 701 (2023)

Ivana Herrera, José Alex Lourenço Fernandes, Khatereh Shir-Mohammadi, Jasmine Levesque & Pierre Mattar

Abstract

Neurodegenerative diseases are accompanied by dynamic changes in gene expression, including the upregulation of hallmark stress-responsive genes. While the transcriptional pathways that impart adaptive and maladaptive gene expression signatures have been the focus of intense study, the role of higher order nuclear organization in this process is less clear. Here, we examine the role of the nuclear lamina in genome organization during the degeneration of rod photoreceptors. Two proteins had previously been shown to be necessary and sufficient to tether heterochromatin (HC) at the nuclear envelope. The LBR is expressed during development, but downregulates upon rod differentiation. A second tether is the intermediate filament lamin A (LA), which is not normally expressed in murine rods. Here, we show that in the *rd1* model of retinitis pigmentosa, LA ectopically upregulates in rod photoreceptors at the onset of degeneration. LA upregulation correlated with increased HC tethering at the nuclear periphery in *rd1* rods, suggesting that LA reorganizes the nucleus. To determine how HC tethering affects the genome, we used *in vivo* electroporation to misexpress LA or LBR in mature rods in the absence of degeneration, resulting in the restoration of conventional nuclear architecture. Using scRNA-seq, we show that reorganizing the nucleus via LA/LBR misexpression has relatively minor effects on rod gene expression. Next, using ATAC-seq, we

show that LA and LBR both lead to marked increases in genome accessibility. Novel ATAC-seq peaks tended to be associated with stress-responsive genes. Together, our data reveal that HC tethers have a global effect on genome accessibility, and suggest that HC tethering primes the photoreceptor genome to respond to stress.

Introduction

Photoreceptor cells are highly susceptible to degeneration – perhaps due to their very high metabolic demands[256]. Cone photoreceptors are responsible for high-acuity color vision, whereas rod photoreceptors mediate vision in low-light conditions. Indeed, rods are sensitive enough to respond to individual photons[185]. To achieve this feat, rods must maintain high-level expression of at least 50 genes that can lead to degeneration when misregulated[188,189]. Genome regulation is thus essential for photoreceptor survival.

The importance of genome organization in photoreceptors is further underscored by their specialized nuclear architecture. In mice, rods undergo a process called chromatin inversion[211,210,208]. Whereas most cells tether heterochromatin (HC) in LADs at the nuclear periphery, rod photoreceptors localize HC centrally[211,210,208,34]. Throughout mammalian evolution, chromatin inversion is correlated with nocturnal lifestyle, as the inverted configuration decreases light scattering and enhances contrast sensitivity[208,209]. At the molecular level, two proteins have been shown to be sufficient for HC tethering.

1) The Lbr is a multi-pass transmembrane receptor that contains an intra-nuclear Tudor domain. Murine rods naturally express Lbr during development, although Lbr levels decline once rods differentiate. However, when Lbr expression in rods was artificially sustained, chromatin inversion was prevented[66].

2) The *Lmna* gene encodes two splice variants – LA and LC, neither of which is normally expressed in murine rod photoreceptors[66,215,219,216]. These A-type lamins are IFs that form a network across the surface of the inner nuclear membrane. In *Lmna* knockout mice, HC tethering was lost in various tissues, but transgenic misexpression of LC in rods had no effect on their inverted organization[66], initially suggesting that A-type lamins were not sufficient for HC tethering. However, we showed that LA is sufficient to tether HC in rods[219], resolving this conundrum. Interestingly, the unique LA C-terminus was recently shown to interact with histone H3, while the equivalent domain of LC cannot[91], which potentially explains this functional divergence.

Interestingly, degenerating rods were found to exhibit altered nuclear organization in a variety of mice harbouring mutations in chromatin proteins[66,219,257,23,193,258,201]. While these data potentially link the associated chromatin proteins to nuclear architecture, the observed alterations might instead be driven by cell death. Alternatively, chromatin proteins might act indirectly by altering gene expression. For example, mutants for the Nrl and Nr2e3 transcription factors lead to a rod-to-cone fate switch that reorganizes the nucleus[259,260]. Additionally, A-type lamins have been shown to upregulate in some knockouts[66,219,23] raising the possibility that HC tethers might contribute to degeneration-associated nuclear reorganization.

Here, we show that LA upregulates in the *rd1* mouse – one of the best studied models for retinitis pigmentosa. Rod degeneration in the *rd1* mutant is triggered via toxic accumulation of cGMP - a chromatin-independent process. Using genomic and transcriptomic approaches, we find that heterochromatin tethering may help to reconfigure the genome to respond to environmental insults.

Results

3.1. Lamin A upregulates during rod photoreceptor degeneration

LA is sufficient to reorganize the rod nucleus[219], whereas LC has no effect[66]. Using an isoform-specific antibody (Fig. 3.1A, B, C), we found that in wild-type mice, LA was extensively expressed within the inner retina (Fig. 3.2A, B, Supplemental video 1), as reported previously[206].

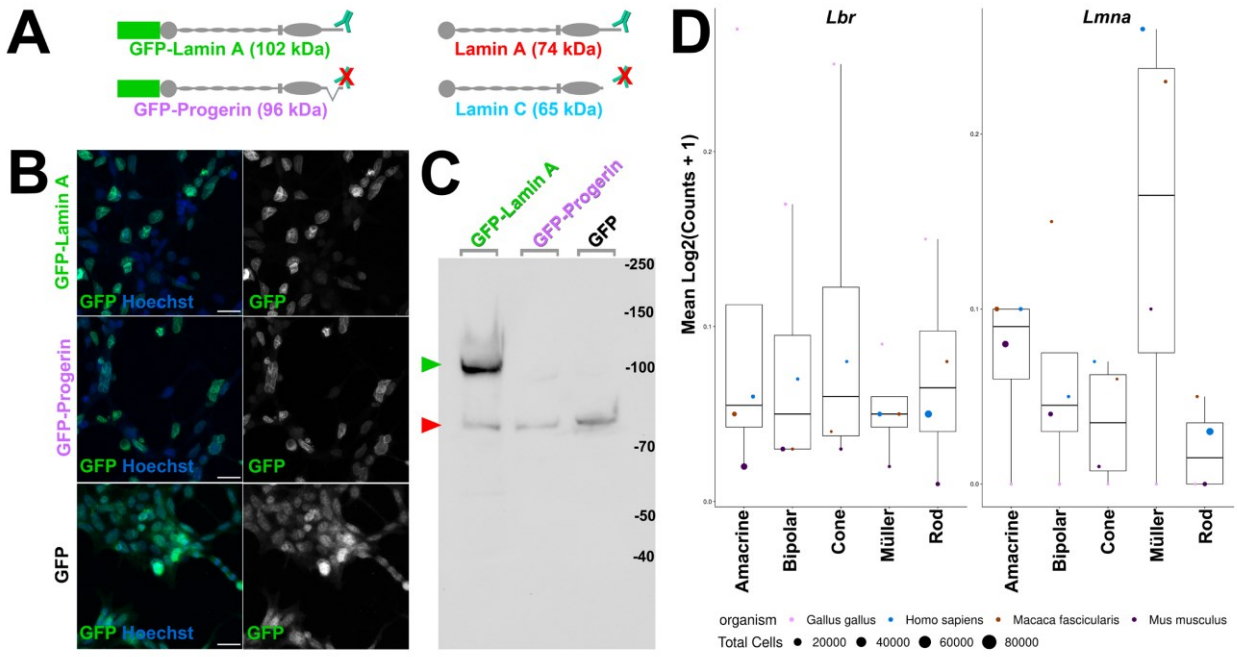

Figure 3.1. Validation of the lamin A -specific antibody. (**A**) Schematic of endogenous and exogenous A-type lamin proteins. (**B**) 293 cell lines stably expressing GFP-lamin A, GFP-progerin, or GFP alone as indicated, imaged for GFP epifluorescence. Scale bar = 20 µm. (**C**) Western blot of stably transfected 293 cell lines expressing GFP-lamin A, GFP-progerin, or GFP alone. Green arrowhead indicates GFP-lamin A band. Red arrowhead indicates endogenous lamin A. (**D**) scRNA-seq expression data for *Lbr* and *Lmna* obtained from chick (*Gallus gallus*), human (*Homo sapiens*), macaque (*Macaca fascicularis*), or mouse (*Mus musculus*) as indicated. The plot was generated using the *Plae* resource[262].

In photoreceptors, LA immunoreactivity was observed only in cones (Fig. 3.2A, B, arrowheads), and was absent from rods (Fig. 3.2A, B). *Lmna* transcription was also little detected in chick, human, or macaque rods as determined via the *Plae* scRNA-seq database[261] (Fig. 3.1D), in accordance with previous studies[66].

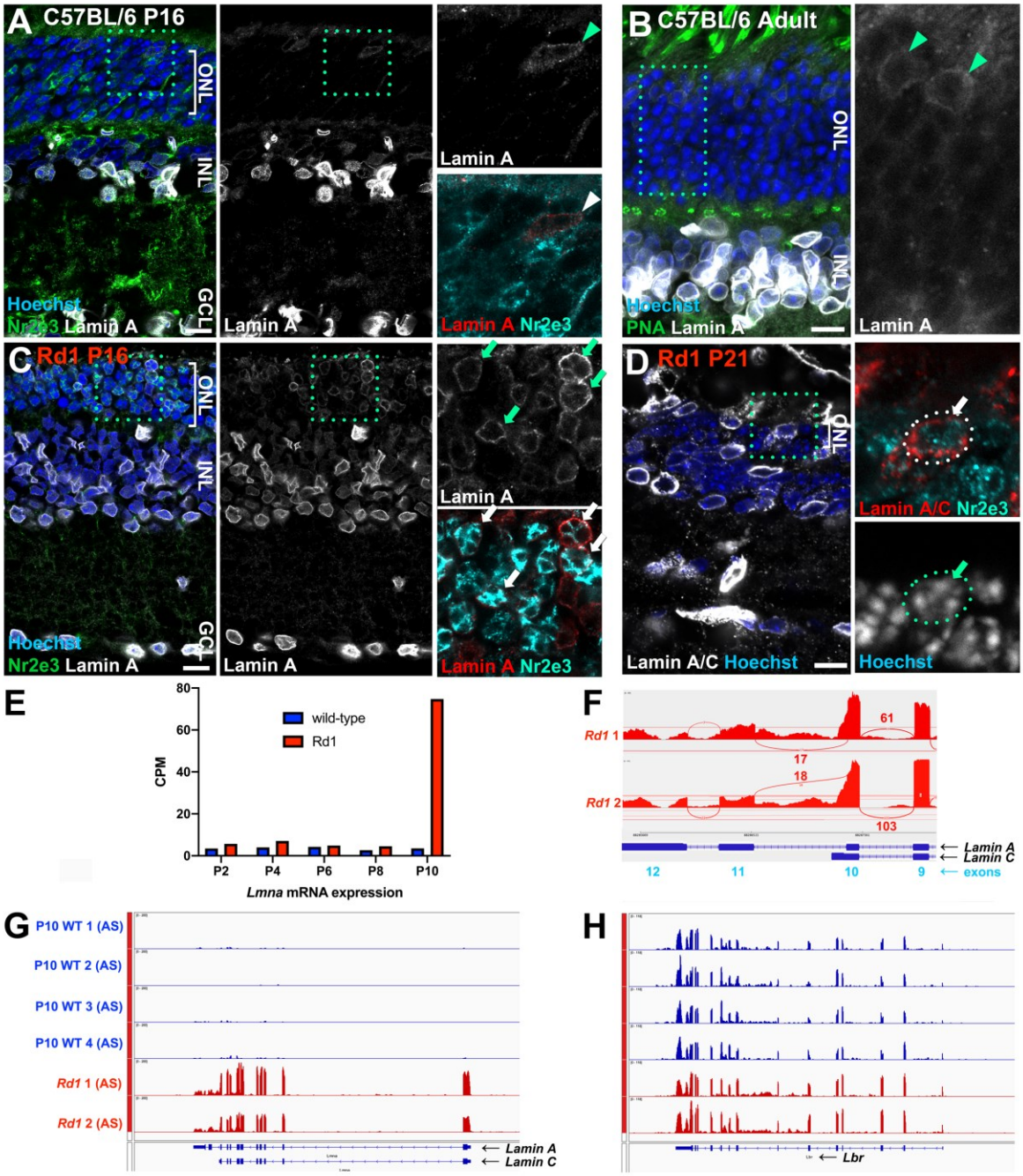

Figure 3.2. Lamin A upregulates at the onset of rod degeneration in *rd1* rods. (A, B) Immunohistochemistry on wild-type C57BL/6 at P16 (**A**) or adult (**B**) stages using a LA-specific antibody (white). The retina was counterstained for the rod marker Nr2e3 (A; green) or the cone marker peanut agglutinin (B; green), as well as the DNA dye Hoechst 33342 (blue). Boxed regions indicate the areas shown in the insets. Arrowheads indicate cone photoreceptors. (**C**, **D**) Immunohistochemistry for LA or LA/LC (white) and the rod-specific

marker Nr2e3 (green) on *rd1* retinas at P16 (**C**) or P21 (**D**). Boxed regions indicate the areas shown in the insets. Arrows indicate LA expression in Nr2e3+ rods. Scale bars = 10 µm. (E-H) Transcript expression at different postnatal stages as indicated - from the Anand Swaroop lab (AS)[245]. (**F**) Sashimi plot of splice junctions from P10 *rd1* RNA-seq data. (**G**, **H**) Transcription at the *Lmna* (**G**) or *Lbr* (**H**) loci from P10 RNA-seq samples as indicated. Data were remapped from Jiang et al.[245] and plotted on the same scale (group autoscale).

Previous studies revealed nuclear disorganization and LA/LC upregulation in mice harboring mutations in essential chromatin proteins (eg. Casz1, Atxn7), but whether this was a general feature of degeneration remained unclear. To address this question, we examined *rd1* mice – a well-studied degenerative model in which rods are completely eliminated by the fourth postnatal week. The *rd1* mutation disrupts the *Pde6b* gene, which is linked to retinitis pigmentosa in humans[207]. Examination of P16 *rd1* mice revealed extensive LA expression within the degenerating photoreceptor layer (Fig. 3.3C). Since cone cell death is more protracted versus rods in the *rd1* model, we co-stained *rd1* retinas with the rod-specific transcription factor Nr2e3 (Fig. 3.3C, D, Supplemental video 2). This confirmed that LA upregulated in *bona fide* rods in the *rd1* retina.

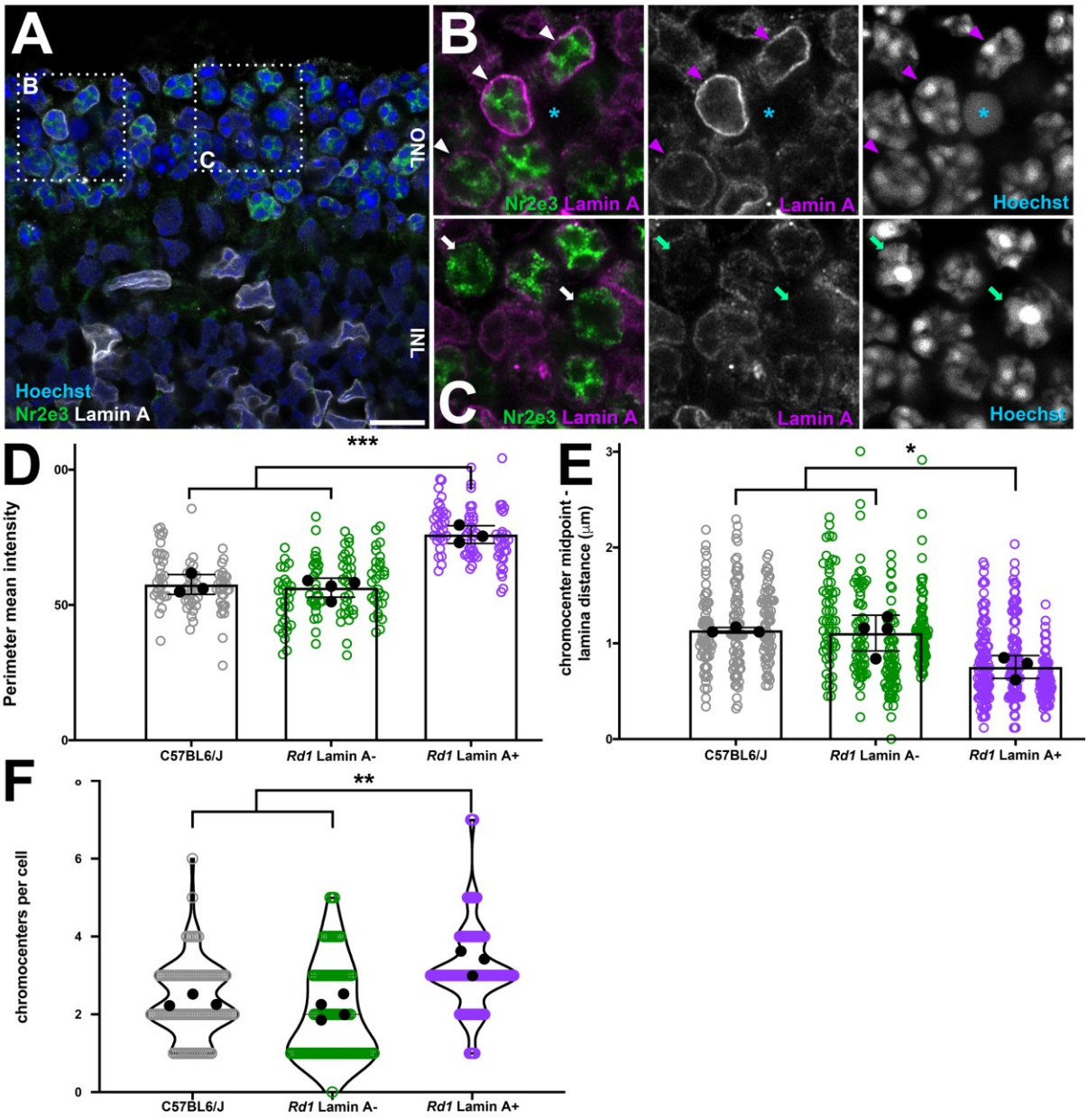

Figure 3.3. Increased heterochromatin tethering in Lamin A+ *rd1* rods. (**A**) Airyscan confocal imaging of P16 *rd1* retinas stained for LA (white), Nr2e3 (green), and Hoechst (blue). Boxed regions indicate the areas shown in (**B**, **C**). Arrowheads indicate LA+ Nr2e3+ rods. Arrows indicate LA-negative Nr2e3+ rods. Asterisk indicates a pyknotic nucleus. Scale bars = 10 μm. (**D**) Mean chromatin intensity at the nuclear margin normalized against the mean chromatin intensity of the whole nucleus. (**E**) Linear distance between chromocenter centroids and the nuclear margin. (**F**) Chromocenters per nucleus. Black datapoints and error bars are

the mean intensity values from each biological replicate (30 cells each; circles) ± SEM. * $p < 0.05$, ** $p < 0.01$, *** $p < 0.001$; ANOVA with Tukey's post-hoc test.

To corroborate these observations, we examined a recently published RNA-seq dataset made from sorted *rd1* rods[245]. In this dataset, *Lmna* was among the most significantly upregulated genes. Moreover, *Lmna* upregulation coincided precisely with the onset of cell death at P10 (Fig. 3.2E). Since pathological gene expression begins as early as P2[245], these data argue that *Lmna* upregulates in response to degeneration. To visualize *Lmna* transcripts directly, we re-mapped Jiang et al.'s RNA-seq data. *Lmna* upregulated significantly in the reanalyzed data (Log_2 fold-change vs. control: 3.40; adj. *p*-value: 5.19E-13). Examination of *Lmna* exon usage revealed that alternative splicing generated bona fide *LA* transcripts (Fig 3.3F, G). Finally, we examined *Lbr* transcripts, but found no difference in wild-type versus *rd1* mice (Log_2 fold-change vs. control: 0.042; adj. p-value: 0.91; Fig. 3.3H; Fig. 3.4). Thus, degenerating rods upregulate LA, raising the possibility that higher order genome organization might be reconfigured in these photoreceptors.

To test this idea directly, we measured HC tethering in LA–positive versus –negative rods. We found that the intensity of DNA at the nuclear periphery was elevated when LA+ cells were compared to LA-negative cells from the *rd1* mouse, or to C57BL6/J controls (Fig. 3.3A-D). Similarly, the distance between each chromocenter and the margin of the nucleus was significantly reduced in LA+ versus C57BL6/J control rods (Fig. 3.3E), suggesting that LA reorganizes the nucleus during degeneration.

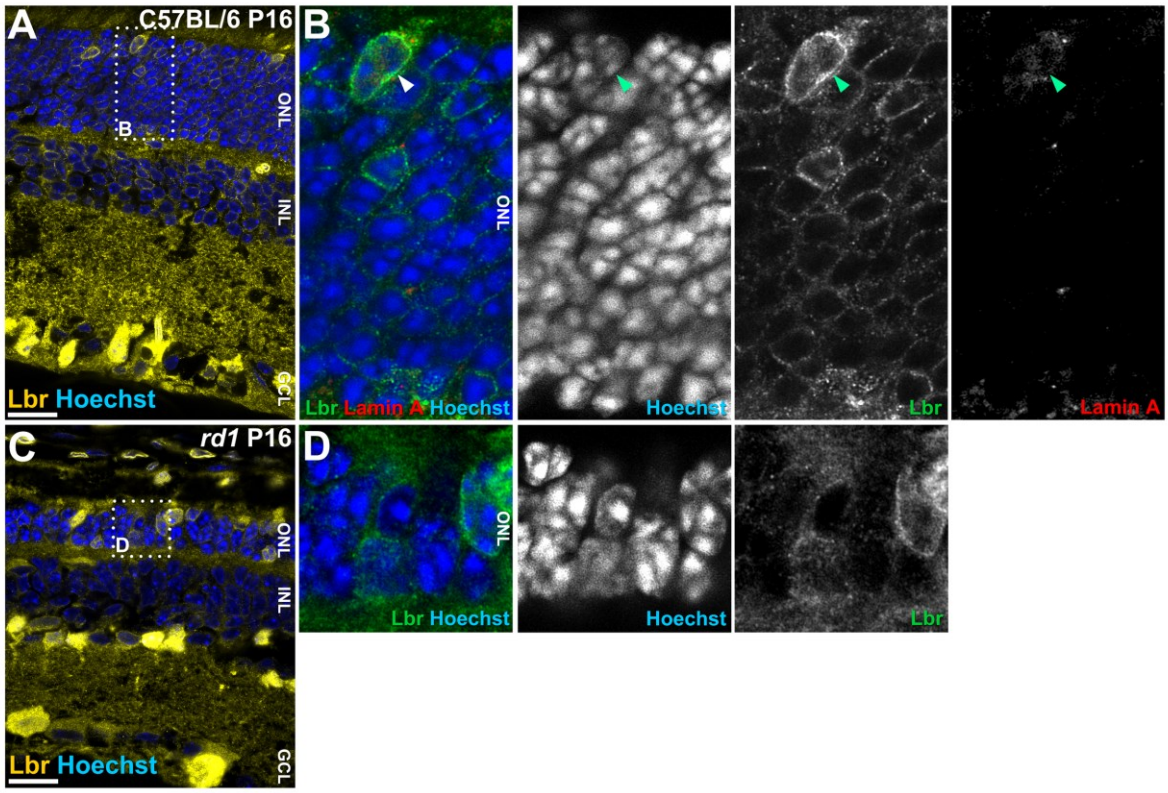

Figure 3.4. Lbr expression in the degenerating *rd1* mutant. (A-D) Airyscan confocal microscopy of P16 wild-type C57BL/6 (**A**) or *rd1* mutant retinas (**C**) with an Lbr-specific antibody (yellow). The retina was also counterstained with DNA dye Hoechst 33342 (blue). Boxed regions indicate the areas shown in the insets. (**B**, **D**) Inset regions showing individual color channels, including lamin A for C57BL/6. Arrowheads indicate cone photoreceptors. Scale bars = 10 µm.

3.2. Heterochromatin tethering by Lamin A versus Lbr

While LA+ rods exhibited increased HC tethering, *Lbr* is still expressed when LA upregulates (Fig. 3.2G, H) raising the question of whether LA and Lbr tether heterochromatin differently. To compare LA versus Lbr –dependent HC tethering, wild-type retinas were electroporated at P0 with control, LA, or Lbr expression constructs cloned into the pCIG2 vector, which contains an IRES2-EGFP reporter cassette. Importantly, due to the exclusively embryonic

temporal window for cone generation, cone photoreceptors are never transfected[262,263,264]. Transfected rods were examined at P42, when chromatin inversion is complete (Fig. 3.5A).

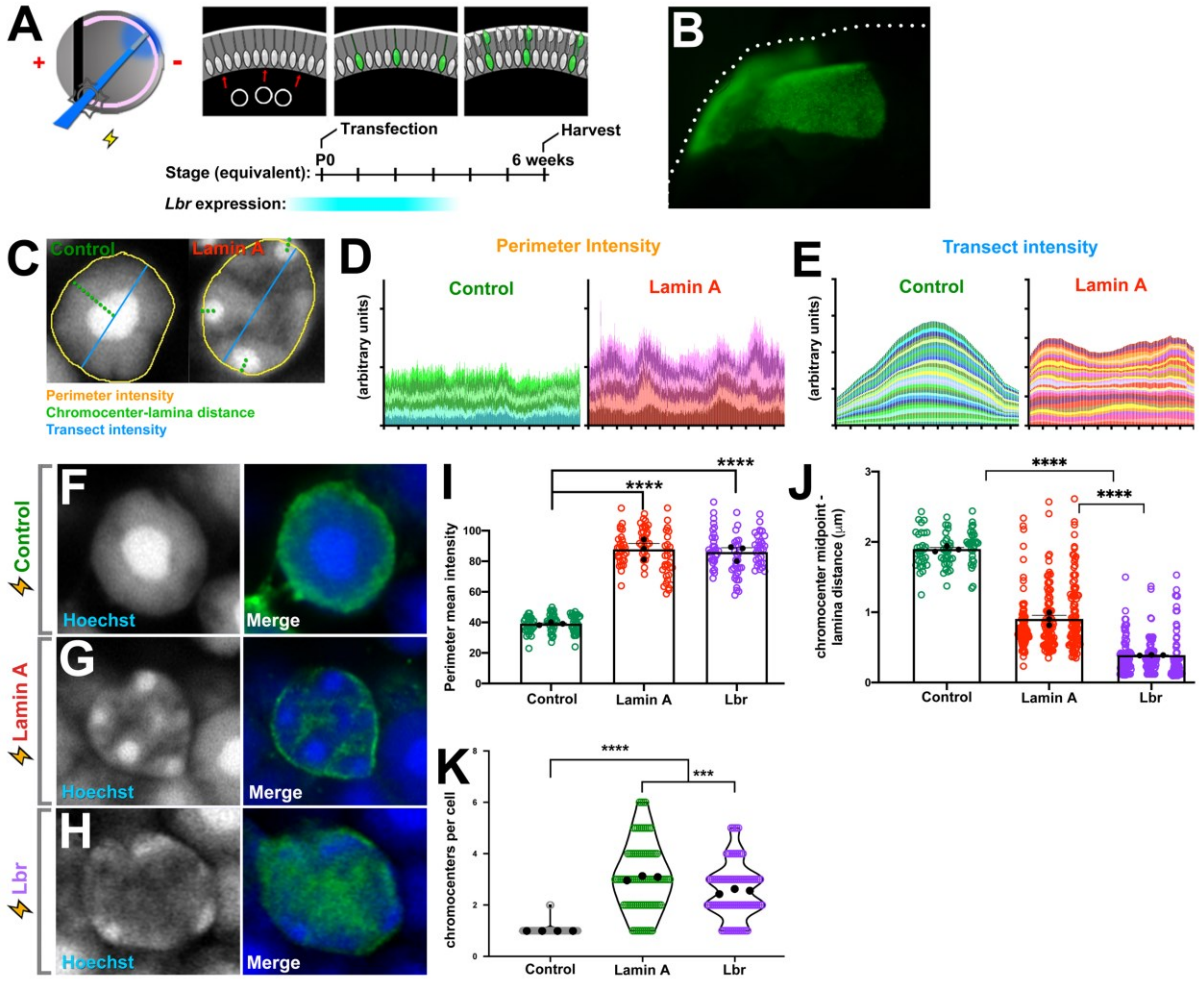

Figure 3.5. Heterochromatin tethering by lamin A versus Lbr. (**A**) In vivo electroporation paradigm. Retinas were subretinally injected with plasmids, electroporated, and harvested after 6 weeks, yielding transfected rod photoreceptors. (**B**) Wholemount epifluorescence image of EGFP expression from a transfected retina. (**C**) Morphometric analysis of transfected nuclei was performed as indicated. (**D**) Densitometry values for chromatin intensity at the nuclear periphery of Control (n=6) or LA -transfected cells (n=6) as indicated, obtained using the "Plot profile" tool in Fiji. Each color represents a different cell. (**E**) Densitometry values for chromatin intensity transecting the center of the nucleus from Control (n=30) or LA -transfected cells (n=30). (F-H) Airyscan confocal imaging of rod photoreceptors transfected with GFP-expressing empty vector control (**F**), LA (**G**), or Lbr (**H**) constructs, and harvested

after 6 weeks. (**I**) Quantitation of chromatin intensity at the nuclear margin measured using the "Freehand Line" tool in Fiji. (**J**) Distance from the chromocenter midpoint to the nuclear periphery. (**K**) Chromocenter number per cell. Black datapoints and error bars are the mean intensity values from each biological replicate (30 cells each; circles) ± SEM. $p < 0.0001$, ANOVA with Tukey's post-hoc test. *** $p < 0.001$, **** $p < 0.0001$, ANOVA with Tukey's post-hoc test.

Using morphometric measures for heterochromatin tethering (Fig. 3.5C-E), we found that both LA and Lbr increased the intensity of DNA at the nuclear periphery equivalently in comparison to control cells (Fig. 3.5F-I; Fig. 3.6). Chromatin inversion progressively reduces the number of chromocenters[208]. In Lbr-transfected cells, the distance between the chromocenter centroid and nuclear lamina was significantly reduced in rods expressing Lbr versus LA (Fig. 3.5J). Moreover, LA increased chromocenter number significantly more than Lbr (Fig. 3.5K). LA and Lbr thus had different effects on nuclear organization. In accordance with these observations, we found no evidence of cross-regulation. Lbr did not upregulate in LA transfections, nor did LA upregulate in Lbr transfections (Fig. 3.7).

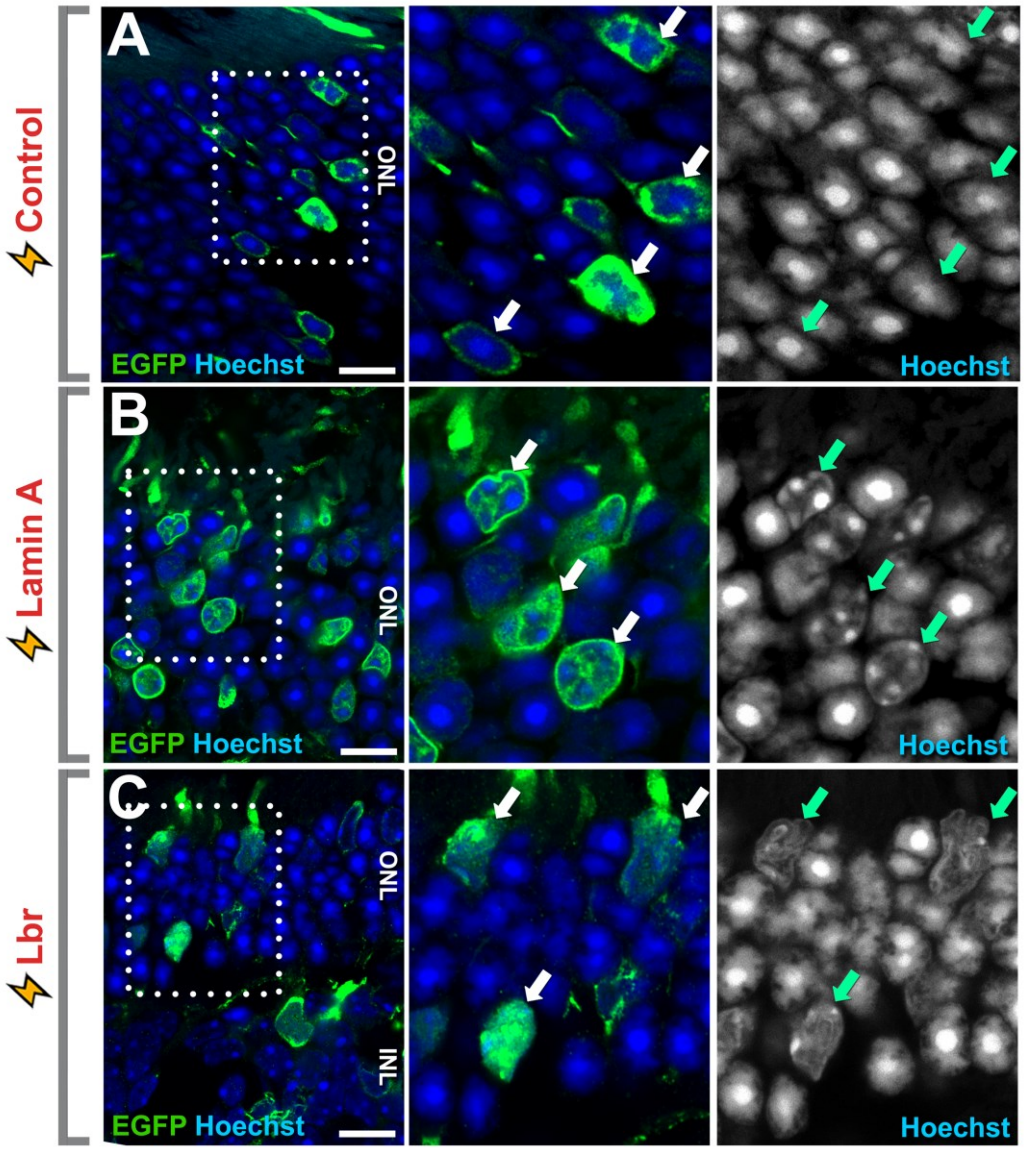

Figure 3.6. Examples of heterochromatin tethering induced by *in vivo* electroporation. (**A**-**C**) Airyscan confocal imaging of retinas transfected with empty vector control (**A**), LA (**B**), or Lbr (**C**) expression constructs, and harvested after 6 weeks. Arrows mark transfected EGFP+ cells Scale bars = 10 µm.

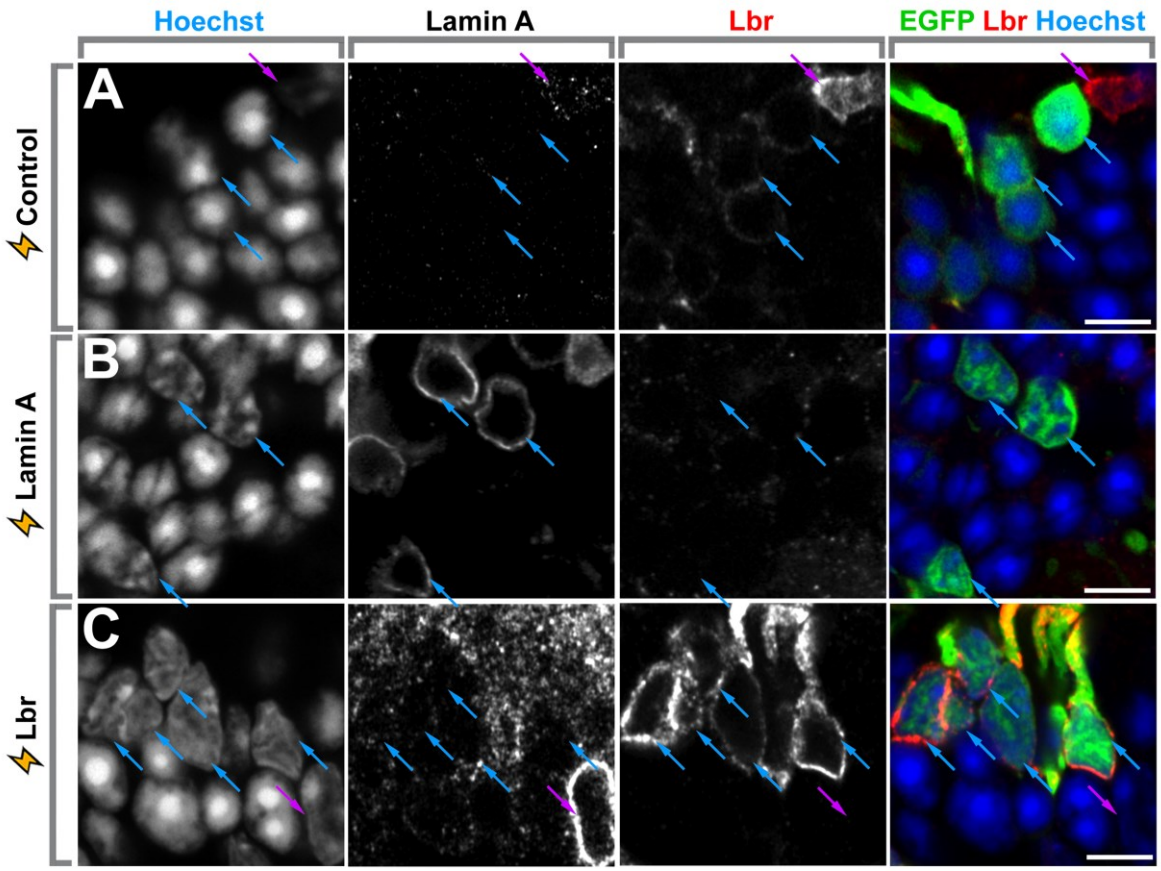

Figure 3.7. Lack of reciprocal upregulation upon lamin A or Lbr misexpression. (**A**-**C**) Airyscan confocal imaging of retinas stained transfected with GFP-expressing empty vector control (**A**), lamin A (**B**), or Lbr (**C**) expression constructs, and harvested after 6 weeks. Retinas were stained for lamin A, Lbr, and Hoechst. Blue arrows mark transfected EGFP+ cells. Magenta arrows indicate cones. Scale bars = 5 μm.

3.3. Heterochromatin tethers have subtle effects on gene expression

To determine how tethering affects gene expression, we misexpressed LA/Lbr in rods using in vivo electroporation. After 8 weeks, we flow-sorted viable EGFP+ cells. As we were only able to obtain a few thousand cells per transfected retina, we opted to perform scRNA-seq using the 10x Genomics Chromium platform. To avoid batch effects, we multiplexed samples using

the Multi-seq barcoding approach. After removing low-quality cells and performing additional filtering (see Methods), we clustered individual cells using Uniform Manifold Approximation and Projection (UMAP; Fig. 3.8A). To annotate cell types in an unsupervised manner, we used scDeepSort[254] trained on a previously published retinal RNA-seq atlas[253]. As expected, most sorted cells in the dataset were rods, but a few bipolars and Müllers were also annotated (Fig. 3.8B).

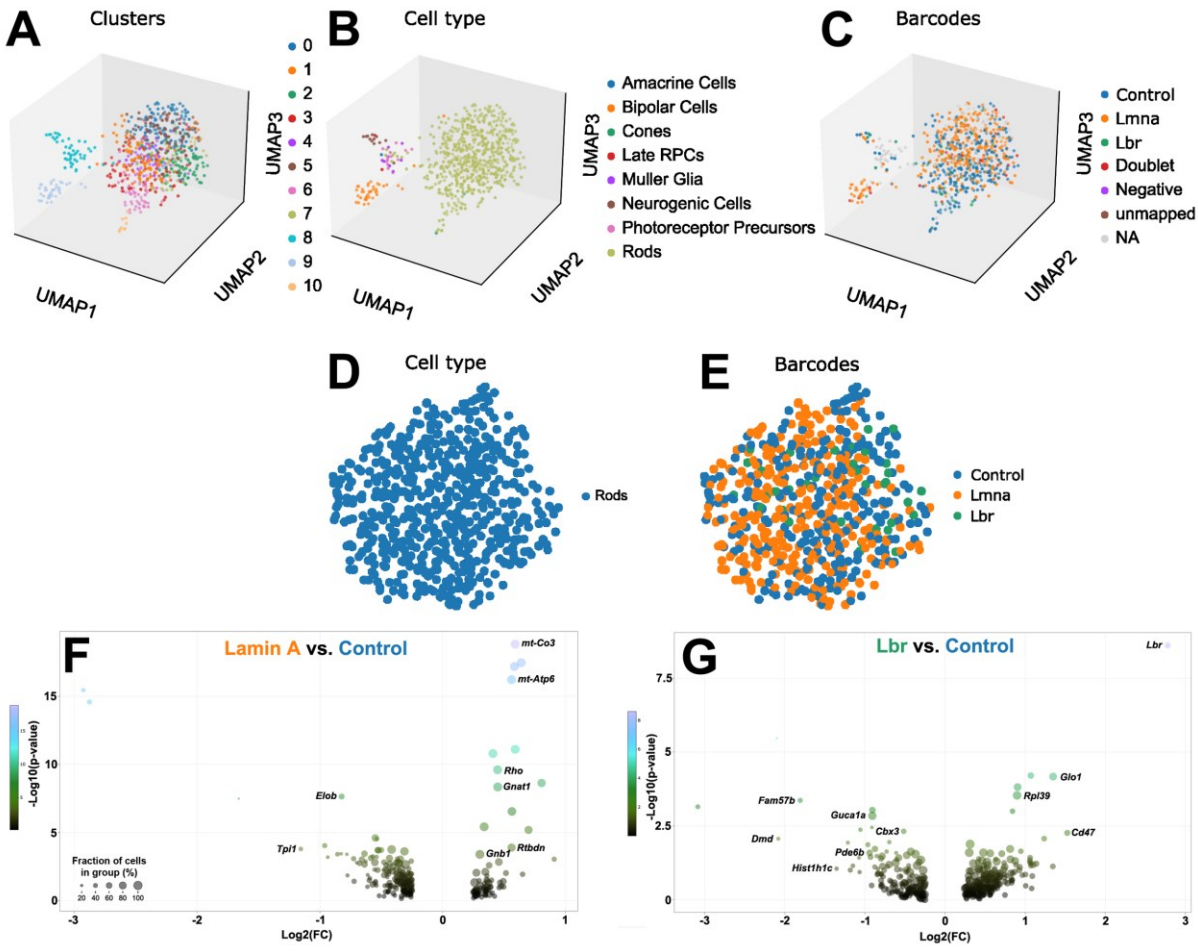

Figure 3.8. Comparison of gene expression in control versus tethered rods. (**A**) UMAP projection of Multi-seq dataset. (**B**) Unsupervised cell-type annotation via scDeepSort trained on a previously published retinal scRNA-seq dataset[253]. (**C**) Demultiplexing of control, lamin A, and Lbr samples. (**D**, **E**) Overlap of Control, lamin A, or Lbr -transfected cells within the

rod cluster. (**F**, **G**) Volcano plots of differential gene expression in annotated rods. (**F**) Lamin A versus control. (**G**) Lbr versus control.

Focusing solely on annotated rods, Control, LA, and Lbr -transfected cells clustered in an overlapping fashion, suggesting little difference between their overall gene expression patterns (Fig. 3.8D, E). Similarly, we found that both LA and Lbr misexpression had relatively modest effects on the expression of individual genes (Fig. 3.8E, F; Table S1). Characteristic photoreceptor genes were significantly elevated in LA-expressing rods (eg. *Rho*, *Gnat1*; Fig. 3.8F), and significantly decreased in Lbr-expressing cells (eg. *Guca1a*, *Pde6b*; Fig. 3.8G). Nonetheless, the overall magnitude of transcriptional changes in tethered rods was generally modest, with only a few genes changing more than 2-fold. Interestingly, *Hist1h1c* and *Cbx3*, which encode key heterochromatic proteins, were significantly downregulated in Lbr-expressing rods (Fig. 3.8G).

3.4. Heterochromatin tethering regulates genome accessibility

Previous studies have reported that rod photoreceptors uniquely exhibit megabase-scale genomic intervals with unusually reduced chromatin accessibility[215]. We reasoned that this unique accessibility signature might be altered by heterochromatin tethering. We therefore performed ATAC-seq on rods transfected with control, LA, or Lbr constructs. To mark rods specifically, we co-transfected the plasmids with a pRho2.2::DsRed reporter[223] (Fig. 3.9A, B). After 8 weeks, rod photoreceptors were sorted using EGFP, DsRed, and Dapi to mark viability.

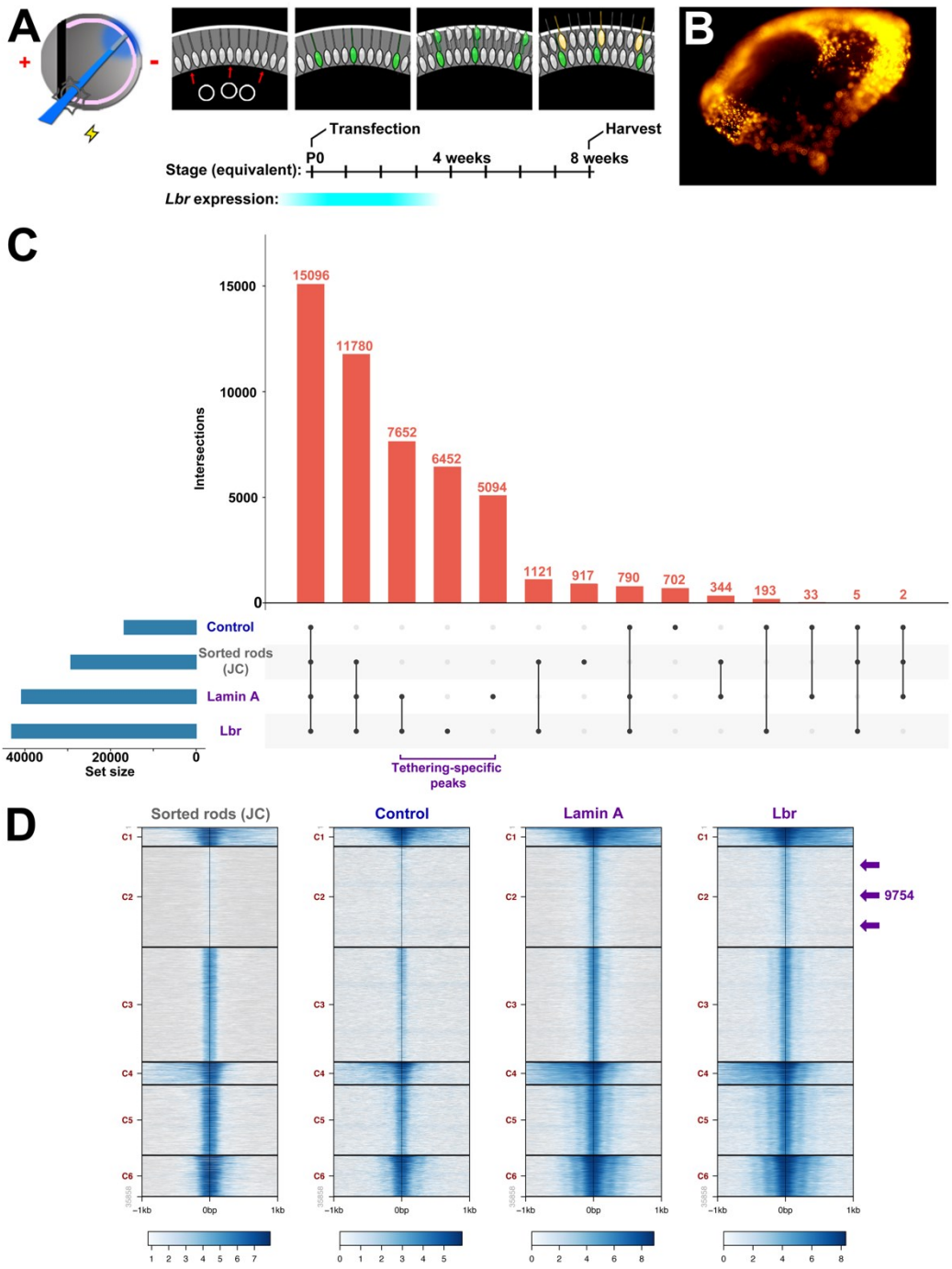

Figure 3.9. Heterochromatin tethering promotes chromatin accessibility. (**A**) *In vivo* electroporation paradigm. Retinas were subretinally injected with expression plasmids, including the rod-specific pRho2.2-DsRed reporter. Electroporated retinas were harvested after 8 weeks, yielding DsRed+ rod photoreceptors. (**B**) Wholemount epifluorescence image of EGFP and DsRed expression from a transfected retina. (**C**) Upset plot of of ATAC-seq peak

intersections from sorted rods transfected with control, LA, or Lbr expression constructs compared against previously published data from the Joe Corbo lab (JC)[215] as indicated. (**D**) Alignment of ATAC-seq data from sorted rods transfected with control, LA, or Lbr expression constructs compared against previously published data[215] as indicated. Plots are centered on peak summits from LA transfected rods. Arrows indicate the tethering-specific cluster C2 peaks.

Next, we processed the ATAC-seq datasets in order to call peaks. We first compared our datasets against previously published ATAC-seq data from sorted rods[215]. In general, we observed that all of our datasets exhibited comparable signal at the rod-specific peak loci previously identified by Hughes et al.[215] (Fig. 3.10). We also observed a lack of signal at the promoters of several marker genes for non-rod cell types, such as cones, bipolars, and Müller glia (Fig. 3.11).

In accordance with the hypothesis that inverted nuclear architecture restricts accessibility[215], we observed an increase in the number of peaks in tethered rods (Fig. 3.9C). We compared LA or Lbr -tethered rod ATAC-seq data versus normal rod datasets using two approaches. First, we examined the overlap between peaks. We found that more than half of the rod-specific peaks identified by Hughes et al. were shared by our ATAC-seq datasets (Fig. 3.9C). The control datasets together contained less than 2000 peaks that were absent from tethered rods. By contrast, LA and Lbr datasets exhibited 5094 and 6452 unique peaks, respectively, and shared an additional 7652 peaks – all of which were absent from the control datasets (Fig. 3.9C).

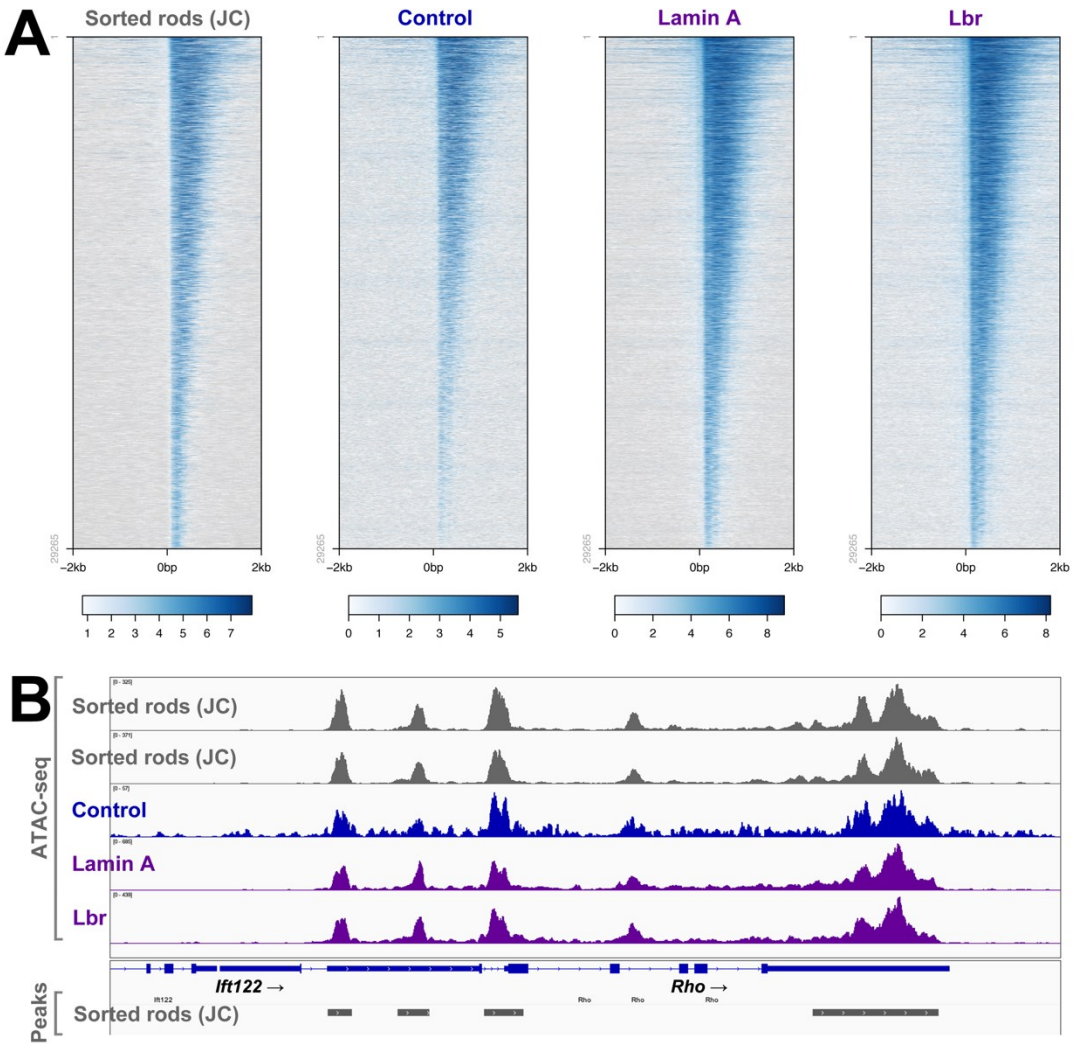

Figure 3.10. Comparison of control and tethered rod ATAC-seq datasets versus previously published data. (**A**) Alignment of ATAC-seq data from sorted rods transfected with control, lamin A, or Lbr expression constructs compared against previously published data from the Joe Corbo lab (JC)[215] as indicated. Peaks are centered on rod-specific peaks (narrowpeaks) published by Hughes et al.[215] (**B**) Visualization of previously published ATAC-seq tracks and called peaks previously generated by Hughes et al. (JC), in comparison with ATAC-seq tracks generated from control, lamin A, or Lbr -transfected rods at the *Rhodopsin* locus. Tracks are plotted on different scales.

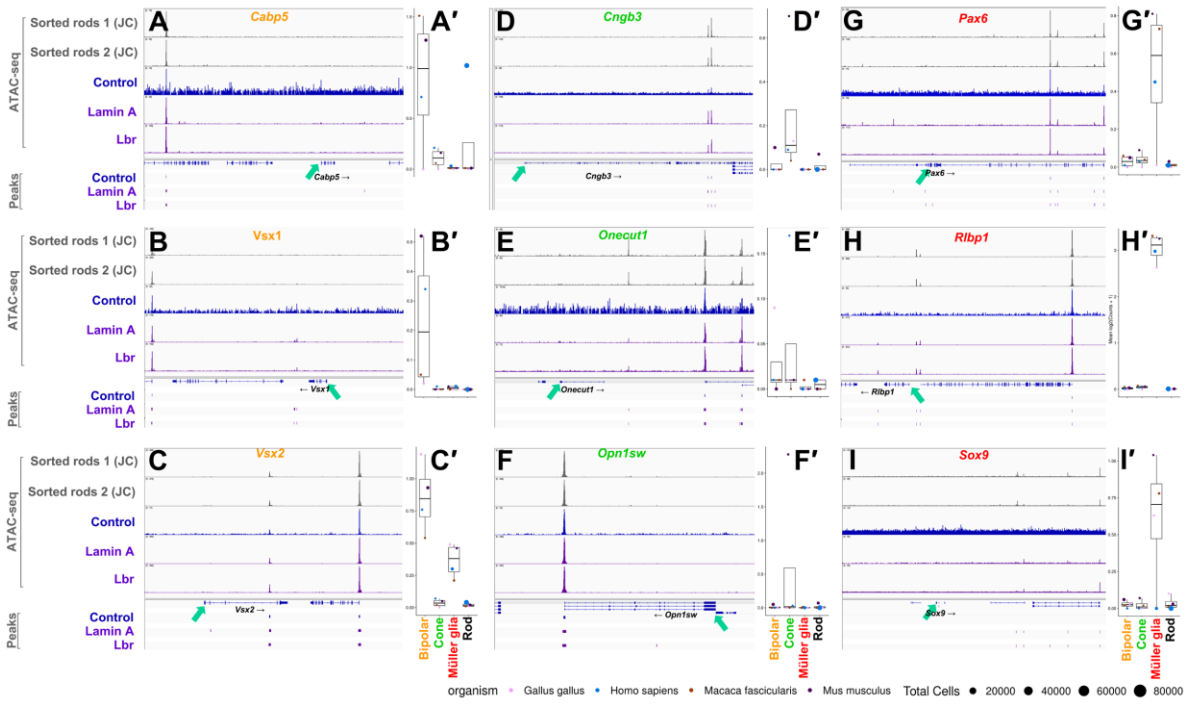

Figure 3.11. Lack of accessibility at selected cell-type-specific marker genes. (**A-I**) Visualization of previously published ATAC-seq tracks previously generated by Hughes et al. (JC)[232], in comparison with ATAC-seq tracks and called peaks generated from control, LA, or Lbr -transfected rods at bipolar (**A-C**), cone (**D-F**), or Müller glia (**G-I**) marker genes. ATAC-seq tracks were plotted on different scales. Arrows indicate the transcription start sites for each marker gene. (**A′-I′**) Comparison of marker gene expression in annotated bipolars, cones, Müller glia, and rods generated using the *Plae* scRNA-seq resource[262].

Secondly, we also plotted the data centered on the 35 858 LA peaks. This analysis revealed a great deal of resemblance between the accessibility signatures of LA+ and Lbr+ rods. We performed K-means clustering which allowed us to separate 9754 peaks that had markedly elevated signal in LA/Lbr tethered rods in comparison to controls (Fig. 3.9D; cluster C2; arrows). Peak-to-gene annotation revealed that only ~10% of these novel peaks were found in gene-proximal regions (Fig. 3.12A). Taken together, these analyses indicate that rods with tethered HC gain thousands of additional peaks – mainly in distal intergenic regions.

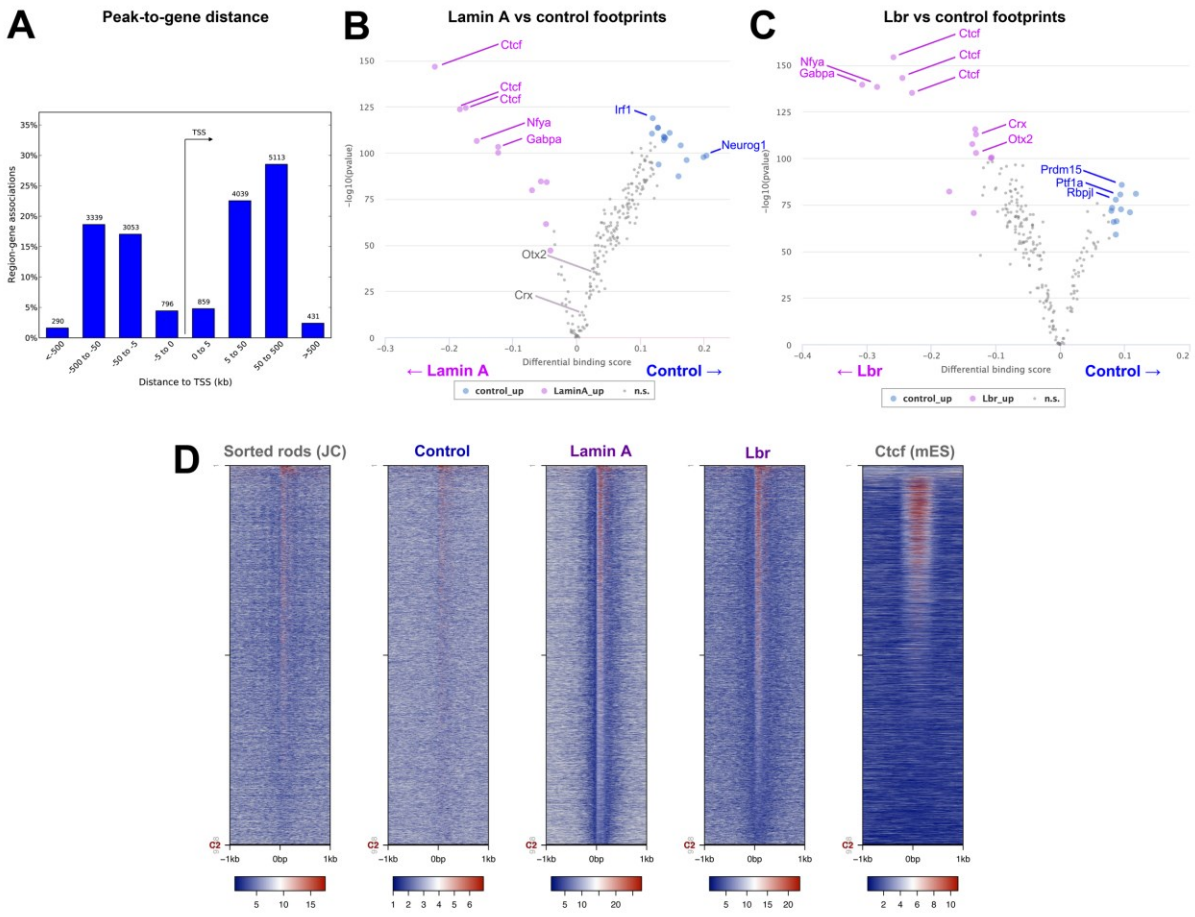

Figure 3.12. Characterizing novel tethering-specific accessible sites. (**A**) Location of tethering-specific cluster C2 peaks in relation to the transcription start site (TSS) of adjacent genes. (**B**, **C**) Motif enrichment in ATAC-seq footprints comparing LA versus control (**B**) or Lbr versus control (**C**) ATAC-seq datasets. (**D**) Alignment of ATAC-seq data from sorted rods transfected with control, LA, or Lbr expression constructs compared against previously published data from the Joe Corbo lab (JC)[215], and Ctcf ChIP-seq data from embryonic stem cells generated by the Encode Consortium. Plots are centered on tethering-specific cluster C2 peak summits (see Fig. 3.8D).

We inspected newly accessible peaks, but they did not appear to overlap with any specific genomic feature. We therefore opted to perform footprinting analysis using the TOBIAS algorithm[244]. TOBIAS examines ATAC-seq peaks to identify regions occluded by proteins,

and to match these 'footprints' to transcription factor motifs. We selected 220 transcription factor motifs from the TRANSFAC database. Using this approach, we found that Ctcf footprints were the most overrepresented motifs in both LA and Lbr datasets (Fig. 3.12B, C). Focusing on novel tethering-specific cluster C2 peaks, we next visualized Ctcf ChIP-seq datasets made from embryonic stem cells by the Bing Ren lab[235]. We found that cluster C2 loci correlated with considerable Ctcf signal (Fig. 3.12D). These data suggest that many of the peaks induced by HC tethering are genuine regulatory elements that are normally decommissioned in rods. Perhaps accordingly, we found that cluster C2 loci exhibited little enrichment for chromatin marks from published rod-specific datasets[34,217] (Fig. 3.13).

Hughes et al. had also previously hypothesized that HC tethering might explain the increased genomic accessibility of cones[215]. However, we found that in terms of genome accessibility, tethered rods are more similar to control rods than to cones – perhaps not surprisingly (Fig. 3.14A). Inspection of cone-specific peaks revealed that most remained inaccessible in tethered rods (Fig. 3.14B; see also Fig. 3.11), except at the *Lmna* locus itself (Fig. 3.14C), which was previously noted to be accessible in cones but not rods[208]. Some loci might therefore take on cone-like accessibility signatures in response to tethering.

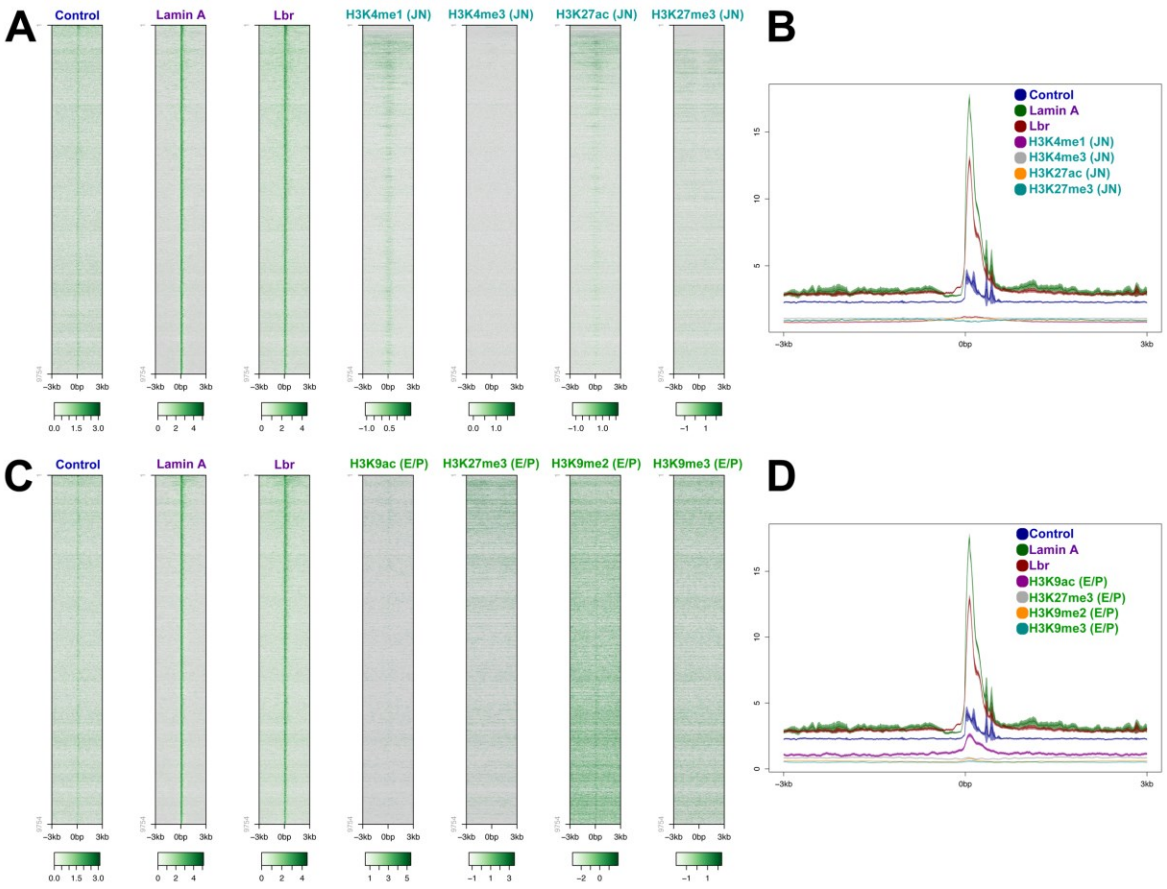

Figure 3.13. Comparison of control and tethered rod ATAC-seq datasets versus previously published rod-specific ChIP-seq and cut&run-seq data. (**A**, **B**) Alignment of ATAC-seq data from sorted rods transfected with GFP control, lamin A, or Lbr expression constructs compared against previously published ChIP-seq data from the Jeremy Nathans lab (JN)[217] as indicated. Plots are centered on tethering-specific cluster C2 peak summits (see Fig. 3.8D). (**C**, **D**) Alignment of ATAC-seq data from sorted rods transfected with GFP control, lamin A, or Lbr expression constructs compared against previously published cut&run-seq data from the Epstein and Poleshko laboratories (E/P)[34] as indicated. Plots are centered on tethering-specific cluster C2 peak summits (see Fig. 3.8D). Tracks are plotted on different scales.

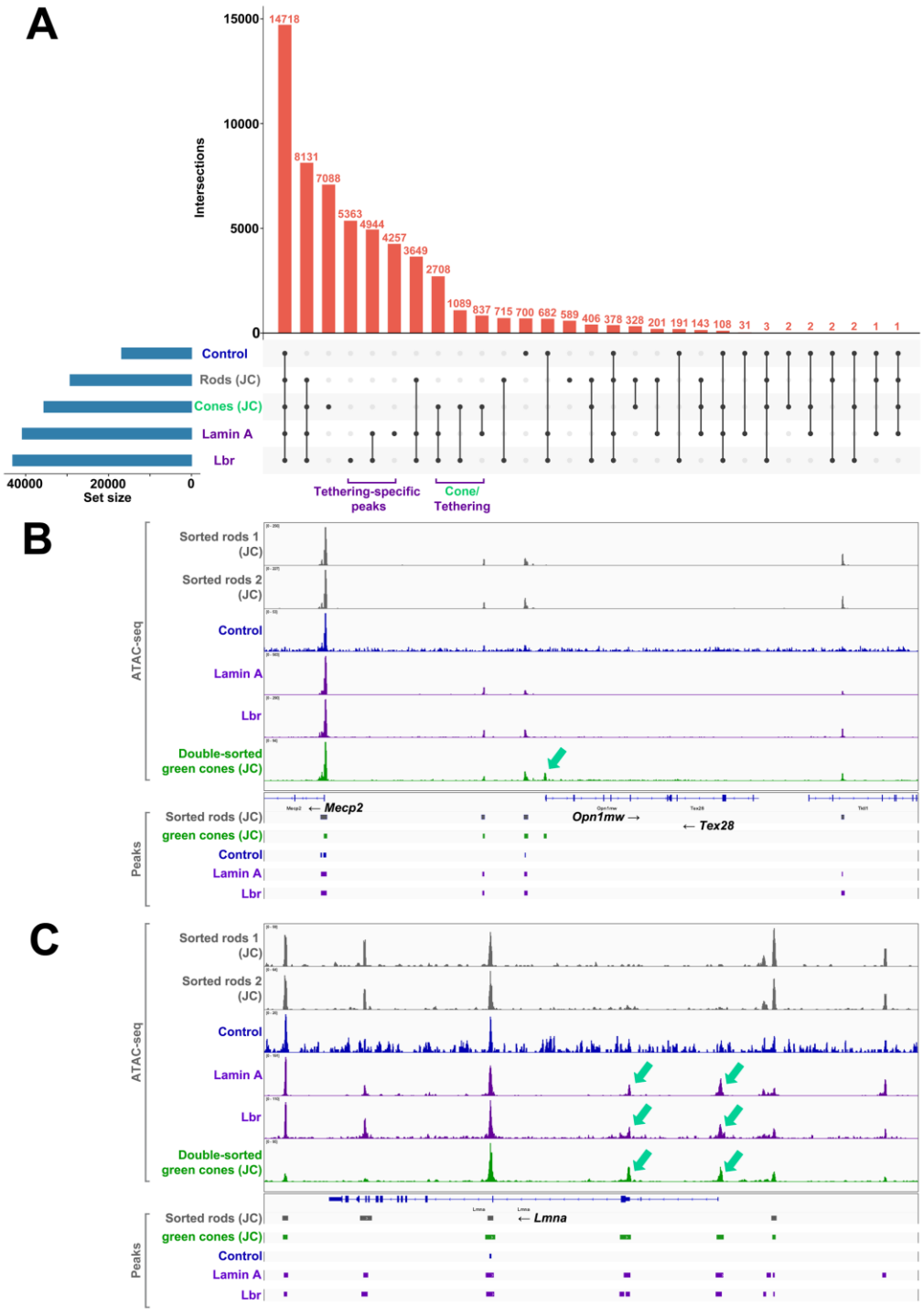

Figure 3.14. Comparison of ATAC-seq data from control rods, tethered rods, and green cones. (**A**) Upset plot of of ATAC-seq peak intersections from sorted rods transfected with control, LA, or Lbr expression constructs compared against previously published sorted rod and (double-sorted) green cone data from the Joe Corbo lab (JC)[215] as indicated. (**B**, **C**)

Comparison of previously published ATAC-seq tracks and called peaks versus ATAC-seq tracks generated from control, LA, or Lbr -transfected rods as indicated, visualizing the cone-specific genes *Opn1mw* (green cone opsin; **B**) or *Lmna* (**C**). ATAC-seq tracks are plotted on different scales. Arrows indicate peaks present in cones and/or tethered rods, but not control rods. Tracks are plotted on different scales.

Finally, to address the hypothesis that heterochromatin tethering might affect the accessibility of B compartment topologically associating domains (TADs), we examined rod-specific Hi-C experiments[23]. Surprisingly, we found that almost all of the novel cluster C2 peaks were present in the euchromatic A compartment (Fig. 3.15A). We did observe a few notable exceptions, where B compartment accessibility was altered, including at the *Myc* gene (Fig. 3.15B), which was previously reported to be localized within a large inaccessible interval[215], as well as across a TAD that contains the chemokines *Ccl1*, *Ccl2*, *Ccl7*, *Ccl8*, *Ccl11*, and *Ccl12* (Fig. 3.15C). Nonetheless, effects on B compartment accessibility were the exception.

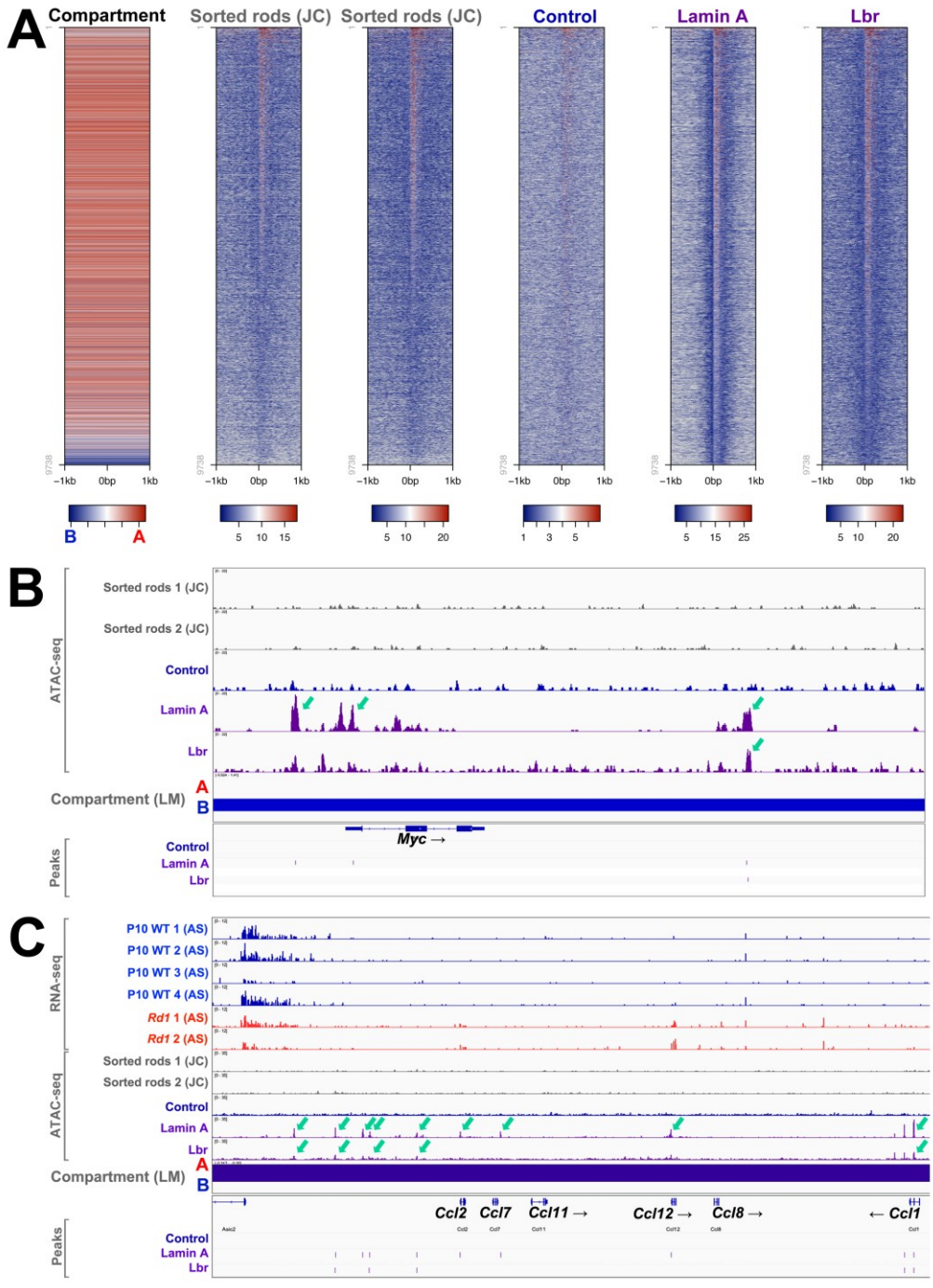

Figure 3.15. Alteration of genome accessibility in the A versus B -compartments. (**A**) Alignment of ATAC-seq data from sorted rods transfected with control, LA, or Lbr expression constructs compared against previously published data from the Joe Corbo lab (JC)[215], and compartment data from Falk et al.[23] as indicated. Peaks are centered on tethering-specific cluster C2 peak summits (see Fig. 3.8D). (**B**, **C**) Control vs. *rd1* RNA-seq from the Anand

Swaroop lab (AS)[245], ATAC-seq tracks and called peaks from the Joe Corbo lab (JC)[215], and compartment data from the Leonid Mirny lab (LM)[23], compared against ATAC-seq tracks generated from control, LA, or Lbr -transfected rods. B-compartment TADs included the *Myc* (**B**) and *Ccl2*, *Ccl7*, *Ccl11*, *Ccl12*, *Ccl8*, and *Ccl1* (**C**) loci. RNA-seq and ATAC-seq tracks were respectively group-autoscaled. Arrows indicate peaks present specifically in tethered rods.

3.5. Heterochromatin tethering promotes accessibility at a subset of stress-responsive genes

To understand how heterochromatin tethering might relate to function, we performed GO terms analysis on the tethering-specific cluster C2 peaks using Panther and ReViGO[238,239]. Since 9754 peaks were obtained in the cluster, peak-to-gene annotation would retrieve a large fraction of all genes. To reduce false discovery, we restricted our analysis to gene-proximal peaks located from 5 kb upstream to 1 kb downstream of a given gene. This reduced the overall peak count to only ~1400 peaks, corresponding to 1224 genes. Significantly enriched GO terms related to the stress response, including "immune system process", and "inflammatory response" (Fig. 3.16A; Table S2).

To determine whether the same group of stress-responsive genes might upregulate in *rd1* rods, we intersected the 1224 tethering-specific cluster C2 genes with the RNA-seq data generated by Jiang et al., but observed no systematic change in the expression of these genes (Fig. 3.16B). Moreover, we also examined the viability of transfected cells using flow cytometry, but did not observe any elevation in LA or Lbr expressing rods (Fig. 3.16C), nor did stress-responsive transcripts upregulate in our Multi-seq dataset (Fig. 3.16D, E). Nonetheless, a few cluster C2 genes exhibited notable increases in accessibility, including the putative tumor suppressor

Tusc1 (Fig. 3.16F). Novel peaks were also seen at the *Ccl3* and *Ccl4* chemokine genes (Fig. 3.17A), as well as the interferon activated gene *Ifi204* and the *Cd68* surface marker (Fig. 3.17B, C) – both of which were shown to become acutely accessible in a light damage model of retinal degeneration[265].

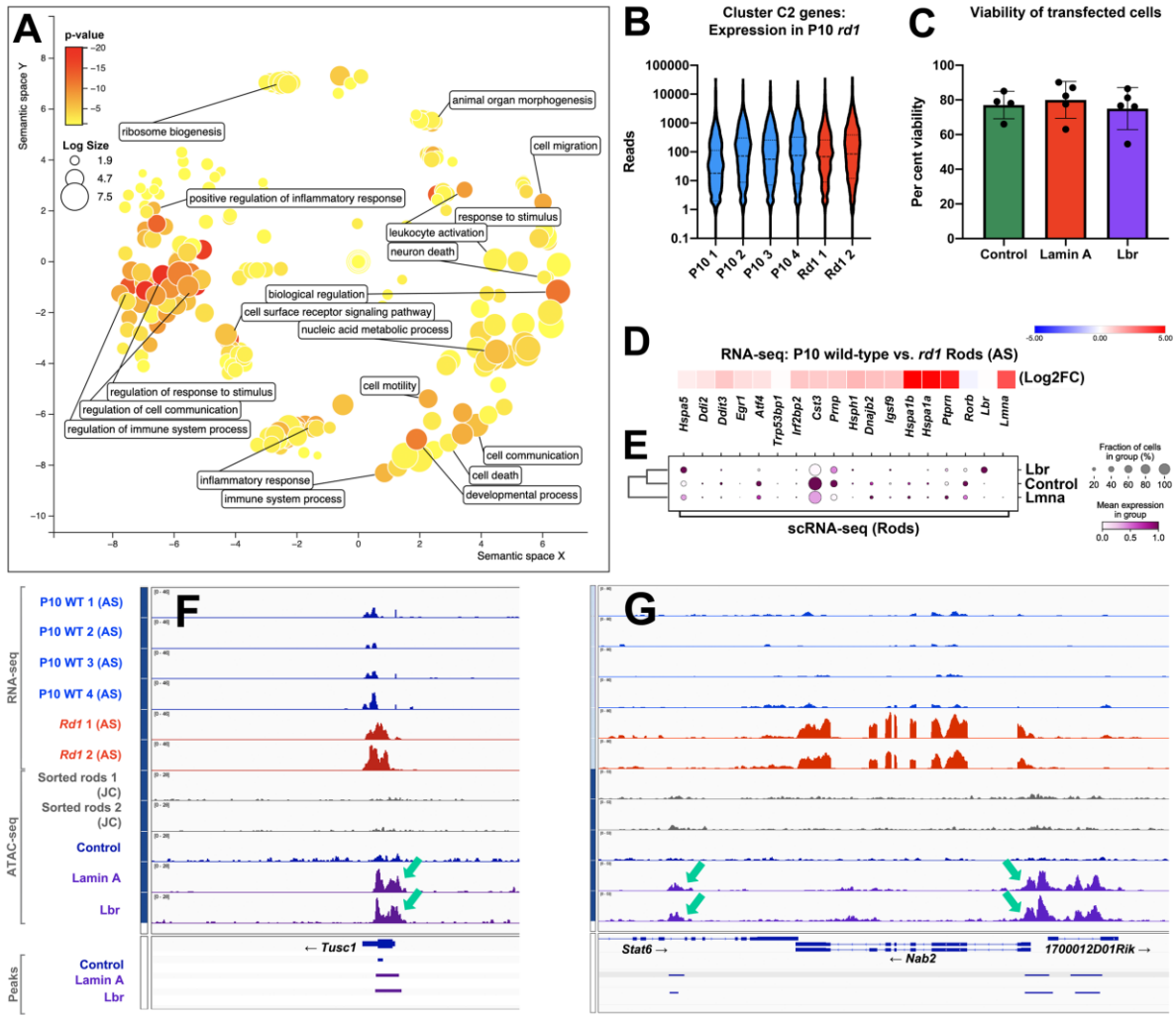

Figure 3.16. Heterochromatin tethering promotes accessibility at stress responsive genes. (**A**) GO terms analysis of tethering-specific cluster C2 genes (see Fig. 3.8D) via PantherDB and ReViGO. Peak-to-gene annotation was restricted to gene proximal peaks as described in the text. (**B**) Violin plot of mRNA expression for genes associated with cluster C2 peaks from P10 control or *rd1* sorted rods. RNA-seq data were generated by the Swaroop lab[245]. (**C**) Cell viability data from transfected (GFP/DsRed+) cells harvested after 8 weeks, based on Dapi

exclusion. (**D**, **E**) Expression changes for selected stress-responsive genes, comparing RNA-seq data from control versus *rd1* sorted rods from the Anand Swaroop lab (AS)[245] (**D**) versus scRNA-seq data from rods transfected with control, lamin A, or Lbr plasmids (**E**). (**F**, **G**) Control vs. *rd1* RNA-seq, and ATAC-seq tracks and called peaks from Hughes et al. (JC)[215], compared against ATAC-seq tracks generated from control, LA, or Lbr -transfected rods at the *Tusc1* (**F**) and *Nab2* (**G**) loci. RNA-seq and ATAC-seq tracks were respectively group-autoscaled. Arrows indicate peaks present specifically in tethered rods, but not control rods.

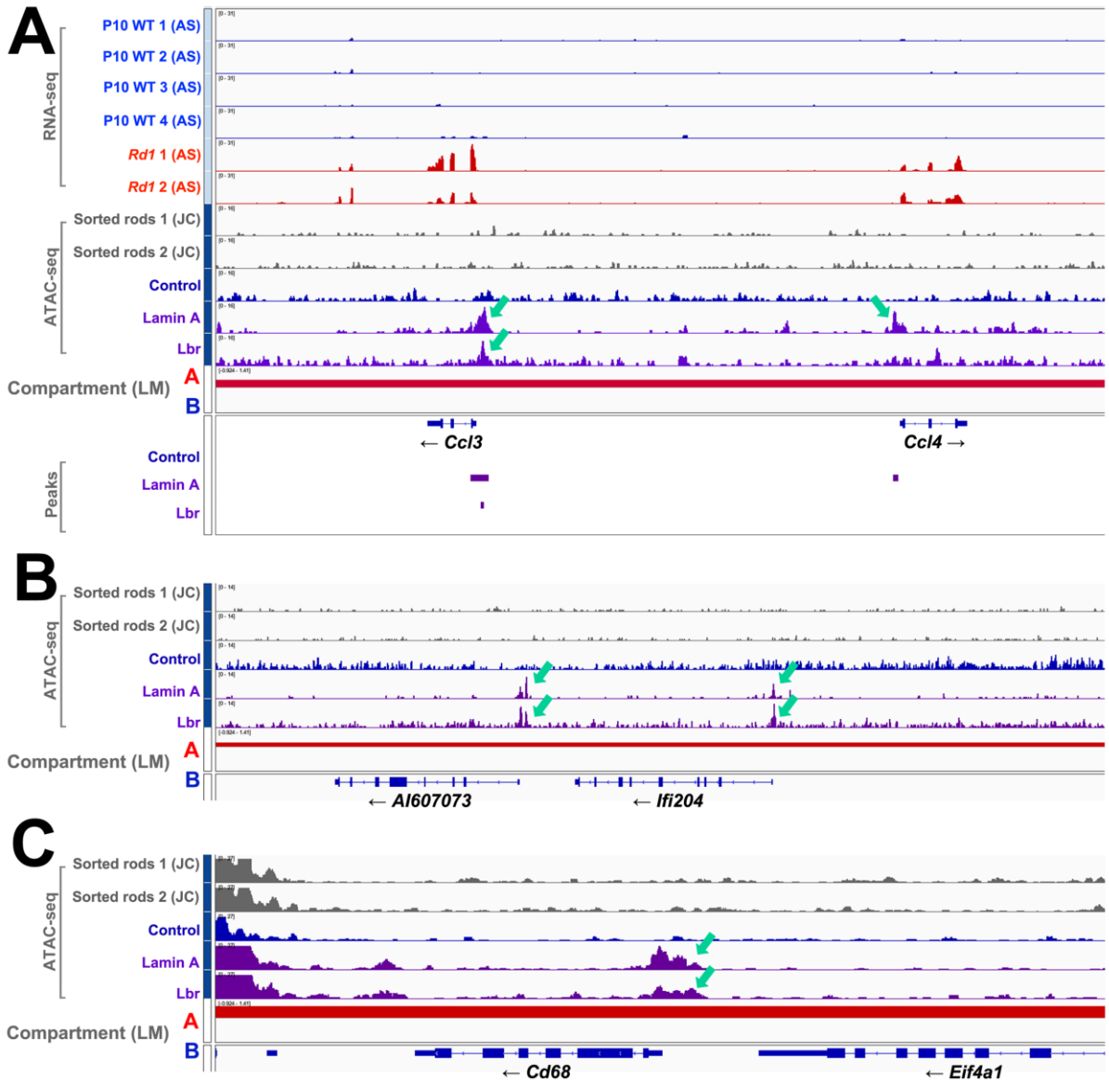

Figure 3.17. Heterochromatin tethering promotes accessibility at a subset of degeneration-associated genes. (**A**-**C**) Control vs. *rd1* RNA-seq from the Anand Swaroop lab (AS)[245], ATAC-seq tracks and called peaks from the Joe Corbo lab (JC)[215], and compartment data from the Leonid Mirny lab (LM)[23], compared against ATAC-seq tracks generated from control, LA, or Lbr -transfected rods as indicated. RNA-seq and ATAC-seq tracks were respectively group-autoscaled. Arrows indicate peaks present specifically in tethered rods, but not control rods.

We also observed novel tethering-specific peaks at the immediate early gene *Nab2* (Fig. 3.16G). Interestingly, *Nab2* has been shown to upregulate during cone degeneration[266]. Taken together, these data suggest that heterochromatin tethering might 'poise' regulatory elements to facilitate the stress response, but that additional steps are necessary for full gene activation.

Discussion

The rod photoreceptors of nocturnal animals are perhaps the only eukaryotic cells that normally function without heterochromatin tethering. Here, we report that LA upregulates in the *rd1* model of retinitis pigmentosa. Since LA/LC upregulates in two other degenerative models[66,219], and since *Pde6b* does not directly regulate gene expression, we conclude that *Lmna* upregulation is likely a general response to degeneration.

How does LA upregulation affect the photoreceptor genome? Previous studies suggested that the absence of tethering leads to a strikingly 'closed' accessibility signature[215,212]. Perhaps counterintuitively, our data suggest that tethering the heterochromatic B-compartment at the nuclear periphery mainly affects accessibility within the euchromatic A-compartment. Acting like the fingers in a "cat's cradle", heterochromatin tethering might be important for disentangling and segregating B compartment TADs away from the A compartment (Fig.

3.18). Alternatively, tethering might provide tensile force to chromosomes that could facilitate gene expression. *LMNA* mutations have accordingly been shown to have extensive effects on genome accessibility in other contexts[168].

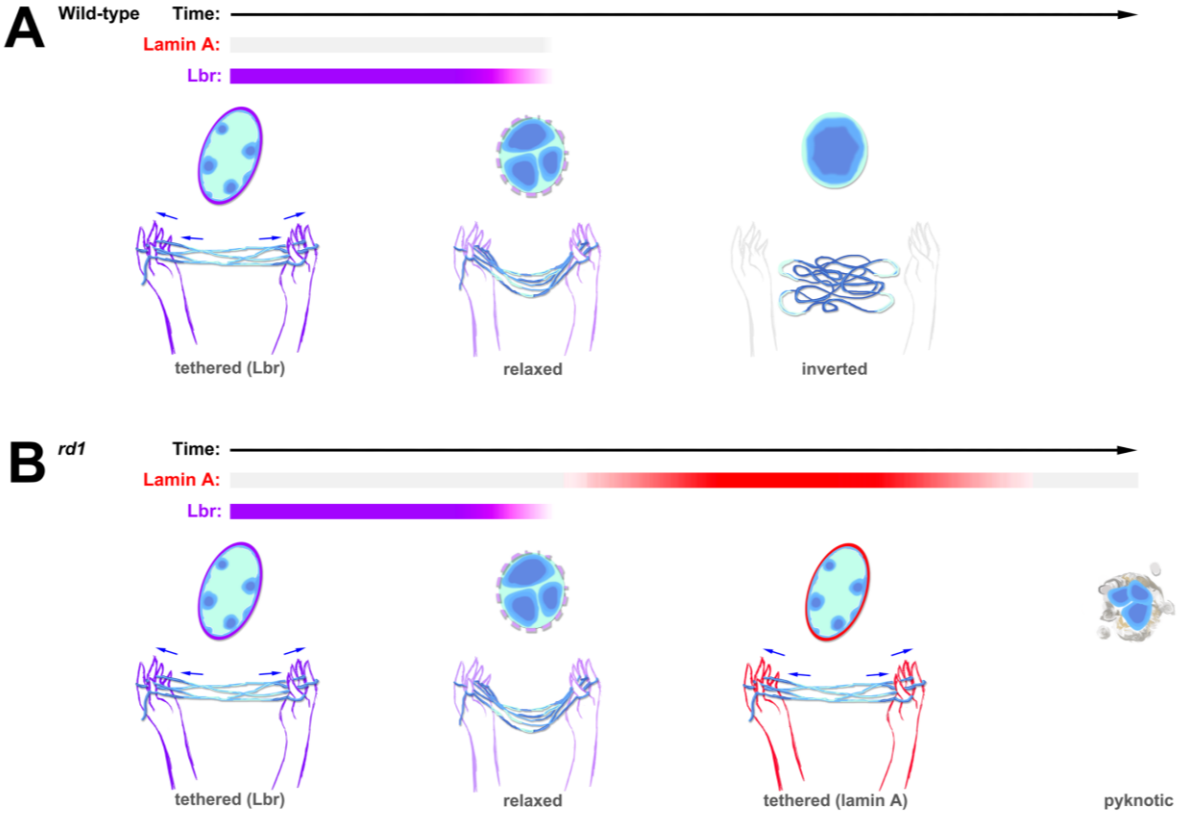

Figure 3.18. Cat's cradle model for tethering-dependent effects on genome accessibility. (**A**) During the differentiation of wild-type rods, the tethering of heterochromatin (dark blue) by Lbr (purple) stretches the chromosomes, promoting accessibility in the A-compartment (cyan). Over time, Lbr expression is downregulated leading to chromatin relaxation, and finally chromatin inversion. As the chromatin relaxes, accessibility decreases. (**B**) During the differentiation of *rd1* rods, lamin A (red) upregulates at the onset of tissue damage. The prolongation of tethering promotes accessibility at genomic regions that would normally be decommissioned. *Rd1* rods downregulate lamin A prior to cell death.

Based on genome modeling, the Solovei and Mirny labs predicted that the introduction of heterochromatin tethering in fully inverted rods would fail to restore conventional architecture[23]. Results from SCA7 and Casz1 mutant mice, in which LA/LC upregulates in mature rods agree with this prediction[23,219]. By contrast, the upregulation of LA in *rd1* rods occurs prior to full inversion. Nonetheless, since tethering mainly induced novel peaks within the A-compartment, we predict that LA upregulation might have similar effects on genome accessibility during the degeneration of mature rods with fully inverted architecture.

Heterochromatin tethers are permissive—but not instructive—for gene expression

We found that LA/Lbr both increased genome accessibility similarly—mainly at distal intergenic regions. Focusing on cluster C2 peaks, we found that Ctcf footprints were increased, suggesting that these loci might be bona fide regulatory elements that are normally decommissioned in inverted rods. Accordingly, we found that many of these loci exhibited Ctcf occupancy in murine ES cells. While the accessibility signatures of LA/Lbr were similar, they differed in footprint enrichment profiles and elicited subtle but divergent changes in gene expression, in agreement with previous research[66]. Moreover, morphometric analysis of HC tethering revealed that LA/Lbr had different effects on chromocenters.

In the literature, LA/Lbr are thought to interact with LADs that are characterized by localization within the B-compartment, and enrichment for heterochromatic marks. As our transfection paradigm only permitted the purification of small numbers of cells, we focused on methods such as scRNA-seq and ATAC-seq. However, ATAC-seq would be unlikely to identify elements directly bound by LA/Lbr. In the future, it will be important to use a battery

of ‘omics’ and microscopic approaches in order to determine how the genome interacts with LA/Lbr, and to perform more extensive time coursing and replication.

One alternative possibility is that the increased accessibility observed in tethered rod datasets might arise if samples were contaminated with non-rod cells. However, we disfavor this interpretation. First, in our ATAC-seq experiments, we found that cell-type-specific marker genes exhibited equivalent accessibility when compared to control rod datasets. Second, most of the observed novel peaks were distal to genes. Third, even for gene-proximal peaks, GO terms were mainly associated with the stress response rather than cell fate, suggesting that changes in cell composition are unlikely to account for the novel peaks.

Another alternative interpretation is that the observed accessibility signature might be a by-product of toxicity introduced by construct overexpression. Again, we disfavor this scenario. First, while LA/LC overexpression has been associated with toxicity, these effects are often linked to mitotic catastrophe or nuclear rupture, which are mitigated in non-motile post-mitotic rods. We harvested rods at least 6 weeks after transfection, and observed no effect on cell viability, suggesting that LA was well-tolerated over the long-term. Second, similar changes in accessibility were observed when rods were transfected with Lbr, which has been shown to be well-tolerated in transgenic mice[209,66]. Third, LA/Lbr are both expressed in the rods of various vertebrates[66].

Lamin A reorganizes the nucleus during degeneration

ATAC-seq has been recently used to characterize degenerating retinas in age-related macular degeneration and murine light damage models, revealing a marked decrease in genome accessibility[266,267]. Examination of RNA-seq data from the light damage model revealed that

Lmna was similarly upregulated by ~10–20-fold—both at 6 h and one day post-injury, but not at 3 days[266]. While the reported decrease in genomic accessibility thus conflicts with our observations, the ATAC-seq data from the above studies were generated using whole retinas, whereas we studied sorted rods. Moreover, we note that several genes that were reported to become accessible upon light damage, including Ccl4, Ifi204, and Cd68, similarly became accessible upon heterochromatin tethering via LA/Lbr (Fig. 3.17). Luu et al. also reported that light damage increased accessibility at distal intergenic regions, in accordance with our observations.

Elsewhere in the CNS, changes in nuclear lamins have previously been linked to neurodegeneration. For example, alterations in the expression and integrity of B-type lamins have been documented in tauopathies and Alzheimer's disease[268,176]. A potential linkage between LA and photoreceptor degeneration nonetheless seemed unlikely, given that the expression of the LA splice variant is usually suppressed in neurons[99], and has been repeatedly shown to be absent in rods[66,215,219,216]. However, LA was recently found to upregulate in hippocampal neurons in Alzheimer's disease[269]. Indeed, *Lmna* upregulation was recently linked to tissue damage in a variety of other organs[270], although the responsible regulatory mechanisms have not yet been defined.

What might be the purpose of upregulating LA in response to pathology? Tethering heterochromatin via LA/Lbr transfection appears to 'poise' the regulatory elements of stress-responsive genes. However, the limited effect on transcription suggests that LA upregulation may serve additional purposes. One possibility is that heterochromatin tethering may be important for facilitating DNA repair. Indeed, previous studies have shown that DNA repair is inefficient in inverted rod photoreceptors, and this inefficiency is ameliorated via transgenic

misexpression of Lbr[110,111]. Given the well-documented linkage between LA/LC and DNA repair[112], it would be interesting to test whether LA upregulation improves the efficiency of DNA repair even further.

Appendix

Nab2 stress responsive protein expression in Lamin A+ rods

To help validate the ATAC-seq data generated using sorted rods (Chapter 3), we opted to look for the expression of selected genes that exhibit increased promoter accessibility. Nab2 is one of the highly upregulated immediate-early stress responsive proteins in *rd1* rods, and has a highly accessible genomic region in LA/Lbr expressing rods (Figure 3.16G). It has also been shown to upregulate in degenerating cones[267]. Accordingly, in our unpublished data, we found a distinct nuclear Nab2 protein expression in *rd1* LA expressing rods and transfected LA rods (Fig. S1B, D) versus control-tranfected nuclei where Nab2 is limited to the NL (Fig. S1A, C).

Although our scRNA-seq data did not reveal elevated *Nab2* mRNA expression in LA expressing rods, these immunohistochemical data might provide validation for the increased accessibility observed in LA expression rods in the ATAC-seq dataset.

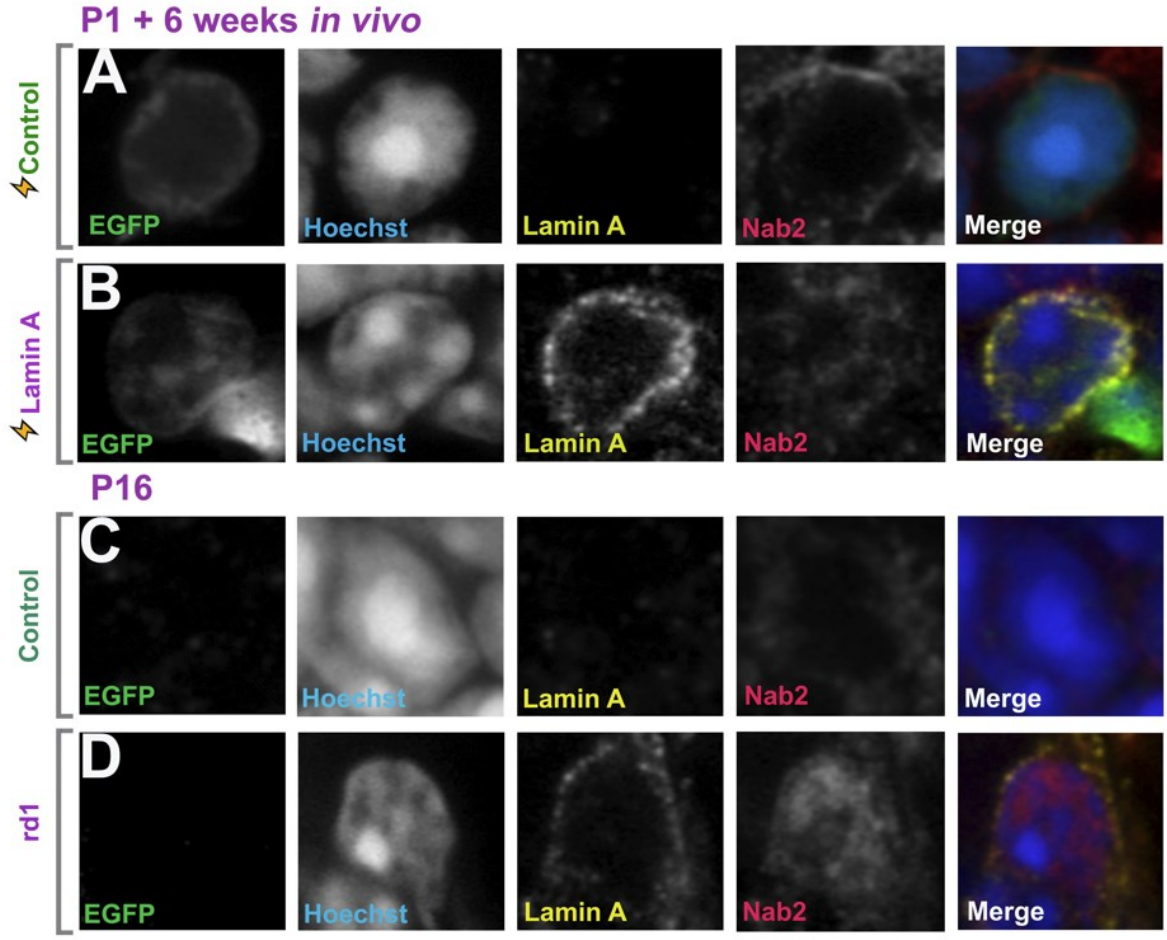

Figure S1. Nuclear Nab2 expression in lamin A expressing rods. Airyscan confocal imaging of transfected rod photoreceptors with EGFP-expressing empty vector Control (**A**) and Lamin A (**B**), harvested after 6 weeks. C57BL/6J wild-type Control (**C**), *rd1* (**D**), harvested after 16 days.

Chapter 4. A link between Lamin A upregulation and the DNA damage response during rod photoreceptor degeneration

Abstract

Photoreceptor cells are highly vulnerable to neurodegenerative disease. In retinitis pigmentosa, rod photoreceptors degenerate via cell death mechanisms that are not fully understood. Evidence suggests that the process may be multi-phasic, with stress-responsive gene expression signatures evident long before rods succumb to die, but the molecular mechanisms that link pathophysiological events to gene regulation are unclear. In previous work, we showed that lamin A (LA) upregulated at the onset of rod photoreceptor degeneration in the *rd1* mouse model of retinitis pigmentosa, suggesting that it might be an early marker of cellular pathology. Here, we show that LA upregulation correlates with the DNA damage response. Using phosphorylated KAP1 (pKAP1) immunohistochemistry, we show that LA upregulation correlates tightly with rods harboring an active DNA damage response. Time course analysis suggests that LA transiently marks an early phase of the cell death process, whereas pKAP1 cumulatively marks rods throughout degeneration. Next, to determine how LA modifies rod degeneration, we performed siRNA knock-down or overexpression of LA in the *rd1* via *in vivo* electroporation. We found that siRNA-mediated knockdown of LA accelerated cell death, whereas LA overexpression reduced cell death. These data suggest that LA upregulation is adaptive, and promotes rod photoreceptor survival. Together, these data suggest that DNA damage and KAP1 phosphorylation converges with LA upregulation to reorganize heterochromatin (HC) during rod photoreceptor degeneration.

Introduction

The death of retinal photoreceptor cells accounts for several of the most common forms of neurodegeneration. Cone photoreceptor degeneration in age-related macular degeneration has a particularly large burden, afflicting more than 10% of all individuals above age 40[271]. Retinitis pigmentosa (RP) – in which rod photoreceptors degenerate, is among the most common genetic disorders, afflicting as many as 1 in 4,000 people, with at least 84 genes contributing to the RP genetic landscape[191]. Since photoreceptor vulnerability contributes to the disease process in both cases, improving our understanding of RP pathophysiology should provide important insight into neurodegeneration.

In RP, mutations often misregulate the phototransduction process, leading to profound ionic and metabolic imbalances, as well as oxidative stress[272,273,274]. While these insults are ultimately fatal to the cell, many data suggest that photoreceptors go through distinct phases of degeneration. While RP is generally driven by inherited mutations, degeneration typically occurs during adulthood, and progresses slowly over years or even decades[191].

Transcriptomics has been used to profile cell death in RP models, revealing that initial insults drive a cascade of gene expression changes that occur prior to overt cell death. In many cases, genes are strikingly upregulated in response to damage[245,267,268]. Moreover transcription factors or co-factors are genetically linked to RP, including CRX, NRL, NR2E3, and OTX2, implying that some forms of RP are 'transcriptionopathies'. However, even when RP is driven by defects in phototransduction, studies have revealed consequent alterations to the transcriptome and epigenome. Previous studies have linked photoreceptor degeneration to changes in chromatin accessibility[266,268], DNA methylation[275], histone modifications[276,277,278], and DNA damage[279,280].

While the order-of-events underlying the transcriptomic component of the cell death process in RP has been studied previously, the underlying pathophysiological and regulatory mechanisms remain largely unclear. Relatively few markers that distinguish between early and later phases of rod photoreceptor cell death have been established thus far. In previous work, we showed that in the *rd1* mouse model of RP, rod photoreceptors upregulate LA, which in turn reorganizes the nucleus[220]. LA upregulation coincided with the onset of the initial wave of cell death[220], but how exactly cell stress led to altered gene regulation remained unclear.

To begin to understand the upstream events responsible for this process, we performed co-staining experiments with other markers of cellular stress response. We report that LA is highly co-expressed with phospho (p) KAP1, a marker of the DNA damage response. Whereas LA expression peaks early in the degenerative process, we found that pKAP1 continues to mark photoreceptor nuclei throughout degeneration. These data suggest that LA upregulates in cells in response to DNA damage. Next, to determine how LA affects cell death, we knocked-down or overexpressed LA in the *rd1* mouse model using retinal electroporation. We find that LA knock down accelerates cell death. Together, these data establish LA upregulation as an adaptive response to DNA damage during rod degeneration. Our data suggest that both LA and KAP1 phosphorylation may converge to reorganize heterochromatin (HC) during early stages of rod photoreceptor degeneration. Lamin A and pKAP1 should be useful markers with which to identify photoreceptors in distinct phases of degeneration.

Results

4.1. Lamin A expression peaks at P16 in the *rd1* mouse model

RP is often age-dependent and slowly progressive. This implies that individual photoreceptors may exhibit extensive heterogeneity in their response to insult, with some photoreceptors persisting for longer than others. Despite this fact, very few molecular markers can be used to discriminate between different stages of degeneration. Using the *rd1* mutant as a model system, we previously reported that LA upregulates during rod photoreceptor degeneration[220]. Analysis of previously published RNA-seq data from sorted *rd1* rods revealed that upregulation of *Lmna* – the gene encoding LA – coincided precisely with the onset of cell death at postnatal day (P) 10[245,220], suggesting that LA might mark rods during early phases of degeneration.

To determine how LA expression correlates with cell death in the *rd1* retina, Jasmine Levesque, an Honour's student in Dr. Mattar lab, focused on P10, P16 and P21 stages and found that as the retina of the *rd1* mouse degenerates, the width of the photoreceptor layer drastically decreases between P10 and P16 (Figure 4.1D-G). At P10, the width of the photoreceptor layer was 58.86 μm ± 5.3 μm. The photoreceptor layer underwent drastic degeneration between P16 and P21, decreasing in width to 9.7 μm ± 1.9 μm and 4.4μm ± 0.8 μm, respectively. Comparing the photoreceptor layer in the *rd1* versus that of C57BL6/J controls, we found no significant difference at P10, but a marked reduction in thickness at P16 and P21, as expected (Figure 4.1G). Similar results were obtained when we measured the photoreceptor layer by counting cell rows. Next, we performed IHC for LA to determine how LA expression in rods changes during degeneration. In wild-type mice, LA was nearly absent in the photoreceptor layer (Figure 4.1A-C).

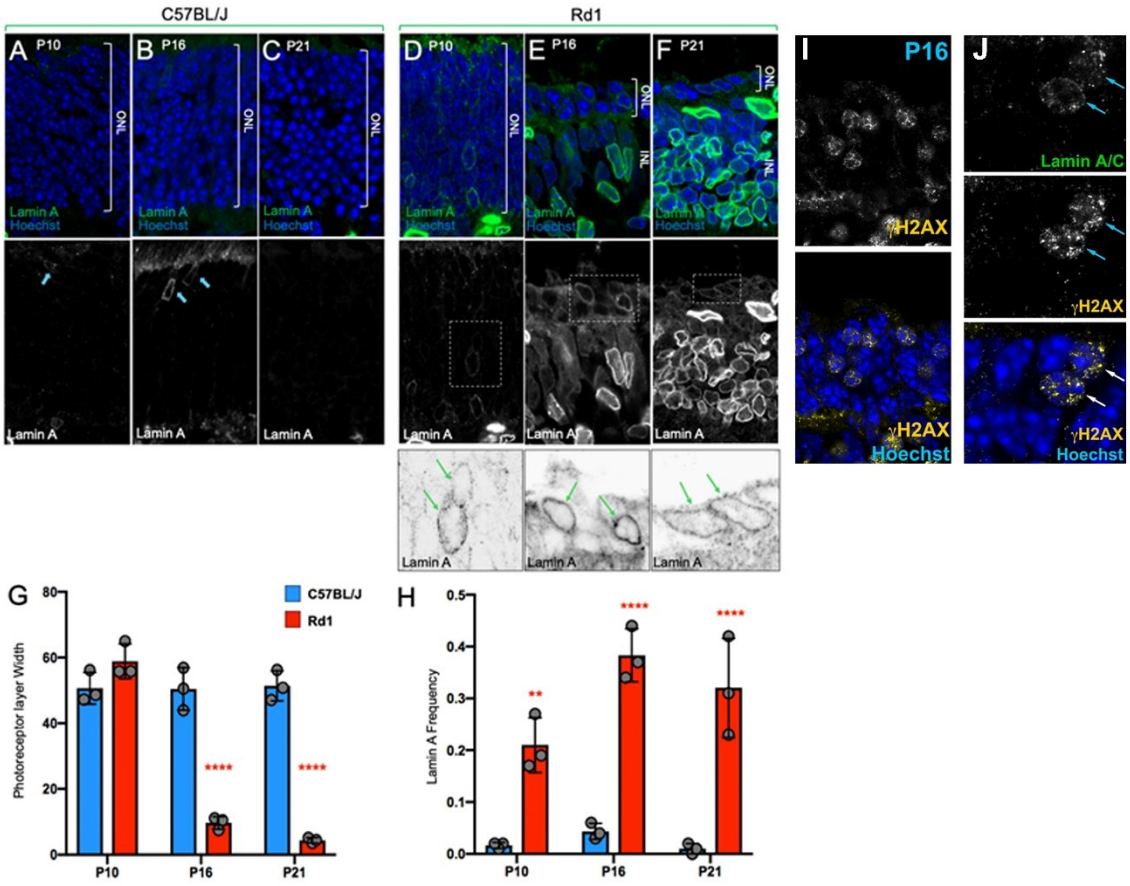

Figure 4.1. Kinetics of lamin A/C upregulation in the *rd1* retina.

Lamin A expression in C57BL6/J retinas (**A**-**C**) or *rd1* (**D**-**F**) retinas at P10 (**A**, **D**), P16 (**B**, **E**), or P21 (**C**, **F**). (**G**) Width of the photoreceptor layer (micrometers). (**H**) Proportion of photoreceptors that are Lamin A positive. (**I, J**) H2A.X and Lamin A expression in P16 *rd1* rods.

The few LA+ cells were found at the apical margin of the layer, and were probably cone photoreceptors as shown previously[216,66,219]. By contrast, in the P10 *rd1* retina, prior to the overt loss of rods, 22% of photoreceptor cells expressed LA (Figure 4.1D, H). By P16 (Figure 4.1E, H), 39% of photoreceptors express LA, which decreased to 32% at P21 (Figure 4.1F, H). In each case, these proportions were significantly elevated versus wild-type controls.

Additionally, we performed γH2AX IHC in P16 *rd1* rods. The data suggest that there is fairly widespread DNA damage in the *rd1*. Individual foci might arise from oxidative stress (Figure 4.1I). However, most of the cells have the whole nucleus marked (Figure 4.1J), suggesting that many LA+ cells may be undergoing DNA fragmentation associated with apoptosis.

4.2. Phospho-KAP1 is upregulated in lamin A -expressing rods

In response to DNA damage, cells mount repair responses. However, degenerating rod photoreceptors repair DNA very inefficiently[110]. It is reported that DNA double-strand break repair efficiency in rods correlates with the level of KAP1 expression and phosphorylation, which are low in mature rods after DNA damage[110]. KAP1 protein is a co-repressor that binds to HP1 during gene silencing but is also phosphorylated at Serine 824 in response to DNA damage[281,282]. Therefore, pKAP1 (S824) is a marker of DNA damage. The mechanism of photoreceptor death in the *rd1* retina is not fully understood, and identifying specific mechanisms contributing to rod cell death, (eg. DNA damage), may provide an insight into this mechanism.

While the rod photoreceptors in the wild-type C57BL/J retina rarely express pKAP1, there is an increasing expression of pKAP1 in the *rd1* model (Figure 4.2G), at every chosen time point (P10, P16 and P21). This suggests that as degeneration occurs in the *rd1* model, DNA damage is increasing. First, we examined how LA and pKAP1 were expressed during rod photoreceptor degeneration in the *rd1* mutant. Compared to control (Figure 4.2A-C), we found that LA upregulation strongly correlated with pKAP1 expression. Approximately 80% of rods that expressed LA were observed to co-express pKAP1 (Figure 4.2D-F, H).

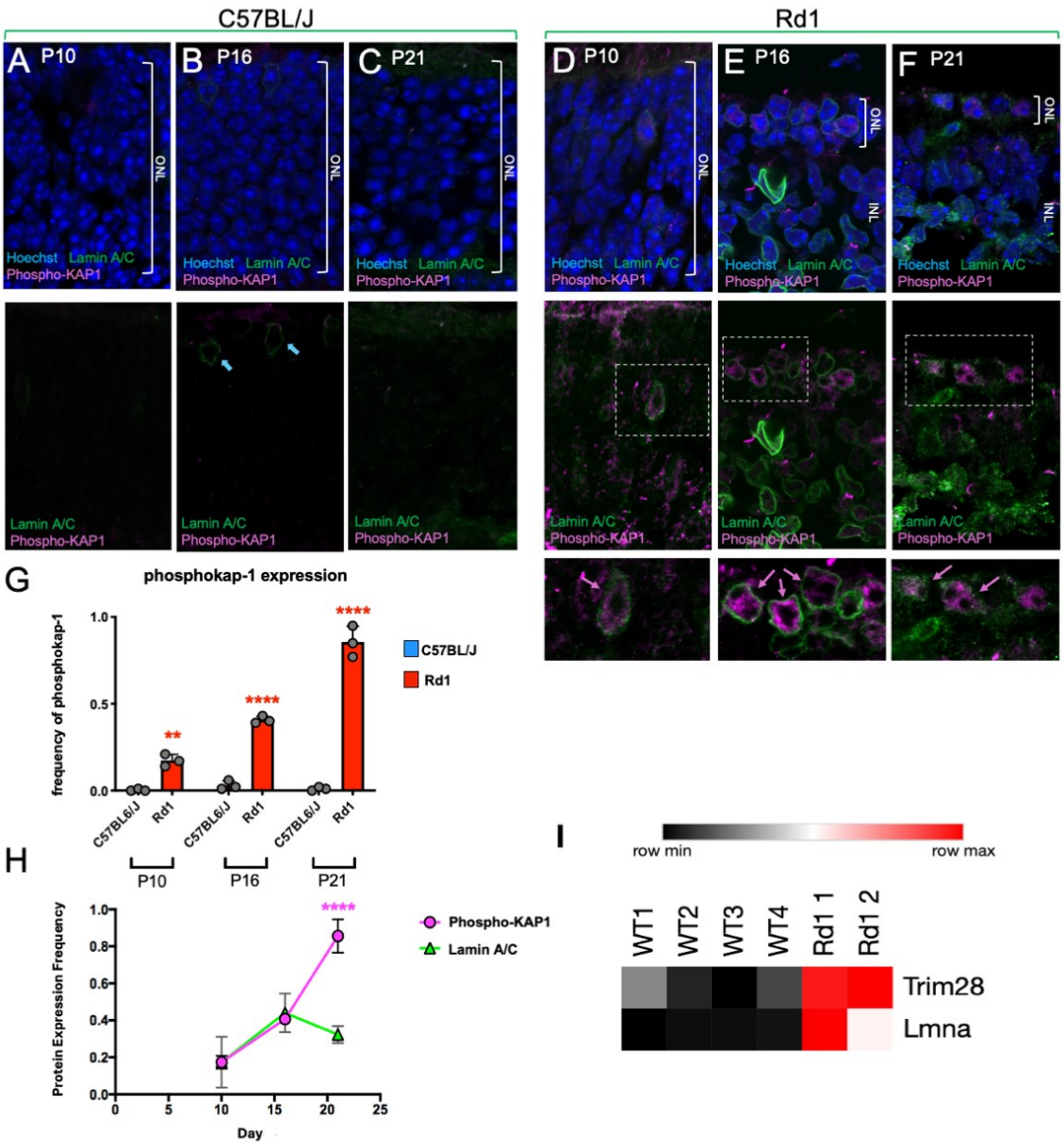

Figure 4.2. Co-expression of phospho KAP1 and Lamin A/C in the control and *rd1* mutant. (**A**-**F**) P10 - P16 cells co-expressing Lamin A/C and pKAP-1 are highlighted with a purple arrow. (**G**) Proportion of photoreceptors that are pKAP1 positive at P10, P16 and P21. (**H**) Comparison of Lamin A+ versus pKAP1+ proportions at P10, P16 and P21. (**I**) Analysis of the published RNA-seq dataset[245], *Trim28* was upregulated in *rd1* rods 1.54 -fold versus control rods (adj. *p*-value < 0.001).

We examined RNA-seq data from sorted P10 control and *rd1* rods. Interestingly, like *Lmna*, *Trim28*, which is the transcript that encodes KAP1, was significantly upregulated in *rd1* versus control, albeit to a lesser extent versus *Lmna*. In our re-analysis of the published RNA-seq dataset[245], *Trim28* was upregulated approximately 1.54 -fold versus control rods (adj. *p*-value < 0.001) (Figure 4.2I). Increases in pKAP1 in degenerating rods therefore likely have both a transcriptional and post-translational basis.

While the correlation between LA/C and pKAP1 co-expression in *rd1* from P10 to P16 remains stable (Figure 4.2D-F), LA/C does not upregulate past P16, while pKAP1 does (Figure 4.2H). As there is no significant difference in expression levels between the LA/C and pKAP1 at P10 and P16 of the *rd1* retina, this suggests that these stress markers may appear in an ordered fashion. Since LA/C and pKAP1 are commonly coexpressed in dying photoreceptors, there may be a functional link between DNA damage and LA.

4.3. Lamin A upregulation is an adaptive response to degeneration

In order to gain a better understanding of how LA is affecting cell survival versus death in the *rd1* model of retinitis pigmentosa, I have tranfected siRNA to suppress LA upregulation (Figure 4.3B, C). Transfected cells were marked by co-injecting a GFP plasmid. To validate the siRNA strategy, I first examined LA upregulation. In general, based on our data, 30-40% of the rods should be LA+ at this stage of *rd1* development. Accordingly, we readily found LA protein expression in rods transfected with an siRNA negative control (NC) (Fig. 4.3A). However, on a qualitative level, LA was absent from siRNA LA transfected *rd1* rods (Fig. 4.3B, C).

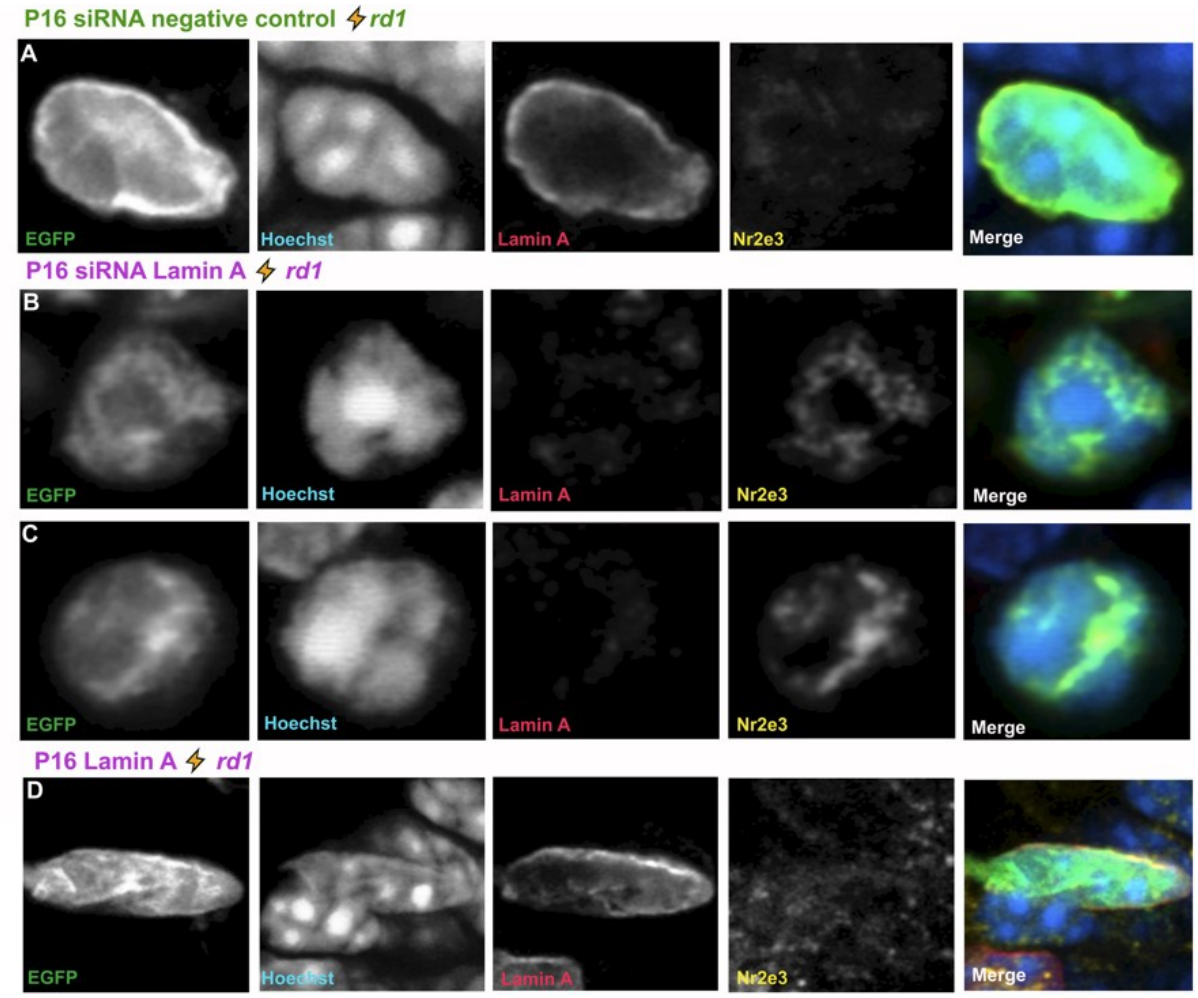

Figure 4.3. siRNA Lamin A expression in *rd1* rods to supress Lamin A upregulation. Airyscan confocal imaging of *rd1* rod photoreceptors transfected with siRNA LA negative control (NC) (**A**), siRNA lamin A (**B**, **C**), and pCIG Lamin A (**D**), harvested after 16 days, with Lamin A/Nr2e3 rod-specific marker expression (red/yellow).

Next, we examined the viability of rod photoreceptors to determine whether their survival was altered. We counted pyknotic nuclei, as degenerating rods do not express many conventional apoptotic markers, including activated caspase 3[283]. As *rd1* rods undergo rapid degeneration, pyknotic nuclei are readily observed at P16.

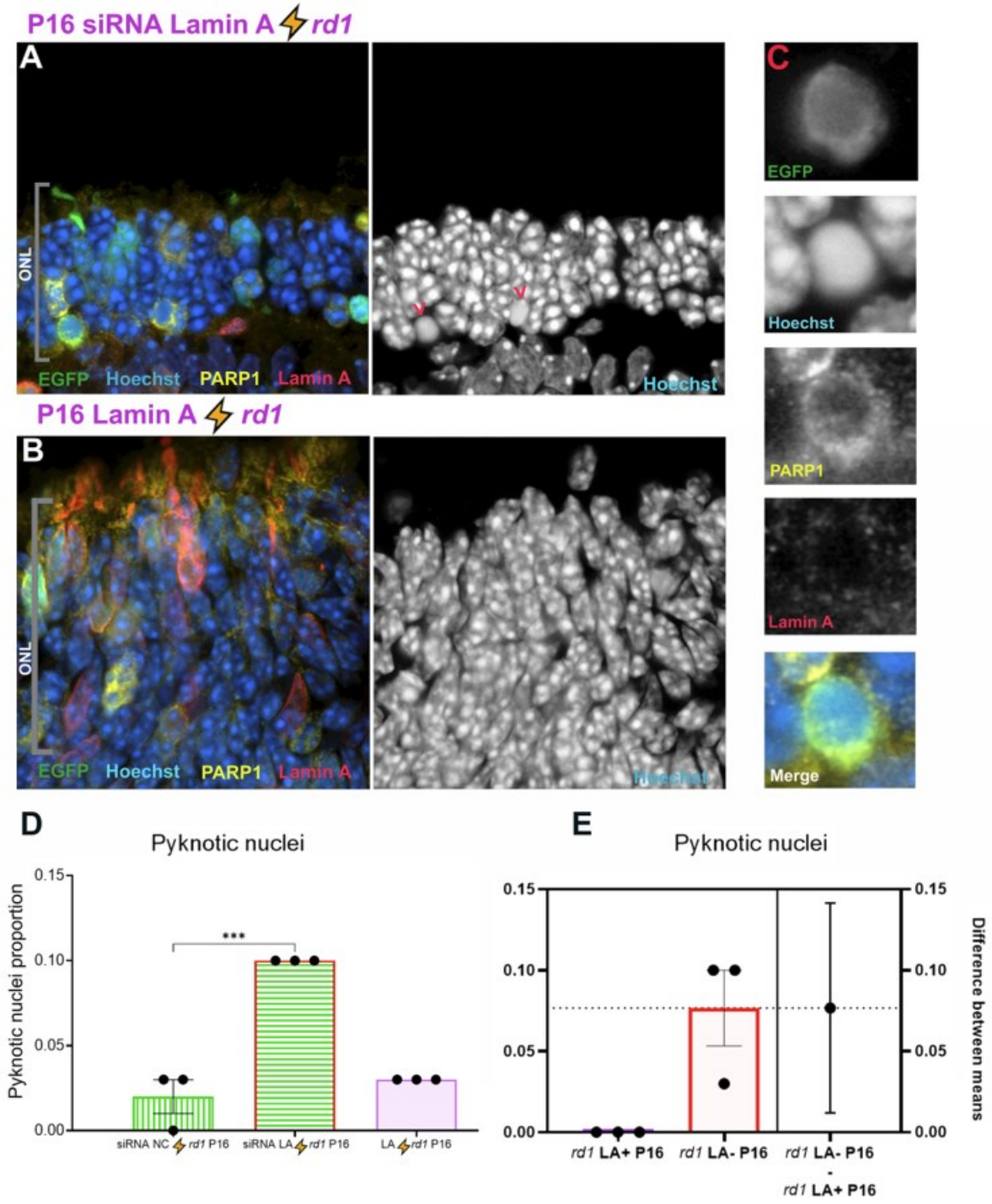

Figure 4.4. Lamin A overexpression and depletion in *rd1* rods affects viability.

Airyscan confocal imaging of transfected (*rd1* rod photoreceptors with siRNA lamin A (**A**), Lamin A (**B**), siRNA lamin A pyknotic nucleus expressing PARP1 magnified (**C**) harvested after 16 days. **D**. Proportion of pyknotic nuclei per 30 (transfected) nuclei (n=3) comparing rods transfected with siRNA NC (negative control) with siRNA Lamin A and pCIG Lamin A.

E. Proportion of Lamin A positive (LA+) or Lamin A negative (LA-) nuclei per 30 untransfected *rd1* pyknotic rods at P16 (n=3) (t-test). Black datapoints and error bars are the mean intensity values from each biological replicate (30 cells each; circles) ± SEM. $p < 0.0001$, one-way ANOVA with Tukey's post-hoc test. ***$p < 0.001$, ****$p < 0.0001$, ANOVA with Tukey's post-hoc test. Data are compared to negative control transfected with non-targeting siRNA negative control (*rd1)* and positive control *rd1* LA+ harvested at P16.

We found that the proportion of pyknotic *rd1* rod nuclei (P16) was higher in rods transfected with siRNA LA versus negative control (NC) (Figure 4.4A, D). Since LA knockdown reduced viability, we next performed the converse experiment by overexpressing LA in *rd1* rods (Figure 4.3D, 4.4B, D). We found that LA overexpression significantly increased survival (Figure 4.4B, D). Next, we examined untransfected *rd1* rods, counting LA+ versus LA- pyknotic nuclei. We similarly found that rods endogenously expressing LA were never pyknotic, whereas *rd1* rods devoid of LA expression were frequently found to be pyknotic (Figure 4.4E). Together, these data suggest that rods depleted of LA may be degenerating faster in comparison with LA transfected/upregulating *rd1* rod nuclei (Figure 4.4A, B, D). What is more peculiar is that the pyknotic nuclei highly express PARP1 (Figure 4.4C).

Discussion

DNA fragmentation has long been associated with photoreceptor apoptosis in mouse models of RP[284,285]. Apoptosis is well-known to drive DNA damage, but in photoreceptors, high intensity light also leads to DNA damage. Careful analysis of DNA fragmentation has suggested that light initially induces an acute phase of random DNA damage that is related to oxidative attack, followed later by a second wave of enzyme-mediated damage that is likely apoptotic[286,287]. Since many RP mutations and high intensity light both lead to excessive

activation of the phototransduction cascade, we think that oxidative stress likely explains the widespread DNA damage that we observed.

In the *rd1* mouse, activation of the DNA damage response has been visualized via EdU incorporation, as well as via the aberrant upregulation of cell cycle markers such as PCNA and damage responsive proteins such as DNA Ligase IV and P53[279,288]. In many cases these proteins are found mainly in pyknotic rods. For this reason, it has been argued that the damage response is a relatively late event during degeneration[279]. Moreover, DNA repair has been shown to proceed slowly in murine rod photoreceptors, with radiation inducing DNA damage and γH2AX foci efficiently, but mobilization of pKAP1 and 53BP1 proceeding inefficiently[110,111]. Similarly, in the *rd1* and *rd10* mutant photoreceptors, elevations in γH2AX and 53BP1 foci were not previously observed[280].

By contrast, we find that pKAP1 expression marks rods at a very early stage in degeneration, and continues to cumulatively report the degenerative process. We found considerable numbers of pKAP1+ rods at the onset of degeneration at P10. Moreover, relatively few of these nuclei exhibited evidence of pyknosis. Indeed, we found that a considerable proportion of these cells co-expressed LA. Since *Lmna* is upregulated via transcriptional mechanisms[245,220], these data argue that pKAP1 marks a proportion of rods early in the degenerative process, when the cells are actively upregulating stress-responsive genes. It is thus possible that the LA+ *rd1* population exhibits less pyknotic nuclei because LA is marking an early phase of degeneration, suggesting that the LA+ nuclei are in the initial stages of degeneration. Moreover, when we reanalyzed RNA-seq data from sorted *rd1* rods, we found that KAP1 transcript (Trim28) was itself significantly upregulated at P10.

It is interesting to ponder on the role of LA in the correlation with PARP1 expression. It is reported that retinal degeneration may lead to the overactivation of PARP-1, triggering PARP-dependent cell death[289,290]. It seems that when LA is absent, a cell death process associated with PARP1 upregulation may be increased. LA seems to be a restraining factor for PARP1-associated cell death, since LA upregulation in *rd1* nuclei did not cause an increase in degeneration. Upregulated PARP1 expression in LA-depleted pyknotic *rd1* nuclei could explain PARP1 involvement in photoreceptor cell death in different models of retinitis pigmentosa[291,292].

Moreover, DNA repair mechanism in inverted rods was shown to be inefficient[110,111]. Interestingly, LBR-mediated HC tethering improved DNA repair capacity[111]. Therefore, it is tempting to propose that the simultaneous upregulation of PARP1 with tethering competent LA would allow HC tethering with chromatin PARylation to facilitate DNA damage repair efficiency. This is supported with our finding that LA upregulation strongly correlated with pKAP1, as DNA repair efficiency in rods requires a strong expression of pKAP1[110,111]. In future work, using electroporation, we aim to determine whether phospho-mimetic versions of KAP1 are sufficient to induce LA.

Taken together, these data indicate that LA upregulation forestalls degeneration, suggesting that LA upregulation might facilitate the DNA damage response.

Chapter 5. Structure-function analysis of Lamin A heterochromatin tethering

Abstract

The nuclear lamina cytoskeleton plays a critical role in higher order genome organization by tethering heterochromatin (HC) at the inner nuclear membrane. Genome disorganization is accordingly implicated in laminopathic diseases, many of which arise due to mutations in the *LMNA* gene. *LMNA* encodes the nuclear intermediate filaments lamin A (LA) and lamin C (LC). However, the mechanism through which nuclear lamins tether HC remains unknown. Importantly, previous experiments revealed that LA is sufficient to tether HC at the nuclear lamina, but that its alternative splice variant LC cannot. Since LA differs from LC only at its C-terminus, we performed a structure-function study of the LA C-terminus. We used murine rod photoreceptors as a model system since these cells naturally lack HC tethering. Our analyses indicate that the C-terminus of LA provides two essential functions. First, molecular modelling predicts that the C-terminus interacts directly with nucleosomes. Second, we found that the LA C-terminus must be defarnesylated in order to tether HC. We additionally found that HC tethering depends on C-terminal amino acids that are mutated in both progeroid and non-progeroid diseases, including surface IG-fold domain residues. Finally, to demonstrate sufficiency, we exchanged the LA C-terminus into the Lamin B1 gene. Misexpression of this recombinant "Lamin BA" in rod photoreceptors was sufficient to tether HC. Taken together, these data provide a framework for understanding how HC tethering is controlled, and how this function is disrupted in disease.

Introduction

Nuclear organization is thought to play a critical role in gene regulation[293,294]. Whereas cytoplasmic functions are often partitioned within membrane-enclosed organelles, the nucleus lacks such structures, and so functional compartmentalization must be achieved through different mechanisms. In many cases, large domains of the genome that are enriched with specific epigenetic modifications associate with particular nuclear structures. For example, the nucleolus is associated with HC, whereas nuclear pore complexes tend to associate with euchromatin (EC)[295,296]. The nuclear lamina has perhaps the most well-studied importance in nuclear organization. In virtually every eukaryotic cell, HC is tethered at the nuclear lamina. Both facultative (H3K27me3) and constitutive (H3K9me2/3, H4K20me3) HC can interact with the lamina[25,27,297,34,298]. Moreover, the artificial recruitment of reporter genes to the lamina suppresses transcription[35], suggesting that the lamina normally has a repressive influence on the genome.

What are the molecular mechanisms that control HC tethering at the nuclear lamina? Addressing this question using genetic approaches is complicated by the highly redundant expression of putative tethering proteins – many of which are essential for viability. Uniquely, the rod photoreceptors of nocturnal mammals naturally lack the expression of HC tethering proteins (both known and as-yet unidentified), and exhibit an inverted chromatin organization with centrally localized HC and peripherally localized EC[211,210,208]. HC inversion reduces light scattering and improves contrast sensitivity in low-light conditions[211,210,208,209]. Interestingly, in diurnal animals, rod photoreceptors maintain a conventional nuclear organization[208,66]. Rods of nocturnal mammals invert during development, as retinal progenitors initially exhibit conventionally organized nuclei, and chromatin inversion takes place slowly over the course of weeks in the differentiating rods[209]. Using murine rods as a model system, gain-of-function

approaches have revealed that the lamin B receptor (LBR) and Lamin A (LA) proteins are sufficient to tether HC[66,219,220]. LBR is a transmembrane protein that localizes within the inner nuclear membrane. Heterozygous and homozygous mutations in *LBR* lead to the Pelger-Huet anomaly, in which the nuclear morphology of granulocytes is aberrant[299,300]. In knockout mice, HC tethering is lost in many tissues[66]. LBR is thought to bind HC directly through an N-terminal tudor domain.

LA is an intermediate filament protein encoded by the *LMNA* gene. Like *LBR*, *LMNA* mutations are associated with laminopathic disease, but mutations lead to markedly different phenotypes[92,301]. In contrast with LBR, LA lacks a canonical chromatin binding domain. Lamin genes do encode an IG-fold domain, which is a structure utilized by some transcription factors to bind DNA. However, the lamin IG-fold is thought to lack critical residues that might allow it to bind DNA[43]. Curiously, LA shares extensive homology with the ubiquitously expressed B-type lamins that are encoded by the *LMNB1* and *LMNB2* genes. Moreover, LA is nearly identical to lamin C (LC) - an alternative splice variant that differs from LA only at its C-terminus. However, only LA is capable of tethering HC in rod photoreceptors[66,219,220]. Intriguingly, the C-terminal domain of LA was recently shown to bind histone H3 *in vitro*, and exhibited a preference for heterochromatic modifications[91]. By contrast, the analogous domain of LC could not bind H3. These data suggest that LA (but not LC) might interact with histones directly, but whether this mechanism accounts for HC tethering *in vivo* remains unclear.

Here, we used a variety of approaches to decipher the molecular logic of LA-dependent HC tethering. First, we used Alphafold3[302] to model the interaction between lamin proteins and nucleosomes. Second, we validated these data by performing a structure/function study of LA -dependent HC tethering in murine rod photoreceptors. Taken together, our results point to a

two-fold importance of the unique LA C-terminal domain. First, Alphafold3 predicts direct contacts between the unique LA C-terminus and nucleosomes. Second, we find that C-terminal post-translational defarnesylation is critical for establishing tethering competence.

Results

Rod photoreceptors are perhaps the best model system with which to assess the effectiveness of candidate HC tethers. As shown previously, rods do not express LA or LC, but they do express Lamin B1 (LB1)[66], indicating that B-type lamins are not sufficient to tether HC. Mature rods do not express LBR, as shown previously[66]. Retinas can be readily transfected by performing subretinal plasmid injections and electroporation on perinatal mouse pups[223], which targets progenitor cells during the peak of rod photoreceptor production. Rods transfected with control plasmids undergo chromatin inversion on the normal schedule (Figure 5.1A). As shown previously[66,219,220], LA robustly tethers HC, leading to a complete reversal of chromatin inversion (Fig. 5.1B), but LC is not sufficient to tether HC (Fig. 5.1C, F-H). Likewise, overexpression of LB1 has no effect on nuclear organization (Fig. 5.1D, F-H), suggesting that endogenous LB1 does not fail to tether HC due to insufficient expression levels.

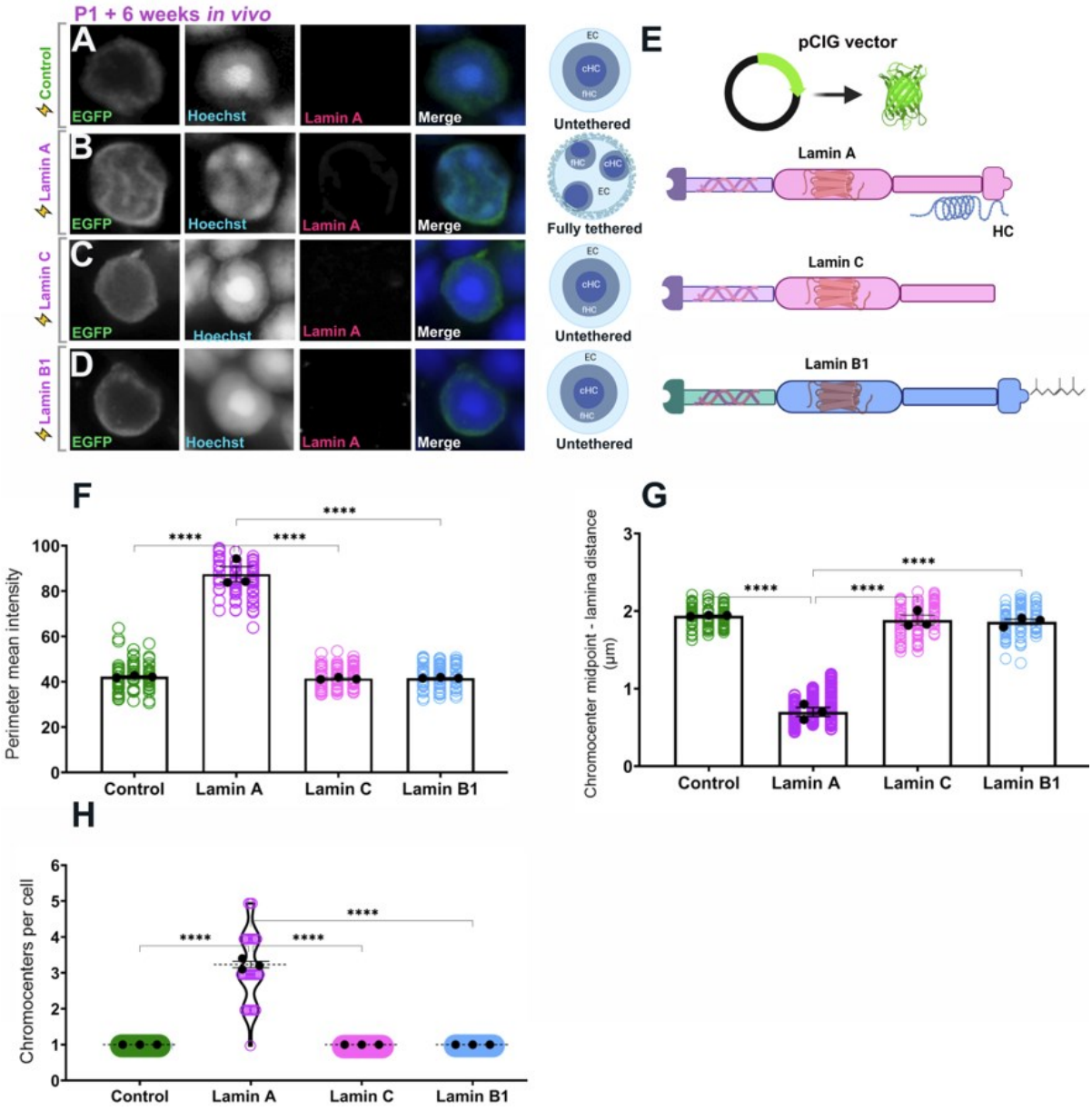

Figure 5.1. Lamin A, but not lamin B1 and lamin C, is sufficient for heterochromatin tethering.

Airyscan confocal imaging of rod photoreceptors transfected with GFP-expressing empty vector control (**A**), Lamin A (**B**), Lamin C (**C**) or Lamin B1 (**D**) constructs, and harvested after 6 weeks (P42). **E.** Illustration of different lamin proteins, of which only Lamin A can tether heterochromatin (HC). **F.** Quantitation of chromatin intensity at the nuclear margin measured using the "Freehand Line" tool in Fiji. **G.** Distance from the chromocenter midpoint to the nuclear periphery. **H.** Chromocenter number per cell. Black datapoints and error bars are the

mean intensity values from each biological replicate (30 cells each; circles) ± SEM. $p < 0.0001$, one-way ANOVA with Tukey's post-hoc test. ***$p < 0.001$, ****$p < 0.0001$, ANOVA with Tukey's post-hoc test.

Moreover, we tested misexpressing LA with different promoters, including the Rho2.2 promoter that is active only in differentiating rods [303]. Changing promoters made no appreciable difference (Figure 5.2), suggesting that HC tethering in rods is quantitatively robust, and little altered by differences in timing. Analysis of the tethering intensity associated with transfection (GFP) intensity implied that LA tethers HC independently on the expression stage/level (Figure 5.2G).

In our published manuscript[219], we additionally determined that LA (or LBR) overexpression does not alter cell viability, and does not lead to the marked upregulation of stress-responsive genes (Chapter 3.1, Fig.3.16). Moreover, upregulation of endogenous LA reorganized HC in degenerating rods.

Together, these data confirm the utility of rod photoreceptors as a model system for studying LA-dependent HC tethering.

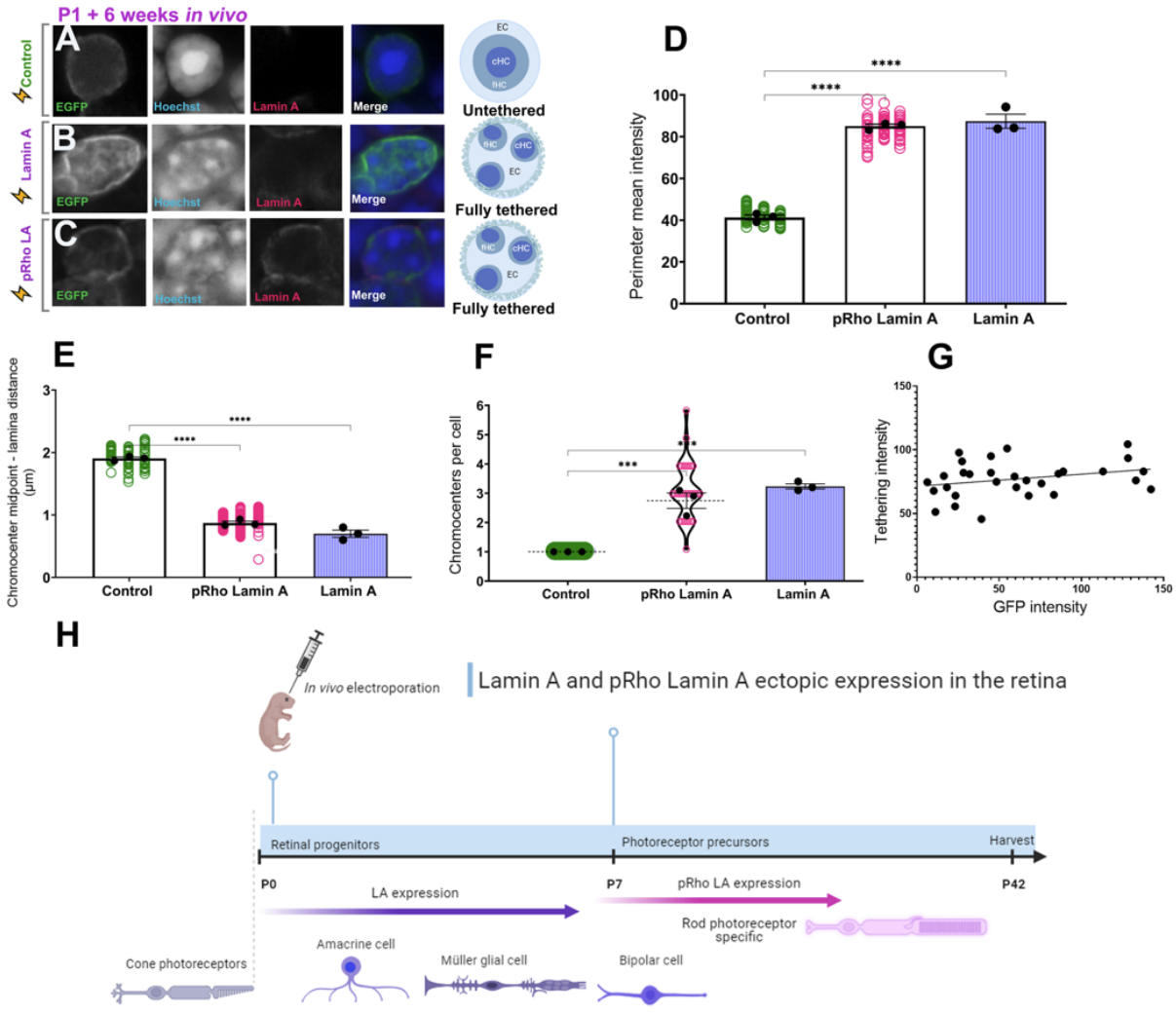

Figure 5.2. Lamin A expression paradigm.

Airyscan confocal imaging of rod photoreceptors transfected with GFP-expressing empty vector control (**A**), along with Lamin A (**B**), or pRho Lamin A (**C**) constructs, and harvested after 6 weeks (P42). Tethering activity was not significantly different between LA and pRho LA, based on nucleo-morphometric analysis. **D** Quantitation of chromatin intensity at the nuclear margin measured using the "Freehand Line" tool in Fiji. **E** Distance from the chromocenter midpoint to the nuclear periphery. **F** Chromocenter number per cell. Black datapoints and error bars are the mean intensity values from each biological replicate (30 cells each; circles) ± SEM. $p < 0.0001$, one-way ANOVA with Tukey's post-hoc test. ***$p < 0.001$, ****$p < 0.0001$, ANOVA with Tukey's post-hoc test. **G** Quantitation of chromatin and transfection (EGFP) intensity at the nuclear margin measured using the "Freehand Line" tool

in Fiji. **H** Illustration of the difference between Lamin A and pRho Lamin A expression. Data are compared to negative control pCIG and positive control wild-type Lamin A average values generated from replicates in Figure 5.1.

5.1. Modelling lamin-nucleosome interactions

What is the structural basis for tethering competence? Previous results have suggested that the LA C-terminus can interact directly with histone H3 *in vitro*, whereas the corresponding C-terminal domain of LC cannot[91]. Using AlphaFold3[305], we first simulated the interaction between two lamin proteins. We found that LA, LC and LB1 all formed braided filament-like structures. Next, we modelled the interactions between lamin dimers and a nucleosome octamer (Figure 5.3). We found that LC dimers maintained their filamentous configuration, and that the nucleosome self-assembled into an octamer, but no robust interaction between LC and the octamer was evident (Figure 5.3B). Next, we performed the same simulation with two LA proteins. We found that instead of forming a rod-like structure, the two LA subunits took on a hoop-like configuration which encircled the nucleosome. Closer inspection revealed that the LA dimers formed a number of Van der Waals bonds with histones, and the IG-fold domains took on an oriented alignment over and under the nucleosome (Figure 5.3C). While this interaction was striking, we thought that LA would be unlikely to take on this configuration once polymerized into intermediate filaments. The hoop-like structure seemed much more likely to be formed by nucleoplasmic, soluble lamin.

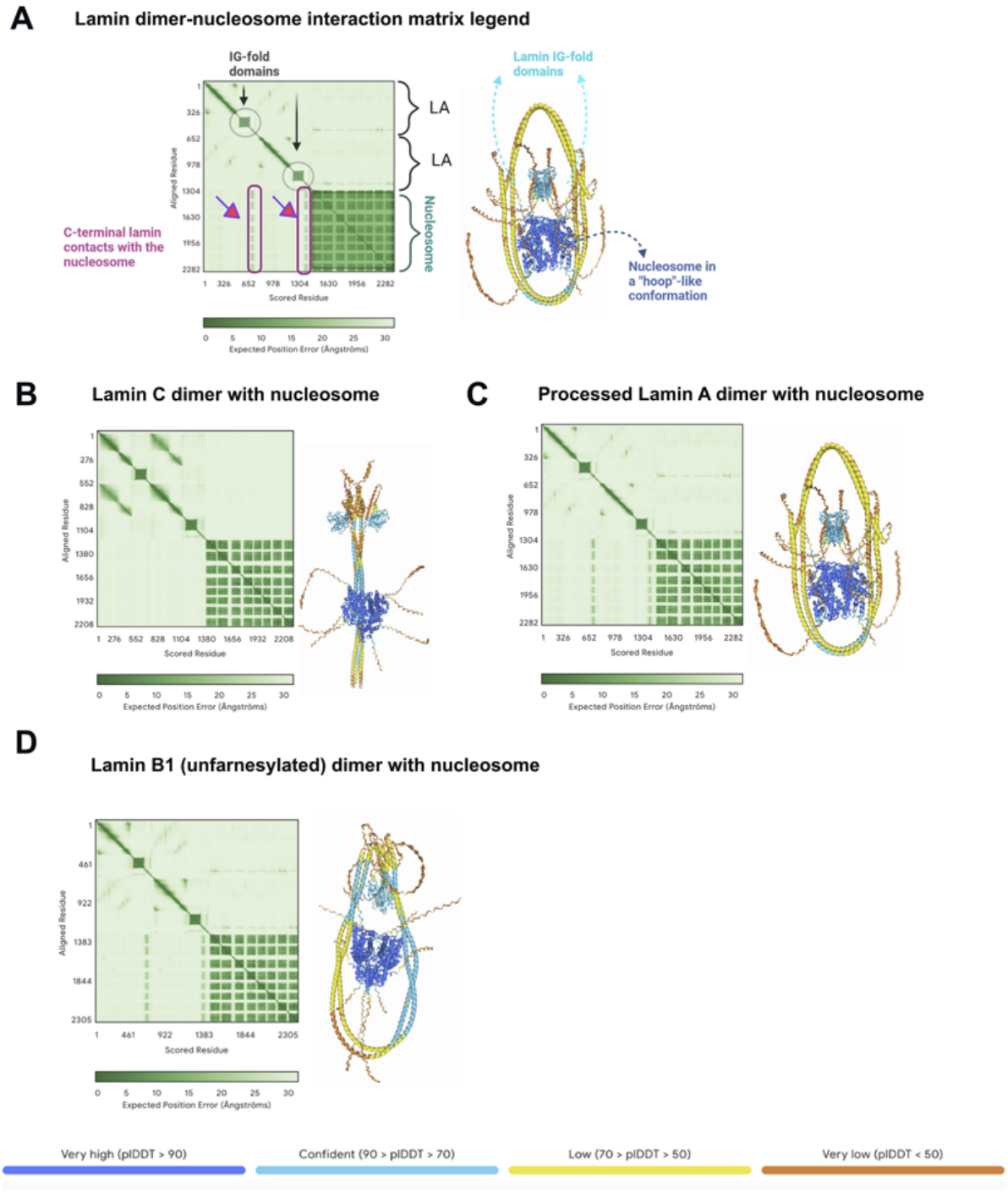

Figure 5.3. Alphafold3 projection of A- and B-type lamins and nucleosomes.

A legend for the lamin dimer and nucleosome interaction matrix (Lamin A as an example), with a highlighted Lamin A C-termini contacts (**A**). Modelling of the Lamin C dimer with the unmethylated nucleosome (**B**). Modelling of the processed Lamin A dimer with the

unmethylated nucleosome (**C**). Modelling of the Lamin B1 dimer with the unmethylated nucleosome (**D**). In a modeled Lamin A dimer, the colours blue, turquoise, yellow, orange signify the model prediction confidence – with blue representing the highest level of prediction confidence.

Moreover, when we tested a LB1 dimer, we found that it could take on a similar hoop-like configuration (Figure 5.3D). Indeed, for both LC and lamin B1, the IG folds and C-terminus were oriented away from the nucleosome (Figure 5.3B, D).

Next, we simulated a series of euchromatic and heterochromatic modifications of histone tails, including H3K27me3, H3K27ac, and H4K20me2/3. Strikingly, when the nucleosome was modified to contain the H3K9me2 modification, we noted that the contacts between the LA C-terminus could be retained while the LA dimer remained in the filamentous configuration (Figure 5.4A).

Of note, H3K9me2 is particularly enriched at the nuclear lamina in conventional cells, and is a key modification that defines lamina-associated domains (LADs) in the genome[33,34]. Similar results were observed when the nucleosome was supplemented with the H1.2 linker histone (HIST1H1C) (Figure 5.4B). By contrast, nucleosomes containing H3K9me2 did not form bonds with LB1 or LC (Figure 5.4C, D).

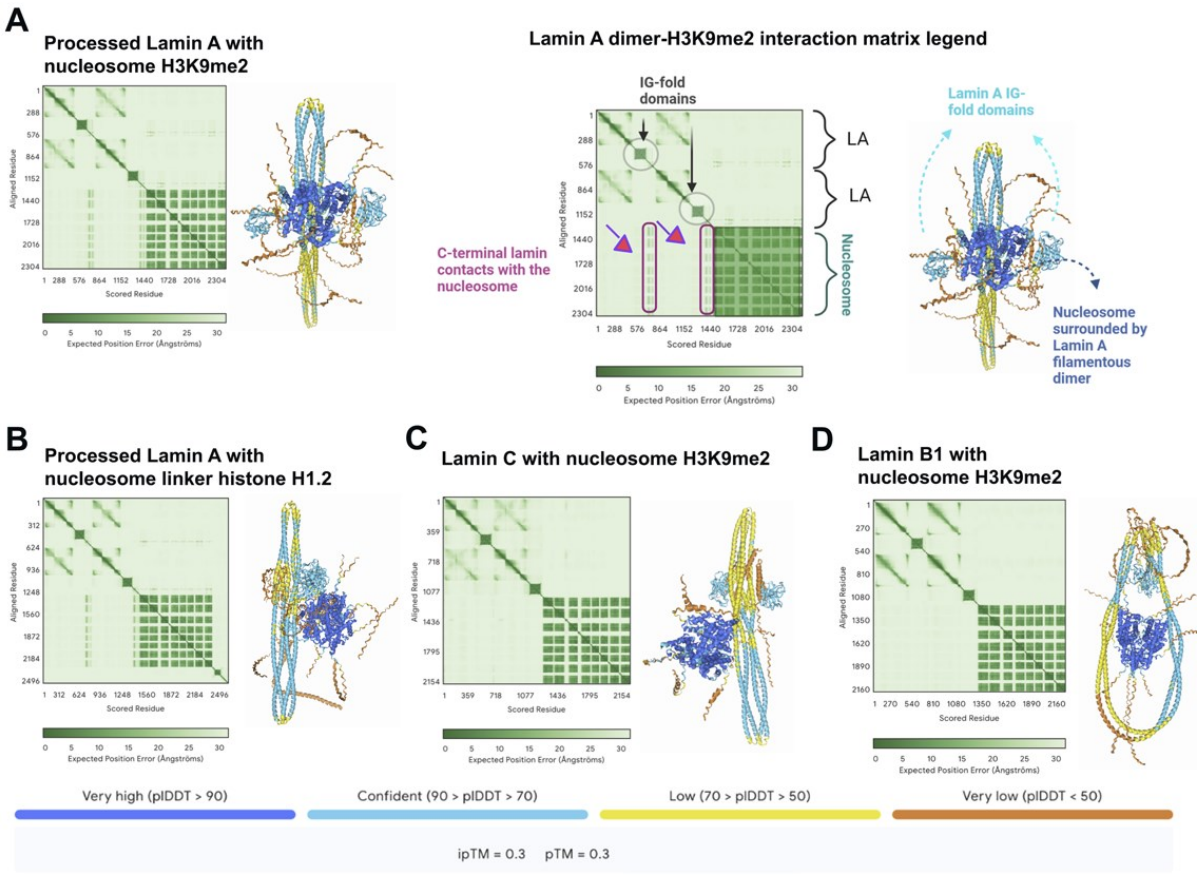

Figure 5.4. Alphafold3 projection of Lamin A, Lamin C and Lamin B1 with modified nucleosomes. Alphafold3 modeling of fully processed mature Lamin A protein interaction with H3K9me2 nucleosome (**A**), with nucleosome linker histone H1.2 (**B**). Alphafold modeling of Lamin C (**C**) and Lamin B1 (**D**) protein interaction with H3K9me2 nucleosome. The colours blue, turquoise, yellow, orange signify the model prediction confidence – with blue representing the highest level of prediction confidence.

Next, we inspected Van der Waals bonds predicted to form between residues in the LA dimers and the nucleosome. In all cases, LA/histone bonds were found to be symmetrical, with each LA subunit pairing with one side of the nucleosome in a mirrored fashion. Alphafold3 predicted a number of such bonds (visualized via ChimeraX[304]), including one in the N-terminus (Figure 5.5A), as well as V629 and E578 in the LA C-terminus, which paired with

histone H2A and H2B, respectively, while Y579 paired with H4 (Figure 5.5B). Interestingly, a recent preprint by the Medalia lab shows that LA residues between 579-585 contact H2A-H2B histones[305].

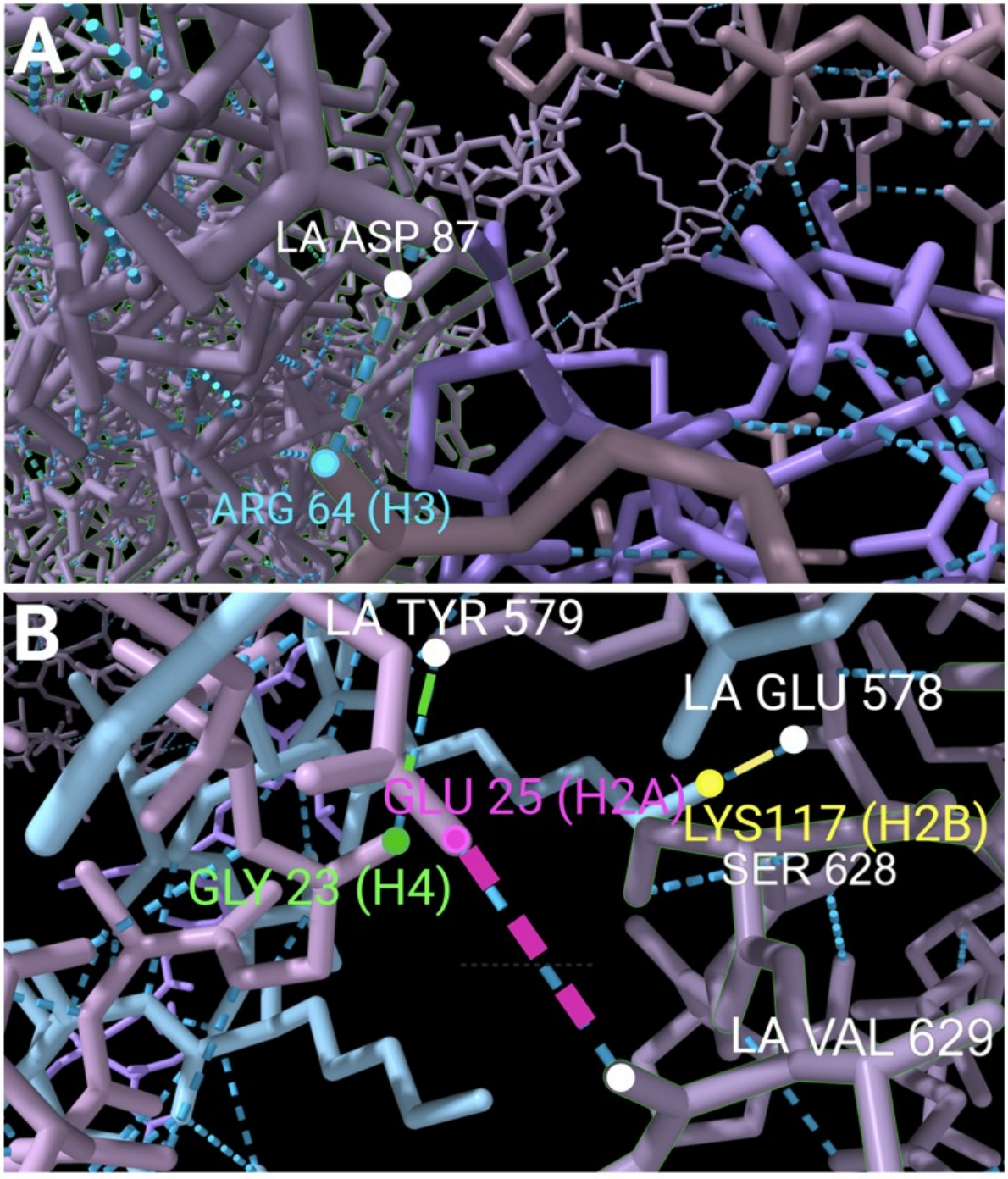

Figure 5.5. ChimeraX modeling of direct Lamin A C-terminal tail and N-terminal head interactions with histones.

A. Arginine 63 of histone H3 contacts the LA N-terminal residue Asp 87.

B. LA C-terminal contacts between Valine 629 and Glutamic acid 25 of histone H2A (pink). LA C-terminal Glutamic acid 578 interacts with the Lysine 117 of histone H2B (yellow), and C-terminal Tyrosine 579 interacts with Glycine 23 of histone H4 (green).

The most extensive set of interactions were made by a patch of interface amino acid residues (LA578-585), specific to the unique LA C-terminus (not found in LC), which interacted with both H2B and H4 (Figure 5.5B). Interestingly, some of those AA are also implicated in disease (eg. E578V; R582H; R584H)[306]. Extensive internal Van der Waals interactions within a large internally looping stretch of the LA C-terminal tail appear to be important for exposing and orienting a C-terminal loop harboring most of the residues that made contacts with the nucleosome. Together, these simulations provide a framework for understanding HC tethering by LA that we tested experimentally below.

5.2. The IG-fold domain is necessary for tethering

To test the predictions of the Alphafold3 model, we decided to simulate interactions between nucleosomes and laminopathic LA variants, and then to compare these predictions with results from *in vivo* tethering assays in rod photoreceptors. We first examined mutations associated with the IG-fold domain. Previous work has implied that the IG-fold can bind DNA directly[307], although other work suggests that it cannot bind histones by itself[91]. While Alphafold3 modelling suggests that the IG-fold does not make direct contacts with the nucleosome, IG-

fold missense mutations are associated with laminopathic disease. We first examined LA R453W and LA R482W, which cause Emery-Dreifuss muscular dystrophy and dilated cardiomyopathy, respectively[82]. In simulations, LA R453W dimers retained a filamentous configuration, but LA R482W was rearranged into a loose hoop-like configuration (Figure 5.6B, C). Compared to wild-type LA (Figure 5.6A), simulations reveal that both mutants lose Van der Waals contacts with the H3K9me2 nucleosome.

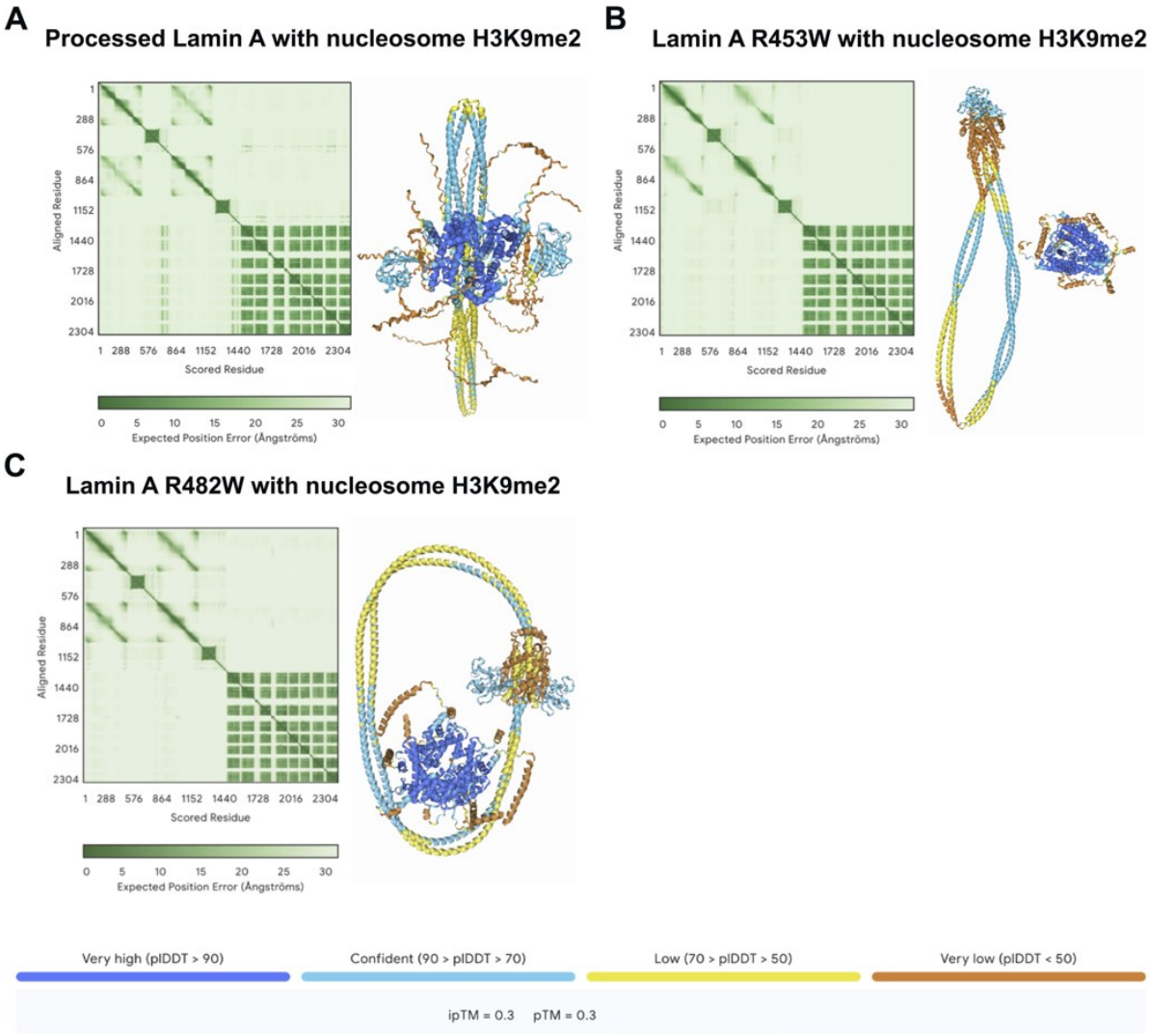

Figure 5.6. Alphafold3 projection of Lamin A IG-fold mutants with the nucleosome.

Alphafold3 modeling of the processed Lamin A-H3K9me2 interaction matrix as a control (**A**), Lamin A IG-fold mutant LA R453W-H3K9me2 (**B**), and Lamin A IG-fold mutant LA R482W-H3K9me2 interaction (**C**). The colours blue, turquoise, yellow, orange signify the model prediction confidence – with blue representing the highest level of prediction confidence.

In both cases, the IG-folds and C-termini were oriented away from the nucleosome and the 3D structure of the IG-fold appeared to be disorganized (Fig. 5.6B, C).

In perfect agreement, overexpressing both LA R453W and LA R482W in rod photoreceptors completely failed to tether HC (Fig. 5.7A-H). LA immunostaining confirmed that the failure to tether was not due to lack of protein expression or incorrect localization. Likewise, LA IG-fold mutant expression in 3T3 cells revealed that mutant proteins form precipitates (Figure 5.7I-L). These data suggest that the IG-fold plays an important role in lamin function, but that with respect to HC tethering, its likely role is to orient more C-terminal regions of LA in order to surface-expose regions that directly contact the nucleosome.

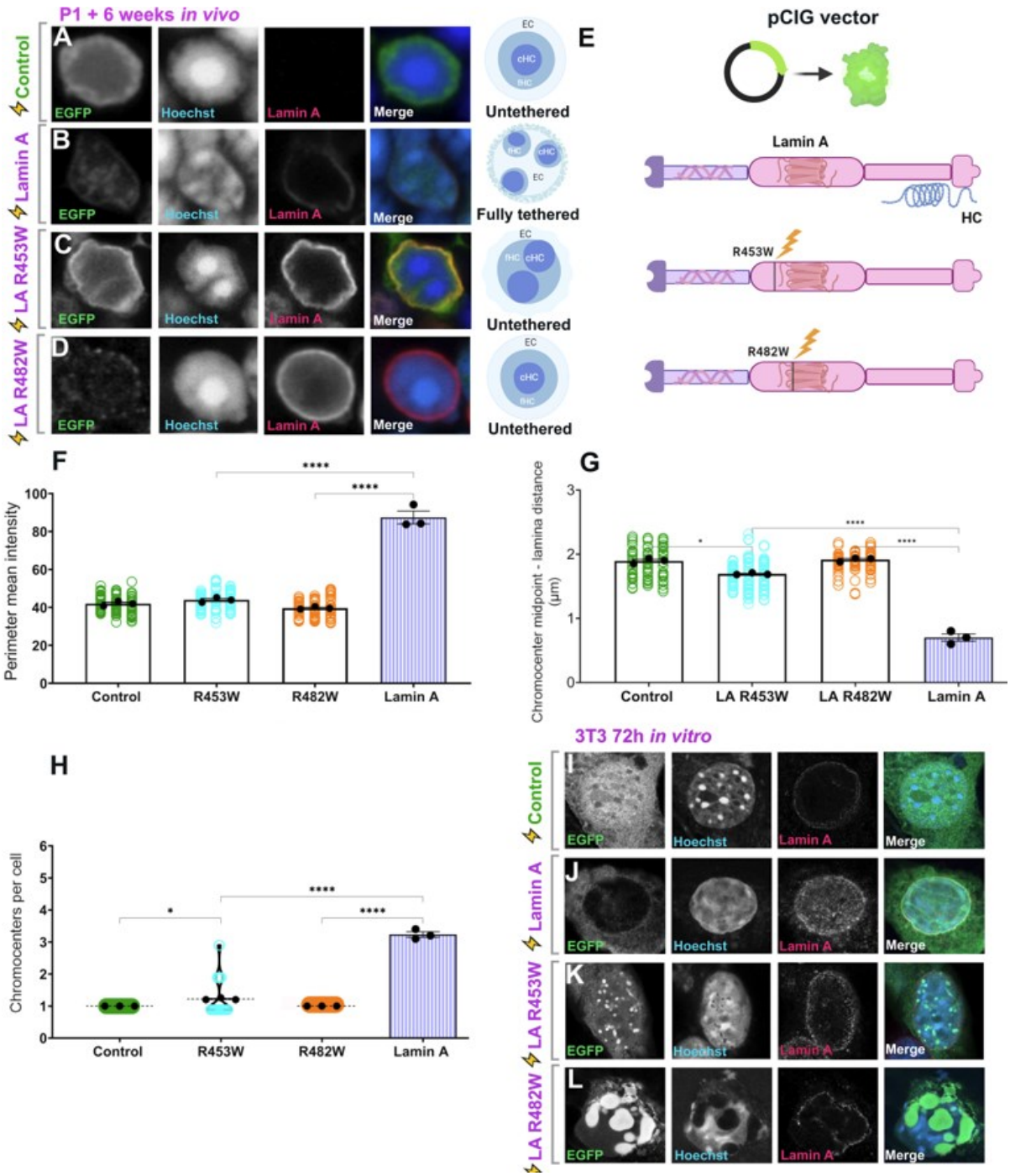

Figure 5.7. Loss of tethering in IG-fold non-progeroid disorders.

Airyscan confocal imaging of rod photoreceptors transfected with GFP-expressing empty vector control (**A**), Lamin A (**B**), Lamin A R53W (**C**) Lamin A R482W (**D**) constructs, and harvested after 6 weeks. **E.** Illustration of IG-fold lamin A point mutants. **F.** Quantitation of chromatin intensity at the nuclear margin measured using the "Freehand Line" tool in Fiji. **G.**

Distance from the chromocenter midpoint to the nuclear periphery. **H.** Chromocenter number per cell. Black datapoints and error bars are the mean intensity values from each biological replicate (30 cells each; circles) ± SEM. $p < 0.0001$, one-way ANOVA with Tukey's post-hoc test. ***$p < 0.001$, ****$p < 0.0001$, ANOVA with Tukey's post-hoc test. Data are compared to negative Control pCIG and positive control wild-type Lamin A average values generated from replicates in Figure 5.1. 3T3 cell line transfected with (**I**) Control, (**J**) Lamin A, (**K**) R453W and (**L**) R482W.

5.3. Post-translational processing is essential for tethering competence

In addition to the histone tails, post-translational processing occurs on lamin proteins. Both LA and B-type lamins are farnesylated on the Cysteine residues of their C-terminal CAAX motifs. To approximate this in Alphafold3, we added palmitoyl to the C-terminal CAAX motifs. After C-terminal palmitoylation, we noted that LA maintained its hoop-like encirclement of the nucleosome, but now failed to make contacts with the nucleosome (Figure 5.8). Upon farnesylation, LA undergoes subsequent processing that culminates in the cleavage of amino acids 647-665 by the ZMPSTE24 protease, which removes the farnesylated cysteine. When we simulated this cleavage, we found that processed LA C-terminus resumed a robust interaction with the nucleosome (Figure 5.8).

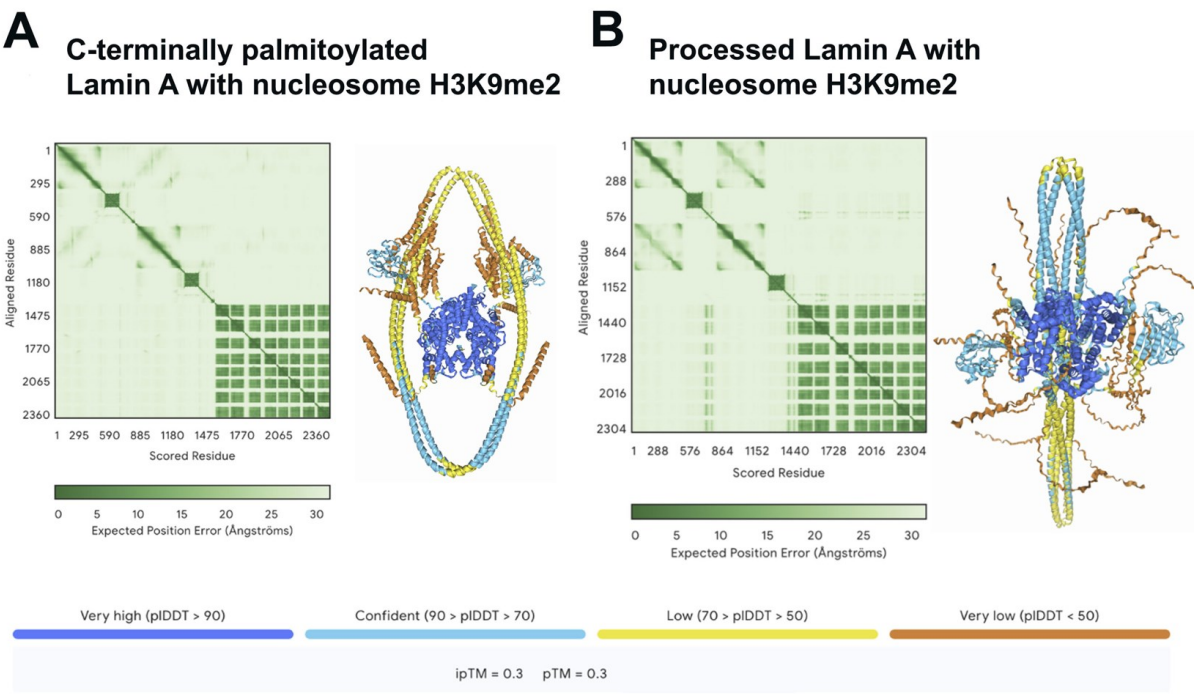

Figure 5.8. Alphafold3 projection of palmitoylated Lamin A with the nucleosome H3K9me2.

Alphafold3 modeling of C-terminally palmitoylated Lamin A protein interaction with H3K9me2 nucleosome (**A**) and processed (cleaved) Lamin A protein interaction with H3K9me2 nucleosome (**B**). The colours blue, turquoise, yellow, orange signify the model prediction confidence – with blue representing the highest level of prediction confidence.

Since Alphafold3 predicted that farnesylation would block HC tethering, we next examined the effects of mutations that block LA processing. The most famous LA mutation is likely progerin, which is associated with Hutchinson-Guilford progeria syndrome. Progerin usually arises due to the activation of a cryptic premature splice donor, resulting in generation of a protein that lacks 50 C-terminal amino acids, including the proteolytic cleavage site at Leucine 647. We simulated the interaction between progerin and the nucleosome. We found that palmitoylated progerin lost the normal contacts exhibited between LA and histones, even

though many of the relevant amino acids remain present in the protein (AA578-585) (Figure 5.9B).

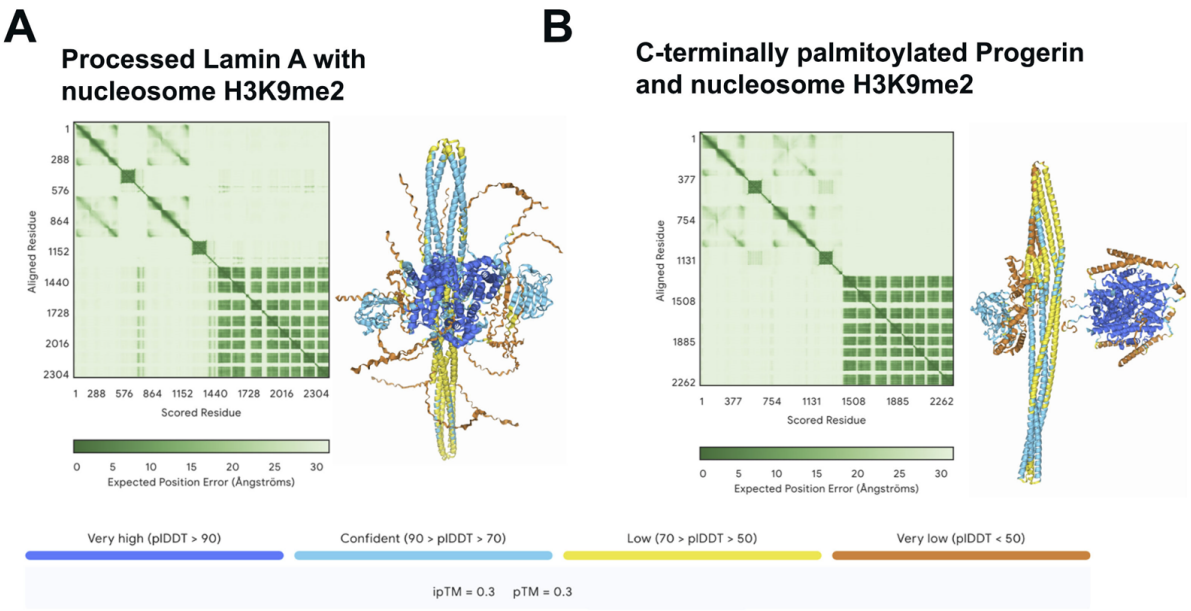

Figure 5.9. Alphafold3 projection of palmitoylated Progerin with the nucleosome H3K9me2.

Alphafold3 modeling of processed Lamin A protein interaction with H3K9me2 nucleosome as a control (**A**) and C-terminally palmitoylated Progerin protein interaction with H3K9me2 nucleosome (**B**). The colours blue, turquoise, yellow, orange signify the model prediction confidence – with blue representing the highest level of prediction confidence.

When we misexpressed progerin in rod photoreceptors, we accordingly observed that rod nuclei became markedly misshapen (Figure 5.10C). However, when we performed densitometric measurements, we found that progerin completely failed to tether HC to the periphery (Figure 5.10C-F).

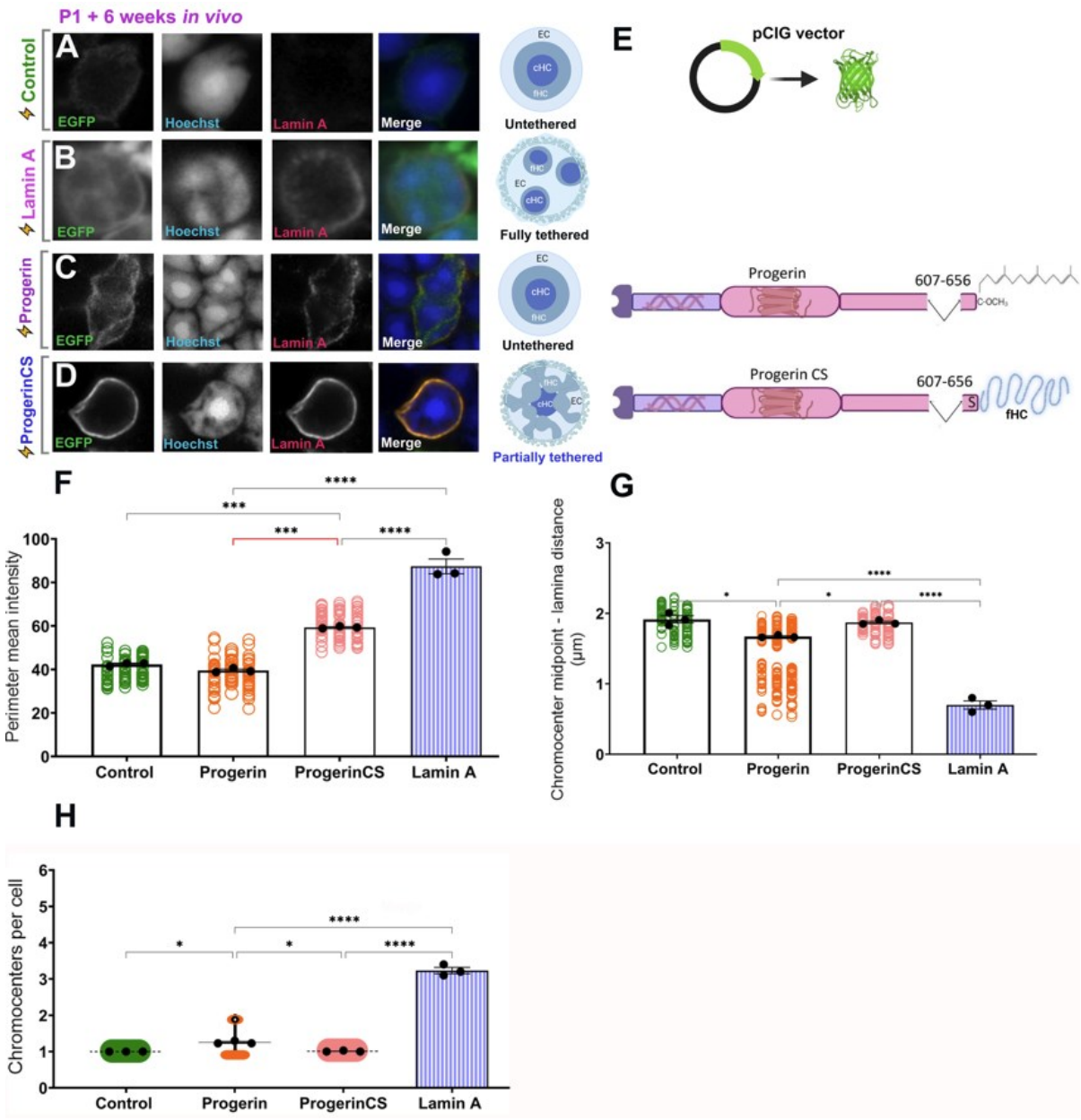

Figure 5.10. Abolished tethering in Progerin is partially recovered via defarnesylation.

Airyscan confocal imaging of rod photoreceptors transfected with GFP-expressing empty vector control (**A**), Lamin A (**B**), along with Progerin (**C**), or Progerin-CS (**D**) constructs, and harvested after 6 weeks. **E**) Illustration of post-translational mutants. *Progerin* is missing 50 aa residues at the C-terminus (including the cleavage site at Leucine 647), and is permanently farnesylated at terminal Cysteine. *Progerin-CS* has an additional mutation at this C-terminal Cysteine, replacing it with Serine, so farnesylation is prevented, which partially rescues

tethering. **F.** Quantitation of chromatin intensity at the nuclear margin measured using the "Freehand Line" tool in Fiji. **G.** Distance from the chromocenter midpoint to the nuclear periphery. **H.** Chromocenter number per cell. Black datapoints and error bars are the mean intensity values from each biological replicate (30 cells each; circles) ± SEM. $p < 0.0001$, one-way ANOVA with Tukey's post-hoc test. ***$p < 0.001$, ****$p < 0.0001$, ANOVA with Tukey's post-hoc test. Data are compared to negative control pCIG and positive control wild-type Lamin A average values generated from replicates in Figure 5.1.

To examine whether permanent farnesylation underlies the loss of tethering by progerin, we next tested a progerin mutant that lacks the ZMPSTE24 cleavage site, but additionally contains a C663S mutation that abrogates the thiol sidechain required for CAAX box farnesylation (Progerin-CS). Strikingly, this farnesylation incompetent mutant regained partial tethering ability - with facultative HC (fHC) being tethered at the nuclear lamina (Figure 5.10D-F).

To further confirm that failure to tether HC is due to permanent farnesylation, and not due to the 50 amino acid deletion, we next examined LA L647R. The L647R substitution retains the 50 amino acid lost in progerin, but prevents LA C-terminal cleavage leading to permanent farnesylation and progeria[142]. Interestingly, LA L647R also failed to tether HC, suggesting that cleavage/defarnesylation is critical (Figure 5.11C-F). Moreover, addition of the C663S mutation (LA L647R-CS) restored some tethering activity (Figure 5.11D-F). Thus, farnesylation-incompetent progeroid mutants regained partial tethering ability.

Taken together, these data indicate that both, cleavage and defarnesylation are essential for HC tethering competence.

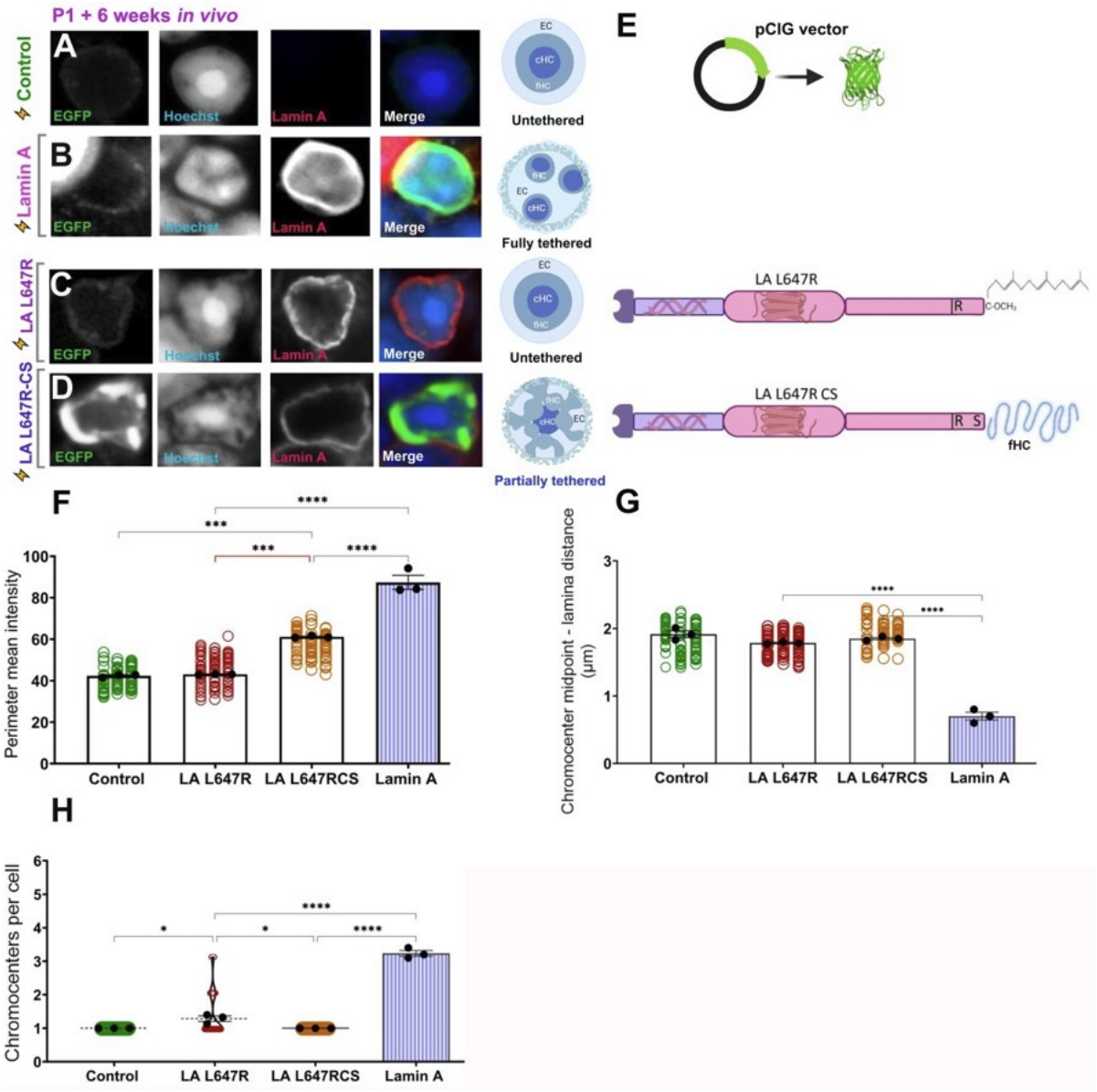

Figure 5.11. Abolished tethering in progeroid misprocessed mutant LA L647R is partially recovered via defarnesylation.

Airyscan confocal imaging of rod photoreceptors transfected with GFP-expressing empty vector control (**A**), Lamin A (**B**), along with Lamin A L647R (**C**), or Lamin A L647R-CS (**D**) constructs and harvested after 6 weeks. **E**) Illustration of post-translational mutants. *LA L647R* is a point mutant that abolishes the cleavage site and is permanently farnesylated. *LA L647R-CS* point mutant has an additional mutation at C-terminal Cysteine, replacing it with Serine, so farnesylation is prevented, which partially rescues tethering. **F.** Quantitation of chromatin

intensity at the nuclear margin measured using the "Freehand Line" tool in Fiji. **G.** Distance from the chromocenter midpoint to the nuclear periphery. **H.** Chromocenter number per cell. Black datapoints and error bars are the mean intensity values from each biological replicate (30 cells each; circles) ± SEM. $p < 0.0001$, one-way ANOVA with Tukey's post-hoc test. ***$p < 0.001$, ****$p < 0.0001$, ANOVA with Tukey's post-hoc test. Data are compared to negative control pCIG and positive control wild-type Lamin A average values generated from replicates in Figure 5.1.

5.4. The unique lamin A C-terminus is sufficient to tether facultative heterochromatin

In order to test the sufficiency of the LA C-terminus, we reasoned that it would need to be expressed in the context of a functional full-length lamin protein. We therefore fused the N-terminus of the tethering incompetent LB1 protein, with the LA IG-fold and C-terminal domains to generate a recombinant Lamin BA protein.

We found it was able to tether HC from the outer chromocenter layer to the nuclear periphery, and localizing at the NL (Figure 5.12C). Lamin BA produced the "partial tethering" phenotype that was very similar to the Progerin-CS and LA L647R-CS constructs, pulling what appears to be the fHC at the nuclear lamina.

Interestingly, wild-type LA is observed to produce the "partial tethering" phenotype in some instances (Figure 5.13). This suggests that the HC tethering mechanism observed in Lamin BA and LA-CS mutants is identical to wild-type LA, but exhibited at a quantitatively reduced level.

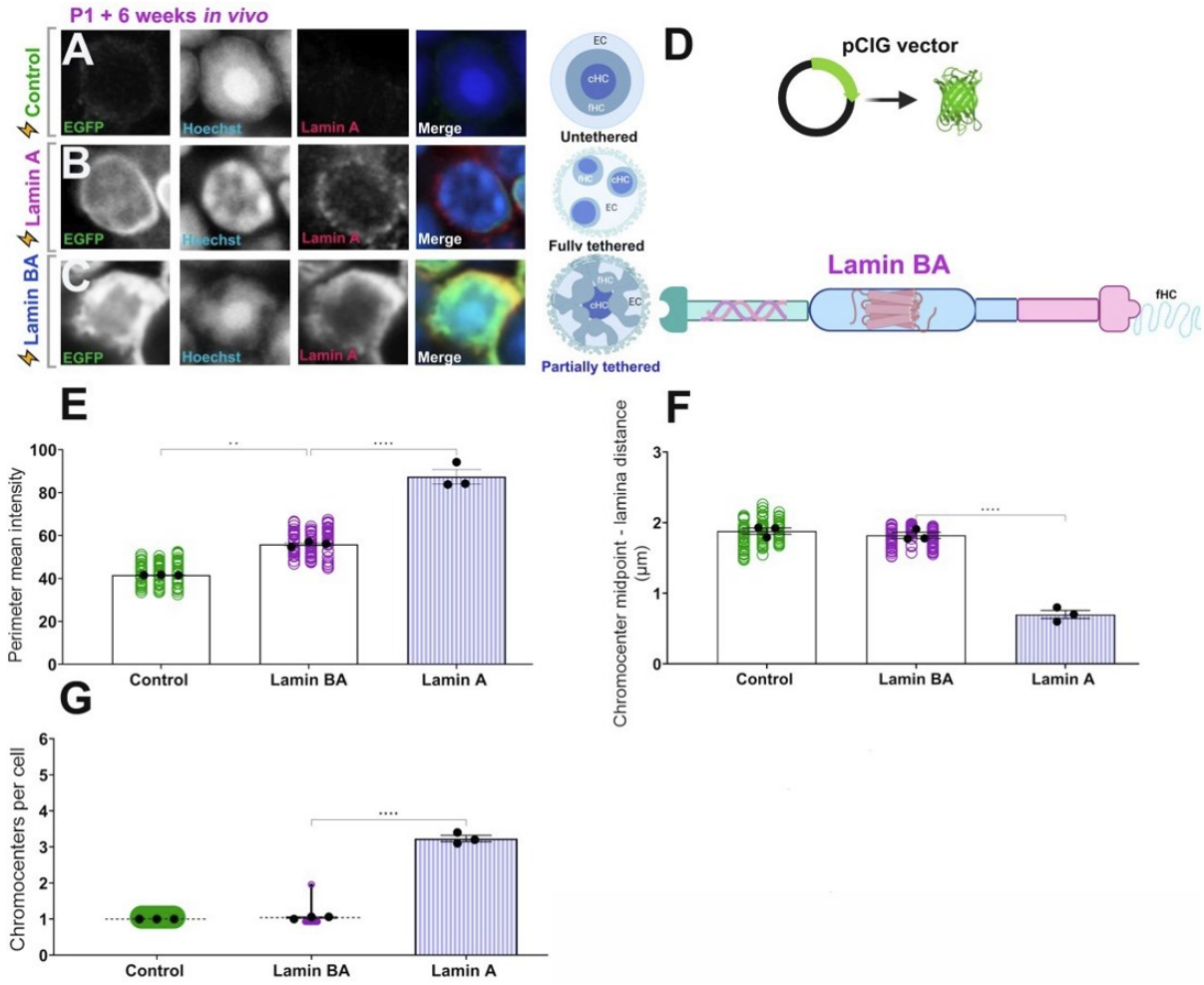

Figure 5.12. The unique Lamin A C-terminus is sufficient to tether heterochromatin.

Airyscan confocal imaging of rod photoreceptors transfected with GFP-expressing empty vector control (**A**), Lamin A (**B**), along with a Lamin BA construct (**C**), and harvested after 6 weeks. **D.** Illustration of lamin BA recombinant protein. *Lamin BA* is a recombinant protein between N-terminal domain of lamin B1 and C-terminal domain of lamin A (534 to 664), partially tethering HC. **E.** Quantitation of chromatin intensity at the nuclear margin measured using the "Freehand Line" tool in Fiji. **F.** Distance from the chromocenter midpoint to the nuclear periphery. **G.** Chromocenter number per cell. Black datapoints and error bars are the mean intensity values from each biological replicate (30 cells each; circles) ± SEM. $p < 0.0001$, one-way ANOVA with Tukey's post-hoc test. ***$p < 0.001$, ****$p < 0.0001$, ANOVA with Tukey's post-hoc test. Data are compared to negative control pCIG and positive control wild-type Lamin A average values generated from replicates in Figure 5.1.

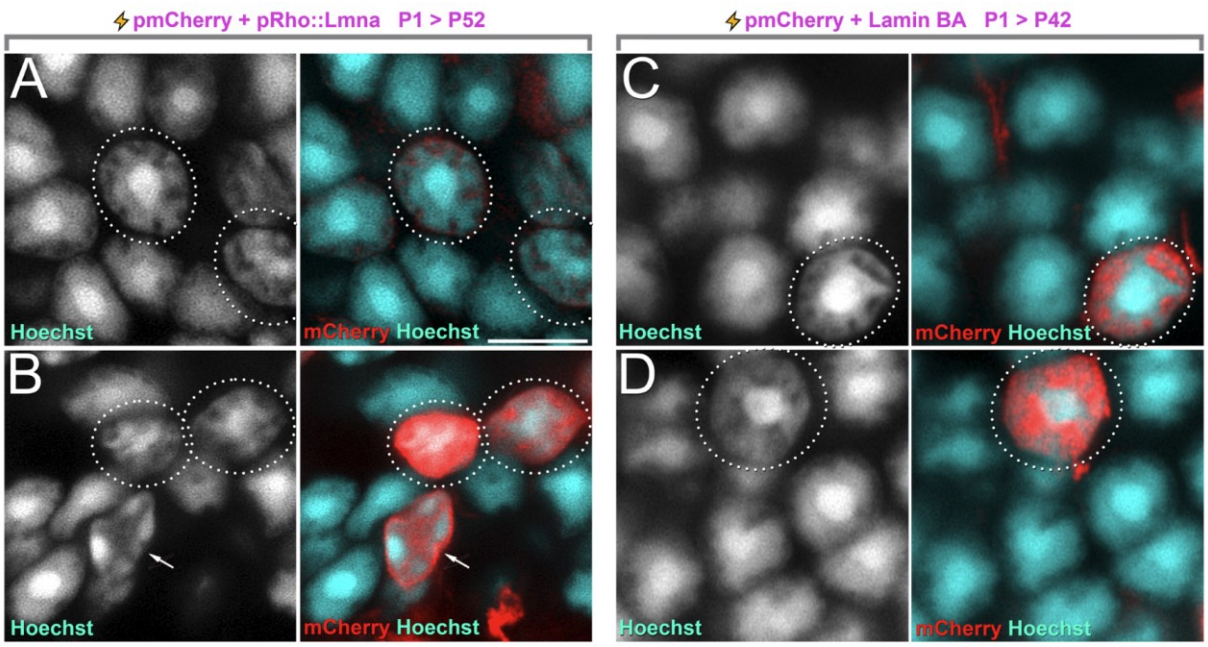

Figure 5.13. Wild-type Lamin A and Lamin BA partial tethering phenotype.

Airyscan confocal imaging of rod photoreceptors transfected with mCherry (red) and pRho Lamin A at P1 and harvested at P52 (**A**, **B**), along with mCherry (red) and Lamin BA at P1 and harvested at P42 (**C**, **D**).

5.5. Bypassing of Lamin A post-translational processing does not affect heterochromatin tethering

Finally, to determine whether post-translational processing is neccessary for targeting of LA to the nuclear lamina, we tested a LA 646-Stop construct designed to generate a mature form of LA that bypasses all processing steps. However, although it was never farnesylated, LA 646-Stop was normally incorporated into the NL and tethered HC at similar levels vs. wild-type LA (Figure 5.14C-F). These data suggest that mature LA protein is competent to tether HC, whether it is directly synthesized or post-translationally processed, similar to reports from Coffinier et al[308].

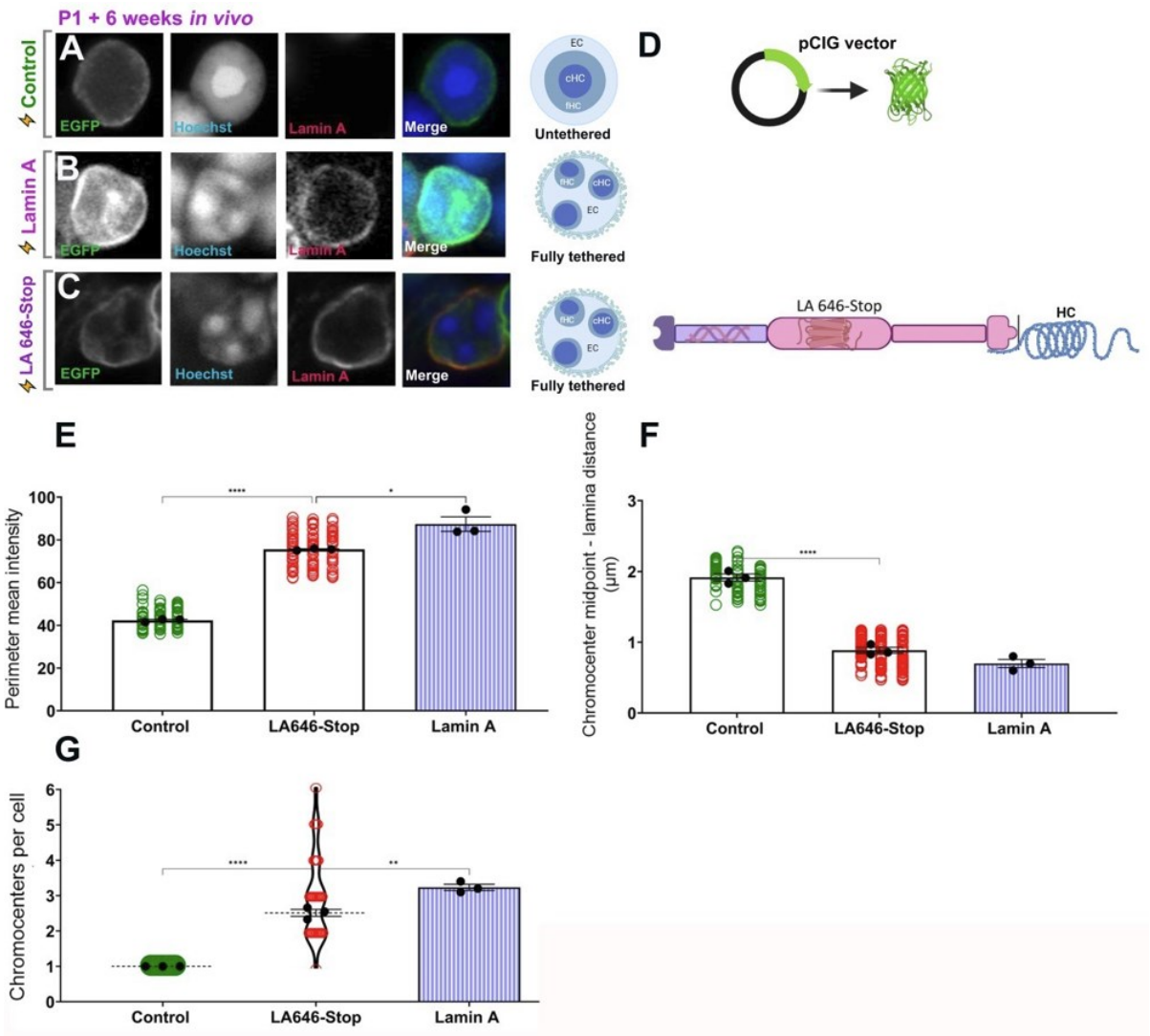

Figure 5.14. Bypassing post-translational processing does not alter heterochromatin tethering.

Airyscan confocal imaging of rod photoreceptors transfected with GFP-expressing empty vector control (**A**), Lamin A (**B**), Lamin A 646-Stop (**C**) constructs and harvested after 6 weeks. **D.** Illustration of post-translational mutants. *LA 646-Stop* terminates at the mature lamin A residues so it doesn't go through farnesylation/cleavage and defarnesylation. **E.** Quantitation of chromatin intensity at the nuclear margin measured using the "Freehand Line" tool in Fiji. **F.** Distance from the chromocenter midpoint to the nuclear periphery. **G.** Chromocenter number per cell. Black datapoints and error bars are the mean intensity values from each biological replicate (30 cells each; circles) ± SEM. $p < 0.0001$, one-way ANOVA

with Tukey's post-hoc test. ***$p < 0.001$, ****$p < 0.0001$, ANOVA with Tukey's post-hoc test. Data are compared to negative control pCIG and positive control wild-type Lamin A average values generated from replicates in Figure 5.1.

5.6. Histone modifications demarcating heterochromatin tethering

Next, to determine which type of HC is tethered by LA, we performed IHC experiments on several histone marks. To test the Alphafold3 modeling predictions, we performed IHC staining for H3K9me2 on untransfected and LA transfected rod nuclei (Figure 5.15). Accordingly, LA can relocate H3K9me2, which seems to mark fHC in the untethered and tethered nuclei.

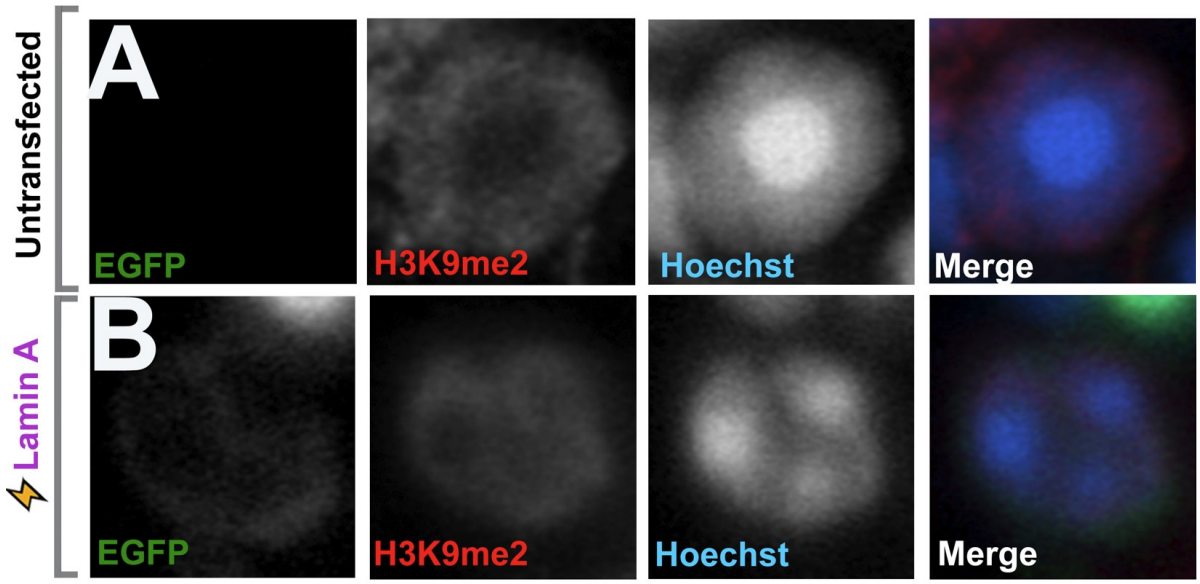

Figure 5.15. H3K9me2 heterochromatin mark deposition by wild-type Lamin A.

Airyscan confocal imaging of untransfected rod photoreceptor (**A**), and transfected rod with Lamin A (**B**) construct and harvested after 6 weeks. Nuclei were stained for H3K9me2.

Next, we performed IHC experiments for H3K9me3 constitutive HC mark. In nuclei transfected with a control GFP plasmid, the H3K9me3 marked the central constitutive HC (cHC), while H3K9me3 marked the chromocenters in wild-type LA transfected rods and appeared to be pulled towards the periphery. In LA L647R-CS transfected rods, where HC is tethered more weakly, H3K9me3 was pulled to the periphery in correlation with whorls of denser chromatin (Figure 5.16).

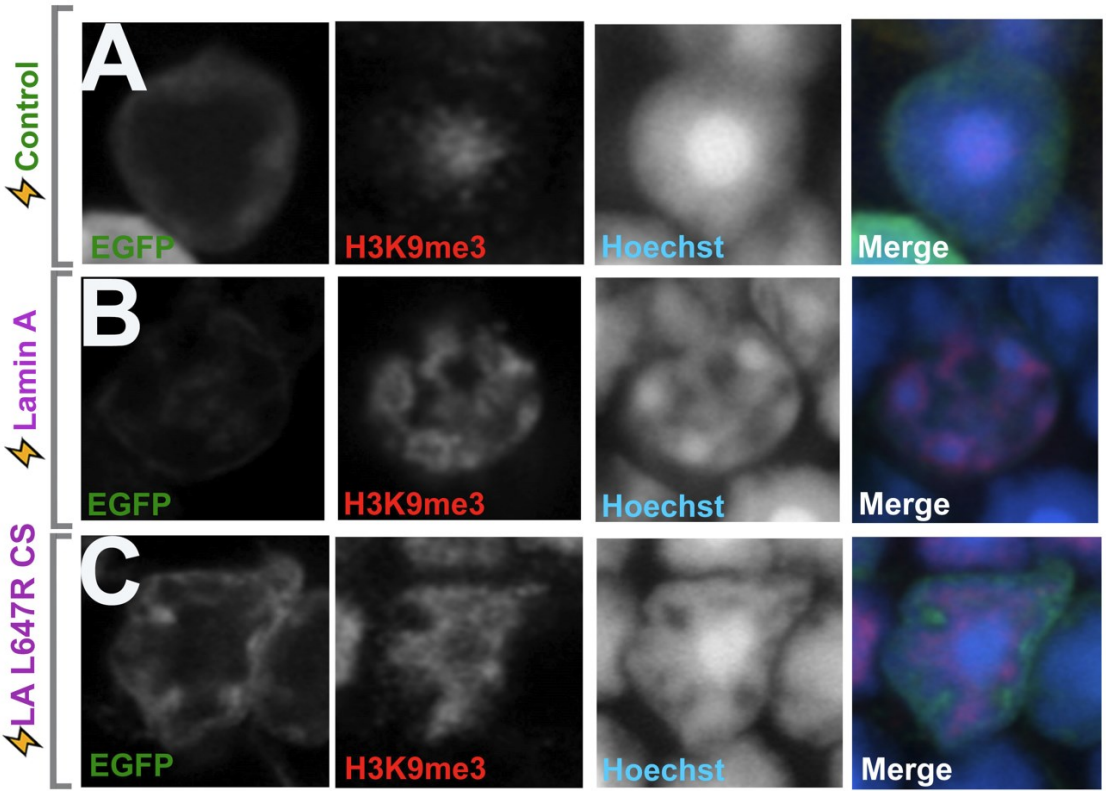

Figure 5.16. H3K9me3 constitutive heterochromatin mark deposition by defarnesylated Lamin A L647R-CS mutant. Airyscan confocal imaging of rod photoreceptors transfected with GFP-expressing empty vector control (**A**), along with Lamin A L647R (**B**), or Lamin A L647R-CS (**C**) constructs and harvested after 6 weeks. Nuclei were stained for H3K9me3.

To examine whether LA C-terminus is indeed sufficient to interact with fHC and cHC, we performed IHC experiments for H3K9me3 and H3K27me3 which demarcate cHC and fHC, respectively (Figure 5.17, 5.18).

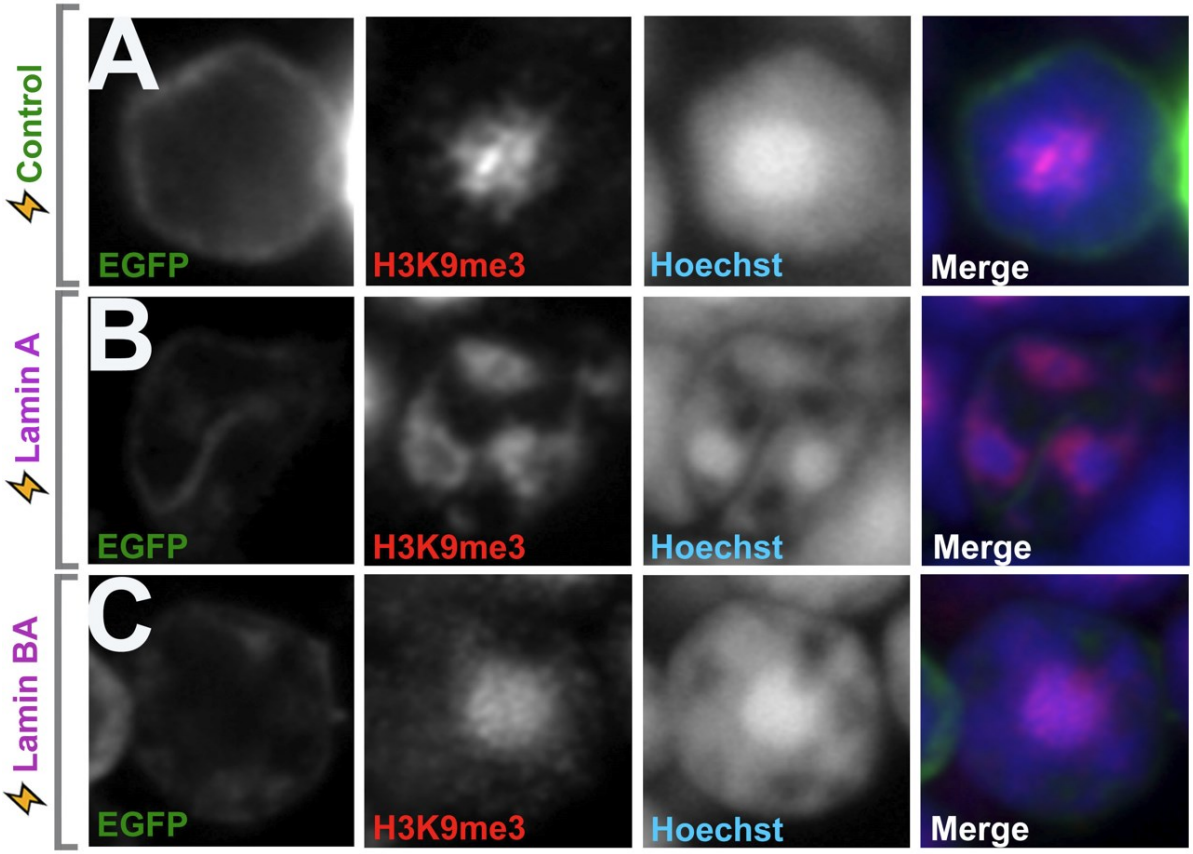

Figure 5.17. H3K9me3 constitutive heterochromatin mark deposition by Lamin BA recombinant protein.

Immunohistochemistry for facultative heterochromatin mark H3k27me3 (red). Airyscan confocal imaging of rod photoreceptors transfected with GFP-expressing empty vector control (**A**), wild-type Lamin A (**B**) and Lamin BA (**C**).

H3K9me3 marked the central chromocenter (Figure 5.17A). In LA transfected nuclei, we found that H3K27me3 fHC mark appeared to surround the chromocenters on the periphery

(Figure 5.18B), while H3K9me3 was mainly limited to chromocenters (Figure 5.17B). In accordance with partial tethering phenotype, Lamin BA affected the H3K27me3 mark, relocalizing it towards the nuclear periphery (Figure 5.18C), with little effect on H3K9me3 (Figure 5.17C).

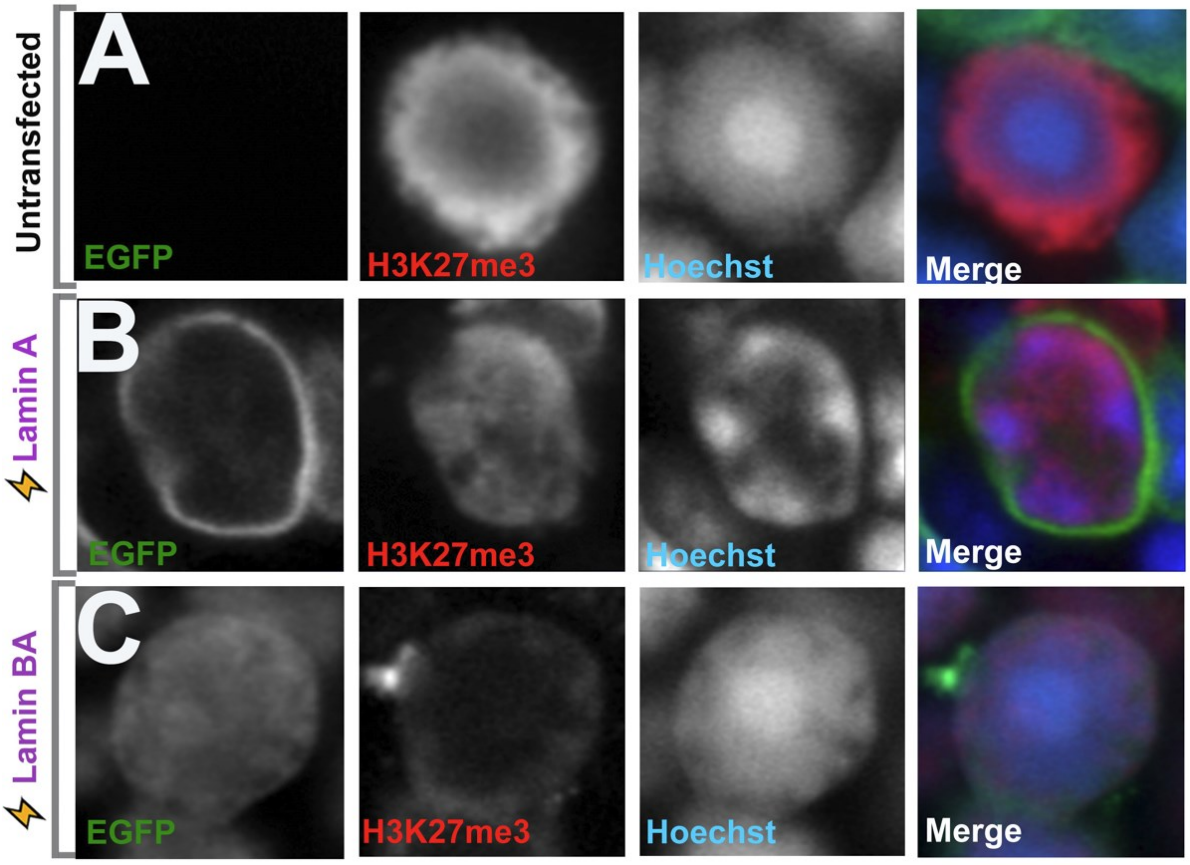

Figure 5.18. H3K27me3 facultative heterochromatin mark deposition by Lamin BA recombinant protein.

Immunohistochemistry for facultative heterochromatin mark H3k27me3 (red). Airyscan confocal imaging of rod photoreceptors transfected with GFP-expressing empty vector control (**A**), wild-type Lamin A (**B**) and Lamin BA (**C**).

In nuclei transfected with a control GFP plasmid, H3K27me3 marked the LINE-rich outer heterochromatic ring, and dimly stained the peripheral EC as well as the central constitutive HC (cHC) (Figure 5.18A). These data suggest that LA is sufficient for tethering of facultative and/or LINE-rich HC (marked by H3K27me3), and might tether cHC (ie. the chromocenters) marked by H3K9me3 more indirectly.

5.7. Laminopathic mutants affect heterochromatin recessively, but cell shape dominantly

A key advantage of the rod photoreceptor model system is that it allows the functions of individual LA variants and isoforms to be examined without interference from any other A-type lamins that might potentially provide compensation. However, in most cells, LA variants are expressed heterozygously. To examine if HC tethering by wild-type LA would be disrupted by laminopathic point mutants, we misexpressed LA along with progerin (Figure 5.19C). We found that when co-expressed together, wild-type LA continued to tether HC with progerin making no detectable impact (Figure 5.19). These results predict that laminopathic mutations will affect HC tethering in a recessive manner.

In previous work, we showed that LA transfected rods exhibit alterations in nuclear position and appeared elongated[219]. LA affects the stiffness and shape of the nucleus – both by providing intrinsic rigidity and by interacting with the Linker of Nucleoskeleton and Cytoskeleton (LINC) complex, which transduces forces between the nuclear and cytoplasmic cytoskeletons. We therefore additionally analyzed the shape of the rod nuclei transfected with LA progeroid mutants.

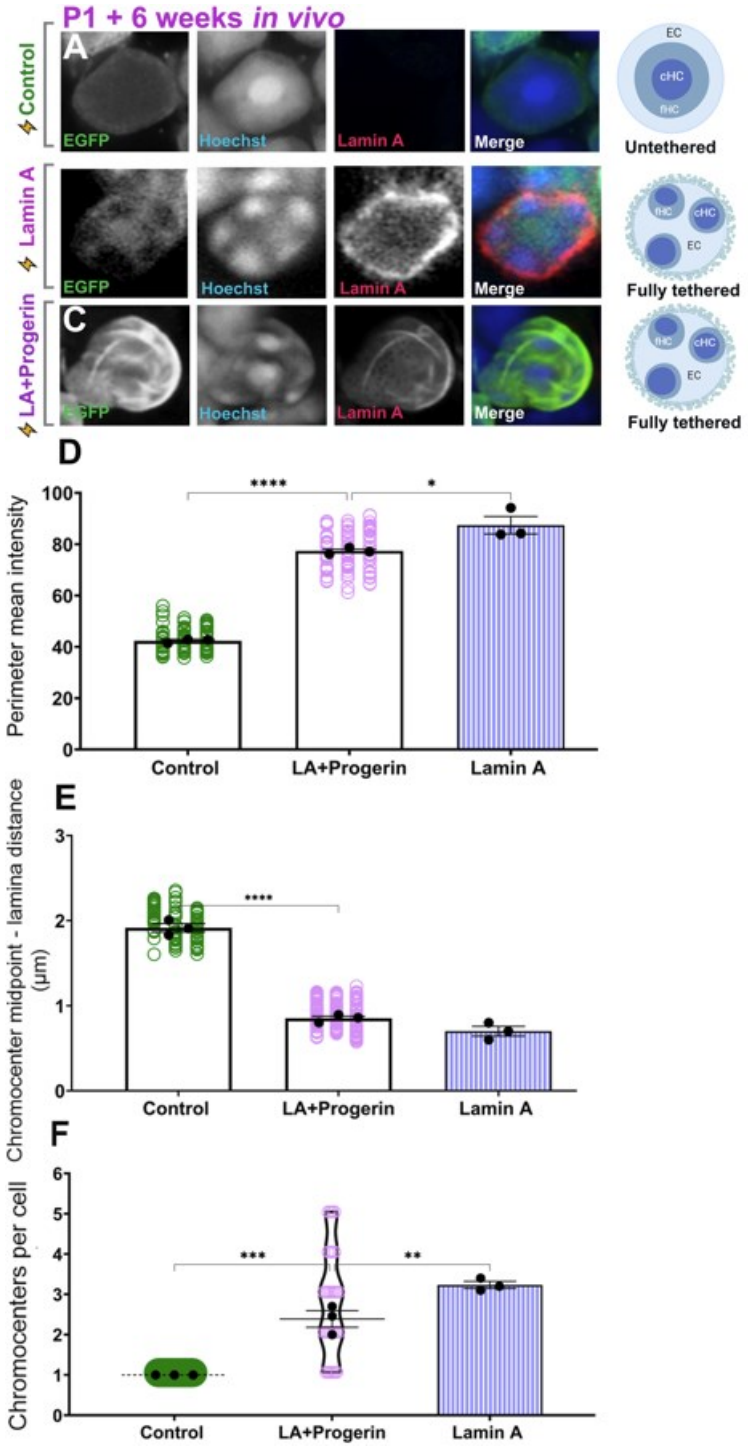

Figure 5.19. Lamin A and Progerin co-expression in rods.

Airyscan confocal imaging of rod photoreceptors transfected with GFP-expressing empty vector control (**A**), Lamin A (**B**), Lamin A and Progerin (**C**) constructs, and harvested after 6 weeks. **D.** Quantitation of chromatin intensity at the nuclear margin measured using the

"Freehand Line" tool in Fiji. **E.** Distance from the chromocenter midpoint to the nuclear periphery. **F.** Chromocenter number per cell. Black datapoints and error bars are the mean intensity values from each biological replicate (30 cells each; circles) ± SEM. $p < 0.0001$, one-way ANOVA with Tukey's post-hoc test. ***$p < 0.001$, ****$p < 0.0001$, ANOVA with Tukey's post-hoc test. Data are compared to negative control pCIG and positive control wild-type Lamin A average values generated from replicates in Figure 5.1.

Since rod nuclei are usually spherical or hexagonal in shape, we reasoned that nuclear length and perimeter measurements would reveal cell shape distortions. We found that LA significantly increased nuclear length (elongation) and deviated from the circular shape (circularity), but progeroid mutants distorted nuclear shape significantly more than wild-type LA (Figure 5.20A, B). This distortion was greatly diminished when progerin was modified with the C-terminal CS mutation. Similar results were seen with LA L647R and LA L647R-CS (Figure 5.20A, B). These data might suggest that increased tethering can ameliorate nuclear shape phenotypes. However, when we co-expressed progerin with wild-type LA, tethering was fully restored (Figure 5.19B) but the nuclear shape phenotype was not rescued (Figure 5.20A, B). Taken together, these data suggest that the nuclear distortions associated with laminopathic mutations are intrinsic to the cytoskeleton, and likely modified by farnesylation, but are not modified by lamina-HC interactions. Moreover, they suggest that laminopathic mutants have a dominant action on nuclear shape that cannot be rescued by wild-type LA in trans.

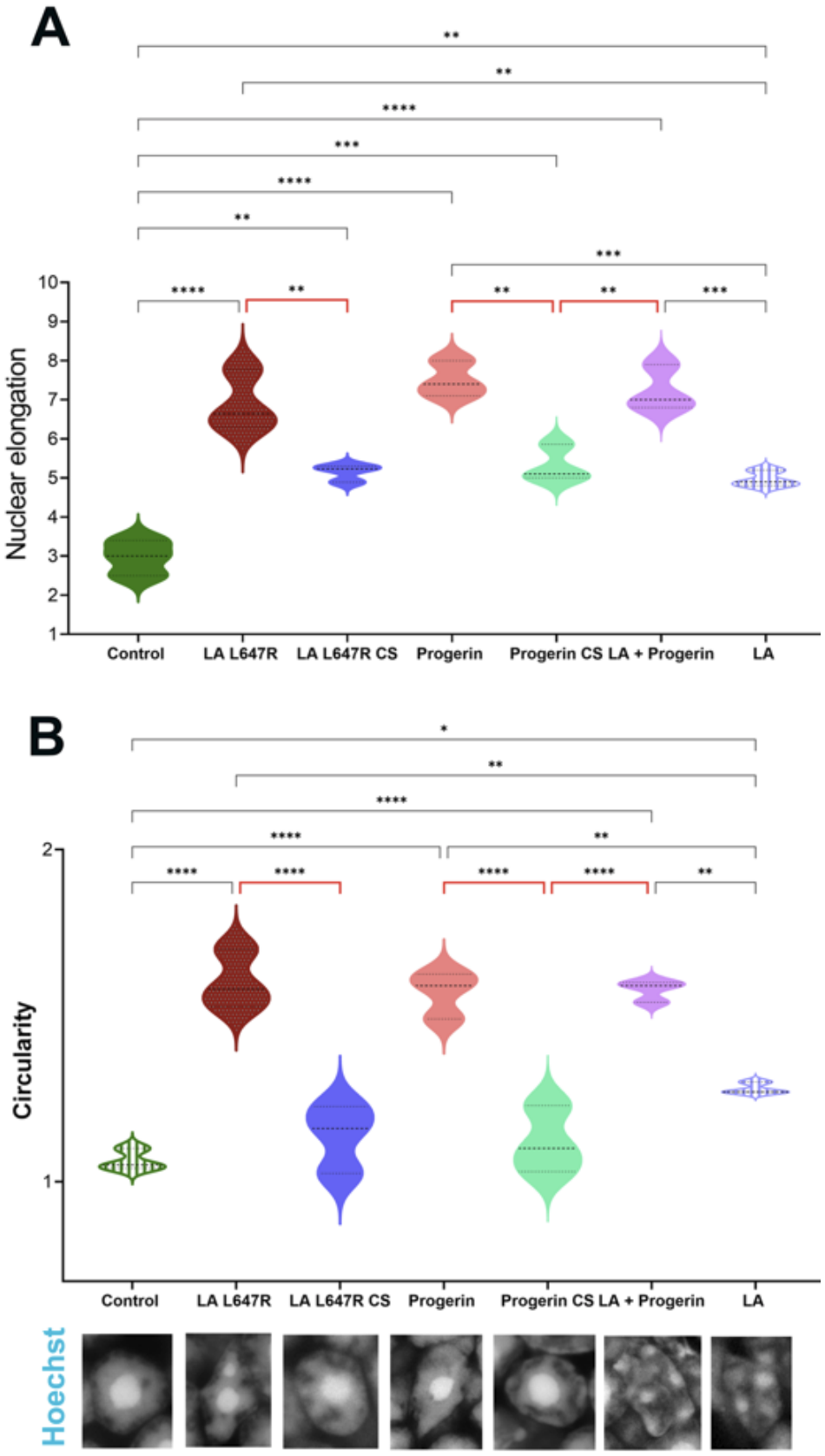
A
Nuclear elongation
Control
LA L647R
LA L647R CS
Progerin
Progerin CS
LA + Progerin
LA
B
Circularity
Hoechst

Figure 5.20. Defarnesylation can reverse elongated progeroid nuclear phenotypes.

A. Quantitation of the length of the nuclei using the "Straight line" tool in Fiji with microscopy images (Hoechst) of the nuclei. Defarnesylated mutants (LA L647R CS, Progerin CS) induce less elongated nuclei versus progeroid mutants (LA L647R, Progerin). **B**. Circularity ($Perimeter^2/4\pi Area$). Violin plots are compiled from biological replicates (30 cells each; n=3) ± SEM. $p < 0.0001$, one-way ANOVA with Tukey's post-hoc test. ***$p < 0.001$, ****$p < 0.0001$, ANOVA with Tukey's post-hoc test.

Discussion

Lamins have a well-established connection to genome organization. Fibroblasts from patients harboring laminopathic mutations were repeatedly shown to exhibit reduced peripheral HC and loss of epigenetic marks such as H3K9me3 and H3K27me3 within the nucleus. Such epigenetic distortions were an appealing mechanistic explanation for diseases like progeria, in which the striking acceleration of aging seemed unlikely to be due to structural defects in cells or tissues alone. Moreover, *Lmna* knockouts were shown to lose HC tethering in particular cell types[66]. However, whether nuclear lamins were sufficient to tether HC was much less clear. Rod photoreceptors have been a key model system with which to resolve such questions, and while rods do not express A-type lamins, they do express structurally similar B-type lamins. Moreover, transgenic misexpression of LC in rods had no effect on HC. In previous work[66] as well as this study, we showed that LA can tether HC[219], and confirmed that LC cannot. However, these data do not resolve the key question of <u>how</u> LA might tether HC. Indeed, the only difference between LA and LC is approximately 100 C-terminal amino acids that do not contain a DNA or chromatin-binding domain.

Here, we addressed this question by using a combination of molecular modelling and tethering sufficiency assays in rod photoreceptors. Our data collectively suggest that defarnesylation is absolutely required for HC tethering. Interestingly, using *Drosophila* polytene chromosomes [309] it has been demonstrated that defarnesylated B-type lamins might be competent to tether HC. However, B-type lamins don't have the corresponding 'interface' amino acids (578-585) found to contact the nucleosomes in LA Alphafold3 modeling. Moreover, our modelling predicts that the C-terminus of LA takes on a conformation that enables direct Van der Waals bonding between histone subunits and the LA C-terminus (Figure 5.21).

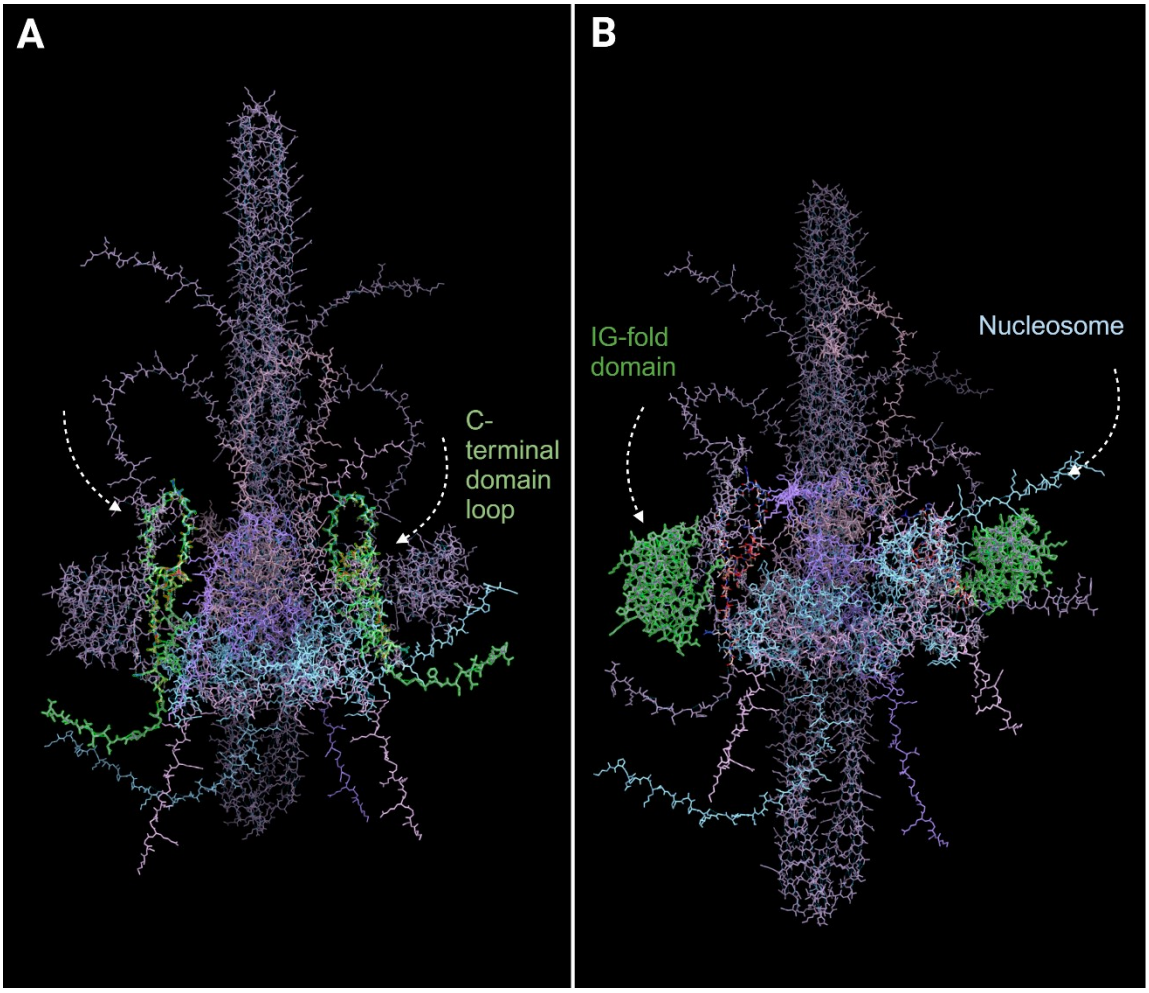

Figure 5.21. Alphafold3 modelling of the Lamin A dimer C-terminal loop configuration in order to contact H3K9me2.

The IG-fold of Lamin A takes on a conformation that enables direct Van der Waals bonding between histone subunits and the Lamin A C-terminus.

This prediction already has experimental support from the Misteli lab, who previously showed that an interval spanning the IG-fold through to the LA C-terminus is sufficient to bind histone H3 *in vitro*, with a preference for H3K9me2 modifications[91]. The C-terminal amino acids that are unique to LA and not shared with B-type lamins or LC, appear to directly bond with histones, as suggested by the Medalia lab[306]. An interface of residues that follow the IG-fold domain appear to make the majority of lamin-histone Van der Waals bonds. These residues are present in progerin, but are absent in B-type lamins and LC. However, the lack of tethering in progerin can be explained by a conformational change that fails to form contacts with the nucleosomes, as predicted with Alphafold3.

In modelling results, lamins normally took on filamentous braided structures, but were reconfigured into hoop like structures that encircled nucleosomes. We think that these sorts of structures might be able to occur within the nucleoplasm. However, only defarnesylated LA could interact with the nucleosome while maintaining a filamentous configuration, and only when nucleosomes contained heterochromatic modifications, such as H3K9me2 or linker histones.

To test the sufficiency of the LA C-terminus to tether HC, we expressed the LA IG-fold and C-terminal domain into the N-terminus of Lamin B1, which is normally tethering-incompetent. We found that this artificial lamin BA construct was sufficient to tether HC, albeit partially.

Next, we performed immunohistochemistry in order to understand what type of chromatin was tethered. We found that wild-type LA could relocalize H3K9me2, H3K27me3 and H3K9me3 chromatin. However, H3K9me3 did not appear to directly contact the nuclear periphery. In previous comparisons between LA and Lbr, we showed that Lbr tethers chromocenters much more directly to the nuclear lamina versus LA[220], suggesting that chromocenters might be recruited to LA indirectly. Many additional results agree with this interpretation. First, Lamin BA led to reorganization of H3K27me3, but did not dramatically affect H3K9me3. Moreover, we identified several additional constructs with similar 'partial tethering' phenotypes, including Progerin-CS and LA L647R-CS. Since the latter presumably bind to the same type of HC as wild-type LA, but to a reduced degree, we think that these partial tethering phenotypes represent a quantitative difference in binding strength rather than a qualitative difference in chromatin type, but further investigation is warranted. Although we demonstrated that GFP levels do not correlate with tethering levels (Figure 5.2G), GFP construct was co-expressed with LA, which means that the GFP levels might not reflect LA levels. Taken together, these results suggest a molecular logic that we think can explain HC tethering by LA (Figure 5.22). In summary, Alphafold3 predicted direct contacts between the unique LA C-terminus (578 – 585, V629 in green) and H2/H4 histones in a looping conformation (similarly to Medalia critical interval *in vitro* 579 – 585 in purple). We find that LA IG-fold domain residues (orange/red) are crucial for tethering conformation (similar to Misteli critical intervals in blue). We show unique LA C-terminus (in pink) is sufficient for tethering of the fHC and required for cleavage/defarnesylation.

Interestingly, CS-mutants did not achieve full tethering effect like wild-type LA. Partial tethering CS mutant phenotypes might be due to lack of cleavage. This is the main structural

difference between LA-L647R-CS and wild-type LA after C-terminal processing. Indeed, when simulated in Alphafold3, uncleaved LA, even if it isn't farnesylated, doesn't bind nucleosomes well.

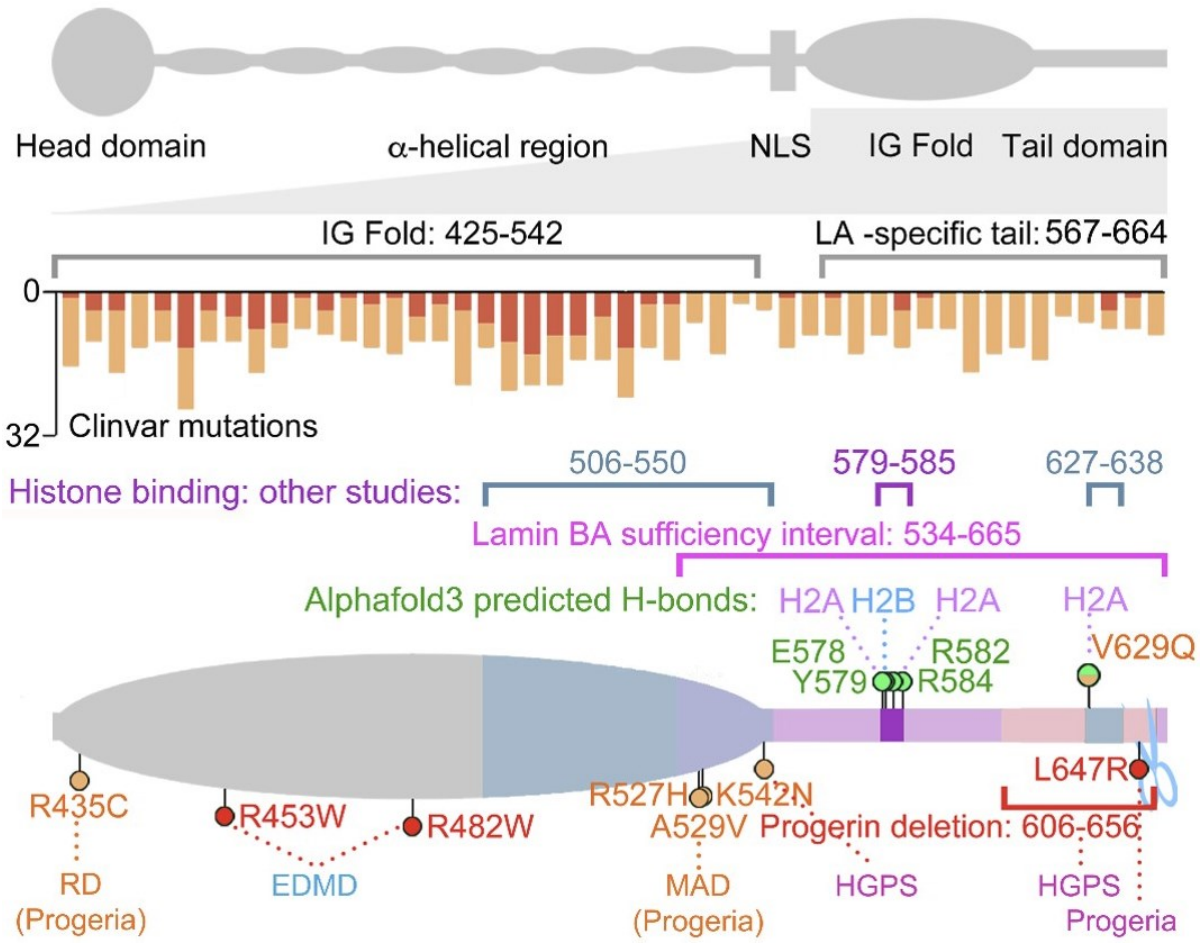

Figure 5.22. Structure-function analysis of Lamin A heterochromatin tethering. Lamin A IG- fold (AA 425-542) and unique C-terminal tail (AA 565-665) domains containing mutations (via variant interpretation database ClinVar). Missense mutations (in orange) are of uncertain significance, while likely pathogenic mutations are in red. Misteli critical intervals for histone binding *in vitro* (AA 506-550, AA 627-638) highlighted in blue. Lamin BA *in vivo* sufficieny interval (AA 534-665) highlighted in pink. Medalia critical interval highlighted in purple. Alphafold3 predicted Van der Waals histone bonds (E578, Y579, S582, R584, V629)

highlighted in green. IG-fold non-progeroid and progeroid mutations reflect residues required for heterochromatin tethering (highlighted in red), whereas residues partially required for tethering are coloured in orange. See also Chapter 6 below.

On Laminopathic mutations

Lamins provide the nucleus with mechanical stability and nuclear shape, and are involved in establishing connections between the nucleoskeleton and the cytoskeleton. In addition to impacting nuclear organization, loss or mutation in lamina proteins can lead to nuclear fragility, undermine nuclear movement and cell migration, increase DNA damage or defective DNA repair[340], and lead to cell division defects. Given this pleiotropy, it is not surprising that LA mutations lead to diverse pathologies, such as muscular dystrophy, lipodystrophy, or premature aging disorders. Here, we assessed the tethering sufficiency of several LA variants. We had predicted that disruptions in HC tethering would be observed only for disorders linked to premature aging. Surprisingly, we saw defective tethering associated with most laminopathic mutants that we tested. Indeed, IG-fold mutants linked to atypical progeria were among the few variants that exhibited some residual tethering activity (Chapter 6). However, in combinatorial co-expression experiments with wild-type LA and Progerin, we found that wild-type LA could fully restore tethering – even in the presence of a LA variant associated with profound effects on the nucleus and a rapidly progressing, lethal phenotype. These data perhaps match prior work using patient fibroblasts, where effects on HC tethering have been reported, but residual tethering generally remains present. By contrast, we found that the effect of Progerin on cell shape was dominant, and not rescued by supplying wild-type LA in trans. The effect was however partially rescued by preventing farnesylation via the CS mutation.

Whereas Progerin-CS exhibited an elevated ability to tether HC, tethering was fully restored in cells expressing Progerin when LA was co-transfected, yet cell-shape was not rescued, suggesting that Progerin's dominant effect on the nucleus is intrinsic to the nucleoskeleton. We think that the results of the Progerin-CS mutation imply that this nucleoskeletal phenotype is modified by farnesylation rather than by HC interactions. Progerin contains two defects – permanent farnesylation and a 50 amino acid deletion in the LA C-terminus. Interestingly, in our hands, all progerin phenotypes were perfectly recapitulated by LA L647R, suggesting that permanent farnesylation underlies progerin phenotypes.

Taken together, our work provides a partial explanation for how LA tethers HC, while LC and B-type lamins do not. We find that the LA C-terminus is necessary to allow for lamin defarnesylation, and structural modelling additionally suggests that the unique C-terminus can additionally contact nucleosomes. In the future, it will be important to determine whether the amino acid residues found to form Van der Waals bonds with nucleosomes, including LA578-585, and LA V629, are required for HC tethering.

Chapter 6. Evaluation of lamin A partner protein importance in tethering

Abstract

It is increasingly clear that lamins support a broad range of cellular processes, in part, by acting as an interaction hub to interlink the nuclear lamina with a large number of proteins that function in a variety of cellular pathways. Heterochromatin (HC) is also tethered to the nuclear lamina, but the mechanisms responsible for this tethering are unclear. Mutations in A-type lamins (*LMNA*), or lamin-binding membrane proteins such as emerin (*EMD*) or lamin-B receptor (*LBR*), cause a wide range of heritable or sporadic human diseases (laminopathies), which include muscular dystrophy, cardiomyopathy and accelerated aging (progeria) syndromes, many of which are characterized by defective protein-protein interactions as well as disrupted HC tethering. Moreover, previous work by ourselves and others has shown that lamin A (LA) and LBR are sufficient for tethering of the HC to the nuclear lamina. LBR's Tudor domain has been shown to directly bind H4K20me3 rich HC. However, LA doesn't have a defined DNA binding domain. LA has been shown to be capable of binding DNA and histones directly *in vitro*, however it additionally interacts with a variety of chromatin binding proteins like Cbx (Hp1) proteins, PRR14, LEMD2/3, RBBP4 or BAF (BANF1), suggesting that it might bind chromatin indirectly. To evaluate whether LA can tether HC through these identified partners, we examined several LA protein candidates in order to identify potential members of LA-HC binding complex. However, none of these factors was capable of altering HC tethering in sufficiency assays. Comparisons between tethering competent versus incompetent LA interactomes indicate that PARP1, H2A and H4 histones are significantly

enriched in LA tethering competent interactomes. Taken together, our data suggest that LA likely associates with nucleosomes directly.

Introduction

Lamins play a crucial role in genome organization by constraining LADs and through interactions with HC at the inner nuclear membrane. Lamin A (LA) has been shown to be capable of binding naked DNA directly *in vitro*[74]. However, under these experimental conditions, proteins such as lamin C (LC) LC[73] and B-type lamins also bind DNA[74,75], and yet these latter proteins have been shown not to be capable of tethering heterochromatin (HC) *in vivo*[66]. Despite the abundance of research conducted to resolve the molecular mechanism of HC tethering, the mechanism responsible for lamin-dependent HC tethering remains unclear, due to complexity of dynamic chromatin protein-nuclear lamina (NL) interactions and the dearth of model systems that lack tethering.

Murine rod photoreceptors have recently been utilized as a convenient *in vivo* model system for understanding principles of nuclear architecture in living cells. Rod photoreceptors exhibit an inverted chromatin organization, with euchromatin (EC) localized within a ring at the nuclear periphery, and HC concentrated at the center of the nucleus. This organization is achieved in part due to a lack of HC tethers, including LA and LBR[66]. Unlike other model systems, in which genetic mutations disrupt HC tethering, the inverted organization of murine rod photoreceptors arises in the absence of pathology or phenotypes. Moreover, rod photoreceptors convert between conventional and inverted organization during development[208] and degeneration[193,220]. Rod photoreceptors are therefore an ideal model with which to understand molecular mechanisms of genome partitioning and HC tethering at the nuclear periphery[310,66,214,215].

Since LA/C knockout leads to chromatin inversion in cell types such as dermal fibroblasts, but transgenically expressed LC in mouse rods did not lead to HC tethering[66], previous studies concluded that LA/C is necessary but not sufficient for HC tethering, and likely requires a partner protein for tethering[66]. According to this model, the absence of tethering exhibited by LC would reflect the requirement for a second protein that is absent or insufficiently expressed in rod photoreceptors. While we later showed that misexpression of LA by itself is sufficient to tether HC in rods, this does not negate the idea that additional proteins are required to mediate the interaction between A-type lamins and HC. If so, modifying the levels of these adapters would be expected to modify HC tethering. Here, we wished to address the hypothesis that LA/C tethers HC indirectly through an adapter protein.

While LA lacks a known DNA binding motif, it additionally interacts with a variety of chromatin binding proteins. Genetic and biochemical data nominate several partner proteins as potential mediators of LA-dependent HC tethering. Researchers have described 337 LA/C–interacting proteins in total[64], although many of these proteins may bind LA/C indirectly. Moreover, several of these partner proteins require LA/C for their positioning at the NL, since they mislocalize in absence of A-type lamins[311]. It has been established that emerin is a dispensable component of the LA/C-dependent HC tether[66]. It is also reported that a LEM-domain protein mutation, which disrupts interaction with LA, causes dilated cardiomyopathy[312]. In humans, *LEMD2* mutations have also been linked to arrhythmic cardiomyopathy[313] and a benign progeroid disorder[314]. Intriguingly, the lamin -interacting protein BAF (BANF1) has also been suggested to mediate the interaction between A-type lamins and chromatin, and *BANF1* mutations are associated with a form of progeria that strongly resembles a laminopathic disorder[135]. Since LA does not contain a canonical DNA

binding motif, we hypothesized that LA might potentially interact with HC through LA partner proteins, including BAF[83], RBBP4[86-90], PRR14[85], LEMD[76-78]. While all of these proteins appear to be endogenously expressed in murine rods based on transcriptomic data (Figure 6.1), we hypothesized that increasing the levels of these proteins might alter tethering in the presence of modified A-type lamins. However, in sufficiency assays, we found little evidence that these known partners affect HC tethering – either when expressed alone, or with LA. Additionally, we provide proteomic data that tethering competence increases the interaction between LA and nucleosomes. Along with our structure/function study of LA/HC interactions (Chapter 5), our data together imply that LA likely binds chromatin directly.

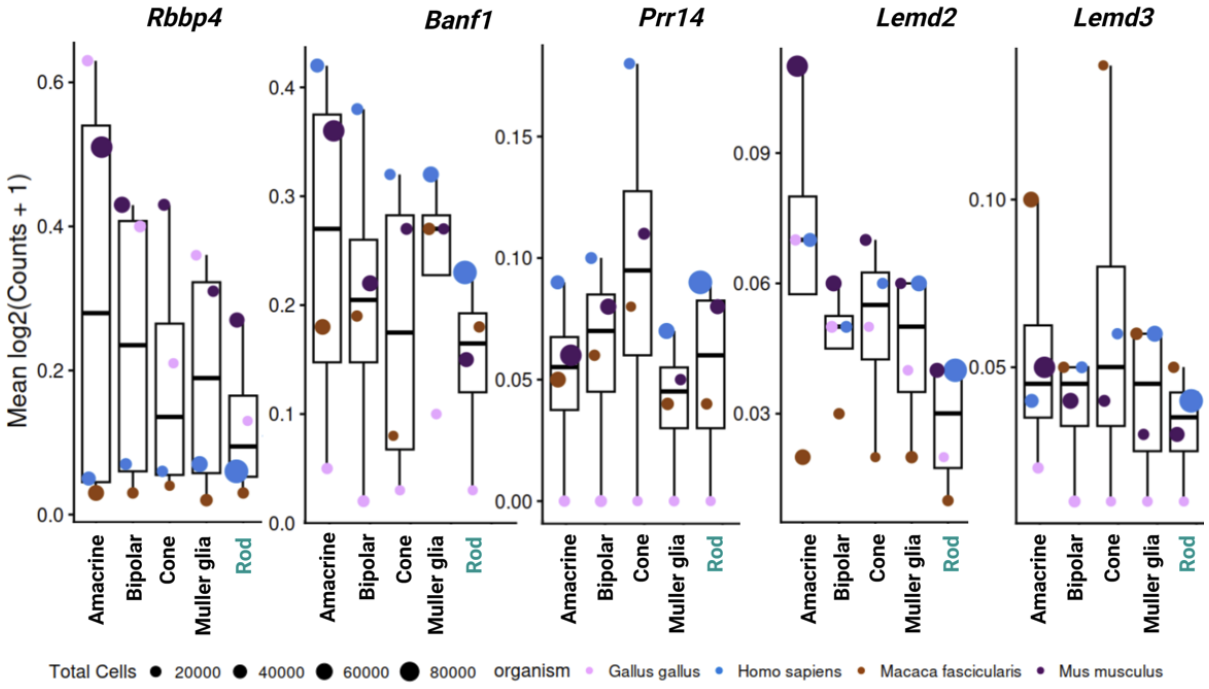

Figure 6.1. Lamin A-interacting proteins expression in the retina between species.

scRNA-seq expression data for *Rbbp4*, *Banf1*, *Prr14*, *Lemd2* and *Lemd3* obtained from chick (*Gallus gallus*), human (*Homo sapiens*), macaque (*Macaca fascicularis*), or mouse (*Mus musculus*) as indicated. The plot was generated using the *Plae* resource[262].

Results

6.1. Absence of functional tethers in the nuclear lamina of murine rod photoreceptors

The *Lmna* gene gives rise to two splice variants, LA and LC. It has been suggested that the translation of LA, but not LC, is blocked in neurons[99]. However, we previously reported that LA is the dominant *Lmna* gene transcript in murine cone photoreceptors[219]. The expression of LA by retinal neurons is further supported by immunohistochemical staining of the P42 retina (Figure 6.2A, D and Razafsky et al[216]). In contrast, the NL of rod photoreceptors is organized exclusively by B-type lamins (Figure 6.2B). Murine rod photoreceptors never express LA/C[67] (Figure 6.2A, D). Instead, the alternative tether LBR is expressed in rods during development[66] but falls below functional level threshold in adult rods (Figure 6.2C, D). LBR is responsible for the maintenance of the conventional nuclear architecture[66], prior to complete genome inversion by P28[209].

To examine the sufficiency of putative tethers, we performed retinal transfections as described above. As a negative control, we performed morphometric analysis of untransfected rods.

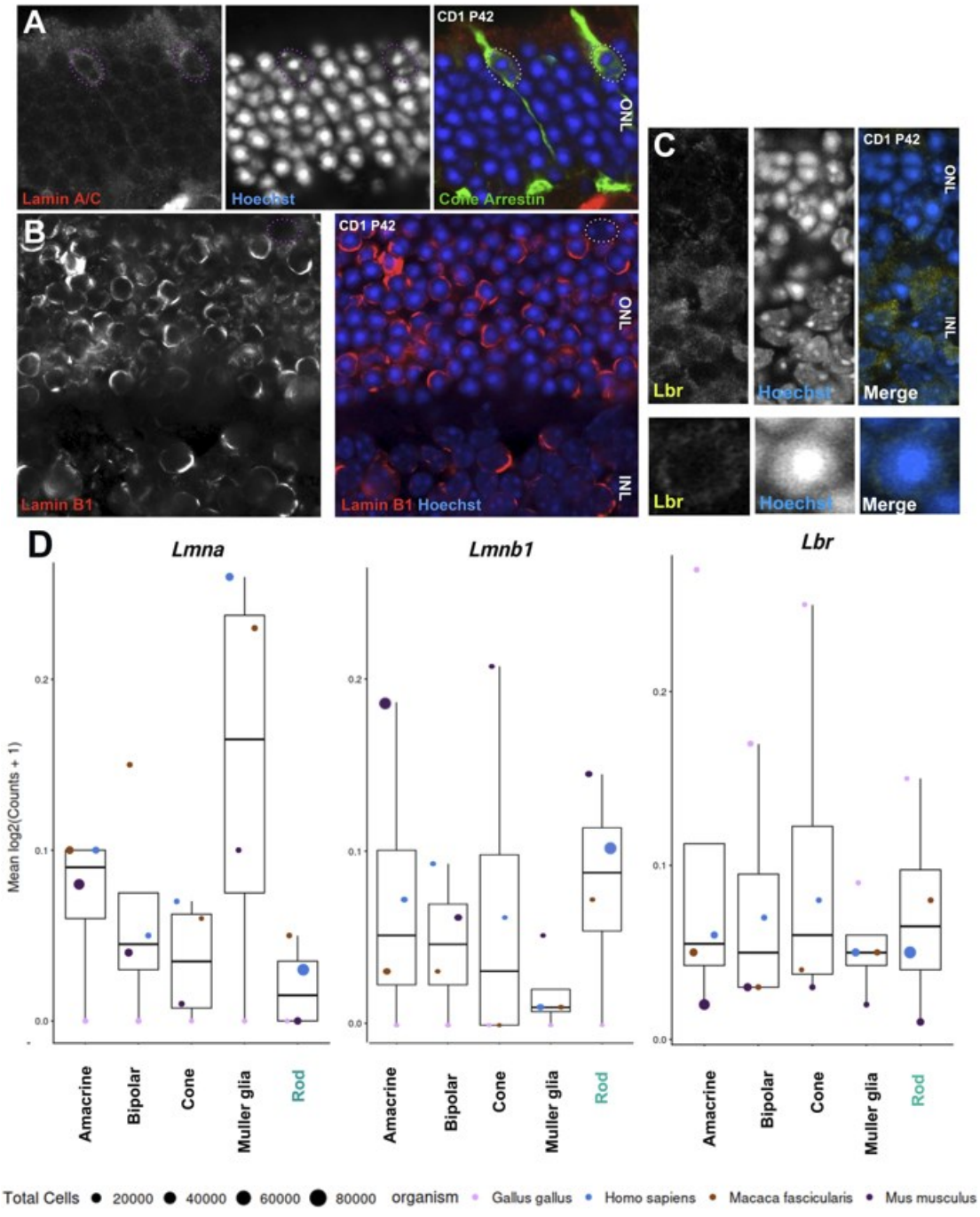

Figure 6.2. Lamin A/C, Lamin B1 and LBR expression in wild-type rod photoreceptors.

Airyscan confocal microscopy of P42 wild-type CD1, with LA/C specific antibody (red) and cone-arrestin (green) (**A**), with an Lamin B1-specific antibody (red) (**B**), and with LBR-specific antibody (yellow) (**C**). The retina was also counterstained with DNA dye Hoechst 33342 (blue). Cones are marked by cone arrestin and express Lamin A/C, while rods never

express Lamin A/C. Lamin B1 is expressed ubiquitously. (**D**) scRNA-seq expression data for *Lmna*, *Lmnb1* and *Lbr* obtained from chick (*Gallus gallus*), human (*Homo sapiens*), macaque (*Macaca fascicularis*), or mouse (*Mus musculus*) as indicated. The plot was generated using the *Plae* resource[262].

To ensure that untransfected rods were similar to rods transfected with a control plasmid, we compared EGFP-transfected cells (control) versus untransfected (neighbouring) nuclei, but found no statistical difference between the two (Figure 6.3).

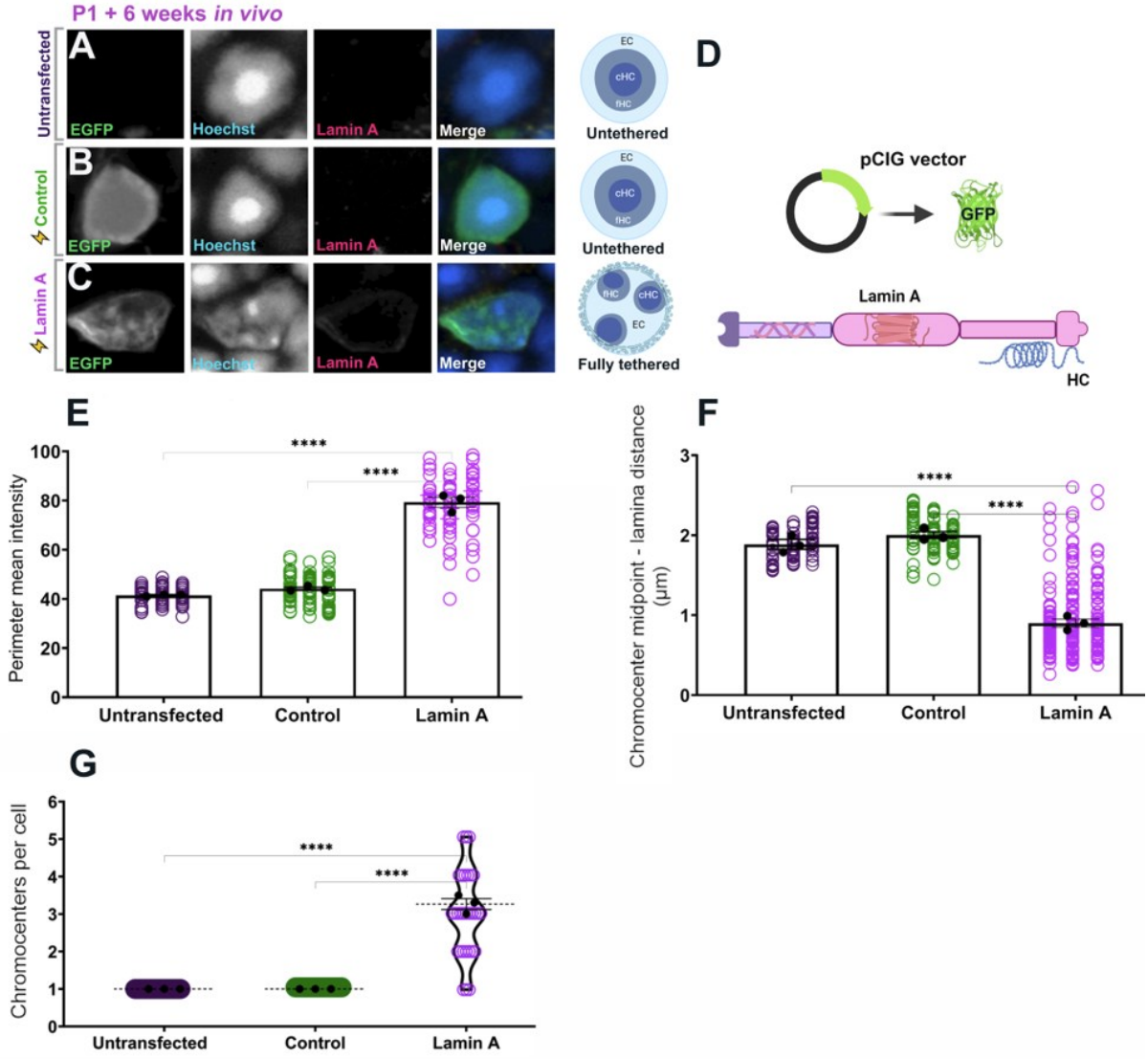

Figure 6.3. Tethering profiles of untransfected and Control (pCIG vector expressing GFP) nuclei. Airyscan confocal imaging of untransfected (**A**) and transfected rod photoreceptors with GFP-expressing empty vector control (**B**), along with Lamin A (**C**) constructs, and harvested after 6 weeks. **D.** Illustration of an empty pCIG vector and lamin A. **E.** Quantitation of chromatin intensity at the nuclear margin measured using the "Freehand Line" tool in Fiji. **F.** Distance from the chromocenter midpoint to the nuclear periphery. **G.** Chromocenter number per cell. Black datapoints and error bars are the mean intensity values from each biological replicate (30 cells each; circles) ± SEM. $p < 0.0001$, one-way ANOVA with Tukey's post-hoc test. ***$p < 0.001$, ****$p < 0.0001$, ANOVA with Tukey's post-hoc test.

Untransfected nuclei served as an internal technical control and were used to quantify the internal variation and normalize the chromatin intensity values between replicates.

6.2. BAF is dispensable for the tethering function of lamin A

The Barrier-to-Autointegration Factor (BAF; BANF1) is a chromatin-interacting protein that forms a complex between lamins and the LEM- domain family of nuclear proteins[315,316] including TMPO (LAP2α), emerin and LEMD3[317]. Interestingly, BAF protein mutation is associated with Néstor-Guillermo progeria syndrome (NGPS)[318] characterized by accelerated aging with severe skeletal abnormalities - placing BAF within the progeroid disease spectrum[319]. Besides premature aging phenotype, NGPS patients suffer from progressive bone degeneration. However, they don't exhibit signs of cardiovascular complications like HGPS patients[320]. In contrast, they suffer profound skeletal abnormalities that affect their quality of life. Additionally, the BAF, LA and emerin complex was shown to be disrupted in atypical progeroid disorders[82].

BAF-DNA complexes formed *in vitro* show remarkable stability as BAF can compact or loop DNA[320]. In photoreceptors, BAF associates indirectly (via DNA) with transcription factor Crx, and with other paired rule homeodomain proteins *in vitro*[321,322]. BAF also directly binds to histones H1.1, H3 and H4 which suggests a role in HC organization[323,324]. Moreover, depletion of BAF in *C. elegans* affects peripheral HC and gene repression[325]. BAF is thus a potential candidate for tethering chromatin through the interaction with LA.

We hypothesized that LA might depend on BAF to tether HC. In order to test if the LA interaction with BAF is indispensable for HC tethering function of LA, we obtained several homozygous IG-fold LA point mutants (R435C, K542N, R527H, A529V) associated with atypical progeroid syndromes, with reduced or no affinity for BAF (courtesy of Zinn-Justin Laboratory, France)[82]. These *LMNA* mutations are associated with progeroid laminopathies RD (R435C), HGPS (K542N), and MAD (R527H, A529V). LA R435C, LA K542N, and LA R527H lose the ability to bind BAF, while LA A529V has a significantly lower affinity for BAF. Mutants were confirmed to be well folded and had a thermal stability close to that of the wild-type LA IG-fold[82].

Nuclear-morphometric analysis revealed that ectopically expressed LA/BAF mutants were nonetheless sufficient for HC tethering in rods. However, they tethered less efficiently than wild-type LA (Figure 6.4). In all examined LA mutants, we observed occlusions (protein precipitates) in the interior of the nucleus. Since BAF is reported to form a complex with LA, LA mutations at BAF binding sites most likely interrupt the protein localization at the NL. We confirmed LA protein localization at the NL and on the occlusions in the interior of the transfected rod nuclei, using IHC (Figure 6.4).

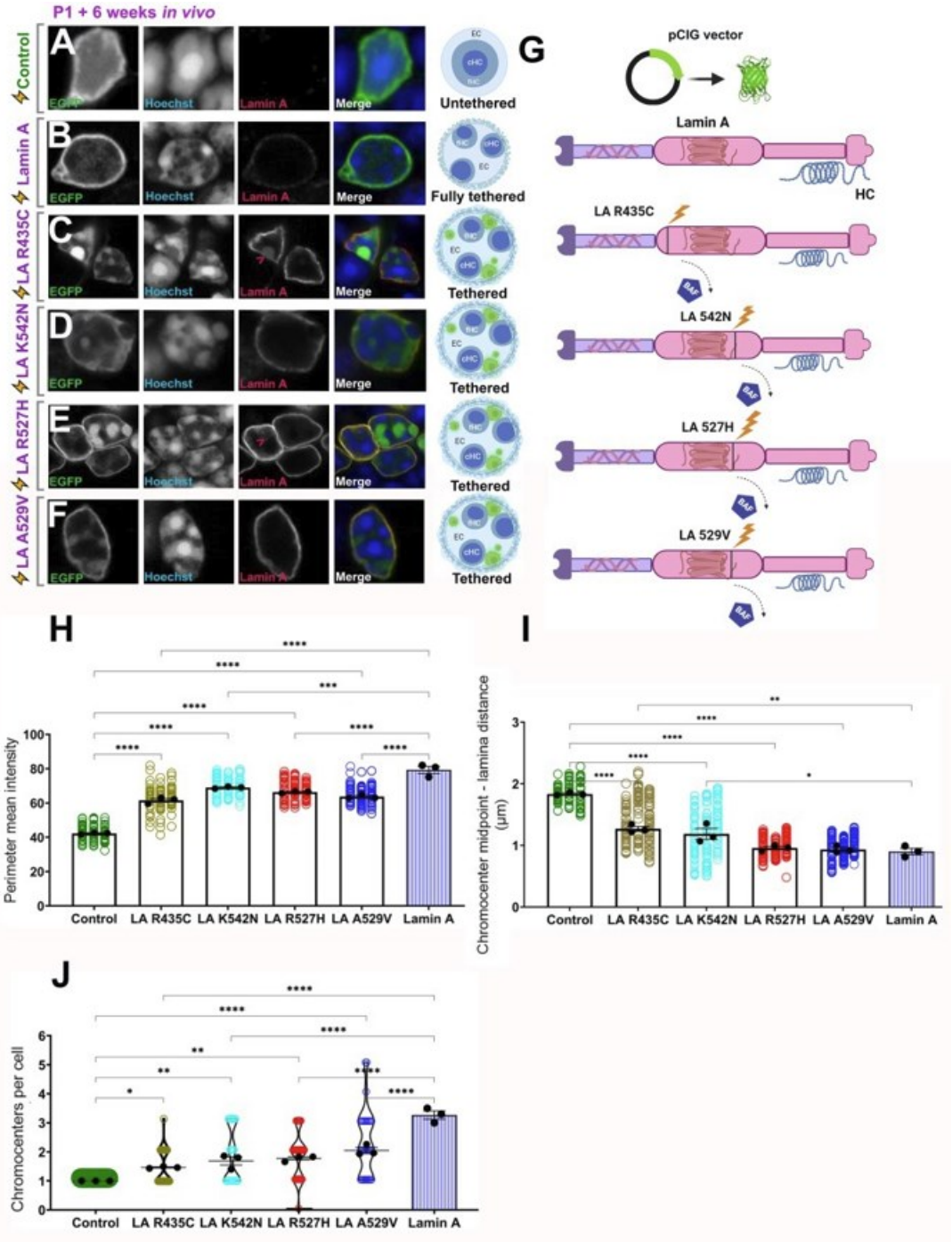

Figure 6.4. Lamin A mutants with reduced or no affinity for BAF tether heterochromatin.

Airyscan confocal imaging of rod photoreceptors transfected with GFP-expressing empty vector control (**A**), along with Lamin A (**B**), Lamin A R435C (**C**), Lamin A K542N (**C**) Lamin A R527H (**E**) Lamin A A529V (**F**) constructs, and harvested after 6 weeks. Red arrows

indicate Lamin A staining on the occlusions and in the nuclear interior. **G.** Illustration of lamin A mutants with no or reduced affinity for BAF. **H.** Quantitation of chromatin intensity at the nuclear margin measured using the "Freehand Line" tool in Fiji mutants against the negative (pCIG) and positive control (Lamin A). **I.** Distance from the chromocenter midpoint to the nuclear periphery. **J.** Chromocenter number per cell. Black datapoints and error bars are the mean intensity values from each biological replicate (30 cells each; circles) ± SEM. $p < 0.0001$, one-way ANOVA with Tukey's post-hoc test. ***$p < 0.001$, ****$p < 0.0001$, ANOVA with Tukey's post-hoc test. Data are compared to negative control pCIG and positive control wild-type LA average values (purple bar) generated from replicates in Figure 6.3.

We additionally overexpressed these LA mutants in 3T3 cells and spotted occlusions that included EGFP protein that we co-expressed to mark transfected cells, which might suggest that lamina targeting of the mutant LA proteins might be impaired, leading to aggregate formation (Figure 6.5C-F).

To further examine BAF, we transfected wild-type EGFP-BAF or a EGFP-BAF L58R dominant negative mutant, containing a point mutation associated with NGPS. These BAF constructs were transfected with or without LA (cloned into a pBABE vector that does not co-express GFP). Misexpression of BAF by itself was not sufficient for tethering (Figure 6.6C). Misexpression of BAF with wild-type LA did not increase tethering (Figure 6.6D), nor did misexpression of LA with the NGPS L58R BAF mutant disrupt HC tethering (Figure 6.6F). Together, experiments with mutant LA or BAF constructs suggest that BAF doesn't affect HC organization (Fig. 6.6C, E), and is dispensable for tethering function of LA (Figure 6.6D, F).

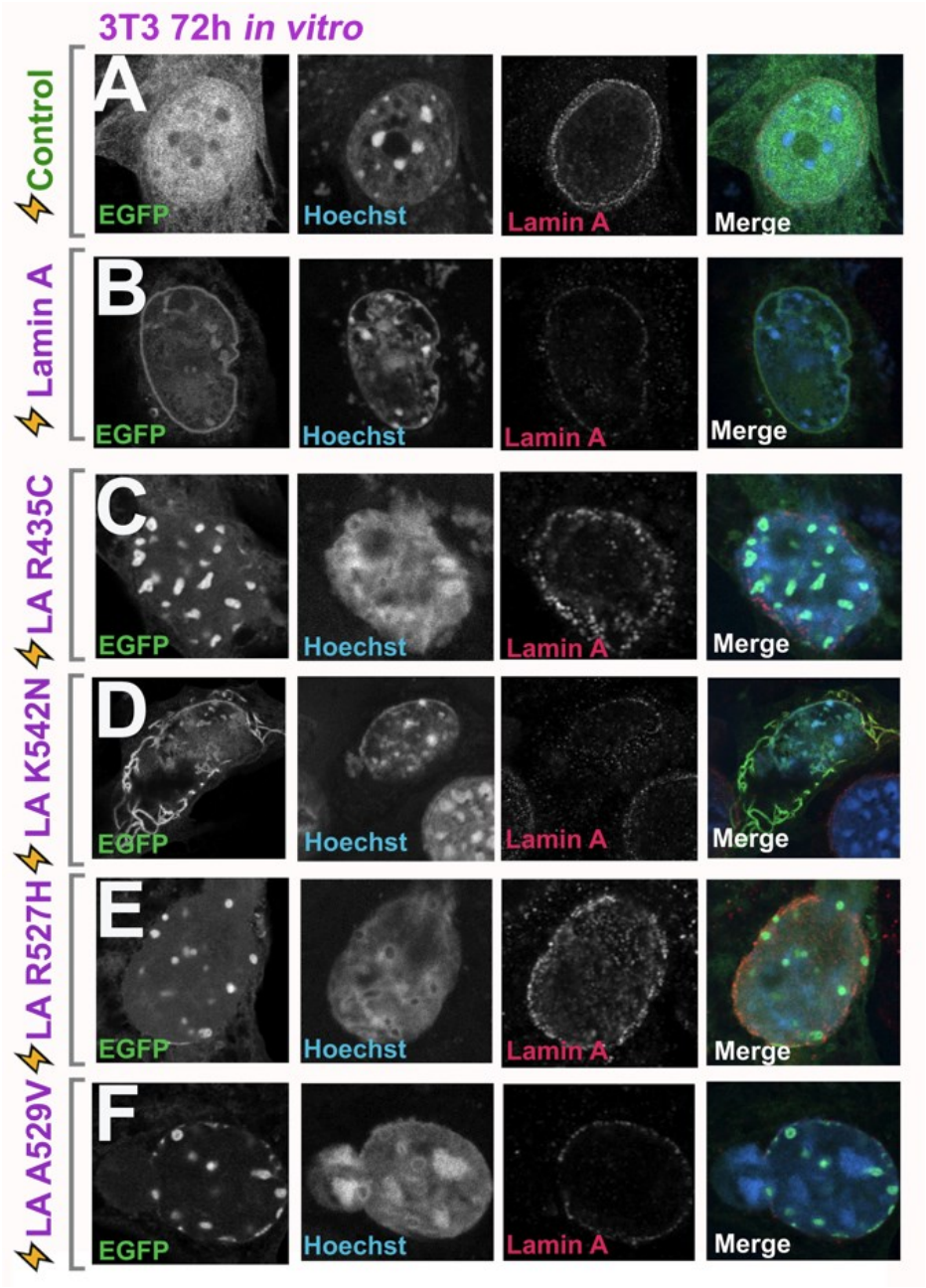

Figure 6.5. Lamin A mutants with reduced or no affinity for BAF form occlusions in 3T3 cells. Airyscan confocal imaging of 3T3 cell line transfected with control (**A**), along with Lamin A (**B**), R435C (**C**) K542N (**D**) R527H (**E**) A529V (**F**). Note that EGFP was co-transfected to mark cells, and is not directly tagged onto the LA constructs.

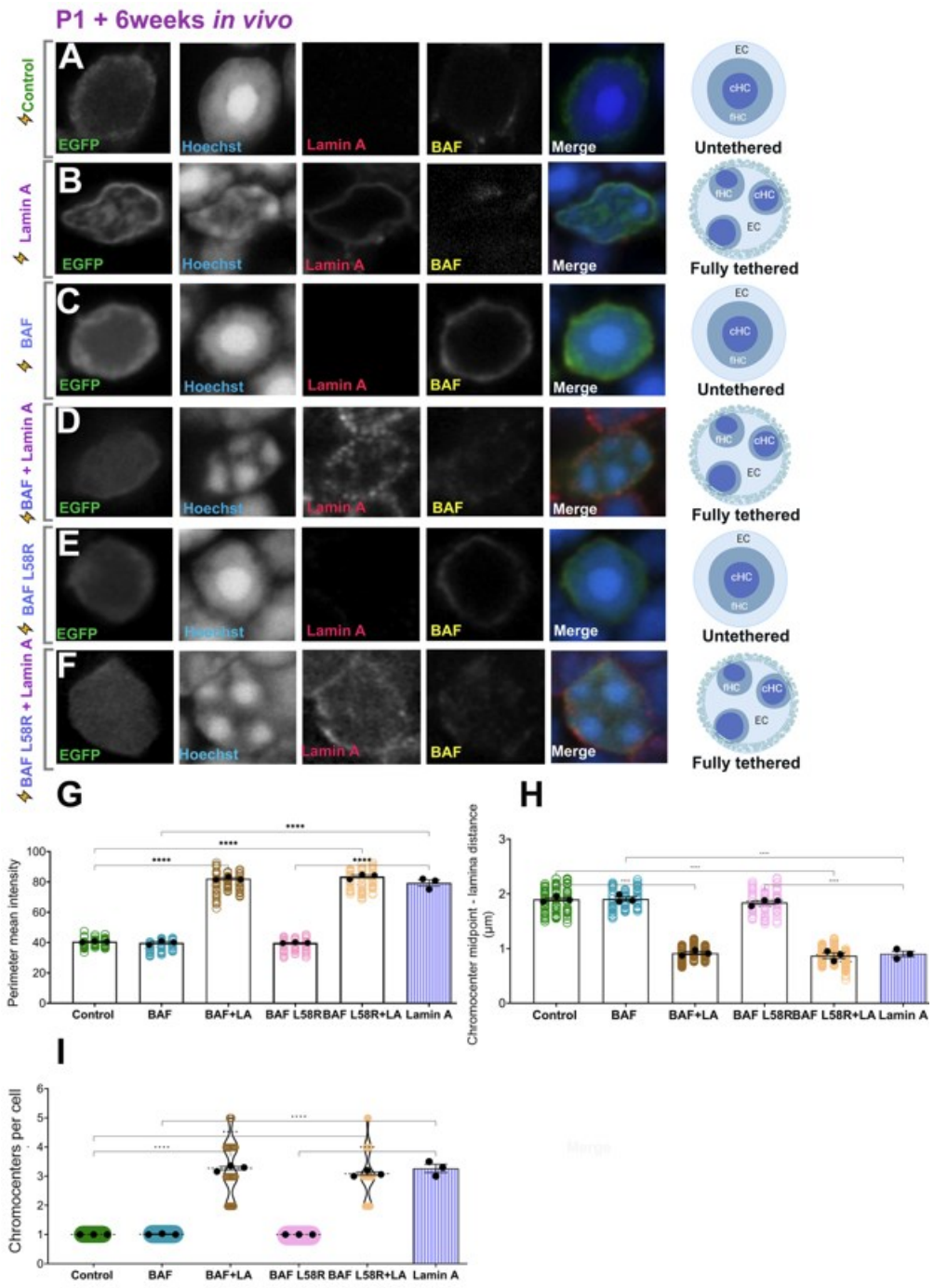

Figure 6.6. BAF L58R dominant negative mutant does not disrupt heterochromatin tethering. Airyscan confocal imaging of rod photoreceptors transfected with GFP-expressing empty vector control (**A**), along with Lamin A (**B**), EGFP-BAF (**C**) EGFP-BAF and pBabe Lamin A (**D**) EGFP-BAF L58R (**E**) EGFP-BAF L58R and pBabe Lamin A (**F**) constructs, and harvested after 6 weeks. **G.** Quantitation of chromatin intensity at the nuclear margin measured using the "Freehand Line" tool in Fiji. **H.** Distance from the chromocenter midpoint

to the nuclear periphery. **I.** Chromocenter number per cell. Black datapoints and error bars are the mean intensity values from each biological replicate (30 cells each; circles) ± SEM. $p < 0.0001$, one-way ANOVA with Tukey's post-hoc test. ***$p < 0.001$, ****$p < 0.0001$, ANOVA with Tukey's post-hoc test. Data are compared to negative control pCIG and positive control wild-type Lamin A average values generated from replicates in Figure 6.3.

6.2.1. LEMD2/3 proteins are not sufficient for heterochromatin tethering

In addition to experiments focused on BAF, I additionally examined the importance of LEMD proteins in HC tethering. LEMD proteins like emerin are involved in the complex with BAF and LA. LEMD proteins share an ~45-residue bihelical domain[326,327,328]. There are several LEMD proteins known, which are all localized mainly at the NL[329,330]. Mutations in genes encoding the lamina LEMD proteins are associated with several human diseases. The loss of LEMD proteins is the cause of bone disorders, cardiomyopathies and muscular dystrophies[331]. Like laminopathies, these diseases are tissue specific and linked to advanced aging phenotypes. Structural analyses of LEMD proteins suggest that some of these proteins also interact directly with chromatin. LEMD3 (MAN1) contains a MAN1-Src1p C-terminal (MSC) domain that forms a winged helix DNA-binding domain[332]. Therefore, LEMD3 is a DNA-bridging protein that contributes to nuclear organization. It was suggested recently that LEMD proteins mediate the association between lamins and chromatin[333]. Additionally, heterozygous mutations in the human *MAN1* gene are associated with osteopoikilosis and the Buschke–Ollendorff syndrome[334]. Disease phenotypes caused by *LMNA* mutations overlap with those caused by the loss of *MAN1*, implying that the loss of one NL component may alter the function of other proteins in the network.

LMNA mutations lead to significant loss and aberrant positioning of LEMD2[81]. These results suggest that LEMD2 requires LA/C for its localization. Accordingly, it was shown that LEMD2 binds LC C-terminal tail *in vitro*[335]. However, LEMD2 (or co-expressed with LC), was not able to restore the conventional nuclear architecture in murine rod nuclei[81]. Solovei et al. reported that emerin deletion did not produce chromatin inversion in the murine cell types, but it was compensated in a cell-type specific manner by another LEMD protein[66].

To test the hypothesis that HC tethering depends on LEMD proteins[336], we overexpressed LEMD2 and LEMD3 in rods. In accordance with previous research[81], we confirmed LEMD2, and LEMD3 (MAN1) are not sufficient to tether HC (Figure 6.7). Based on immunohistochemistry, we nonetheless observe that both LEMD2 and LEMD3 correctly localized to the nuclear periphery – even in the absence of LA/C.

Although we confirmed that LEMD2 nor LEMD3 (MAN1) are not probable mediators of LA-dependent tethering, they are likely to be co-localized with the lamin scaffold (as other proteins we studied). Despite the strong implication of DNA-bridging BAF and LEMD proteins in LA-mediated HC tethering, we found that BAF or LEMD protein overexpression in rod photoreceptors don't affect HC tethering.

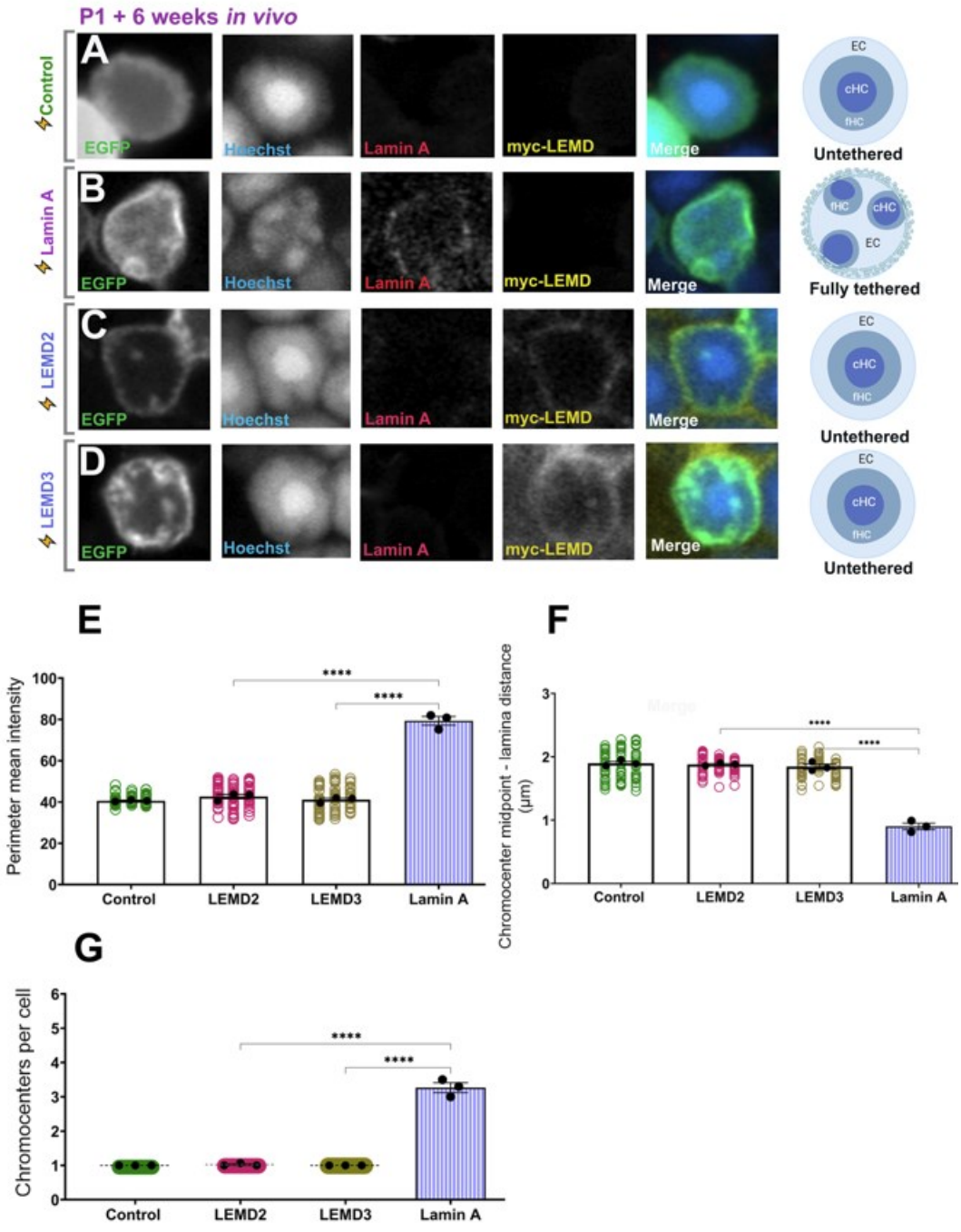

Figure 6.7. LEMD proteins are not sufficient for heterochromatin tethering. Airyscan confocal imaging of rod photoreceptors transfected with GFP-expressing empty vector control (**A**), along with Lamin A (**B**), myc-LEMD2 (**C**) myc-LEMD3 (**D**) constructs, and harvested after 6 weeks. **E.** Quantitation of chromatin intensity at the nuclear margin measured using the "Freehand Line" tool in Fiji. **F.** Distance from the chromocenter midpoint to the nuclear

periphery. **G.** Chromocenter number per cell. Black datapoints and error bars are the mean intensity values from each biological replicate (30 cells each; circles) ± SEM. $p < 0.0001$, one-way ANOVA with Tukey's post-hoc test. ***$p < 0.001$, ****$p < 0.0001$, ANOVA with Tukey's post-hoc test. Data are compared to negative control pCIG and positive control wild-type Lamin A average values generated from replicates in Figure 6.3.

6.3. RBBP4 is not involved in Lamin A heterochromatin tethering

Retinoblastoma-binding protein 4 (RBBP4) is a reported physical interactor of LA, BAF[337] and histones[86]. RBBP4, along with RBBP7, is a shared subunit of several multi-protein complexes involved in the establishment of HC, including the Nucleosome Remodeling and Deacetylase (NuRD) complex[338] and the Polycomb PRC2 complex[339]. RBBP4 is also a component of the CAF-1 complex, which assembles chromatin upon DNA replication and DNA damage repair[340]. Interestingly, Pegoraro et al. showed that RBBP4 interacts with wild-type LA, but not with progerin[167], suggesting that the LA-RBBP4 interaction might depend on the unique LA C-terminus, and that this interaction is disrupted by progeroid LA mutation. Accordingly, fibroblast cells from patients with HGPS showed reduced protein levels of RBBP4. Furthermore, loss of RBBP4 correlated with lower levels of HP1[173], pointing to global chromatin defects. Silencing of RBBP4 recapitulated chromatin defects associated with aging, followed by DNA damage accumulation[173]. Considering that HGPS cells exhibit several chromatin defects which are also characteristic for physiological aging, including loss of HC structure, RBBP4 might be a key LA partner in HC tethering.

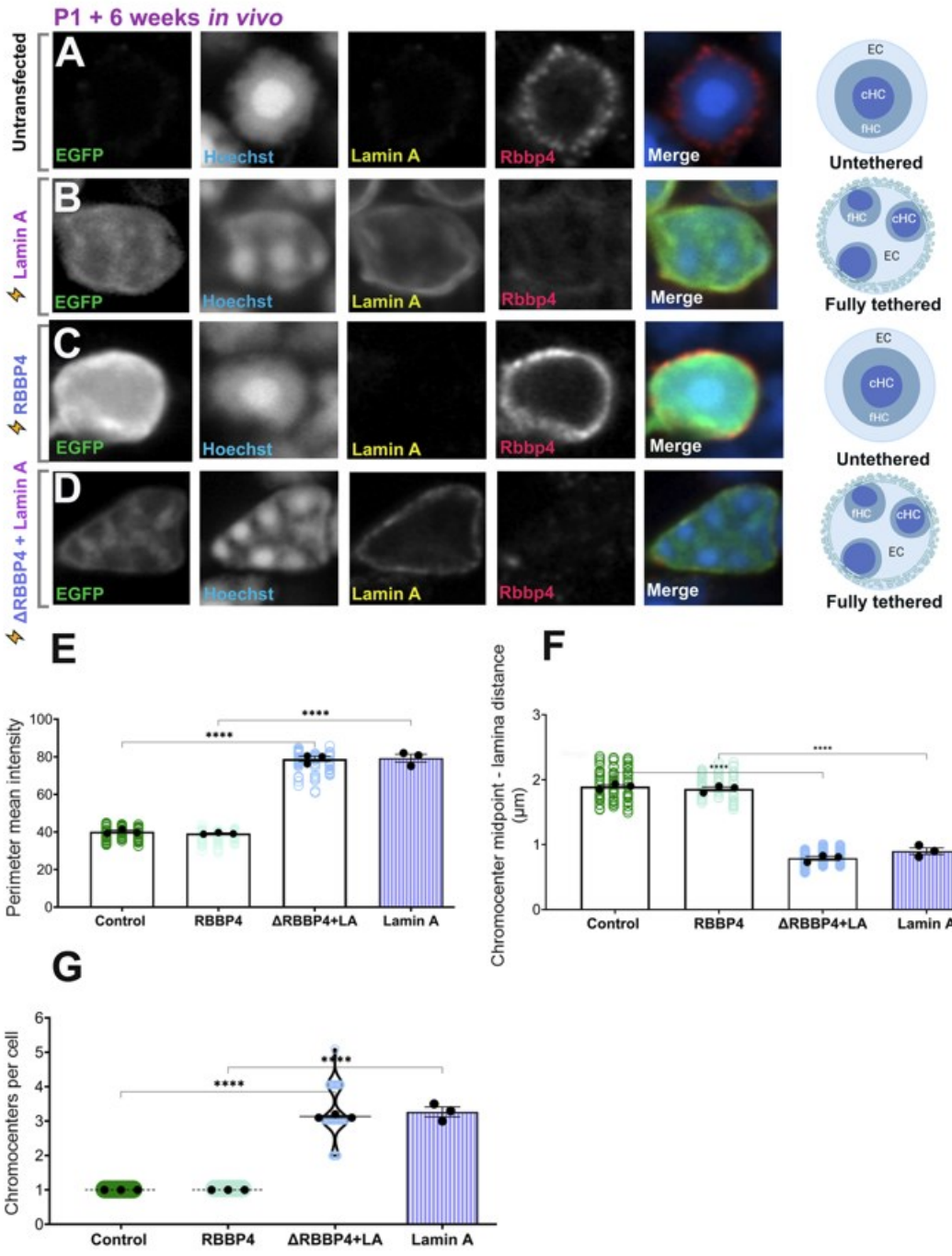

Figure 6.8. ΔRBBP4 dominant negative mutant does not disrupt Lamin A heterochromatin tethering. Airyscan confocal imaging of rod photoreceptors transfected with GFP-expressing empty vector control (**A**), along with Lamin A (**B**), RBBP4 (**C**) truncated ΔRBBP4 and pCIG Lamin A (**D**) constructs, and harvested after 6 weeks. **E.** Quantitation of chromatin intensity at the nuclear margin measured using the "Freehand Line" tool in Fiji. **F.** Distance from the chromocenter midpoint to the nuclear periphery. **G.** Chromocenter number

per cell. Black datapoints and error bars are the mean intensity values from each biological replicate (30 cells each; circles) ± SEM. $p < 0.0001$, one-way ANOVA with Tukey's post-hoc test. ***$p < 0.001$, ****$p < 0.0001$, ANOVA with Tukey's post-hoc test. Data are compared to negative control pCIG and positive control wild-type Lamin A average values generated from replicates in Figure 6.3.

We tested the tethering sufficiency of RBBP4, by overexpressing wild-type and dominant negative mutant ΔRBBP4 along with LA, to test whether it will block LA-dependent tethering. ΔRBBP4 mutant is missing 54 N-terminal residues, essential for the interaction with histone H4[341,342]. However, ectopic expression of RBBP4 (and truncated ΔRBBP4 along with wild-type LA) in rods didn't alter the genome, which suggests that RBBP4 doesn't play a role in tethering of HC (Figure 6.8C, D).

To examine the NuRD complex relationship to LA more closely, we expressed a dominant negative NuRD protein (GATAD2A 335-486) in rods[219]. This GATAD2A mutant led to LA upregulation and genome reorganization (Figure 6.9). These data suggests that NuRD is suppressing LA expression. This is supported by our published research, where we show that Casz1 cooperates with polycomb and NuRD repressor complexes to control rod genome organization, in part by silencing LA/C[219]. While we did not quantitate HC tethering in these cells, qualitative inspection of the nucleus suggests that LA does alter HC in the presence of the dominant negative NuRD protein. Taken together, these data suggest that NuRD is dispensable for HC tethering. Although RBBP4 is a chromatin protein interacting with LA, our results suggest that RBBP4 is not a relevant player in genome organization via LA tethering. Again, future genetic work will be required to confirm these observations.

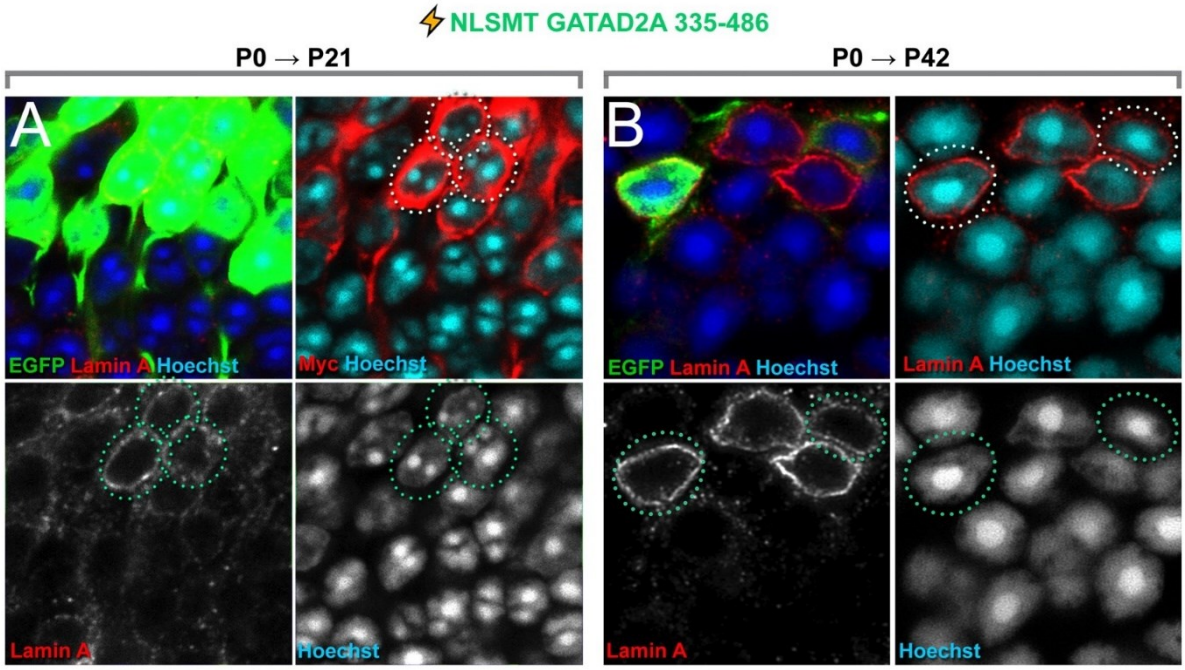

Figure 6.9. Mutated NuRD protein expression in rod photoreceptors.

GATAD2A 335-486 construct was transfected at P0 and harvested at P21/P42. Lamin A expression (red) in transfected rods (green).

6.4. PRR14 is not sufficient for heterochromatin tethering in murine rods

Proline-rich protein 14 (PRR14) is a nuclear protein that was reported to tether HC and suggested to localize at the lamina in a LA/C dependent fashion[85]. PRR14 was shown to bind HC and the NL via different domains. PRR14 associates with the NL through central lamina-binding domains[343]. The N-terminal domain of PRR14 contains HP1-binding LxVxL motifs allowing PRR14 to bind HC. Two HP1-binding sites have a major role in HC binding and stabilizing the interaction with HC[344]. PRR14 is able to alter the localization of all three mammalian HP1 isoforms *in vivo*[334]. Tethering to the nuclear periphery in the context of PRR14 overexpression was associated with the HP1α and HP1β isoforms[85], in contrast to the

HP1γ isoform which has been found in both HC and EC regions[345]. PRR14 was reported to tether HC by associating with H3K9me2/3[85]. During interphase, PRR14 localization at the nuclear periphery is disrupted by siRNA knockdown of the NL components LA and LC, but not by knockdown of LB1 or LB2[85], which indicates PRR14 localization at the lamina depends directly on LA/C. These findings suggested that PRR14 functions to tether HP1-marked HC directly, or indirectly, to LA/C. SiRNA knockdown of PRR14 is associated with partial loss of perinuclear H3K9me3 HC and misshapen nuclei[85], as seen in laminopathies[346]. Compelled by all these data, we hypothesized that PRR14 and LA might be co-dependent in their localization and tethering function.

However, PRR14 was not sufficient for HC tethering and it didn't affect rod photoreceptor genome organization when expressed by itself (Figure 6.10C). We next decided to test whether PRR14 might enhance tethering in the presence of LA. We opted to co-express PRR14 with a GFP-LA fusion construct which was shown to lose tethering sufficiency[219] (see also Figure 6.11 below). Although GFP-LA is not competent to tether, it contains the whole LA protein and it is correctly localized at the NL[219]. From previous studies, we know that other N-terminally tagged proteins like Flag-LA polymerize into filaments[347].

However, we found that PRR14 wasn't able to restore tethering when co-expressed with a tethering-incompetent GFP-LA construct that localizes to the NL (Figure 6.9). While it is unclear whether PRR14 can interact properly with GFP-LA, PRR14 appeared to be concentrated at the nuclear periphery in these transfected cells – both in the presence or absence of GFP-LA.

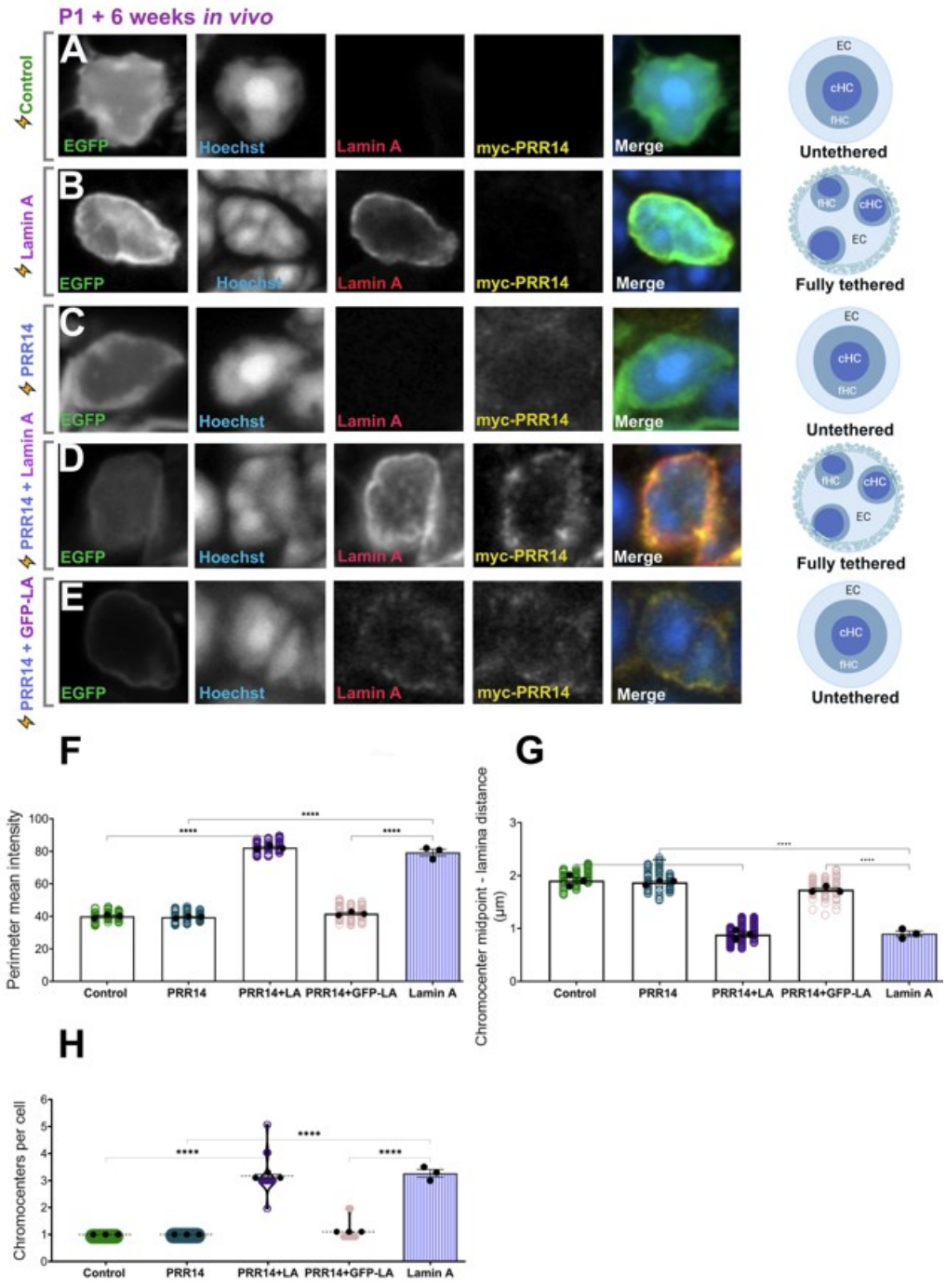

Figure 6.10. **PRR14 is not sufficient for heterochromatin tethering.** Airyscan confocal imaging of rod photoreceptors transfected with GFP-expressing empty vector control (**A**), along with Lamin A (**B**), myc-PRR14 (**C**) myc-PRR14 and pCIG Lamin A (**D**) myc-PRR14 and GFP-Lamin A (**E**) constructs, and harvested after 6 weeks. **F.** Quantitation of chromatin intensity at the nuclear margin measured using the "Freehand Line" tool in Fiji. **G.** Distance

from the chromocenter midpoint to the nuclear periphery. **H.** Chromocenter number per cell. Black datapoints and error bars are the mean intensity values from each biological replicate (30 cells each; circles) ± SEM. $p < 0.0001$, one-way ANOVA with Tukey's post-hoc test. ***$p < 0.001$, ****$p < 0.0001$, ANOVA with Tukey's post-hoc test. Data are compared to negative control pCIG and positive control wild-type Lamin A average values generated from replicates in Figure 6.3.

Importantly, while epitope tags are function-blocking in the context of LA fusion proteins, it was previously shown that PRR14 could tether HC even when fused to GFP, so we surmise that the failure to tether HC is not due to the addition of the Myc epitope tag onto the PRR14 construct. However, further experiments would be required in order to fully confirm the validity of our assumptions.

6.5. N-terminal tags obstruct Lamin A heterochromatin tethering

To further understand how tethering competence changes the LA interactome, we decided to compare wild-type LA with tethering-incompetent forms of the protein. We previously reported that ectopically expressed N-terminal GFP-fusion proteins encoding LA (prelamin A) and Progerin had no effect on chromatin inversion or nuclear position in rods, while wild-type

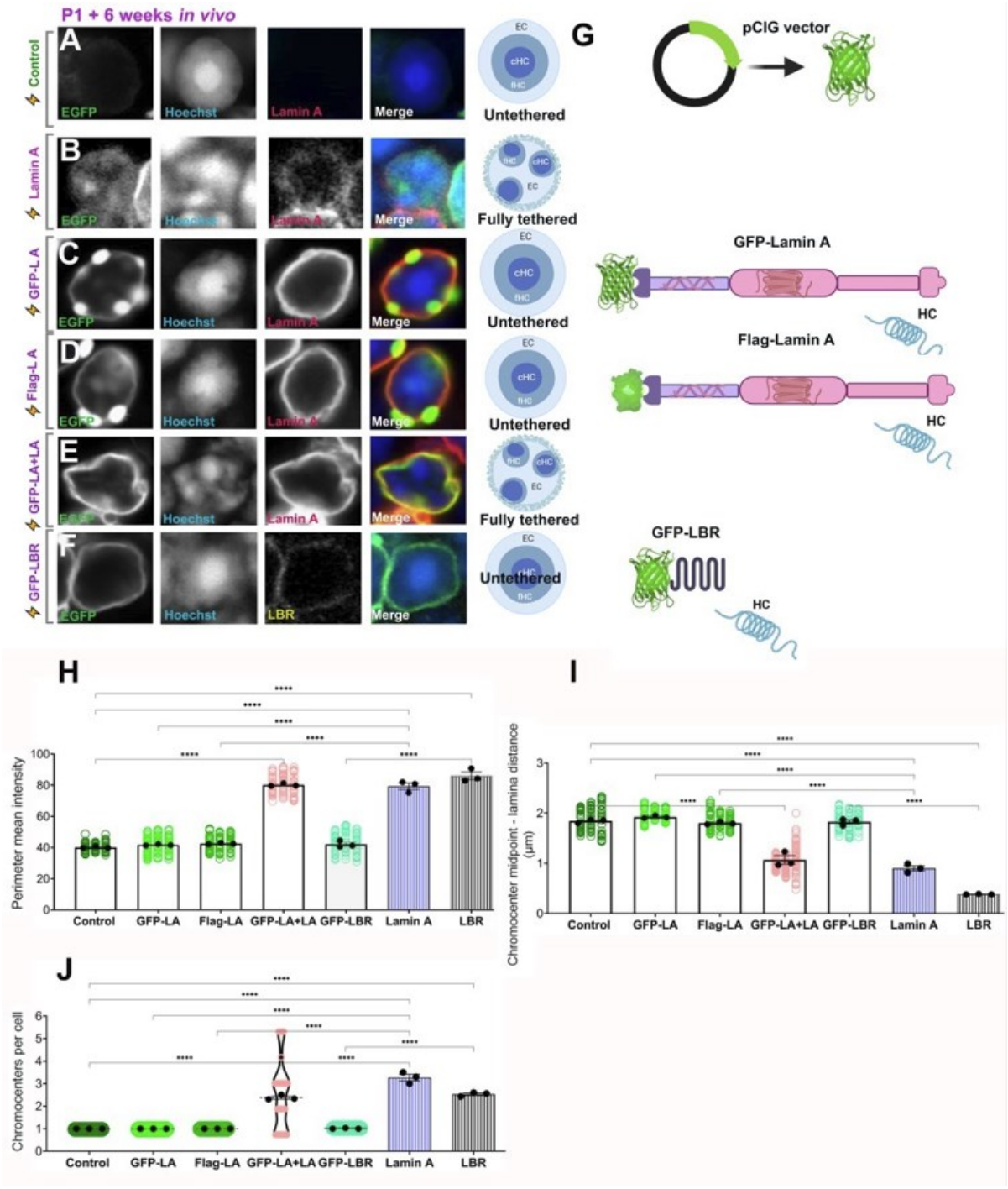

Figure 6.11. N-terminally tagged constructs lose tethering function.

Airyscan confocal imaging of rod photoreceptors transfected with GFP-expressing empty pCIG vector control (**A**), Lamin A (**B**), along with GFP-Lamin A (**C**), Flag-Lamin A (**D**) or co-transfected with GFP-Lamin A/Lamin A (**E**) GFP-LBR (**F**) constructs, and harvested after 6 weeks. **G.** Illustration of N-terminally tagged Lamin A proteins, which lose tethering

function. **H.** Quantitation of chromatin intensity at the nuclear margin measured using the "Freehand Line" tool in Fiji. **I.** Distance from the chromocenter midpoint to the nuclear periphery. **J.** Chromocenter number per cell. Black datapoints and error bars are the mean intensity values from each biological replicate (30 cells each; circles) ± SEM. $p < 0.0001$, one-way ANOVA with Tukey's post-hoc test. ***$p < 0.001$, ****$p < 0.0001$, ANOVA with Tukey's post-hoc test. Data are compared to negative control pCIG, positive control wild-type Lamin A average values (purple bar) generated from replicates in Figure 6.3. and positive control wild-type LBR average values (black/white bar) generated from replicates in Figure 3.5.

untagged LA was sufficient for HC tethering, and for relocalizing of photoreceptor soma to the apical side of the neural retina[219]. These results suggest that the N-terminal GFP tag is function blocking. Both tagged and untagged LA proteins localized correctly to the nuclear periphery, in accordance with dozens of studies that previously validated fusion constructs. However, the GFP-LA construct generated protein inclusions that were not apparent in cells transfected with the untagged version. We additionally tested a panel of Flag- and GFP-tagged LA and LBR constructs. However, these constructs seem to have lost tethering function as a consequence of the N-terminal tags, although they localize correctly at the NL (Figure 6.11).

6.7. Comparing the interactome of tethering competent vs. incompetent LA

To determine whether LA depends on any protein partners for HC tethering, we performed a co-IP/MS experiment (n=3) on endogenous LA (n=3), GFP-LA (n=3) and GFP-Progerin (n=2) stably transfected in HEK 293 cells (Figure 6.12A, B). The experiment was designed to identify proteins that would interact with LA to tether HC, but whose interactions with LA would be disrupted by the presence of the function-blocking GFP tag. As expected, we

detected NL proteins (LA, LB1, LB2, and the LEMD proteins TMPO and EMD) enriched in LA, GFP-LA and GFP-Progerin co-IPs (Fig. 6.12C). Interestingly, when proteins enriched by

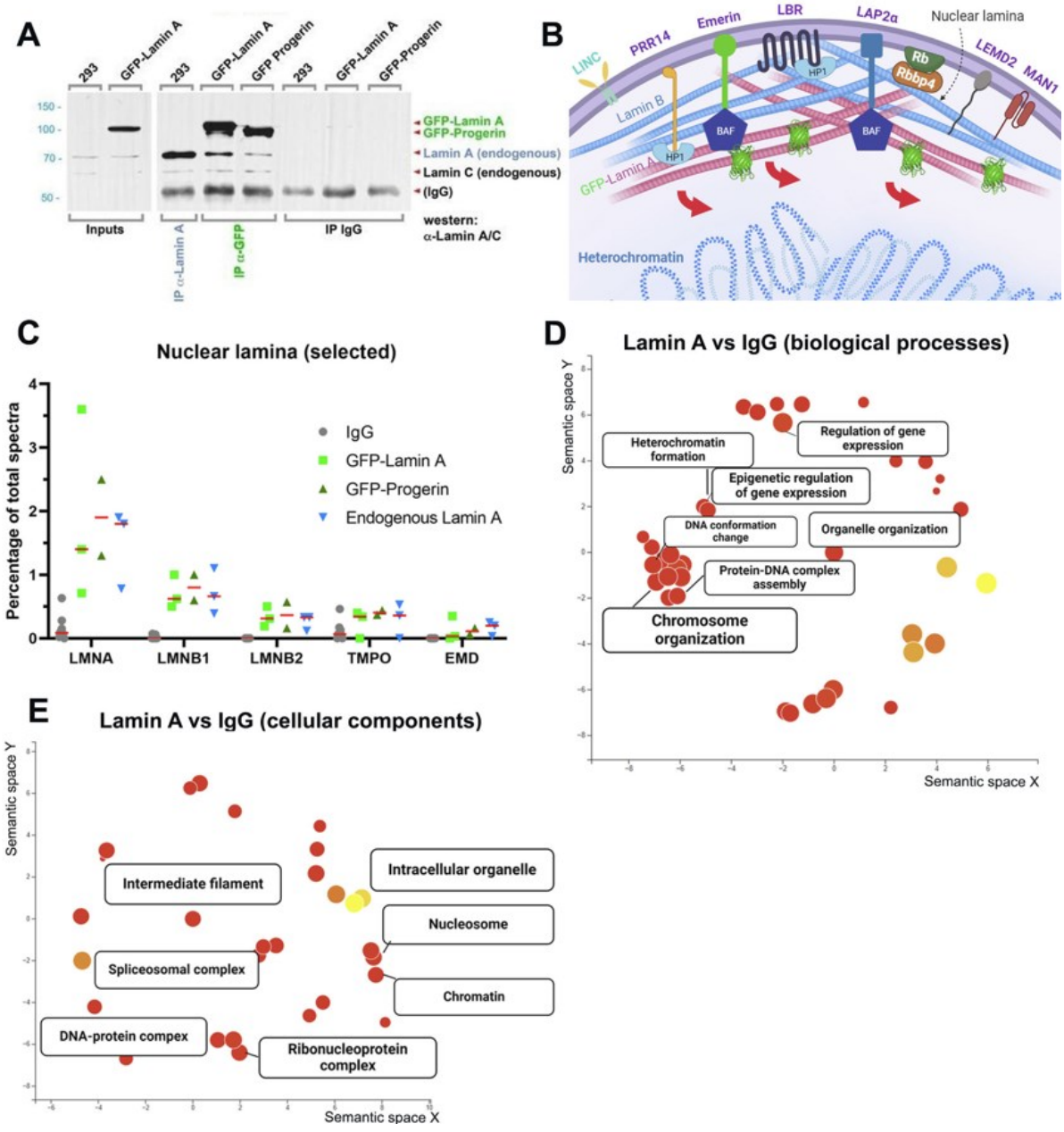

Figure 6.12. coIP-MS experiment on lamin A interacting proteins.

A. Western blot of co-immunoprecipitated non-functional GFP-Lamin A or GFP-Progerin, IgG and endogenous functional Lamin A (293), using a Lamin A-specific antibody performed by myself and Samuel Clémot-Dupont. **B.** Illustration of tethering non-competent GFP-Lamin

A, GFP-progerin (function blocking). **C**. Mass spectrometry hits graphed to detect common binding partners (nuclear lamina proteins) between Lamin A, GFP-lamin A, GFP-Progerin, and IgG. **D**. GO terms analysis of biological processes associated with Lamin A interactome (top 50) (Lamin A vs IgG). **E.** GO terms analysis of cellular components associated with Lamin A interactome (top 50 enriched proteins) (Lamin A vs IgG).). Analysis via Shiny GO and ReViGO.

GFP or LA were compared against the IgG control, enriched GO terms included gene expression, chromosome organization, DNA-protein complex assembly (Figure. 6.12D). GO terms analysis of biological components specified nucleosomes, organelles and filaments (Figure 6.12E). However, as determined by peptide counts, enrichments for LA and other lamina -associated proteins were very similar when GFP coIPs were compared against LA coIPs.

We found that only three proteins reached statistical significance when the LA tethering competent interactome was compared against incompetent GFP-LA, namely PARP1, H2A and H4 (Figure 6.13A), suggesting that LA might interact with nucleosomes directly rather than through additional partner proteins. When we examined the top 50 proteins enriched by endogenous LA vs. GFP-LA, GO terms analysis of biological processes showed that LA-partner proteins were highly correlated with DNA damage response, stress response, chromatin organization, HC formation, DNA conformation change (Figure 6.13B). The GO terms analysis of biological components revealed that tethering competence is associated with DNA repair complexes and chromatin (Figure 6.13C).

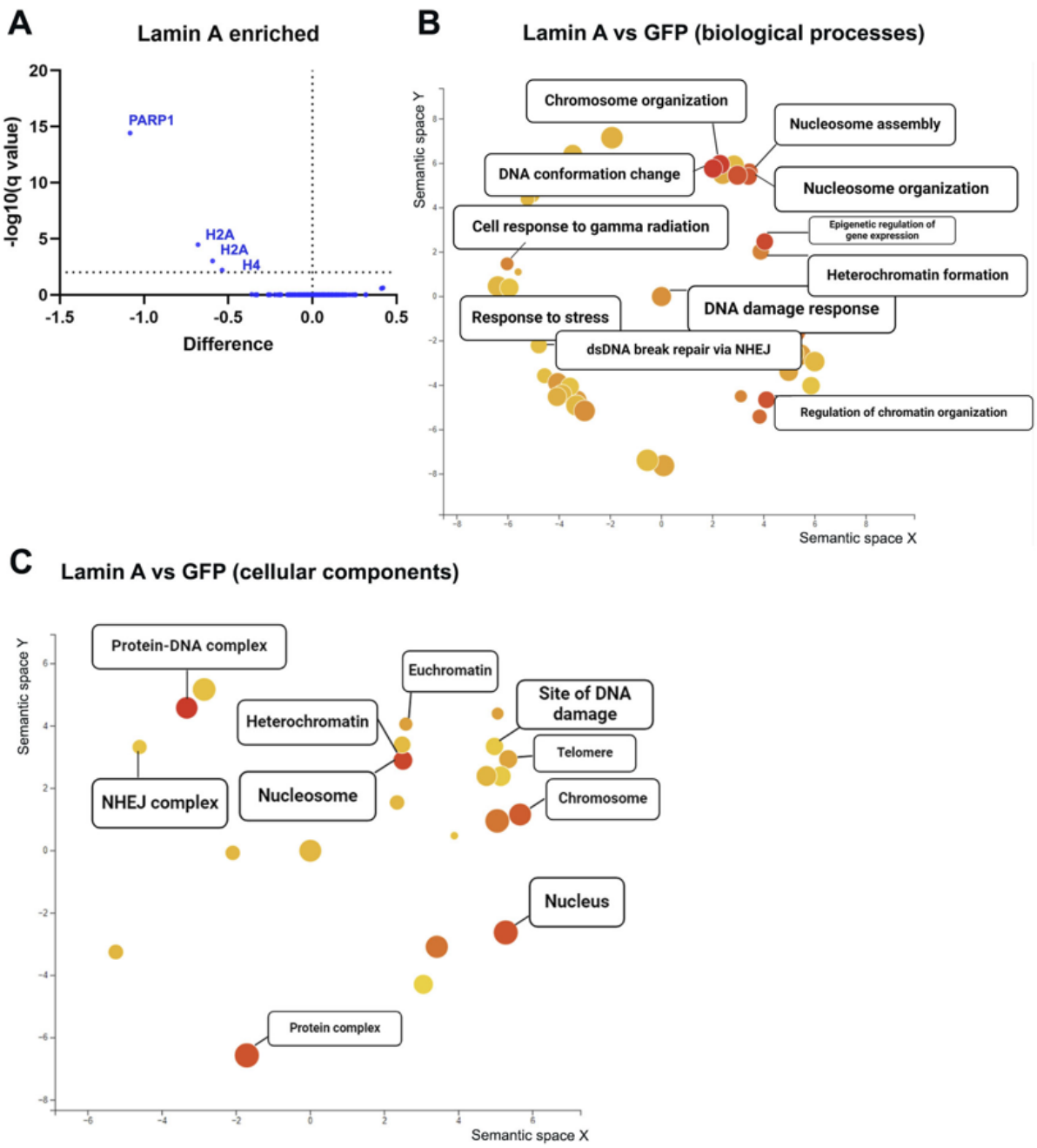

Figure 6.13. Lamin A-tethering competent interactome.

A. Mass spectrometry hits graphed to detect differential binding partners between Lamin A and GFP-lamin A. **B**. GO terms analysis of biological processes associated with Lamin A interactome (top 50) (Lamin A vs GFP). **C**. GO terms analysis of cellular components associated with Lamin A interactome (top 50 enriched proteins) (Lamin A vs GFP). Analysis via Shiny GO and ReViGO.

Discussion

The nuclear envelope has an essential role in the 3D organization of the genome. The inner nuclear membrane interior is lined by a network of filamentous lamin proteins that represents a multifunctional interface for different cellular processes. A subset of NL- and inner nuclear membrane-associated proteins function as anchors to hold transcriptionally silent heterochromatic regions (LADs) at the nuclear periphery. A major question is how LAD–NL interactions are mediated and controlled?

Several proteins have been proposed to be key players in HC tethering at the lamina. Previous work has shown that the transmembrane multi-pass protein LBR is necessary and sufficient for HC tethering[66]. Previous data further show that LBR tethers HC through a direct interaction via its Tudor chromatin binding domain[69]. Based on transgenic LC expression in rods, it was previously concluded that LA/C is necessary, but not sufficient for tethering of the HC to the NL and that it most likely tethers through a mediator protein[66]. However, while many proteins that interact with both chromatin and LA/C have been identified, none have been shown to be sufficient for HC tethering, and the majority of these proteins interact with LA, but additionally interact with LC or B-type lamins. Although we subsequently discovered that LA is able to restore conventional nuclear architecture, when ectopically expressed in mouse rods[219], LA might nonetheless require a partner protein in order to achieve this effect. Here we performed experiments in order to evaluate the potential contribution of known partner proteins to HC tethering by A-type lamins. Here we addressed the hypothesis that altering the expression of putative co-factors would modulate HC tethering – either in the absence or presence of LA. However, we were unable to identify LA partner proteins that altered HC tethering. Our results show that none of the tested proteins are sufficient to tether HC, and only LA mutants that lose

affinity for BAF seem to modify HC tethering. Another explanation is that the LA mutations affecting affinity for BAF simply destabilize the LA IG-fold domain conformation. Accordingly, dominant negative BAF L58R mutation didn't affect LA –mediated HC tethering, suggesting that BAF might be irrelevant for HC tethering. However, limitations of the experiments used for answering the question of LA tethering mediator are significant. For example, we did not include dominant negative mutants of all the examined proteins, such as PRR14 and LEMD2/3. To definitively address their requirement in LA-dependent HC tethering, it will be necessary to knock-down or knockout these proteins alongside LA misexpression in future experiments.

Our data further suggests that LA doesn't need an intermediate protein to tether HC since nucleosomes H2 and H4, along with PARP, are primary partners enriched in a comparison between tethering competent versus incompetent versions of LA. Accordingly, the Misteli lab showed that LA (but not LC) can bind H3 *in vitro*[91], which supports our proteomics data (see also Chapter 5 above). We conclude that LA doesn't require an intermediate and the C-terminus might be sufficient for tethering.

Lamin A might promote DNA repair via PARP1

To determine whether LA requires protein partners for HC tethering in an unbiased proteome-wide fashion, we used a co-IP/MS experiment using tethering competent endogenous LA and incompetent GFP-LA transfected in 293 cells. The experiment was designed to identify the specific proteins interacting with tethering competent endogenous LA versus the tethering incompetent GFP-LA construct. Understandably, both complexes had proteins in common, since both localize at the NL and both include identical LA amino acid sequences. B-type lamins, emerin (*EMD*), Lap2α (*TMPO*) proteins were found to be equally enriched in LA and

GFP-LA interactomes. Co-IP experiment revealed that only histones H2 and H4, and PARP1 were significantly enriched by tethering competent LA.

The interaction between PARP1 and LA might reflect the role of tethering in DNA damage repair. Previous studies have shown that DNA repair is inefficient in inverted mouse rod photoreceptors, and this effect is improved through tethering activity by the transgenically expressed LBR[110,111]. It is reported that absence of LA/C induces loss of 53BP1 protein[105] and aberrant DNA repair mechanism (non-homologous end joining), causing persistent DNA damage. Similarly, deletion of lamins was shown to supress the efficiency of the DNA damage repair mechanism of homologous recombination, through the loss of BRCA1 and RAD51[108,348,349,350]. Therefore, A-type lamins might be responsible for regulation of genomic stability through interaction with proteins crucial for DNA double-strand break repair. In LA/C-depleted cells, there was a noted reduction in base excision repair efficiency, through downregulation of poly-ADP-ribose (PAR), PARP1, and other enzymes important in this DNA repair pathway[351]. Thus, our results are in accordance with a notion that LA/C might promote DNA base excision repair which involves PARP1. Interestingly, this is supported by our LA interactome analysis, where PARP1 is the strongest binding partner for tethering-competent LA, but not GFP-LA. This makes the connection between tethering activity and DNA damage repair even more compelling.

Chapter 7. Discussion

Although interactions between heterochromatic regions drive compartmentalization of EC and HC into A and B compartments, respectively, interactions of HC with the NL are essential for the conventional organization of the nucleus[23]. The NL therefore has a major role in 3D genome organization and gene regulation. Lamina proteins such as LBR and LA play a key role in organizing the genome[66]. However, both the mechanisms responsible for these effects, and the cellular functions served by HC tethering remain poorly defined[352]. This is partly due to a lack of useful and convenient experimental systems for studying lamina functions. The murine rod photoreceptor is a striking exception to this rule. Rods express a much-reduced complement of lamina proteins, and are perhaps the only cell known not to express any heterochromatic tethers in the adult stage[66]. Here, we used mouse rod photoreceptors as an assay system for HC tethering sufficiency.

Previous work showed that transgenically expressed Lbr in murine rods is sufficient for HC tethering[66]. However, since transgenically expressed LC was shown not to be sufficient for HC tethering, it was suggested that LA isoform is not sufficient either[66]. Although LA/C was found to be genetically required for tethering in hair follicles, and despite the fact that HC tethering is reduced in laminopathic cells, LA was dismissed as a protein capable of directly tethering HC. While researchers focused their attention on the rich LA/C interactome[64], we ectopically expressed untagged wild-type LA in murine rods and finally concluded that LA is indeed sufficient for HC tethering[219]. However, we still had many questions to answer about the logic and the purpose of LA/C-dependent HC tethering, with respect to rod photoreceptor genome organization.

Interestingly, we and others found that degenerating rods (SCA7[66], *Casz1-KO*[219], *rd1*[220]) upregulate LA/C, and these mutants were shown to exhibit higher order genome reorganization. It was reported that HC drives compartmentalization of inverted and conventional nuclei[23]. However, it was yet unclear whether nuclear reorganization is a consequence of degenerative changes or if LA/C expression mediated these changes directly. Similarly, reduced HC at the nuclear periphery is correlated with laminopathic mutations[353,162], and accumulation of DNA damage[354,355], but it is unclear whether disruption in HC tethering directly or indirectly contributes to this pathology.

In Chapter 3, we found that LA upregulates in response to degeneration. In Chapter 4, we show that this is likely in response to DNA damage. LA upregulation was sufficient to reorganize the rod nucleus in degenerating *rd1* rods and prolong HC tethering. In Chapter 5, I performed a structure/function study designed to test the hypothesis that the unique LA C-terminus is necessary and sufficient to tether HC. In Chapter 6, we addressed the alternative hypothesis that LA might require a partner protein to tether HC. We screened several proteins (BAF, PRR14, RBBP4, LEMD) that were implicated in the chromatin organization. We also performed a proteomic study designed to identify the interactome of tethering competent vs. incompetent lamins. However, our data did not support the idea that these proteins are essential LA partners in HC tethering.

Taken together, our data suggest the following model (Figure 6.1): The NL consists of inter-dependent networks of A- and B-type lamins and inner nuclear membrane proteins. Murine rod photoreceptors uniquely lack HC tethering under normal conditions. However, during degeneration and DNA damage accumulation, LA/C upregulates in rods. The LA isoform directly interacts with heterochromatic nucleosomes to tether HC to the nuclear periphery via

its defarnesylated and cleaved C-terminal tail. At the same time, HC tethering stretches the chromosomes, promoting accessibility in the transcriptionally active A-compartment and poising the regulatory elements for stress-responsive gene activation. Additionally, LA/C might facilitate DNA damage repair in concert with PARP1 and KAP1.

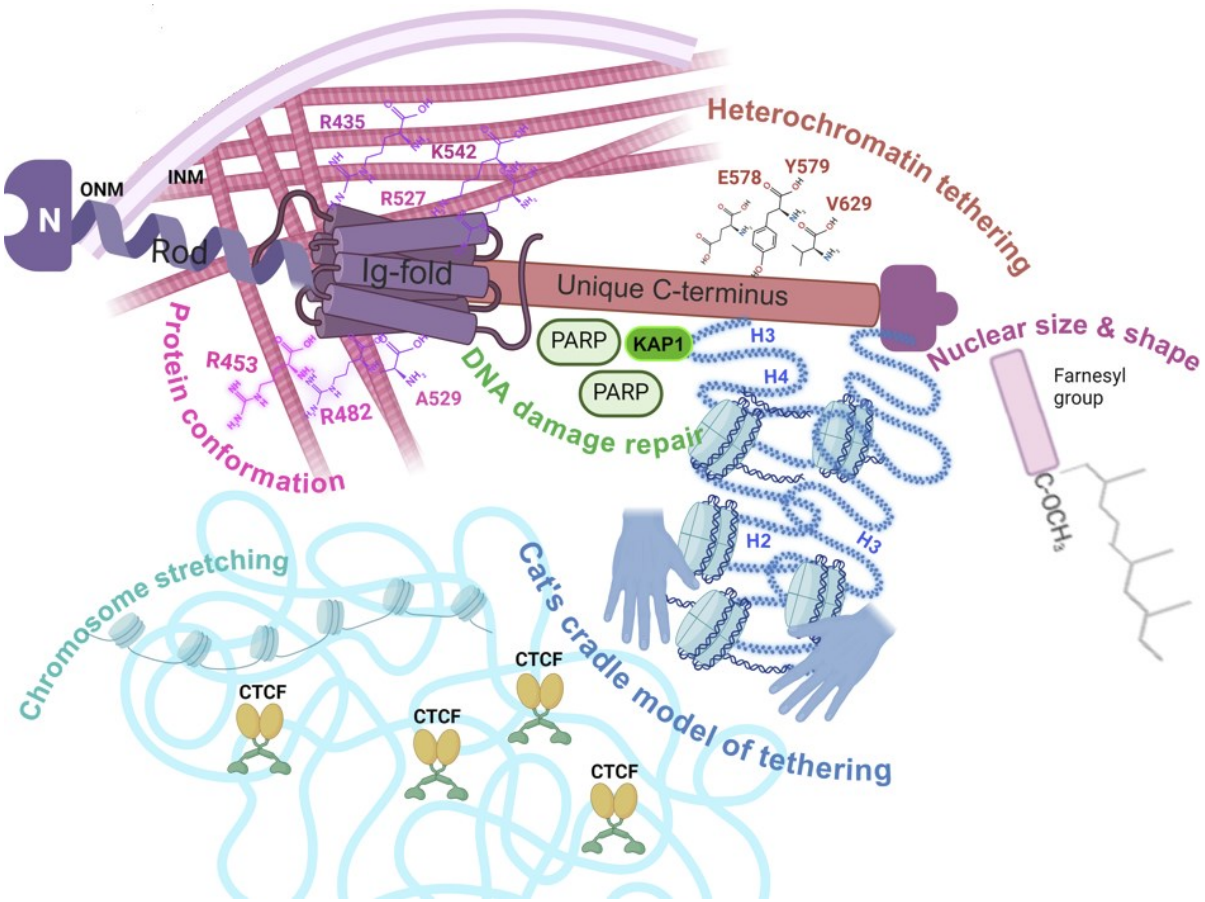

Figure 7.1. Proposed model of Lamin A functions.

Unique Lamin A C-terminal residues (red) directly bind nucleosomes (blue). IG-fold residues (pink) are important for Lamin A conformational structure. By tethering the heterochromatin at the nuclear periphery, the chromosomes are stretched (turquoise), and the nuclear area is expanded. Lamin A binds KAP1/PARP1 (green), important in DNA damage repair. Defarnesylation is an important determinant of Lamin A heterochromatin tethering, and it affects nuclear size and shape.

Interestingly, in Chapter 4 we report high PARP1 expression by degenerating *rd1* rods devoid of LA expression. This suggests that excessive PARP1 activation could contribute to retinal degeneration. It would be interesting to directly test the role of LA/C in PARP1-dependant DNA damage response.

The logic of Lamin A heterochromatin tethering

Recently, lamin proteins have been a focus of intense studies[35,66,219,220], but their role in HC tethering is unclear in the literature. A-type lamins have been portrayed as being insufficient for tethering, while B-type lamins and LC are often portrayed as exhibiting equivalent tethering competence versus LA. Here, we define and reinforce LA's position as an independent HC tethering organizer and a major regulator of genome architecture. In agreement with Misteli and Medalia study on the LA C-terminal domain sufficiency, using Alphafold3 modeling, we found that the LA C-terminus interacted directly with the heterochromatic nucleosomes H2A, H2B and H4. However, the internal LA C-terminal contacts between the IG-fold and C-terminal tail were also required for full HC tethering function.

Here, we find that the LA isoform tethers H3K9me2, H3K27me3 and H3K9me3 histones to the nuclear periphery via its defarnesylated C-terminal tail. Fusion of epitope tags (Flag, GFP) to the N-terminal head of lamins has been a consistent practice in cell biology research for a number of years. However, we[219] and others reported[347,356] that tags interfere with normal LA function. It is likely that N-terminal tags affect the ability of LA to form a functional filamentous network[337] and thereby cause complete function-blocking of HC tethering[219].

While our functional experiments perhaps cannot definitively prove that LA binds HC independently of protein partners, we addressed this question by using biochemical experiments.We took advantage of the tethering-incompetent LA constructs, in order to reveal the differences between the wild-type LA and GFP-LA interactomes. We showed that indeed, the interactomes differed very little. Only histones and PARP1 were significantly enriched in the LA-tethering competent interactome. These observations argue against the requirement for partner proteins in HC tethering. PARP1 might be an exception to this conclusion, but we think that PARP1 is more likely to reflect an interaction between tethering-competent LA and damaged DNA present in the 293 cell lines, rather than with undamaged HC.

By overexpressing laminopathic mutants in mouse rods, we revealed that complete loss of tethering function is a common trait of different non-progeroid and progeroid laminopathies, suggesting this can have a significant effect on disease pathology. Interestingly, defarnesylation can partially rescue tethering of permanently farnesylated progeroid mutants. This is in line with previous research which revealed that progeroid cells treated with farnesyltransferase inhibitors restore nuclear shape [357]. Interestingly, it was shown that defarnesylated B-type lamin in *Drosophila* can tether chromatin[310]. In the future, defarnesylated LB1/2 C-terminal domain would be an interesting target for HC tethering sufficiency tests in rod photoreceptors. However, our data would predict that LB1/2 will not tether HC very well, as these proteins do not include the V629 and *interface* amino acids that form bonds with histone proteins in our models. Moreover, in preliminary experiments (not shown), we cultured adult retinas in the presence of farnesylatransferase inhibitors, but did not observe obvious HC tethering. Considering the loss or defective HC tethering in virtually all laminopathic mutants inspected in this study, it would be useful to transgenically express

specific LA disease mutations in rods and examine the consequences of aberrant tethering on the disease-specific interactome without the interference of other potential tethers[358,64].

Future perspectives on LA functions in genome organization and degeneration

Photoreceptors are extremely prone to degeneration, as they are among the most metabolically expensive cells in the body[257]. Higher order genome organization has a well-established and fundamental importance in gene regulation, especially in photoreceptors[66,199,200,201,202,203,204]. The dynamic changes in the photoreceptor epigenome during retinal development have been thoroughly explored by Aldiri et al[212]. Interestingly, dynamic DNA methylation during retinogenesis accounts for a small percentage of developmental gene regulation. Epigenetic modifications that happen in parallel with rod genome inversion seem to be the drivers for the activation of differentiation genes, rather than silencing of progenitor genes. Interestingly, rod genes have been characterized by some of the most dramatic changes during development, through activated promoters and superenhancers. However, non-rod genes are repressed via H3K27me3 deposition in a cell-type specific fashion[212]. More detailed study of the chromatin landscape during retinal development identified cell-type and developmental stage specific enhancers. 25% of rod specific genes increase promoter-enhancer interactions (that span even across EC/fHC domains) that correlate with gene expression during development. Although they report that TAD boundaries in rods are conserved throughout development, there are still major changes in the localization of genes between A and B chromatin compartments[213].

Based on our ATAC-seq (Chapter 3) and Nab2 expression data in LA upregulating rods (Chapter 3 Appendix), HC tethering in the context of degeneration serves to poise regulatory

elements to facilitate the stress response. Our data suggest that LA-mediated HC tethering might reconfigure the genome as a general response to degeneration. This is in line with other reports where LA/C is defined as a part of a proinflammatory response. In insulin resistant obese mice, LA/C upregulates in adipose tissue macrophages[359]. It would be interesting to probe LA and siRNA LA effects on chromatin accessibility and transcriptome in the *rd10* model of retinal degeneration, which is known to degenerate slower than *rd1*. Equally important, transgenic laminopathic mutant expression in rods would potentially reveal an exact effect of aberrant HC tethering on the genome and transcriptome. Rod nuclei have a high level of transcriptional activity[189], so any kind of transcriptomic changes are readily detectable.

What is the purpose of HC tethering? LA/C upregulates in degenerating rod photoreceptors[66,219,220], cancers[360] and neurodegenerative diseases[270]. We showed that LA/C upregulation correlates with the start of rod photoreceptor degeneration, reorganizing the nucleus and prolonging HC tethering in maturing rods. Our experiments in wild-type cells suggest that LA likely stretches the chromosomes and increases genome accessibility[220]. Interestingly, inverted rod photoreceptors repair DNA inefficiently and express low pKAP levels in response to gamma irradiation. Restoration of HC tethering by expressing Lbr in murine rod photoreceptors rescued both of these inefficiencies[110,111]. It is observed that absence of LA/C accelerates aging and causes DNA damage accumulation in laminopathic cells[115,357]. It is reasonable to presume that the LA-tethering mediated stretching of the accessible chromatin favours DNA repair. LA is required to maintain a pool of 53BP1 so it can be recruited to the sites of DNA damage to facilitate non-homologous end joining[103,104].

Interestingly, Lammerding group reported that *LMNA* mutations reduced nuclear stability and caused rupture of the NE in skeletal muscle cells, resulting in DNA damage, DNA damage

response activation and reduced cell viability. Nuclear migration during skeletal muscle maturation correlated with disease and DNA damage severity in the mouse models, while reducing cytoskeletal forces on the myonuclei prevented NE damage and rescued myofiber function and viability in *LMNA* mutant myofibers, indicating that myofiber dysfunction is the result of mechanically induced NE damage and can be observed as a pathogenic contributor for *LMNA* skeletal muscle diseases[361].

To begin to understand the upstream events responsible for LA upregulation during degeneration, we performed co-staining experiments with other markers of cellular stress responses. We report that LA is highly co-expressed with pKAP1, a marker of the DNA damage response. Whereas LA expression peaks early in the degenerative process, we found that pKAP1 marks rod photoreceptor nuclei throughout degeneration. We also show that LA depletion in rods accelerates cell death. Together, these data establish LA upregulation as an adaptive response to DNA damage during rod degeneration. Our data suggest that both LA and KAP1 phosphorylation may converge to reorganize HC during early stages of rod photoreceptor degeneration. LA and pKAP1 may be used as markers of distinct phases of degeneration. Given what we learned in previous chapters, and that in inverted murine rod nuclei DNA repair is inefficient, it would be interesting to see how the competence or incompetence of laminopathic mutants affects DNA repair in photoreceptor degeneration.

Nuclear envelope instability in inflammation and aging

The efficiency of DNA repair is known to decrease with age[362]. It has been theorised that aging arises due to DNA damage accumulation or perhaps the loss of HC. Progeroid and normative aging cells show several common hallmarks such as increased DNA damage, loss of constitutive HC, epigenetic alterations and genome instability. Interestingly, mutations of

proteins which play a crucial role in DNA repair are known to cause progeroid disorders[152]. Lamin A/C modulates healthy aging[363,364] and upregulates in degeneration[220] as an adaptive stress response to DNA damage. Despite a fairly high occurence of HC loss in progeroid and healthy aging cells, our work implies that HC tethering seems to be separable from aging. Our results demonstrate that both progeroid and non-progeroid *LMNA* mutations lead to loss of HC tethering at the nuclear periphery. Additionally, progeroid nuclei are characterized by extreme nuclear size and shape aberrations. Here, we show that LA mutants dominantly affect nuclear morphology, while HC tethering can be rescued by wild-type LA (or Lbr) expression in laminopathic nuclei. These data suggest that destabilization of the nuclear envelope, and perhaps rupture, might be the driving force towards aging. However, nuclear rupture has been demonstrated in non-progeroid laminopathies as well, especially cardiomyopathies[365] and muscular dystrophies, as reported by Lammerding group[361], essentially accelerating the aging process within the muscle itself.

For example, cGas/Sting[366] or extracellular matrix signaling pathways[367] link nuclear rupture with upregulated inflammatory signalling. Interestingly, it was found that laminopathic nuclear rupture precedes transcriptional changes and DNA damage accumulation[365]. In the future, it will be necessary to examine the mechanisms behind nuclear rupture and the role it plays in inflammation and aging.

Conclusion

Since LA/C is frequently upregulated in the conditions of transcriptional stress and DNA damage, there is enough evidence to suggest that heterochromatin tethering may be a cell mechanism important for the regulation of chromatin accessibility, in order to poise the regulatory elements for a stress response. Lamin A-induced heterochromatin tethering might additionally support DNA damage repair. Given all the experimental evidence, we propose that the Lamin A C-terminus is the main heterochromatin tethering domain and a determinant of nuclear size and shape, while the IG-fold domain is required to position C-terminal residues in apposition to the nucleosome. In the future, a further insight into these mechanisms could be the way of understanding longevity and providing therapeutics for many laminopathies. Heterochromatin tethering certainly is an important determinant of the life of the cell.

Chapter 8. References

[1] R. D. Kornberg, "Chromatin Structure: A Repeating Unit of Histones and DNA," *Science (New York, N.Y.)* 184, no. 4139 (May 24, 1974): 868–71, https://doi.org/10.1126/science.184.4139.868.

[2] François Gros and Federation of European Biochemical Societies, *Organization and Expression of the Eukaryotic Genome ; Biochemical Mechanisms of Differentiation in Prokaryotes and Eukaryotes: Federation of European Biochemical Societies Tenth Meeting, Paris, 1975* (North-Holland Publishing Company, 1975).

[3] M. Noll and R. D. Kornberg, "Action of Micrococcal Nuclease on Chromatin and the Location of Histone H1," *Journal of Molecular Biology* 109, no. 3 (January 25, 1977): 393–404, https://doi.org/10.1016/s0022-2836(77)80019-3.

[4] Peter B. Becker and Wolfram Hörz, "ATP-Dependent Nucleosome Remodeling," *Annual Review of Biochemistry* 71, no. Volume 71, 2002 (July 1, 2002): 247–73, https://doi.org/10.1146/annurev.biochem.71.110601.135400.

[5] Sajad Hussain Syed et al., "Single-Base Resolution Mapping of H1-Nucleosome Interactions and 3D Organization of the Nucleosome," *Proceedings of the National Academy of Sciences of the United States of America* 107, no. 21 (May 25, 2010): 9620–25, https://doi.org/10.1073/pnas.1000309107.

[6] Kazuhiro Maeshima, Satoru Ide, and Michael Babokhov, "Dynamic Chromatin Organization without the 30-Nm Fiber," *Current Opinion in Cell Biology*, Cell Nucleus, 58 (June 1, 2019): 95–104, https://doi.org/10.1016/j.ceb.2019.02.003.

[7] Job Dekker and Tom Misteli, "Long-Range Chromatin Interactions," *Cold Spring Harbor Perspectives in Biology* 7, no. 10 (October 2015): a019356, https://doi.org/10.1101/cshperspect.a019356.

[8] Jesse R. Dixon et al., "Topological Domains in Mammalian Genomes Identified by Analysis of Chromatin Interactions," *Nature* 485, no. 7398 (April 11, 2012): 376–80, https://doi.org/10.1038/nature11082.

[9] Geoffrey Fudenberg et al., "Formation of Chromosomal Domains by Loop Extrusion," *Cell Reports* 15, no. 9 (May 31, 2016): 2038–49, https://doi.org/10.1016/j.celrep.2016.04.085.

[10] Job Dekker and Leonid Mirny, "The 3D Genome as Moderator of Chromosomal Communication," *Cell* 164, no. 6 (March 10, 2016): 1110–21, https://doi.org/10.1016/j.cell.2016.02.007.

[11] Thomas Cremer, Christoph Cremer, and Peter Lichter, "Recollections of a Scientific Journey Published in Human Genetics: From Chromosome Territories to Interphase Cytogenetics and Comparative Genome Hybridization," *Human Genetics* 133, no. 4 (April 1, 2014): 403–16, https://doi.org/10.1007/s00439-014-1425-5.

[12] Robin C. Allshire and Hiten D. Madhani, "Ten Principles of Heterochromatin Formation and Function," *Nature Reviews. Molecular Cell Biology* 19, no. 4 (April 2018): 229–44, https://doi.org/10.1038/nrm.2017.119.

[13] Olivia Morrison and Jitendra Thakur, "Molecular Complexes at Euchromatin, Heterochromatin and Centromeric Chromatin," *International Journal of Molecular Sciences* 22, no. 13 (June 28, 2021): 6922, https://doi.org/10.3390/ijms22136922.

[14] Nehmé Saksouk, Elisabeth Simboeck, and Jérôme Déjardin, "Constitutive Heterochromatin Formation and Transcription in Mammals," *Epigenetics & Chromatin* 8, no. 1 (January 15, 2015): 3, https://doi.org/10.1186/1756-8935-8-3.

[15] Patrick Trojer and Danny Reinberg, "Facultative Heterochromatin: Is There a Distinctive Molecular Signature?," *Molecular Cell* 28, no. 1 (October 12, 2007): 1–13, https://doi.org/10.1016/j.molcel.2007.09.011.

[16] Antoine H. F. M. Peters et al., "Loss of the Suv39h Histone Methyltransferases Impairs Mammalian Heterochromatin and Genome Stability," *Cell* 107, no. 3 (November 2, 2001): 323–37, https://doi.org/10.1016/S0092-8674(01)00542-6.

[17] Zachary L. Watson et al., "Histone Methyltransferases EHMT1 and EHMT2 (GLP/G9A) Maintain PARP Inhibitor Resistance in High-Grade Serous Ovarian Carcinoma," *Clinical Epigenetics* 11, no. 1 (November 27, 2019): 165, https://doi.org/10.1186/s13148-019-0758-2.

[18] Jun-ichi Nakayama et al., "Role of Histone H3 Lysine 9 Methylation in Epigenetic Control of Heterochromatin Assembly," *Science* 292, no. 5514 (April 6, 2001): 110–13, https://doi.org/10.1126/science.1060118.

[19] Thomas Schalch et al., "High-Affinity Binding of Chp1 Chromodomain to K9 Methylated Histone H3 Is Required to Establish Centromeric Heterochromatin," *Molecular Cell* 34, no. 1 (April 10, 2009): 36–46, https://doi.org/10.1016/j.molcel.2009.02.024.

[20] Monika Lachner et al., "Methylation of Histone H3 Lysine 9 Creates a Binding Site for HP1 Proteins," *Nature* 410, no. 6824 (March 2001): 116–20, https://doi.org/10.1038/35065132.

[21] Ru Cao et al., "Role of Histone H3 Lysine 27 Methylation in Polycomb-Group Silencing," *Science (New York, N.Y.)* 298, no. 5595 (November 1, 2002): 1039–43, https://doi.org/10.1126/science.1076997.

[22] Erez Lieberman-Aiden et al., "Comprehensive Mapping of Long-Range Interactions Reveals Folding Principles of the Human Genome," *Science (New York, N.Y.)* 326, no. 5950 (October 9, 2009): 289–93, https://doi.org/10.1126/science.1181369.

[23] Martin Falk et al., "Heterochromatin Drives Compartmentalization of Inverted and Conventional Nuclei," *Nature* 570, no. 7761 (June 2019): 395–99, https://doi.org/10.1038/s41586-019-1275-3.

[24] Jenny A. Croft et al., "Differences in the Localization and Morphology of Chromosomes in the Human Nucleus," *The Journal of Cell Biology* 145, no. 6 (June 14, 1999): 1119–31.

[25] Máté Borsos et al., "Genome–Lamina Interactions Are Established de Novo in the Early Mouse Embryo," *Nature* 569, no. 7758 (May 2019): 729–33, https://doi.org/10.1038/s41586-019-1233-0.

[26] Nolwenn Briand and Philippe Collas, "Lamina-Associated Domains: Peripheral Matters and Internal Affairs," *Genome Biology* 21, no. 1 (April 2, 2020): 85, https://doi.org/10.1186/s13059-020-02003-5.

[27] Lars Guelen et al., "Domain Organization of Human Chromosomes Revealed by Mapping of Nuclear Lamina Interactions," *Nature* 453, no. 7197 (June 12, 2008): 948–51, https://doi.org/10.1038/nature06947.

[28] Sergey V. Ulianov et al., "Nuclear Lamina Integrity Is Required for Proper Spatial Organization of Chromatin in Drosophila," *Nature Communications* 10, no. 1 (March 12, 2019): 1176, https://doi.org/10.1038/s41467-019-09185-y.

[29] Xiaobin Zheng et al., "Lamins Organize the Global Three-Dimensional Genome from the Nuclear Periphery," *Molecular Cell* 71, no. 5 (September 2018): 802-815.e7, https://doi.org/10.1016/j.molcel.2018.05.017.

[30] Wouter Meuleman et al., "Constitutive Nuclear Lamina-Genome Interactions Are Highly Conserved and Associated with A/T-Rich Sequence," *Genome Research* 23, no. 2 (February 2013): 270–80, https://doi.org/10.1101/gr.141028.112.

[31] Daan Peric-Hupkes et al., "Molecular Maps of the Reorganization of Genome-Nuclear Lamina Interactions during Differentiation," *Molecular Cell* 38, no. 4 (May 28, 2010): 603–13, https://doi.org/10.1016/j.molcel.2010.03.016.

[32] Jop Kind et al., "Genome-Wide Maps of Nuclear Lamina Interactions in Single Human Cells," *Cell* 163, no. 1 (September 24, 2015): 134–47, https://doi.org/10.1016/j.cell.2015.08.040.

[33] Andrey Poleshko et al., "H3K9me2 Orchestrates Inheritance of Spatial Positioning of Peripheral Heterochromatin through Mitosis," ed. Andrés Aguilera, Jessica K Tyler, and Andrew S Belmont, *eLife* 8 (October 1, 2019): e49278, https://doi.org/10.7554/eLife.49278.

[34] Cheryl L. Smith et al., "Global Chromatin Relabeling Accompanies Spatial Inversion of Chromatin in Rod Photoreceptors," *Science Advances* 7, no. 39 (September 24, 2021): eabj3035, https://doi.org/10.1126/sciadv.abj3035.

[35] Jennifer C. Harr et al., "Directed Targeting of Chromatin to the Nuclear Lamina Is Mediated by Chromatin State and A-Type Lamins," *Journal of Cell Biology* 208, no. 1 (January 5, 2015): 33–52, https://doi.org/10.1083/jcb.201405110.

[36] F. Lin and H. J. Worman, "Structural Organization of the Human Gene Encoding Nuclear Lamin A and Nuclear Lamin C," *The Journal of Biological Chemistry* 268, no. 22 (August 5, 1993): 16321–26.

[37] C. Stewart and B. Burke, "Teratocarcinoma Stem Cells and Early Mouse Embryos Contain Only a Single Major Lamin Polypeptide Closely Resembling Lamin B," *Cell* 51, no. 3 (November 6, 1987): 383–92, https://doi.org/10.1016/0092-8674(87)90634-9.

[38] Ruth-Ariane Röber, Klaus Weber, and Mary Osborn, "Differential Timing of Nuclear Lamin A/C Expression in the Various Organs of the Mouse Embryo and the Young Animal: A Developmental Study," *Development* 105, no. 2 (1989): 365–78.

[39] Harald Herrmann and Ueli Aebi, "Intermediate Filaments: Structure and Assembly," *Cold Spring Harbor Perspectives in Biology* 8, no. 11 (November 1, 2016): a018242, https://doi.org/10.1101/cshperspect.a018242.

[40] H. Herrmann and R. Foisner, "Intermediate Filaments: Novel Assembly Models and Exciting New Functions for Nuclear Lamins," *Cellular and Molecular Life Sciences: CMLS* 60, no. 8 (August 2003): 1607–12, https://doi.org/10.1007/s00018-003-3004-0.

[41] Dale K. Shumaker et al., "Functions and Dysfunctions of the Nuclear Lamin Ig-Fold Domain in Nuclear Assembly, Growth, and Emery-Dreifuss Muscular Dystrophy," *Proceedings of the National Academy of Sciences of the United States of America* 102, no. 43 (October 25, 2005): 15494–99, https://doi.org/10.1073/pnas.0507612102.

[42] Isabelle Krimm et al., "The Ig-like Structure of the C-Terminal Domain of Lamin A/C, Mutated in Muscular Dystrophies, Cardiomyopathy, and Partial Lipodystrophy," *Structure (London, England: 1993)* 10, no. 6 (June 2002): 811–23, https://doi.org/10.1016/s0969-2126(02)00777-3.

[43] Sirano Dhe-Paganon et al., "Structure of the Globular Tail of Nuclear Lamin *," *Journal of Biological Chemistry* 277, no. 20 (May 17, 2002): 17381–84, https://doi.org/10.1074/jbc.C200038200.

[44] Jacques Young et al., "Type A Insulin Resistance Syndrome Revealing a Novel Lamin A Mutation," *Diabetes* 54, no. 6 (June 2005): 1873–78, https://doi.org/10.2337/diabetes.54.6.1873.

[45] Larisa E. Kapinos et al., "Simultaneous Formation of Right-and Left-Handed Anti-Parallel Coiled-Coil Interfaces by a Coil2 Fragment of Human Lamin A," *Journal of Molecular Biology* 408, no. 1 (2011): 135–46.

[46] Robert D. Goldman, Anne E. Goldman, and Dale K. Shumaker, "Nuclear Lamins: Building Blocks of Nuclear Structure and Function," *Novartis Foundation Symposium* 264 (2005): 3–16; discussion 16-21, 227–30.

[47] Brandon S. J. Davies et al., "The Posttranslational Processing of Prelamin A and Disease," *Annual Review of Genomics and Human Genetics* 10, no. Volume 10, 2009 (September 22, 2009): 153–74, https://doi.org/10.1146/annurev-genom-082908-150150.

[48] Dan N. Simon and Katherine L. Wilson, "Partners and Post-Translational Modifications of Nuclear Lamins," *Chromosoma* 122, no. 0 (March 2013): 13–31, https://doi.org/10.1007/s00412-013-0399-8.

[49] Magdalena Machowska, Katarzyna Piekarowicz, and Ryszard Rzepecki, "Regulation of Lamin Properties and Functions: Does Phosphorylation Do It All?," *Open Biology* Open Biol. 5: 150094. (November 18, 2015), https://doi.org/10.1098/rsob.150094.

[50] Jemima Barrowman et al., "Requirements for Efficient Proteolytic Cleavage of Prelamin A by ZMPSTE24," *PLOS ONE* 7, no. 2 (February 15, 2012): e32120, https://doi.org/10.1371/journal.pone.0032120.

[51] Rebecca de Leeuw, Yosef Gruenbaum, and Ohad Medalia, "Nuclear Lamins: Thin Filaments with Major Functions," *Trends in Cell Biology* 28, no. 1 (January 2018): 34–45, https://doi.org/10.1016/j.tcb.2017.08.004.

[52] Yosef Gruenbaum and Roland Foisner, "Lamins: Nuclear Intermediate Filament Proteins with Fundamental Functions in Nuclear Mechanics and Genome Regulation," *Annual Review of Biochemistry* 84 (2015): 131–64, https://doi.org/10.1146/annurev-biochem-060614-034115.

[53] Takeshi Shimi et al., "The A- and B-Type Nuclear Lamin Networks: Microdomains Involved in Chromatin Organization and Transcription," *Genes & Development* 22, no. 24 (December 15, 2008): 3409–21, https://doi.org/10.1101/gad.1735208.

[54] Thomas Dechat, Katrin Pfleghaar, et al., "Nuclear Lamins: Major Factors in the Structural Organization and Function of the Nucleus and Chromatin," *Genes & Development* 22, no. 7 (April 1, 2008): 832–53, https://doi.org/10.1101/gad.1652708.

[55] Wei Xie et al., "A-Type Lamins Form Distinct Filamentous Networks with Differential Nuclear Pore Complex Associations," *Current Biology: CB* 26, no. 19 (October 10, 2016): 2651–58, https://doi.org/10.1016/j.cub.2016.07.049.

[56] Takeshi Shimi et al., "Structural Organization of Nuclear Lamins A, C, B1, and B2 Revealed by Superresolution Microscopy," *Molecular Biology of the Cell* 26, no. 22 (November 5, 2015): 4075–86, https://doi.org/10.1091/mbc.E15-07-0461.

[57] Yagmur Turgay et al., "The Molecular Architecture of Lamins in Somatic Cells," *Nature* 543, no. 7644 (March 9, 2017): 261–64, https://doi.org/10.1038/nature21382.

[58] Q. Ye and H. J. Worman, "Protein-Protein Interactions between Human Nuclear Lamins Expressed in Yeast," *Experimental Cell Research* 219, no. 1 (July 1995): 292–98, https://doi.org/10.1006/excr.1995.1230.

[59] S. D. Georgatos, C. Stournaras, and G. Blobel, "Heterotypic and Homotypic Associations between the Nuclear Lamins: Site-Specificity and Control by Phosphorylation," *Proceedings of the National Academy of Sciences of the United States of America* 85, no. 12 (June 1988): 4325–29, https://doi.org/10.1073/pnas.85.12.4325.

[60] Sergei V. Strelkov et al., "Crystal Structure of the Human Lamin A Coil 2B Dimer: Implications for the Head-to-Tail Association of Nuclear Lamins," *Journal of Molecular Biology* 343, no. 4 (October 29, 2004): 1067–80, https://doi.org/10.1016/j.jmb.2004.08.093.

[61] Kazuhiro Isobe et al., "The Last Twenty Residues in the Head Domain of Mouse Lamin A Contain Important Structural Elements for Formation of Head-to-Tail Polymers in Vitro," *Bioscience, Biotechnology, and Biochemistry* 71, no. 5 (May 2007): 1252–59, https://doi.org/10.1271/bbb.60674.

[62] Johanna Block et al., "Physical Properties of Cytoplasmic Intermediate Filaments," *Biochimica Et Biophysica Acta* 1853, no. 11 Pt B (November 2015): 3053–64, https://doi.org/10.1016/j.bbamcr.2015.05.009.

[63] Bruce Nmezi et al., "Concentric Organization of A- and B-Type Lamins Predicts Their Distinct Roles in the Spatial Organization and Stability of the Nuclear Lamina," *Proceedings of the National Academy of Sciences of the United States of America* 116, no. 10 (March 5, 2019): 4307–15, https://doi.org/10.1073/pnas.1810070116.

[64] Travis A. Dittmer et al., "Systematic Identification of Pathological Lamin A Interactors," *Molecular Biology of the Cell* 25, no. 9 (May 1, 2014): 1493–1510, https://doi.org/10.1091/mbc.E14-02-0733.

[65] Nard Kubben, Jan Willem Voncken, and Tom Misteli, "Mapping of Protein- and Chromatin-Interactions at the Nuclear Lamina," *Nucleus (Austin, Tex.)* 1, no. 6 (2010): 460–71, https://doi.org/10.4161/nucl.1.6.13513.

[66] Irina Solovei et al., "LBR and Lamin A/C Sequentially Tether Peripheral Heterochromatin and Inversely Regulate Differentiation," *Cell* 152, no. 3 (January 2013): 584–98, https://doi.org/10.1016/j.cell.2013.01.009.

[67] Ada L. Olins et al., "Lamin B Receptor: Multi-Tasking at the Nuclear Envelope," *Nucleus (Austin, Tex.)* 1, no. 1 (2010): 53–70, https://doi.org/10.4161/nucl.1.1.10515.

[68] Yasuhiro Hirano et al., "Lamin B Receptor Recognizes Specific Modifications of Histone H4 in Heterochromatin Formation," *The Journal of Biological Chemistry* 287, no. 51 (December 14, 2012): 42654–63, https://doi.org/10.1074/jbc.M112.397950.

[69] Dimitra Makatsori et al., "The Inner Nuclear Membrane Protein Lamin B Receptor Forms Distinct Microdomains and Links Epigenetically Marked Chromatin to the Nuclear Envelope," *The Journal of Biological Chemistry* 279, no. 24 (June 11, 2004): 25567–73, https://doi.org/10.1074/jbc.M313606200.

[70] Pei-Ling Tsai et al., "The Lamin B Receptor Is Essential for Cholesterol Synthesis and Perturbed by Disease-Causing Mutations," *eLife* 5 (n.d.): e16011, https://doi.org/10.7554/eLife.16011.

[71] Monika Zwerger et al., "Induction of a Massive Endoplasmic Reticulum and Perinuclear Space Expansion by Expression of Lamin B Receptor Mutants and the Related Sterol Reductases TM7SF2 and DHCR7," *Molecular Biology of the Cell* 21, no. 2 (January 15, 2010): 354–68, https://doi.org/10.1091/mbc.e09-08-0739.

[72] Shao H. Yang et al., "An Absence of Both Lamin B1 and Lamin B2 in Keratinocytes Has No Effect on Cell Proliferation or the Development of Skin and Hair," *Human Molecular Genetics* 20, no. 18 (September 15, 2011): 3537–44, https://doi.org/10.1093/hmg/ddr266.

[73] Vérène Stierlé et al., "The Carboxyl-Terminal Region Common to Lamins A and C Contains a DNA Binding Domain," *Biochemistry* 42, no. 17 (May 6, 2003): 4819–28, https://doi.org/10.1021/bi020704g.

[74] H Taniura, C Glass, and L Gerace, "A Chromatin Binding Site in the Tail Domain of Nuclear Lamins That Interacts with Core Histones.," *Journal of Cell Biology* 131, no. 1 (October 1, 1995): 33–44, https://doi.org/10.1083/jcb.131.1.33.

[75] R. L. Shoeman and P. Traub, "The in Vitro DNA-Binding Properties of Purified Nuclear Lamin Proteins and Vimentin," *The Journal of Biological Chemistry* 265, no. 16 (June 5, 1990): 9055–61.

[76] Ayelet Margalit et al., "Barrier-to-Autointegration Factor--a BAFfling Little Protein," *Trends in Cell Biology* 17, no. 4 (April 2007): 202–8, https://doi.org/10.1016/j.tcb.2007.02.004.

[77] Dan N. Simon and Katherine L. Wilson, "The Nucleoskeleton as a Genome-Associated Dynamic 'Network of Networks,'" *Nature Reviews. Molecular Cell Biology* 12, no. 11 (October 5, 2011): 695–708, https://doi.org/10.1038/nrm3207.

[78] Brian Burke and Colin L. Stewart, "The Nuclear Lamins: Flexibility in Function," *Nature Reviews. Molecular Cell Biology* 14, no. 1 (January 2013): 13–24, https://doi.org/10.1038/nrm3488.

[79] Jun Liu et al., "MAN1 and Emerin Have Overlapping Function(s) Essential for Chromosome Segregation and Cell Division in Caenorhabditis Elegans," *Proceedings of the National Academy of Sciences of the United States of America* 100, no. 8 (April 15, 2003): 4598–4603, https://doi.org/10.1073/pnas.0730821100.

[80] J. Liu et al., "Essential Roles for Caenorhabditis Elegans Lamin Gene in Nuclear Organization, Cell Cycle Progression, and Spatial Organization of Nuclear Pore Complexes," *Molecular Biology of the Cell* 11, no. 11 (November 2000): 3937–47, https://doi.org/10.1091/mbc.11.11.3937.

[81] Katharina Thanisch et al., "Nuclear Envelope Localization of LEMD2 Is Developmentally Dynamic and Lamin A/C Dependent yet Insufficient for Heterochromatin Tethering," *Differentiation; Research in Biological Diversity* 94 (2017): 58–70, https://doi.org/10.1016/j.diff.2016.12.002.

[82] Camille Samson et al., "Structural Analysis of the Ternary Complex between Lamin A/C, BAF and Emerin Identifies an Interface Disrupted in Autosomal Recessive Progeroid Diseases," *Nucleic Acids Research* 46, no. 19 (November 2, 2018): 10460–73, https://doi.org/10.1093/nar/gky736.

[83] Christina Marchetti Bradley et al., "Structural Basis for DNA Bridging by Barrier-to-Autointegration Factor," *Nature Structural & Molecular Biology* 12, no. 10 (October 2005): 935–36, https://doi.org/10.1038/nsmb989.

[84] Cristina Capanni et al., "Lamin A Precursor Induces Barrier-to-Autointegration Factor Nuclear Localization," *Cell Cycle* 9, no. 13 (July 2010): 2600–2610, https://doi.org/10.4161/cc.9.13.12080.

[85] Andrey Poleshko et al., "The Human Protein PRR14 Tethers Heterochromatin to the Nuclear Lamina during Interphase and Mitotic Exit," *Cell Reports* 5, no. 2 (October 31, 2013): 292–301, https://doi.org/10.1016/j.celrep.2013.09.024.

[86] Agnieszka J. Nowak et al., "Chromatin-Modifying Complex Component Nurf55/P55 Associates with Histones H3 and H4 and Polycomb Repressive Complex 2 Subunit Su(z)12 through Partially Overlapping Binding Sites," *The Journal of Biological Chemistry* 286, no. 26 (July 1, 2011): 23388–96, https://doi.org/10.1074/jbc.M110.207407.

[87] Rebecca Reed Moody et al., "Probing the Interaction between the Histone Methyltransferase/Deacetylase Subunit RBBP4/7 and the Transcription Factor BCL11A in Epigenetic Complexes," *Journal of Biological Chemistry* 293, no. 6 (February 9, 2018): 2125–36, https://doi.org/10.1074/jbc.M117.811463.

[88] Q. Zhang, N. Vo, and R. H. Goodman, "Histone Binding Protein RbAp48 Interacts with a Complex of CREB Binding Protein and Phosphorylated CREB," *Molecular and Cellular Biology* 20, no. 14 (July 2000): 4970–78, https://doi.org/10.1128/MCB.20.14.4970-4978.2000.

[89] Mario Torrado et al., "Refinement of the Subunit Interaction Network within the Nucleosome Remodelling and Deacetylase (NuRD) Complex," *The FEBS Journal* 284, no. 24 (December 2017): 4216–32, https://doi.org/10.1111/febs.14301.

[90] Saad S. M. Alqarni et al., "Insight into the Architecture of the NuRD Complex: Structure of the RbAp48-MTA1 Subcomplex," *The Journal of Biological Chemistry* 289, no. 32 (August 8, 2014): 21844–55, https://doi.org/10.1074/jbc.M114.558940.

[91] Andria C Schibler et al., "Identification of Epigenetic Modulators as Determinants of Nuclear Size and Shape," ed. Megan C King, Detlef Weigel, and Dennis Discher, *eLife* 12 (May 23, 2023): e80653, https://doi.org/10.7554/eLife.80653.

[92] Thomas Dechat, Stephen A. Adam, et al., "Nuclear Lamins," *Cold Spring Harbor Perspectives in Biology* 2, no. 11 (November 2010): a000547, https://doi.org/10.1101/cshperspect.a000547.

[93] Joan M. Sobo et al., "Lamins: The Backbone of the Nucleocytoskeleton Interface," *Current Opinion in Cell Biology* 86 (February 2024): 102313, https://doi.org/10.1016/j.ceb.2023.102313.

[94] Howard J. Worman and Gisèle Bonne, "'Laminopathies:' A Wide Spectrum of Human Diseases," *Experimental Cell Research* 313, no. 10 (June 10, 2007): 2121–33, https://doi.org/10.1016/j.yexcr.2007.03.028.

[95] Mario Amendola and Bas van Steensel, "Nuclear Lamins Are Not Required for Lamina-Associated Domain Organization in Mouse Embryonic Stem Cells," *EMBO Reports* 16, no. 5 (May 2015): 610–17, https://doi.org/10.15252/embr.201439789.

[96] Youngjo Kim, Xiaobin Zheng, and Yixian Zheng, "Proliferation and Differentiation of Mouse Embryonic Stem Cells Lacking All Lamins," *Cell Research* 23, no. 12 (December 2013): 1420–23, https://doi.org/10.1038/cr.2013.118.

[97] T. Sullivan et al., "Loss of A-Type Lamin Expression Compromises Nuclear Envelope Integrity Leading to Muscular Dystrophy," *The Journal of Cell Biology* 147, no. 5 (November 29, 1999): 913–20, https://doi.org/10.1083/jcb.147.5.913.

[98] B. G. M. van Engelen et al., "The Lethal Phenotype of a Homozygous Nonsense Mutation in the Lamin A/C Gene," *Neurology* 64, no. 2 (January 25, 2005): 374–76, https://doi.org/10.1212/01.WNL.0000149763.15180.00.

[99] Hea-Jin Jung et al., "Regulation of Prelamin A but Not Lamin C by miR-9, a Brain-Specific microRNA," *Proceedings of the National Academy of Sciences of the United States of America* 109, no. 7 (February 14, 2012): E423–31, https://doi.org/10.1073/pnas.1111780109.

[100] Catherine Coffinier et al., "Abnormal Development of the Cerebral Cortex and Cerebellum in the Setting of Lamin B2 Deficiency," *Proceedings of the National Academy of Sciences of the United States of America* 107, no. 11 (March 16, 2010): 5076–81, https://doi.org/10.1073/pnas.0908790107.

[101] Catherine Coffinier et al., "Deficiencies in Lamin B1 and Lamin B2 Cause Neurodevelopmental Defects and Distinct Nuclear Shape Abnormalities in Neurons," *Molecular Biology of the Cell* 22, no. 23 (December 2011): 4683–93, https://doi.org/10.1091/mbc.E11-06-0504.

[102] Andrew N. Blackford and Stephen P. Jackson, "ATM, ATR, and DNA-PK: The Trinity at the Heart of the DNA Damage Response," *Molecular Cell* 66, no. 6 (June 15, 2017): 801–17, https://doi.org/10.1016/j.molcel.2017.05.015.

[103] Anne Bothmer et al., "53BP1 Regulates DNA Resection and the Choice between Classical and Alternative End Joining during Class Switch Recombination," *The Journal of Experimental Medicine* 207, no. 4 (April 12, 2010): 855–65, https://doi.org/10.1084/jem.20100244.

[104] Samuel F. Bunting et al., "53BP1 Inhibits Homologous Recombination in Brca1-Deficient Cells by Blocking Resection of DNA Breaks," *Cell* 141, no. 2 (April 16, 2010): 243–54, https://doi.org/10.1016/j.cell.2010.03.012.

[105] Ian Gibbs-Seymour et al., "Lamin A/C-Dependent Interaction with 53BP1 Promotes Cellular Responses to DNA Damage," *Aging Cell* 14, no. 2 (April 2015): 162–69, https://doi.org/10.1111/acel.12258.

[106] Abena B. Redwood et al., "A Dual Role for A-Type Lamins in DNA Double-Strand Break Repair," *Cell Cycle (Georgetown, Tex.)* 10, no. 15 (August 1, 2011): 2549–60, https://doi.org/10.4161/cc.10.15.16531.

[107] Shrestha Ghosh et al., "Lamin A Is an Endogenous SIRT6 Activator and Promotes SIRT6-Mediated DNA Repair," *Cell Reports* 13, no. 7 (November 2015): 1396–1406, https://doi.org/10.1016/j.celrep.2015.10.006.

[108] R. Scully et al., "Association of BRCA1 with Rad51 in Mitotic and Meiotic Cells," *Cell* 88, no. 2 (January 24, 1997): 265–75, https://doi.org/10.1016/s0092-8674(00)81847-4.

[109] Angela T. Noon et al., "53BP1-Dependent Robust Localized KAP-1 Phosphorylation Is Essential for Heterochromatic DNA Double-Strand Break Repair," *Nature Cell Biology* 12, no. 2 (February 2010): 177–84, https://doi.org/10.1038/ncb2017.

[110] Antonia Frohns et al., "Inefficient Double-Strand Break Repair in Murine Rod Photoreceptors with Inverted Heterochromatin Organization," *Current Biology: CB* 24, no. 10 (May 19, 2014): 1080–90, https://doi.org/10.1016/j.cub.2014.03.061.

[111] Florian Frohns et al., "Differences in the Response to DNA Double-Strand Breaks between Rod Photoreceptors of Rodents, Pigs, and Humans," *Cells* 9, no. 4 (April 2020): 947, https://doi.org/10.3390/cells9040947.

[112] Susana Gonzalo, "DNA Damage and Lamins," *Advances in Experimental Medicine and Biology* 773 (2014): 377–99, https://doi.org/10.1007/978-1-4899-8032-8_17.

[113] Mzwanele Ngubo et al., "Progeria-based Vascular Model Identifies Networks Associated with Cardiovascular Aging and Disease," *Aging Cell* 23, no. 7 (April 4, 2024): e14150, https://doi.org/10.1111/acel.14150.

[114] Jonathan Afilalo et al., "Age-Related Changes in Lamin A/C Expression in Cardiomyocytes," *American Journal of Physiology. Heart and Circulatory Physiology* 293, no. 3 (September 2007): H1451-1456, https://doi.org/10.1152/ajpheart.01194.2006.

[115] Gustavo Duque and Daniel Rivas, "Age-Related Changes in Lamin A/C Expression in the Osteoarticular System: Laminopathies as a Potential New Aging Mechanism," *Mechanisms of Ageing and Development* 127, no. 4 (April 1, 2006): 378–83, https://doi.org/10.1016/j.mad.2005.12.007.

[116] Giovanna Lattanzi et al., "Lamins Are Rapamycin Targets That Impact Human Longevity: A Study in Centenarians," *Journal of Cell Science* 127, no. Pt 1 (January 1, 2014): 147–57, https://doi.org/10.1242/jcs.133983.

[117] Jacob O. Spiegel, Bennett Van Houten, and Jacob D. Durrant, "PARP1: Structural Insights and Pharmacological Targets for Inhibition," *DNA Repair* 103 (July 2021): 103125, https://doi.org/10.1016/j.dnarep.2021.103125.

[118] Sarah M. Schreiner et al., "The Tethering of Chromatin to the Nuclear Envelope Supports Nuclear Mechanics," *Nature Communications* 6 (June 15, 2015): 7159, https://doi.org/10.1038/ncomms8159.

[119] Andrew D. Stephens et al., "Chromatin and Lamin A Determine Two Different Mechanical Response Regimes of the Cell Nucleus," *Molecular Biology of the Cell* 28, no. 14 (July 7, 2017): 1984–96, https://doi.org/10.1091/mbc.E16-09-0653.

[120] Kevin J. Chalut et al., "Chromatin Decondensation and Nuclear Softening Accompany Nanog Downregulation in Embryonic Stem Cells," *Biophysical Journal* 103, no. 10 (November 21, 2012): 2060–70, https://doi.org/10.1016/j.bpj.2012.10.015.

[121] Kristina Haase et al., "Extracellular Forces Cause the Nucleus to Deform in a Highly Controlled Anisotropic Manner," *Scientific Reports* 6 (February 19, 2016): 21300, https://doi.org/10.1038/srep21300.

[122] Yuta Shimamoto et al., "Nucleosome-Nucleosome Interactions via Histone Tails and Linker DNA Regulate Nuclear Rigidity," *Molecular Biology of the Cell* 28, no. 11 (June 1, 2017): 1580–89, https://doi.org/10.1091/mbc.E16-11-0783.

[123] Anthony H. B. de Vries et al., "Direct Observation of Nanomechanical Properties of Chromatin in Living Cells," *Nano Letters* 7, no. 5 (May 2007): 1424–27, https://doi.org/10.1021/nl070603+.

[124] Andrew D. Stephens, Edward J. Banigan, and John F. Marko, "Separate Roles for Chromatin and Lamins in Nuclear Mechanics," *Nucleus (Austin, Tex.)* 9, no. 1 (January 1, 2018): 119–24, https://doi.org/10.1080/19491034.2017.1414118.

[125] Bas van Steensel and Andrew S. Belmont, "Lamina-Associated Domains: Links with Chromosome Architecture, Heterochromatin, and Gene Repression," *Cell* 169, no. 5 (May 18, 2017): 780–91, https://doi.org/10.1016/j.cell.2017.04.022.

[126] Eivind G Lund et al., "Distinct Features of Lamin A-Interacting Chromatin Domains Mapped by ChIP-Sequencing from Sonicated or Micrococcal Nuclease-Digested Chromatin," *Nucleus* 6, no. 1 (January 20, 2015): 30–39, https://doi.org/10.4161/19491034.2014.990855.

[127] Dale K. Shumaker et al., "Mutant Nuclear Lamin A Leads to Progressive Alterations of Epigenetic Control in Premature Aging," *Proceedings of the National Academy of Sciences of the United States of America* 103, no. 23 (June 6, 2006): 8703–8, https://doi.org/10.1073/pnas.0602569103.

[128] Ilaria Filesi et al., "Alterations of Nuclear Envelope and Chromatin Organization in Mandibuloacral Dysplasia, a Rare Form of Laminopathy," *Physiological Genomics* 23, no. 2 (October 17, 2005): 150–58, https://doi.org/10.1152/physiolgenomics.00060.2005.

[129] Lee E. Finlan et al., "Recruitment to the Nuclear Periphery Can Alter Expression of Genes in Human Cells," *PLOS Genetics* 4, no. 3 (March 21, 2008): e1000039, https://doi.org/10.1371/journal.pgen.1000039.

[130] K. L. Reddy et al., "Transcriptional Repression Mediated by Repositioning of Genes to the Nuclear Lamina," *Nature* 452, no. 7184 (March 13, 2008): 243–47, https://doi.org/10.1038/nature06727.

[131] Lei Chang et al., "Nuclear Peripheral Chromatin-Lamin B1 Interaction Is Required for Global Integrity of Chromatin Architecture and Dynamics in Human Cells," *Protein & Cell* 13, no. 4 (April 2022): 258–80, https://doi.org/10.1007/s13238-020-00794-8.

[132] Xianrong Wong et al., "Lamin C Is Required to Establish Genome Organization after Mitosis," *Genome Biology* 22 (November 15, 2021): 305, https://doi.org/10.1186/s13059-021-02516-7.

[133] Silvia Bione et al., "Identification of a Novel X-Linked Gene Responsible for Emery-Dreifuss Muscular Dystrophy," *Nature Genetics* 8, no. 4 (December 1994): 323–27, https://doi.org/10.1038/ng1294-323.

[134] Giovanna Lattanzi et al., "Emerging Perspectives on Laminopathies," *Cell Health and Cytoskeleton* 8 (April 7, 2016): 25–35, https://doi.org/10.2147/CHC.S59507.

[135] Vittoria Cenni et al., "Lamin A Involvement in Ageing Processes," *Ageing Research Reviews* 62 (September 1, 2020): 101073, https://doi.org/10.1016/j.arr.2020.101073.

[136] Stephen G. Young et al., "Prelamin A Farnesylation and Progeroid Syndromes *," *Journal of Biological Chemistry* 281, no. 52 (December 29, 2006): 39741–45, https://doi.org/10.1074/jbc.R600033200.

[137] Travis A. Dittmer and Tom Misteli, "The Lamin Protein Family," *Genome Biology* 12, no. 5 (2011): 222, https://doi.org/10.1186/gb-2011-12-5-222.

[138] Julia Rankin et al., "Extreme Phenotypic Diversity and Nonpenetrance in Families with the LMNA Gene Mutation R644C," *American Journal of Medical Genetics. Part A* 146A, no. 12 (June 15, 2008): 1530–42, https://doi.org/10.1002/ajmg.a.32331.

[139] Ivan I. Boubriak et al., "Stress-Induced Release of Oct-1 from the Nuclear Envelope Is Mediated by JNK Phosphorylation of Lamin B1," *PLOS ONE* 12, no. 5 (May 24, 2017): e0177990, https://doi.org/10.1371/journal.pone.0177990.

[140] Martine Caron et al., "Some HIV Protease Inhibitors Alter Lamin A/C Maturation and Stability, SREBP-1 Nuclear Localization and Adipocyte Differentiation," *AIDS (London, England)* 17, no. 17 (November 21, 2003): 2437–44, https://doi.org/10.1097/00002030-200311210-00005.

[141] Francesca Chiarini et al., "The Cutting Edge: The Role of mTOR Signaling in Laminopathies," *International Journal of Molecular Sciences* 20, no. 4 (January 2019): 847, https://doi.org/10.3390/ijms20040847.

[142] J. Capeau et al., "[Primary lipodystrophies]," *Annales D'endocrinologie* 68, no. 1 (February 2007): 10–20, https://doi.org/10.1016/j.ando.2006.12.003.

[143] Elizabeth M. Turner and Christian Schlieker, "Pelger-Huët Anomaly and Greenberg Skeletal Dysplasia: LBR-Associated Diseases of Cholesterol Metabolism," *Rare Diseases* 4, no. 1 (September 27, 2016): e1241363, https://doi.org/10.1080/21675511.2016.1241363.

[144] Agathe Marcelot, Howard J. Worman, and Sophie Zinn-Justin, "Protein Structural and Mechanistic Basis of Progeroid Laminopathies," *The FEBS Journal* 288, no. 9 (2021): 2757–72, https://doi.org/10.1111/febs.15526.

[145] Fabio Coppedè, "Mutations Involved in Premature-Ageing Syndromes," *The Application of Clinical Genetics* 14 (June 2, 2021): 279–95, https://doi.org/10.2147/TACG.S273525.

[146] Giuseppe Novelli et al., "Mandibuloacral Dysplasia Is Caused by a Mutation in LMNA-Encoding Lamin A/C," *American Journal of Human Genetics* 71, no. 2 (August 2002): 426–31.

[147] Anil K. Agarwal et al., "Zinc Metalloproteinase, ZMPSTE24, Is Mutated in Mandibuloacral Dysplasia," *Human Molecular Genetics* 12, no. 16 (August 15, 2003): 1995–2001, https://doi.org/10.1093/hmg/ddg213.

[148] Yuexia Wang et al., "A Mutation Abolishing the ZMPSTE24 Cleavage Site in Prelamin A Causes a Progeroid Disorder," *Journal of Cell Science* 129, no. 10 (May 15, 2016): 1975–80, https://doi.org/10.1242/jcs.187302.

[149] Claire L. Navarro et al., "Lamin A and ZMPSTE24 (FACE-1) Defects Cause Nuclear Disorganization and Identify Restrictive Dermopathy as a Lethal Neonatal Laminopathy," *Human Molecular Genetics* 13, no. 20 (October 15, 2004): 2493–2503, https://doi.org/10.1093/hmg/ddh265.

[150] Minu Jose Chiramel et al., "Restrictive Dermopathy Due to ZMPSTE24 Mutation: A Case Report with a Novel Finding of Corpus Callosum Agenesis," *Indian Journal of Dermatology* 69, no. 1 (February 27, 2024): 95, https://doi.org/10.4103/ijd.ijd_681_23.

[151] Dido Carrero, Clara Soria-Valles, and Carlos López-Otín, "Hallmarks of Progeroid Syndromes: Lessons from Mice and Reprogrammed Cells," *Disease Models & Mechanisms* 9, no. 7 (July 1, 2016): 719–35, https://doi.org/10.1242/dmm.024711.

[152] Ignacio Benedicto, Beatriz Dorado, and Vicente Andrés, "Molecular and Cellular Mechanisms Driving Cardiovascular Disease in Hutchinson-Gilford Progeria Syndrome: Lessons Learned from Animal Models," *Cells* 10, no. 5 (May 2021): 1157, https://doi.org/10.3390/cells10051157.

[153] Maria Eriksson et al., "Recurrent de Novo Point Mutations in Lamin A Cause Hutchinson-Gilford Progeria Syndrome," *Nature* 423, no. 6937 (May 15, 2003): 293–98, https://doi.org/10.1038/nature01629.

[154] Karim Harhouri et al., "Antisense-Based Progerin Downregulation in HGPS-Like Patients' Cells," *Cells* 5, no. 3 (July 11, 2016): 31, https://doi.org/10.3390/cells5030031.

[155] Camilla Pellegrini et al., "All-Trans Retinoic Acid and Rapamycin Normalize Hutchinson Gilford Progeria Fibroblast Phenotype," *Oncotarget* 6, no. 30 (October 6, 2015): 29914–28, https://doi.org/10.18632/oncotarget.4939.

[156] Giovanna Lattanzi, "Prelamin A-Mediated Nuclear Envelope Dynamics in Normal and Laminopathic Cells," *Biochemical Society Transactions* 39, no. 6 (December 2011): 1698–1704, https://doi.org/10.1042/BST20110657.

[157] M. Columbaro et al., "Rescue of Heterochromatin Organization in Hutchinson-Gilford Progeria by Drug Treatment," *Cellular and Molecular Life Sciences: CMLS* 62, no. 22 (November 2005): 2669–78, https://doi.org/10.1007/s00018-005-5318-6.

[158] Robert D. Goldman et al., "Accumulation of Mutant Lamin A Causes Progressive Changes in Nuclear Architecture in Hutchinson-Gilford Progeria Syndrome," *Proceedings of the National Academy of Sciences of the United States of America* 101, no. 24 (June 15, 2004): 8963–68, https://doi.org/10.1073/pnas.0402943101.

[159] Daria Camozzi et al., "Altered Chromatin Organization and SUN2 Localization in Mandibuloacral Dysplasia Are Rescued by Drug Treatment," *Histochemistry and Cell Biology* 138, no. 4 (2012): 643–51, https://doi.org/10.1007/s00418-012-0977-5.

[160] Antonei B. Csoka et al., "Genome-Scale Expression Profiling of Hutchinson-Gilford Progeria Syndrome Reveals Widespread Transcriptional Misregulation Leading to Mesodermal/Mesenchymal Defects and Accelerated Atherosclerosis," *Aging Cell* 3, no. 4 (August 2004): 235–43, https://doi.org/10.1111/j.1474-9728.2004.00105.x.

[161] Baohua Liu et al., "Genomic Instability in Laminopathy-Based Premature Aging," *Nature Medicine* 11, no. 7 (July 2005): 780–85, https://doi.org/10.1038/nm1266.

[162] Alessandra di Masi et al., "The R527H Mutation in LMNA Gene Causes an Increased Sensitivity to Ionizing Radiation," *Cell Cycle* 7, no. 13 (July 1, 2008): 2030–37, https://doi.org/10.4161/cc.7.13.6149.

[163] Shane A. Richards et al., "The Accumulation of Un-Repairable DNA Damage in Laminopathy Progeria Fibroblasts Is Caused by ROS Generation and Is Prevented by Treatment with N-Acetyl Cysteine," *Human Molecular Genetics* 20, no. 20 (October 15, 2011): 3997–4004, https://doi.org/10.1093/hmg/ddr327.

[164] Eric D. Spear et al., "ZMPSTE24 Missense Mutations That Cause Progeroid Diseases Decrease Prelamin A Cleavage Activity and/or Protein Stability," *Disease Models & Mechanisms* 11, no. 7 (July 13, 2018): dmm033670, https://doi.org/10.1242/dmm.033670.

[165] Paola Scaffidi and Tom Misteli, "Lamin A-Dependent Nuclear Defects in Human Aging," *Science (New York, N.Y.)* 312, no. 5776 (May 19, 2006): 1059–63, https://doi.org/10.1126/science.1127168.

[166] B. Villeponteau, "The Heterochromatin Loss Model of Aging," *Experimental Gerontology* 32, no. 4–5 (1997): 383–94, https://doi.org/10.1016/s0531-5565(96)00155-6.

[167] Florian Köhler et al., "Epigenetic Deregulation of Lamina-Associated Domains in Hutchinson-Gilford Progeria Syndrome," *Genome Medicine* 12, no. 1 (May 25, 2020): 46, https://doi.org/10.1186/s13073-020-00749-y.

[168] Paola Scaffidi and Tom Misteli, "Reversal of the Cellular Phenotype in the Premature Aging Disease Hutchinson-Gilford Progeria Syndrome," *Nature Medicine* 11, no. 4 (April 2005): 440–45, https://doi.org/10.1038/nm1204.

[169] Rachel Patton McCord et al., "Correlated Alterations in Genome Organization, Histone Methylation, and DNA-Lamin A/C Interactions in Hutchinson-Gilford Progeria Syndrome," *Genome Research* 23, no. 2 (February 2013): 260–69, https://doi.org/10.1101/gr.138032.112.

[170] Shrestha Ghosh, Baohua Liu, and Zhongjun Zhou, "Resveratrol Activates SIRT1 in a Lamin A-Dependent Manner," *Cell Cycle (Georgetown, Tex.)* 12, no. 6 (March 15, 2013): 872–76, https://doi.org/10.4161/cc.24061.

[171] Elisabetta Mattioli et al., "Statins and Histone Deacetylase Inhibitors Affect Lamin A/C – Histone Deacetylase 2 Interaction in Human Cells," *Frontiers in Cell and Developmental Biology* 7 (January 31, 2019), https://doi.org/10.3389/fcell.2019.00006.

[172] Gianluca Pegoraro et al., "Ageing-Related Chromatin Defects through Loss of the NURD Complex," *Nature Cell Biology* 11, no. 10 (October 2009): 1261–67, https://doi.org/10.1038/ncb1971.

[173] Masashi Narita et al., "Rb-Mediated Heterochromatin Formation and Silencing of E2F Target Genes during Cellular Senescence," *Cell* 113, no. 6 (June 13, 2003): 703–16, https://doi.org/10.1016/S0092-8674(03)00401-X.

[174] Mahito Sadaie et al., "Redistribution of the Lamin B1 Genomic Binding Profile Affects Rearrangement of Heterochromatic Domains and SAHF Formation during Senescence," *Genes & Development* 27, no. 16 (August 15, 2013): 1800–1808, https://doi.org/10.1101/gad.217281.113.

[175] Isadora Matias et al., "Loss of Lamin-B1 and Defective Nuclear Morphology Are Hallmarks of Astrocyte Senescence in Vitro and in the Aging Human Hippocampus," *Aging Cell* 21, no. 1 (January 2022): e13521, https://doi.org/10.1111/acel.13521.

[176] Pekka Taimen et al., "A Progeria Mutation Reveals Functions for Lamin A in Nuclear Assembly, Architecture, and Chromosome Organization," *Proceedings of the National Academy of Sciences* 106, no. 49 (December 8, 2009): 20788–93, https://doi.org/10.1073/pnas.0911895106.

[177] Foteini-Dionysia Koufi et al., "Lamin B1 as a Key Modulator of the Developing and Aging Brain," *Frontiers in Cellular Neuroscience* 17 (August 31, 2023): 1263310, https://doi.org/10.3389/fncel.2023.1263310.

[178] Merel Stiekema et al., "Super-Resolution Imaging of the A- and B-Type Lamin Networks: A Comparative Study of Different Fluorescence Labeling Procedures," *International Journal of Molecular Sciences* 22, no. 19 (September 22, 2021): 10194, https://doi.org/10.3390/ijms221910194.

[179] Richard H. Masland, "The Neuronal Organization of the Retina," *Neuron* 76, no. 2 (October 18, 2012): 266–80, https://doi.org/10.1016/j.neuron.2012.10.002.

[180] Navid Mahabadi and Yasir Al Khalili, "Neuroanatomy, Retina," in *StatPearls* (Treasure Island (FL): StatPearls Publishing, 2024), http://www.ncbi.nlm.nih.gov/books/NBK545310/.

[181] Kevin H. Nguyen, Bhupendra C. Patel, and Prasanna Tadi, "Anatomy, Head and Neck: Eye Retina," in *StatPearls [Internet]* (StatPearls Publishing, 2023), https://www.ncbi.nlm.nih.gov/books/NBK542332/.

[182] Liantian Tian and Paul J. Kammermeier, "G Protein Coupling Profile of mGluR6 and Expression of G Alpha Proteins in Retinal ON Bipolar Cells," *Visual Neuroscience* 23, no. 6 (2006): 909–16, https://doi.org/10.1017/S0952523806230268.

[183] King-Wai Yau and Roger C. Hardie, "Phototransduction Motifs and Variations," *Cell* 139, no. 2 (October 16, 2009): 246–64, https://doi.org/10.1016/j.cell.2009.09.029.

[184] Jürgen Reingruber, David Holcman, and Gordon L. Fain, "How Rods Respond to Single Photons: Key Adaptations of a G-Protein Cascade That Enable Vision at the Physical Limit of Perception," *BioEssays: News and Reviews in Molecular, Cellular and Developmental Biology* 37, no. 11 (November 2015): 1243–52, https://doi.org/10.1002/bies.201500081.

[185] Dale Purves et al., "Phototransduction," in *Neuroscience. 2nd Edition* (Sinauer Associates, 2001), https://www.ncbi.nlm.nih.gov/books/NBK10806/.

[186] Seth Blackshaw et al., "Comprehensive Analysis of Photoreceptor Gene Expression and the Identification of Candidate Retinal Disease Genes," *Cell* 107, no. 5 (November 30, 2001): 579–89, https://doi.org/10.1016/S0092-8674(01)00574-8.

[187] Timothy H.-C. Hsiau et al., "The Cis-Regulatory Logic of the Mammalian Photoreceptor Transcriptional Network," *PloS One* 2, no. 7 (July 25, 2007): e643, https://doi.org/10.1371/journal.pone.0000643.

[188] Sandra Siegert et al., "Transcriptional Code and Disease Map for Adult Retinal Cell Types," *Nature Neuroscience* 15, no. 3 (January 22, 2012): 487–95, S1-2, https://doi.org/10.1038/nn.3032.

[189] Melanie M. Sohocki et al., "Prevalence of Mutations Causing Retinitis Pigmentosa and Other Inherited Retinopathies," *Human Mutation* 17, no. 1 (2001): 42–51, https://doi.org/10.1002/1098-1004(2001)17:1<42::AID-HUMU5>3.0.CO;2-K.

[190] Sanne K. Verbakel et al., "Non-Syndromic Retinitis Pigmentosa," *Progress in Retinal and Eye Research* 66 (September 2018): 157–86, https://doi.org/10.1016/j.preteyeres.2018.03.005.

[191] SP Daiger, LS Sullivan, and SJ Bowne, "Genes and Mutations Causing Retinitis Pigmentosa," *Clinical Genetics* 84, no. 2 (August 2013): 10.1111/cge.12203, https://doi.org/10.1111/cge.12203.

[192] Dominique Helmlinger et al., "Glutamine-Expanded Ataxin-7 Alters TFTC/STAGA Recruitment and Chromatin Structure Leading to Photoreceptor Dysfunction," *PLoS Biology* 4, no. 3 (March 2006): e67, https://doi.org/10.1371/journal.pbio.0040067.

[193] D. A. Bessant et al., "A Mutation in NRL Is Associated with Autosomal Dominant Retinitis Pigmentosa," *Nature Genetics* 21, no. 4 (April 1999): 355–56, https://doi.org/10.1038/7678.

[194] Yi Chun Chen et al., "Gcn5 Loss-of-Function Accelerates Cerebellar and Retinal Degeneration in a SCA7 Mouse Model," *Human Molecular Genetics* 21, no. 2 (January 15, 2012): 394–405, https://doi.org/10.1093/hmg/ddr474.

[195] Qais Farjo et al., "Human bZIP Transcription Factor Gene*NRL:*Structure, Genomic Sequence, and Fine Linkage Mapping at 14q11.2 and Negative Mutation Analysis in Patients with Retinal Degeneration," *Genomics* 45, no. 2 (October 15, 1997): 395–401, https://doi.org/10.1006/geno.1997.4964.

[196] C. L. Freund et al., "Cone-Rod Dystrophy Due to Mutations in a Novel Photoreceptor-Specific Homeobox Gene (CRX) Essential for Maintenance of the Photoreceptor," *Cell* 91, no. 4 (November 14, 1997): 543–53, https://doi.org/10.1016/s0092-8674(00)80440-7.

[197] N. B. Haider et al., "Mutation of a Nuclear Receptor Gene, NR2E3, Causes Enhanced S Cone Syndrome, a Disorder of Retinal Cell Fate," *Nature Genetics* 24, no. 2 (February 2000): 127–31, https://doi.org/10.1038/72777.

[198] Anne K. Hennig, Guang-Hua Peng, and Shiming Chen, "Transcription Coactivators P300 and CBP Are Necessary for Photoreceptor-Specific Chromatin Organization and Gene Expression," *PLoS ONE* 8, no. 7 (July 26, 2013): e69721, https://doi.org/10.1371/journal.pone.0069721.

[199] A. R. La Spada et al., "Polyglutamine-Expanded Ataxin-7 Antagonizes CRX Function and Induces Cone-Rod Dystrophy in a Mouse Model of SCA7," *Neuron* 31, no. 6 (September 27, 2001): 913–27, https://doi.org/10.1016/s0896-6273(01)00422-6.

[200] Nicholas M. Tran et al., "Mechanistically Distinct Mouse Models for CRX-Associated Retinopathy," *PLoS Genetics* 10, no. 2 (February 2014): e1004111, https://doi.org/10.1371/journal.pgen.1004111.

[201] Guang-Hua Peng and Shiming Chen, "Active Opsin Loci Adopt Intrachromosomal Loops That Depend on the Photoreceptor Transcription Factor Network," *Proceedings of the National Academy of Sciences of the United States of America* 108, no. 43 (October 25, 2011): 17821–26, https://doi.org/10.1073/pnas.1109209108.

[202] C. E. Keeler, "The Inheritance of a Retinal Abnormality in White Mice," *Proceedings of the National Academy of Sciences of the United States of America* 10, no. 7 (July 1924): 329–33, https://doi.org/10.1073/pnas.10.7.329.

[203] C. Bowes et al., "Retinal Degeneration in the Rd Mouse Is Caused by a Defect in the Beta Subunit of Rod cGMP-Phosphodiesterase," *Nature* 347, no. 6294 (October 18, 1990): 677–80, https://doi.org/10.1038/347677a0.

[204] D. B. Farber and R. N. Lolley, "Cyclic Guanosine Monophosphate: Elevation in Degenerating Photoreceptor Cells of the C3H Mouse Retina," *Science (New York, N.Y.)* 186, no. 4162 (November 1, 1974): 449–51, https://doi.org/10.1126/science.186.4162.449.

[205] François Paquet-Durand et al., "PKG Activity Causes Photoreceptor Cell Death in Two Retinitis Pigmentosa Models," *Journal of Neurochemistry* 108, no. 3 (February 2009): 796–810, https://doi.org/10.1111/j.1471-4159.2008.05822.x.

[206] M. E. McLaughlin et al., "Recessive Mutations in the Gene Encoding the Beta-Subunit of Rod Phosphodiesterase in Patients with Retinitis Pigmentosa," *Nature Genetics* 4, no. 2 (June 1993): 130–34, https://doi.org/10.1038/ng0693-130.

[207] Irina Solovei et al., "Nuclear Architecture of Rod Photoreceptor Cells Adapts to Vision in Mammalian Evolution," *Cell* 137, no. 2 (April 17, 2009): 356–68, https://doi.org/10.1016/j.cell.2009.01.052.

[208] Kaushikaram Subramanian et al., "Rod Nuclear Architecture Determines Contrast Transmission of the Retina and Behavioral Sensitivity in Mice," *eLife* 8 (December 11, 2019): e49542, https://doi.org/10.7554/eLife.49542.

[209] Caroline Kizilyaprak et al., "In Vivo Chromatin Organization of Mouse Rod Photoreceptors Correlates with Histone Modifications," *PloS One* 5, no. 6 (June 9, 2010): e11039, https://doi.org/10.1371/journal.pone.0011039.

[210] Anja Eberhart et al., "Epigenetics of Eu- and Heterochromatin in Inverted and Conventional Nuclei from Mouse Retina," *Chromosome Research* 21, no. 5 (August 1, 2013): 535–54, https://doi.org/10.1007/s10577-013-9375-7.

[211] Issam Aldiri et al., "The Dynamic Epigenetic Landscape of the Retina During Development, Reprogramming, and Tumorigenesis," *Neuron* 94, no. 3 (May 3, 2017): 550-568.e10, https://doi.org/10.1016/j.neuron.2017.04.022.

[212] Jackie L. Norrie et al., "Nucleome Dynamics during Retinal Development," *Neuron* 104, no. 3 (November 6, 2019): 512-528.e11, https://doi.org/10.1016/j.neuron.2019.08.002.

[213] Marwa Daghsni and Issam Aldiri, "Building a Mammalian Retina: An Eye on Chromatin Structure," *Frontiers in Genetics* 12 (October 25, 2021): 775205, https://doi.org/10.3389/fgene.2021.775205.

[214] Andrew E. O. Hughes et al., "Cell Type-Specific Epigenomic Analysis Reveals a Uniquely Closed Chromatin Architecture in Mouse Rod Photoreceptors," *Scientific Reports* 7 (March 3, 2017): 43184, https://doi.org/10.1038/srep43184.

[215] David S. Razafsky et al., "Developmental Regulation of Linkers of the Nucleoskeleton to the Cytoskeleton during Mouse Postnatal Retinogenesis," *Nucleus (Austin, Tex.)* 4, no. 5 (2013): 399–409, https://doi.org/10.4161/nucl.26244.

[216] Alisa Mo et al., "Epigenomic Landscapes of Retinal Rods and Cones," *eLife* 5 (n.d.): e11613, https://doi.org/10.7554/eLife.11613.

[217] Jung-Woong Kim et al., "Recruitment of Rod Photoreceptors from Short-Wavelength-Sensitive Cones during the Evolution of Nocturnal Vision in Mammals," *Developmental Cell* 37, no. 6 (June 20, 2016): 520–32, https://doi.org/10.1016/j.devcel.2016.05.023.

[218] Pierre Mattar et al., "Casz1 Controls Higher-Order Nuclear Organization in Rod Photoreceptors," *Proceedings of the National Academy of Sciences of the United States of America* 115, no. 34 (August 21, 2018): E7987–96, https://doi.org/10.1073/pnas.1803069115.

[219] Ivana Herrera et al., "Lamin A Upregulation Reorganizes the Genome during Rod Photoreceptor Degeneration," *Cell Death & Disease* 14, no. 10 (October 25, 2023): 1–12, https://doi.org/10.1038/s41419-023-06224-x.

[220] Randal Hand et al., "Phosphorylation of Neurogenin2 Specifies the Migration Properties and the Dendritic Morphology of Pyramidal Neurons in the Neocortex," *Neuron* 48, no. 1 (October 6, 2005): 45–62, https://doi.org/10.1016/j.neuron.2005.08.032.

[221] Gayathri Subramanian et al., "Lamin B Receptor Regulates the Growth and Maturation of Myeloid Progenitors via Its Sterol Reductase Domain: Implications for Cholesterol Biosynthesis in Regulating Myelopoiesis," *Journal of Immunology (Baltimore, Md.: 1950)* 188, no. 1 (January 1, 2012): 85–102, https://doi.org/10.4049/jimmunol.1003804.

[222] Takahiko Matsuda and Constance L. Cepko, "Electroporation and RNA Interference in the Rodent Retina in Vivo and in Vitro," *Proceedings of the National Academy of Sciences of the United States of America* 101, no. 1 (January 6, 2004): 16–22, https://doi.org/10.1073/pnas.2235688100.

[223] Paola Scaffidi and Tom Misteli, "Lamin A-Dependent Misregulation of Adult Stem Cells Associated with Accelerated Ageing," *Nature Cell Biology* 10, no. 4 (April 2008): 452–59, https://doi.org/10.1038/ncb1708.

[224] Luisana Avilan, "Assembling Multiple Fragments: The Gibson Assembly," *Methods in Molecular Biology (Clifton, N.J.)* 2633 (2023): 45–53, https://doi.org/10.1007/978-1-0716-3004-4_4.

[225] Pierre Mattar et al., "A Casz1-NuRD Complex Regulates Temporal Identity Transitions in Neural Progenitors," *Scientific Reports* 11, no. 1 (February 16, 2021): 3858, https://doi.org/10.1038/s41598-021-83395-7.

[226] Caroline A. Schneider, Wayne S. Rasband, and Kevin W. Eliceiri, "NIH Image to ImageJ: 25 Years of Image Analysis," *Nature Methods* 9, no. 7 (July 2012): 671–75, https://doi.org/10.1038/nmeth.2089.

[227] Steven Xijin Ge, Dongmin Jung, and Runan Yao, "ShinyGO: A Graphical Gene-Set Enrichment Tool for Animals and Plants," *Bioinformatics* 36, no. 8 (April 15, 2020): 2628–29, https://doi.org/10.1093/bioinformatics/btz931.

[228] Yong Joon Kim et al., "Multi-Platform Omics Analysis for Identification of Molecular Characteristics and Therapeutic Targets of Uveal Melanoma," *Scientific Reports* 9, no. 1 (December 17, 2019): 19235, https://doi.org/10.1038/s41598-019-55513-z.

[229] Jason D. Buenrostro et al., "ATAC-Seq: A Method for Assaying Chromatin Accessibility Genome-Wide," *Current Protocols in Molecular Biology* 109 (January 5, 2015): 21.29.1-21.29.9, https://doi.org/10.1002/0471142727.mb2129s109.

[230] Christopher S. McGinnis et al., "MULTI-Seq: Sample Multiplexing for Single-Cell RNA Sequencing Using Lipid-Tagged Indices," *Nature Methods* 16, no. 7 (July 2019): 619–26, https://doi.org/10.1038/s41592-019-0433-8.

[231] Daniel Blankenberg et al., "Manipulation of FASTQ Data with Galaxy," *Bioinformatics (Oxford, England)* 26, no. 14 (July 15, 2010): 1783–85, https://doi.org/10.1093/bioinformatics/btq281.

[232] Anthony M. Bolger, Marc Lohse, and Bjoern Usadel, "Trimmomatic: A Flexible Trimmer for Illumina Sequence Data," *Bioinformatics (Oxford, England)* 30, no. 15 (August 1, 2014): 2114–20, https://doi.org/10.1093/bioinformatics/btu170.

[233] Ben Langmead and Steven L. Salzberg, "Fast Gapped-Read Alignment with Bowtie 2," *Nature Methods* 9, no. 4 (March 4, 2012): 2, https://doi.org/10.1038/nmeth.1923.

[234] Jianxing Feng et al., "Identifying ChIP-Seq Enrichment Using MACS," *Nature Protocols* 7, no. 9 (September 2012): 10.1038/nprot.2012.101, https://doi.org/10.1038/nprot.2012.101.

[235] Cory Y. McLean et al., "GREAT Improves Functional Interpretation of Cis-Regulatory Regions," *Nature Biotechnology* 28, no. 5 (May 2010): 495–501, https://doi.org/10.1038/nbt.1630.

[236] M. Ashburner et al., "Gene Ontology: Tool for the Unification of Biology. The Gene Ontology Consortium," *Nature Genetics* 25, no. 1 (May 2000): 25–29, https://doi.org/10.1038/75556.

[237] The Gene Ontology Consortium, "The Gene Ontology Resource: Enriching a GOld Mine," *Nucleic Acids Research* 49, no. D1 (January 8, 2021): D325–34, https://doi.org/10.1093/nar/gkaa1113.

[238] Fran Supek et al., "REVIGO Summarizes and Visualizes Long Lists of Gene Ontology Terms," *PloS One* 6, no. 7 (2011): e21800, https://doi.org/10.1371/journal.pone.0021800.

[239] Przemyslaw Stempor and Julie Ahringer, "SeqPlots - Interactive Software for Exploratory Data Analyses, Pattern Discovery and Visualization in Genomics," *Wellcome Open Research* 1 (November 15, 2016), https://doi.org/10.12688/wellcomeopenres.10004.1.

[240] Yupeng He et al., "Spatiotemporal DNA Methylome Dynamics of the Developing Mouse Fetus," *Nature* 583, no. 7818 (July 2020): 752–59, https://doi.org/10.1038/s41586-020-2119-x.

[241] Yunhai Luo et al., "New Developments on the Encyclopedia of DNA Elements (ENCODE) Data Portal," *Nucleic Acids Research* 48, no. D1 (January 8, 2020): D882–89, https://doi.org/10.1093/nar/gkz1062.

[242] Ian Dunham et al., "An Integrated Encyclopedia of DNA Elements in the Human Genome," *Nature* 489, no. 7414 (September 2012): 57–74, https://doi.org/10.1038/nature11247.

[243] Mette Bentsen et al., "ATAC-Seq Footprinting Unravels Kinetics of Transcription Factor Binding during Zygotic Genome Activation," *Nature Communications* 11, no. 1 (August 26, 2020): 4267, https://doi.org/10.1038/s41467-020-18035-1.

[244] Ke Jiang et al., "Multiomics Analyses Reveal Early Metabolic Imbalance and Mitochondrial Stress in Neonatal Photoreceptors Leading to Cell Death in Pde6brd1/Rd1 Mouse Model of Retinal Degeneration," *Human Molecular Genetics* 31, no. 13 (July 7, 2022): 2137–54, https://doi.org/10.1093/hmg/ddac013.

[245] Enis Afgan et al., "The Galaxy Platform for Accessible, Reproducible and Collaborative Biomedical Analyses: 2016 Update," *Nucleic Acids Research* 44, no. W1 (July 8, 2016): W3–10, https://doi.org/10.1093/nar/gkw343.

[246] Alexander Dobin et al., "STAR: Ultrafast Universal RNA-Seq Aligner," *Bioinformatics (Oxford, England)* 29, no. 1 (January 1, 2013): 15–21, https://doi.org/10.1093/bioinformatics/bts635.

[247] Helga Thorvaldsdóttir, James T. Robinson, and Jill P. Mesirov, "Integrative Genomics Viewer (IGV): High-Performance Genomics Data Visualization and Exploration," *Briefings in Bioinformatics* 14, no. 2 (March 2013): 178–92, https://doi.org/10.1093/bib/bbs017.

[248] Yang Liao, Gordon K. Smyth, and Wei Shi, "featureCounts: An Efficient General Purpose Program for Assigning Sequence Reads to Genomic Features," *Bioinformatics (Oxford, England)* 30, no. 7 (April 1, 2014): 923–30, https://doi.org/10.1093/bioinformatics/btt656.

[249] Michael I Love, Wolfgang Huber, and Simon Anders, "Moderated Estimation of Fold Change and Dispersion for RNA-Seq Data with DESeq2," *Genome Biology* 15, no. 12 (2014): 550, https://doi.org/10.1186/s13059-014-0550-8.

[250] F. Alexander Wolf, Philipp Angerer, and Fabian J. Theis, "SCANPY: Large-Scale Single-Cell Gene Expression Data Analysis," *Genome Biology* 19, no. 1 (February 6, 2018): 15, https://doi.org/10.1186/s13059-017-1382-0.

[251] Samuel L. Wolock, Romain Lopez, and Allon M. Klein, "Scrublet: Computational Identification of Cell Doublets in Single-Cell Transcriptomic Data," *Cell Systems* 8, no. 4 (April 24, 2019): 281-291.e9, https://doi.org/10.1016/j.cels.2018.11.005.

[252] Brian S. Clark et al., "Single-Cell RNA-Seq Analysis of Retinal Development Identifies NFI Factors as Regulating Mitotic Exit and Late-Born Cell Specification," *Neuron* 102, no. 6 (June 19, 2019): 1111-1126.e5, https://doi.org/10.1016/j.neuron.2019.04.010.

[253] Xin Shao et al., "scDeepSort: A Pre-Trained Cell-Type Annotation Method for Single-Cell Transcriptomics Using Deep Learning with a Weighted Graph Neural Network," *Nucleic Acids Research* 49, no. 21 (December 2, 2021): e122, https://doi.org/10.1093/nar/gkab775.

[254] Adam Gayoso et al., "A Python Library for Probabilistic Analysis of Single-Cell Omics Data," *Nature Biotechnology* 40, no. 2 (February 2022): 163–66, https://doi.org/10.1038/s41587-021-01206-w.

[255] Greg Finak et al., "MAST: A Flexible Statistical Framework for Assessing Transcriptional Changes and Characterizing Heterogeneity in Single-Cell RNA Sequencing Data," *Genome Biology* 16 (December 10, 2015): 278, https://doi.org/10.1186/s13059-015-0844-5.

[256] Margaret Wong-Riley, "Energy Metabolism of the Visual System," *Eye and Brain* 2 (July 22, 2010): 99–116.

[257] Andrea Barabino et al., "Loss of Bmi1 Causes Anomalies in Retinal Development and Degeneration of Cone Photoreceptors," *Development (Cambridge, England)* 143, no. 9 (May 1, 2016): 1571–84, https://doi.org/10.1242/dev.125351.

[258] Evgenya Y. Popova et al., "Developmentally Regulated Linker Histone H1c Promotes Heterochromatin Condensation and Mediates Structural Integrity of Rod Photoreceptors in Mouse Retina," *The Journal of Biological Chemistry* 288, no. 24 (June 14, 2013): 17895–907, https://doi.org/10.1074/jbc.M113.452144.

[259] Joseph C. Corbo and Constance L. Cepko, "A Hybrid Photoreceptor Expressing Both Rod and Cone Genes in a Mouse Model of Enhanced S-Cone Syndrome," *PLoS Genetics* 1, no. 2 (August 2005): e11, https://doi.org/10.1371/journal.pgen.0010011.

[260] A. J. Mears et al., "Nrl Is Required for Rod Photoreceptor Development," *Nature Genetics* 29, no. 4 (December 2001): 447–52, https://doi.org/10.1038/ng774.

[261] Vinay S. Swamy et al., "Building the Mega Single-Cell Transcriptome Ocular Meta-Atlas," *GigaScience* 10, no. 10 (October 13, 2021): giab061, https://doi.org/10.1093/gigascience/giab061.

[262] Jimmy de Melo et al., "The Spalt Family Transcription Factor Sall3 Regulates the Development of Cone Photoreceptors and Retinal Horizontal Interneurons," *Development (Cambridge, England)* 138, no. 11 (June 2011): 2325–36, https://doi.org/10.1242/dev.061846.

[263] Mark M. Emerson et al., "Otx2 and Onecut1 Promote the Fates of Cone Photoreceptors and Horizontal Cells and Repress Rod Photoreceptors," *Developmental Cell* 26, no. 1 (July 15, 2013): 59–72, https://doi.org/10.1016/j.devcel.2013.06.005.

[264] Awais Javed et al., "Pou2f1 and Pou2f2 Cooperate to Control the Timing of Cone Photoreceptor Production in the Developing Mouse Retina," *Development (Cambridge, England)* 147, no. 18 (September 28, 2020): dev188730, https://doi.org/10.1242/dev.188730.

[265] Jennings Luu et al., "Epigenetic Hallmarks of Age-Related Macular Degeneration Are Recapitulated in a Photosensitive Mouse Model," *Human Molecular Genetics* 29, no. 15 (August 29, 2020): 2611–24, https://doi.org/10.1093/hmg/ddaa158.

[266] Duygu Karademir et al., "Single-Cell RNA Sequencing of the Retina in a Model of Retinitis Pigmentosa Reveals Early Responses to Degeneration in Rods and Cones," *BMC Biology* 20, no. 1 (April 12, 2022): 86, https://doi.org/10.1186/s12915-022-01280-9.

[267] Jie Wang et al., "ATAC-Seq Analysis Reveals a Widespread Decrease of Chromatin Accessibility in Age-Related Macular Degeneration," *Nature Communications* 9, no. 1 (April 10, 2018): 1364, https://doi.org/10.1038/s41467-018-03856-y.

[268] Bess Frost, Farah H. Bardai, and Mel B. Feany, "Lamin Dysfunction Mediates Neurodegeneration in Tauopathies," *Current Biology: CB* 26, no. 1 (January 11, 2016): 129–36, https://doi.org/10.1016/j.cub.2015.11.039.

[269] Laura Gil et al., "Perinuclear Lamin A and Nucleoplasmic Lamin B2 Characterize Two Types of Hippocampal Neurons through Alzheimer's Disease Progression," *International Journal of Molecular Sciences* 21, no. 5 (March 7, 2020): 1841, https://doi.org/10.3390/ijms21051841.

[270] Léo Machado et al., "Tissue Damage Induces a Conserved Stress Response That Initiates Quiescent Muscle Stem Cell Activation," *Cell Stem Cell* 28, no. 6 (June 3, 2021): 1125-1135.e7, https://doi.org/10.1016/j.stem.2021.01.017.

[271] David B. Rein et al., "Prevalence of Age-Related Macular Degeneration in the US in 2019," *JAMA Ophthalmology* 140, no. 12 (November 3, 2022): 1202, https://doi.org/10.1001/jamaophthalmol.2022.4401.

[272] Peter A. Campochiaro et al., "Is There Excess Oxidative Stress and Damage in Eyes of Patients with Retinitis Pigmentosa?," *Antioxidants & Redox Signaling* 23, no. 7 (September 2015): 643–48, https://doi.org/10.1089/ars.2015.6327.

[273] Keiichi Komeima et al., "Antioxidants Reduce Cone Cell Death in a Model of Retinitis Pigmentosa," *Proceedings of the National Academy of Sciences* 103, no. 30 (July 25, 2006): 11300–305, https://doi.org/10.1073/pnas.0604056103.

[274] Wenjun Xiong et al., "NRF2 Promotes Neuronal Survival in Neurodegeneration and Acute Nerve Damage," *The Journal of Clinical Investigation* 125, no. 4 (April 2015): 1433–45, https://doi.org/10.1172/JCI79735.

[275] P. Farinelli et al., "DNA Methylation and Differential Gene Regulation in Photoreceptor Cell Death," *Cell Death & Disease* 5, no. 12 (December 2014): e1558–e1558, https://doi.org/10.1038/cddis.2014.512.

[276] J. Sancho-Pelluz et al., "Excessive HDAC Activation Is Critical for Neurodegeneration in the Rd1 Mouse," *Cell Death & Disease* 1, no. 2 (2010): e24, https://doi.org/10.1038/cddis.2010.4.

[277] Ruanne YJ Vent-Schmidt et al., "Opposing Effects of Valproic Acid Treatment Mediated by Histone Deacetylase Inhibitor Activity in Four Transgenic X. Laevis Models of Retinitis Pigmentosa," *The Journal of Neuroscience* 37, no. 4 (January 25, 2017): 1039, https://doi.org/10.1523/JNEUROSCI.1647-16.2016.

[278] Dusan Zencak et al., "Retinal Degeneration Depends on Bmi1 Function and Reactivation of Cell Cycle Proteins," *Proceedings of the National Academy of Sciences of the United States of America* 110, no. 7 (January 28, 2013): E593, https://doi.org/10.1073/pnas.1108297110.

[279] Brigitte Müller et al., "Detection of DNA Double Strand Breaks by γH2AX Does Not Result in 53bp1 Recruitment in Mouse Retinal Tissues," *Frontiers in Neuroscience* 12 (2018): 286, https://doi.org/10.3389/fnins.2018.00286.

[280] Yusuke Murakami et al., "MutT Homolog-1 Attenuates Oxidative DNA Damage and Delays Photoreceptor Cell Death in Inherited Retinal Degeneration," *The American Journal of Pathology* 181, no. 4 (October 2012): 1378–86, https://doi.org/10.1016/j.ajpath.2012.06.026.

[281] D. E. White et al., "The ATM Substrate KAP1 Controls DNA Repair in Heterochromatin: Regulation by HP1 Proteins and Serine 473/824 Phosphorylation," *Molecular Cancer Research : MCR* 10, no. 3 (March 2012): 401–14, https://doi.org/10.1158/1541-7786.MCR-11-0134.

[282] Aaron A. Goodarzi et al., "ATM Signaling Facilitates Repair of DNA Double-Strand Breaks Associated with Heterochromatin," *Molecular Cell* 31, no. 2 (July 25, 2008): 167–77, https://doi.org/10.1016/j.molcel.2008.05.017.

[283] Blanca Arango-Gonzalez et al., "Identification of a Common Non-Apoptotic Cell Death Mechanism in Hereditary Retinal Degeneration," *PloS One* 9, no. 11 (2014): e112142, https://doi.org/10.1371/journal.pone.0112142.

[284] Guo-Qing Chang, Ying Hao, and Fulton Wong, "Apoptosis: Final Common Pathway of Photoreceptor Death in Rd, Rds, and Mutant Mice," *Neuron* 11, no. 4 (October 1, 1993): 595–605, https://doi.org/10.1016/0896-6273(93)90072-Y.

[285] C. Portera-Cailliau et al., "Apoptotic Photoreceptor Cell Death in Mouse Models of Retinitis Pigmentosa," *Proceedings of the National Academy of Sciences of the United States of America* 91, no. 3 (February 1, 1994): 974, https://doi.org/10.1073/pnas.91.3.974.

[286] M. Soledad Cortina et al., "DNA Repair in Photoreceptor Survival," *Molecular Neurobiology* 28, no. 2 (October 2003): 111–22, https://doi.org/10.1385/MN:28:2:111.

[287] S. Specht et al., "Damage to Rat Retinal DNA Induced in Vivo by Visible Light," *Photochemistry and Photobiology* 69, no. 1 (January 1999): 91–98.

[288] L. Menu dit Huart et al., "DNA Repair in the Degenerating Mouse Retina," *Molecular and Cellular Neurosciences* 26, no. 3 (July 2004): 441–49, https://doi.org/10.1016/j.mcn.2004.04.002.

[289] Alberto Chiarugi and Michael A. Moskowitz, "PARP-1--a Perpetrator of Apoptotic Cell Death?," *Science* 297, no. 5579 (July 12, 2002): 200–201, https://doi.org/10.1126/science.1074592.

[290] Xun Li et al., "PARP-1 Is a Potential Marker of Retinal Photooxidation and a Key Signal Regulator in Retinal Light Injury," *Oxidative Medicine and Cellular Longevity* 2022 (2022): 6881322, https://doi.org/10.1155/2022/6881322.

[291] François Paquet-Durand et al., "Excessive Activation of Poly(ADP-Ribose) Polymerase Contributes to Inherited Photoreceptor Degeneration in the Retinal Degeneration 1 Mouse," *The Journal of Neuroscience* 27, no. 38 (September 19, 2007): 10311, https://doi.org/10.1523/JNEUROSCI.1514-07.2007.

[292] Jasvir Kaur et al., "Calpain and PARP Activation during Photoreceptor Cell Death in P23H and S334ter Rhodopsin Mutant Rats," *PLOS ONE* 6, no. 7 (July 12, 2011): e22181, https://doi.org/10.1371/journal.pone.0022181.

[293] Tom Misteli, "The Self-Organizing Genome: Principles of Genome Architecture and Function," *Cell* 183, no. 1 (October 2020): 28–45, https://doi.org/10.1016/j.cell.2020.09.014.

[294] Irina Solovei, Katharina Thanisch, and Yana Feodorova, "How to Rule the Nucleus: Divide et Impera," *Current Opinion in Cell Biology* 40 (June 2016): 47–59, https://doi.org/10.1016/j.ceb.2016.02.014.

[295] Asifa Akhtar and Susan M. Gasser, "The Nuclear Envelope and Transcriptional Control," *Nature Reviews. Genetics* 8, no. 7 (July 2007): 507–17, https://doi.org/10.1038/nrg2122.

[296] Sofia A. Quinodoz et al., "Higher-Order Inter-Chromosomal Hubs Shape 3D Genome Organization in the Nucleus," *Cell* 174, no. 3 (July 26, 2018): 744-757.e24, https://doi.org/10.1016/j.cell.2018.05.024.

[297] Helen Pickersgill et al., "Characterization of the Drosophila Melanogaster Genome at the Nuclear Lamina," *Nature Genetics* 38, no. 9 (September 2006): 1005–14, https://doi.org/10.1038/ng1852.

[298] Benjamin D. Towbin et al., "Step-Wise Methylation of Histone H3K9 Positions Heterochromatin at the Nuclear Periphery," *Cell* 150, no. 5 (August 31, 2012): 934–47, https://doi.org/10.1016/j.cell.2012.06.051.

[299] Katrin Hoffmann et al., "Mutations in the Gene Encoding the Lamin B Receptor Produce an Altered Nuclear Morphology in Granulocytes (Pelger–Huët Anomaly)," *Nature Genetics* 31, no. 4 (August 2002): 410–14, https://doi.org/10.1038/ng925.

[300] Leonard D. Shultz et al., "Mutations at the Mouse Ichthyosis Locus Are within the Lamin B Receptor Gene: A Single Gene Model for Human Pelger–Huët Anomaly," *Human Molecular Genetics* 12, no. 1 (January 1, 2003): 61–69, https://doi.org/10.1093/hmg/ddg003.

[301] Katherine H. Schreiber and Brian K. Kennedy, "When Lamins Go Bad: Nuclear Structure and Disease," *Cell* 152, no. 6 (March 14, 2013): 1365–75, https://doi.org/10.1016/j.cell.2013.02.015.

[302] Josh Abramson et al., "Accurate Structure Prediction of Biomolecular Interactions with AlphaFold 3," *Nature* 630, no. 8016 (June 2024): 493–500, https://doi.org/10.1038/s41586-024-07487-w.

[303] Takahiko Matsuda and Constance L. Cepko, "Controlled Expression of Transgenes Introduced by in Vivo Electroporation," *Proceedings of the National Academy of Sciences of the United States of America* 104, no. 3 (January 5, 2007): 1027, https://doi.org/10.1073/pnas.0610155104.

[304] Eric F. Pettersen et al., "UCSF ChimeraX: Structure Visualization for Researchers, Educators, and Developers," *Protein Science: A Publication of the Protein Society* 30, no. 1 (January 2021): 70–82, https://doi.org/10.1002/pro.3943.

[305] Baihui Wang et al., "The Molecular Basis of Lamin-Specific Chromatin Interactions" (bioRxiv, August 5, 2024), https://doi.org/10.1101/2024.08.05.604734.

[306] So-Mi Kang, Min-Ho Yoon, and Bum-Joon Park, "Laminopathies; Mutations on Single Gene and Various Human Genetic Diseases," *BMB Reports* 51, no. 7 (July 2018): 327–37, https://doi.org/10.5483/bmbrep.2018.51.7.113.

[307] Muneyo Mio et al., "Structural Instability of Lamin A Tail Domain Modulates Its Assembly and Higher Order Function in Emery–Dreifuss Muscular Dystrophy," *Biochemical and Biophysical Research Communications* 512, no. 1 (April 23, 2019): 22–28, https://doi.org/10.1016/j.bbrc.2019.02.138.

[308] Catherine Coffinier et al., "Direct Synthesis of Lamin A, Bypassing Prelamin a Processing, Causes Misshapen Nuclei in Fibroblasts but No Detectable Pathology in Mice," *The Journal of Biological Chemistry* 285, no. 27 (July 2, 2010): 20818–26, https://doi.org/10.1074/jbc.M110.128835.

[309] Ryo Uchino et al., "Non-Farnesylated B-Type Lamin Can Tether Chromatin inside the Nucleus and Its Chromatin Interaction Requires the Ig-Fold Region," *Chromosoma* 126, no. 1 (February 2017): 125–44, https://doi.org/10.1007/s00412-016-0581-x.

[310] Yana Feodorova et al., "Viewing Nuclear Architecture through the Eyes of Nocturnal Mammals," *Trends in Cell Biology* 30, no. 4 (April 2020): 276–89, https://doi.org/10.1016/j.tcb.2019.12.008.

[311] Anne T. Bertrand et al., "Lamin A/C Assembly Defects in LMNA-Congenital Muscular Dystrophy Is Responsible for the Increased Severity of the Disease Compared with Emery–Dreifuss Muscular Dystrophy," *Cells* 9, no. 4 (March 31, 2020): 844, https://doi.org/10.3390/cells9040844.

[312] Matthew R. G. Taylor et al., "Thymopoietin (Lamina-Associated Polypeptide 2) Gene Mutation Associated with Dilated Cardiomyopathy," *Human Mutation* 26, no. 6 (December 2005): 566–74, https://doi.org/10.1002/humu.20250.

[313] Nelly Abdelfatah et al., "Characterization of a Unique Form of Arrhythmic Cardiomyopathy Caused by Recessive Mutation in LEMD2," *JACC. Basic to Translational Science* 4, no. 2 (April 2019): 204–21, https://doi.org/10.1016/j.jacbts.2018.12.001.

[314] Felix Marbach et al., "The Discovery of a LEMD2-Associated Nuclear Envelopathy with Early Progeroid Appearance Suggests Advanced Applications for AI-Driven Facial Phenotyping," *American Journal of Human Genetics* 104, no. 4 (April 4, 2019): 749–57, https://doi.org/10.1016/j.ajhg.2019.02.021.

[315] K. K. Lee et al., "Distinct Functional Domains in Emerin Bind Lamin A and DNA-Bridging Protein BAF," *Journal of Cell Science* 114, no. Pt 24 (December 2001): 4567–73, https://doi.org/10.1242/jcs.114.24.4567.

[316] C. Laguri et al., "Structural Characterization of the LEM Motif Common to Three Human Inner Nuclear Membrane Proteins," *Structure (London, England: 1993)* 9, no. 6 (June 2001): 503–11, https://doi.org/10.1016/s0969-2126(01)00611-6.

[317] Katherine L. Wilson and Roland Foisner, "Lamin-Binding Proteins," *Cold Spring Harbor Perspectives in Biology* 2, no. 4 (April 2010): a000554, https://doi.org/10.1101/cshperspect.a000554.

[318] Xose S. Puente et al., "Exome Sequencing and Functional Analysis Identifies BANF1 Mutation as the Cause of a Hereditary Progeroid Syndrome," *American Journal of Human Genetics* 88, no. 5 (May 13, 2011): 650–56, https://doi.org/10.1016/j.ajhg.2011.04.010.

[319] Rubén Cabanillas et al., "Néstor–Guillermo Progeria Syndrome: A Novel Premature Aging Condition with Early Onset and Chronic Development Caused by BANF1 Mutations," *American Journal of Medical Genetics Part A* 155, no. 11 (2011): 2617–25, https://doi.org/10.1002/ajmg.a.34249.

[320] Dunja Skoko et al., "Barrier-to-Autointegration Factor (BAF) Condenses DNA by Looping," *Proceedings of the National Academy of Sciences of the United States of America* 106, no. 39 (September 29, 2009): 16610–15, https://doi.org/10.1073/pnas.0909077106.

[321] Xuejiao Wang et al., "Barrier to Autointegration Factor Interacts with the Cone-Rod Homeobox and Represses Its Transactivation Function," *The Journal of Biological Chemistry* 277, no. 45 (November 8, 2002): 43288–300, https://doi.org/10.1074/jbc.M207952200.

[322] Ying Huang et al., "No Interaction of Barrier-to-Autointegration Factor (BAF) with HIV-1 MA, Cone-Rod Homeobox (Crx) or MAN1-C in Absence of DNA," *PloS One* 6, no. 9 (2011): e25123, https://doi.org/10.1371/journal.pone.0025123.

[323] Rocío Montes de Oca, Paul R. Andreassen, and Katherine L. Wilson, "Barrier-to-Autointegration Factor Influences Specific Histone Modifications," *Nucleus (Austin, Tex.)* 2, no. 6 (2011): 580–90, https://doi.org/10.4161/nucl.2.6.17960.

[324] Rocío Montes de Oca, Kenneth K. Lee, and Katherine L. Wilson, "Binding of Barrier to Autointegration Factor (BAF) to Histone H3 and Selected Linker Histones Including H1.1," *The Journal of Biological Chemistry* 280, no. 51 (December 23, 2005): 42252–62, https://doi.org/10.1074/jbc.M509917200.

[325] B. D. Towbin et al., "Repetitive Transgenes in C. Elegans Accumulate Heterochromatic Marks and Are Sequestered at the Nuclear Envelope in a Copy-Number- and Lamin-Dependent Manner," *Cold Spring Harbor Symposia on Quantitative Biology* 75 (2010): 555–65, https://doi.org/10.1101/sqb.2010.75.041.

[326] Nicole Wagner and Georg Krohne, "LEM-Domain Proteins: New Insights into Lamin-Interacting Proteins," *International Review of Cytology* 261 (2007): 1–46, https://doi.org/10.1016/S0074-7696(07)61001-8.

[327] Malini Mansharamani and Katherine L. Wilson, "Direct Binding of Nuclear Membrane Protein MAN1 to Emerin in Vitro and Two Modes of Binding to Barrier-to-Autointegration Factor," *The Journal of Biological Chemistry* 280, no. 14 (April 8, 2005): 13863–70, https://doi.org/10.1074/jbc.M413020200.

[328] F. Lin et al., "MAN1, an Inner Nuclear Membrane Protein That Shares the LEM Domain with Lamina-Associated Polypeptide 2 and Emerin," *The Journal of Biological Chemistry* 275, no. 7 (February 18, 2000): 4840–47, https://doi.org/10.1074/jbc.275.7.4840.

[329] Kenneth K. Lee and Katherine L. Wilson, "All in the Family: Evidence for Four New LEM-Domain Proteins Lem2 (NET-25), Lem3, Lem4 and Lem5 in the Human Genome," *Symposia of the Society for Experimental Biology*, no. 56 (2004): 329–39.

[330] Jason M Berk, Kathryn E Tifft, and Katherine L Wilson, "The Nuclear Envelope LEM-Domain Protein Emerin," *Nucleus* 4, no. 4 (July 1, 2013): 298–314, https://doi.org/10.4161/nucl.25751.

[331] Howard J. Worman, Cecilia Ostlund, and Yuexia Wang, "Diseases of the Nuclear Envelope," *Cold Spring Harbor Perspectives in Biology* 2, no. 2 (February 2010): a000760, https://doi.org/10.1101/cshperspect.a000760.

[332] Sandrine Caputo et al., "The Carboxyl-Terminal Nucleoplasmic Region of MAN1 Exhibits a DNA Binding Winged Helix Domain," *The Journal of Biological Chemistry* 281, no. 26 (June 30, 2006): 18208–15, https://doi.org/10.1074/jbc.M601980200.

[333] Daria Filipczak et al., "Lamin Chromatin Binding Is Modulated by Interactions of Different LAP2α Domains with Lamins and Chromatin," *iScience* 27, no. 10 (October 18, 2024): 110869, https://doi.org/10.1016/j.isci.2024.110869.

[334] Jan Hellemans et al., "Loss-of-Function Mutations in LEMD3 Result in Osteopoikilosis, Buschke-Ollendorff Syndrome and Melorheostosis," *Nature Genetics* 36, no. 11 (November 2004): 1213–18, https://doi.org/10.1038/ng1453.

[335] Andreas Brachner et al., "LEM2 Is a Novel MAN1-Related Inner Nuclear Membrane Protein Associated with A-Type Lamins," *Journal of Cell Science* 118, no. Pt 24 (December 15, 2005): 5797–5810, https://doi.org/10.1242/jcs.02701.

[336] Andreas Brachner and Roland Foisner, "Evolvement of LEM Proteins as Chromatin Tethers at the Nuclear Periphery," *Biochemical Society Transactions* 39, no. 6 (December 2011): 1735–41, https://doi.org/10.1042/BST20110724.

[337] Rocío Montes de Oca et al., "Barrier-to-Autointegration Factor Proteome Reveals Chromatin-Regulatory Partners," *PloS One* 4, no. 9 (September 16, 2009): e7050, https://doi.org/10.1371/journal.pone.0007050.

[338] Y. Zhang et al., "Analysis of the NuRD Subunits Reveals a Histone Deacetylase Core Complex and a Connection with DNA Methylation," *Genes & Development* 13, no. 15 (August 1, 1999): 1924–35, https://doi.org/10.1101/gad.13.15.1924.

[339] Andrei Kuzmichev et al., "Histone Methyltransferase Activity Associated with a Human Multiprotein Complex Containing the Enhancer of Zeste Protein," *Genes & Development* 16, no. 22 (November 15, 2002): 2893–2905, https://doi.org/10.1101/gad.1035902.

[340] A. Verreault et al., "Nucleosome Assembly by a Complex of CAF-1 and Acetylated Histones H3/H4," *Cell* 87, no. 1 (October 4, 1996): 95–104, https://doi.org/10.1016/s0092-8674(00)81326-4.

[341] D. Vermaak et al., "Functional Analysis of the SIN3-Histone Deacetylase RPD3-RbAp48-Histone H4 Connection in the Xenopus Oocyte," *Molecular and Cellular Biology* 19, no. 9 (September 1999): 5847–60, https://doi.org/10.1128/MCB.19.9.5847.

[342] Elias Pavlopoulos et al., "Molecular Mechanism for Age-Related Memory Loss: The Histone-Binding Protein RbAp48," *Science Translational Medicine* 5, no. 200 (August 28, 2013): 200ra115, https://doi.org/10.1126/scitranslmed.3006373.

[343] Kelly L. Dunlevy et al., "The PRR14 Heterochromatin Tether Encodes Modular Domains That Mediate and Regulate Nuclear Lamina Targeting," *Journal of Cell Science* 133, no. 10 (May 27, 2020): jcs240416, https://doi.org/10.1242/jcs.240416.

[344] Anna A. Kiseleva et al., "PRR14 Organizes H3K9me3-Modified Heterochromatin at the Nuclear Lamina," *Nucleus (Austin, Tex.)* 14, no. 1 (December 2023): 2165602, https://doi.org/10.1080/19491034.2023.2165602.

[345] E. Minc, J. C. Courvalin, and B. Buendia, "HP1gamma Associates with Euchromatin and Heterochromatin in Mammalian Nuclei and Chromosomes," *Cytogenetics and Cell Genetics* 90, no. 3–4 (2000): 279–84, https://doi.org/10.1159/000056789.

[346] Veronika Butin-Israeli et al., "Nuclear Lamin Functions and Disease," *Trends in Genetics: TIG* 28, no. 9 (September 2012): 464–71, https://doi.org/10.1016/j.tig.2012.06.001.

[347] Jacob Odell and Jan Lammerding, "N-Terminal Tags Impair the Ability of Lamin A to Provide Structural Support to the Nucleus" (bioRxiv, July 24, 2024), https://doi.org/10.1101/2024.04.19.590311.

[348] Simona Graziano et al., "Lamin A/C Recruits ssDNA Protective Proteins RPA and RAD51 to Stalled Replication Forks to Maintain Fork Stability," *The Journal of Biological Chemistry* 297, no. 5 (October 11, 2021): 101301, https://doi.org/10.1016/j.jbc.2021.101301.

[349] Abena B. Redwood et al., "A Dual Role for A-Type Lamins in DNA Double-Strand Break Repair," *Cell Cycle* 10, no. 15 (August 1, 2011): 2549–60, https://doi.org/10.4161/cc.10.15.16531.

[350] Abena B. Redwood, Ignacio Gonzalez-Suarez, and Susana Gonzalo, "Regulating the Levels of Key Factors in Cell Cycle and DNA Repair: New Pathways Revealed by Lamins," *Cell Cycle (Georgetown, Tex.)* 10, no. 21 (November 1, 2011): 3652–57, https://doi.org/10.4161/cc.10.21.18201.

[351] Scott Maynard et al., "Lamin A/C Promotes DNA Base Excision Repair," *Nucleic Acids Research* 47, no. 22 (December 16, 2019): 11709–28, https://doi.org/10.1093/nar/gkz912.

[352] Victoria E. Hoskins, Kristiana Smith, and Karen L. Reddy, "The Shifting Shape of Genomes: Dynamics of Heterochromatin Interactions at the Nuclear Lamina," *Current Opinion in Genetics & Development* 67 (April 2021): 163–73, https://doi.org/10.1016/j.gde.2021.02.003.

[353] A. Ognibene et al., "Nuclear Changes in a Case of X-Linked Emery-Dreifuss Muscular Dystrophy," *Muscle & Nerve* 22, no. 7 (July 1999): 864–69, https://doi.org/10.1002/(sici)1097-4598(199907)22:7<864::aid-mus8>3.0.co;2-g.

[354] Susana Gonzalo and Ray Kreienkamp, "DNA Repair Defects and Genome Instability in Hutchinson-Gilford Progeria Syndrome," *Current Opinion in Cell Biology* 34 (June 2015): 75–83, https://doi.org/10.1016/j.ceb.2015.05.007.

[355] Phillip R. Musich and Yue Zou, "DNA-Damage Accumulation and Replicative Arrest in Hutchinson–Gilford Progeria Syndrome," *Biochemical Society Transactions* 39, no. 6 (December 2011): 1764–69, https://doi.org/10.1042/BST20110687.

[356] Mark A. Rizzo, Michael W. Davidson, and David W. Piston, "Fluorescent Protein Tracking and Detection: Applications Using Fluorescent Proteins in Living Cells," *Cold Spring Harbor Protocols* 2009, no. 12 (December 2009): pdb.top64, https://doi.org/10.1101/pdb.top64.

[357] Yuexia Wang, Cecilia Ostlund, and Howard J. Worman, "Blocking Protein Farnesylation Improves Nuclear Shape Abnormalities in Keratinocytes of Mice Expressing the Prelamin A Variant in Hutchinson-Gilford Progeria Syndrome," *Nucleus (Austin, Tex.)* 1, no. 5 (2010): 432–39, https://doi.org/10.4161/nucl.1.5.12972.

[358] Cristina Capanni et al., "Familial Partial Lipodystrophy, Mandibuloacral Dysplasia and Restrictive Dermopathy Feature Barrier-to-Autointegration Factor (BAF) Nuclear

Redistribution," *Cell Cycle* 11, no. 19 (October 1, 2012): 3568–77, https://doi.org/10.4161/cc.21869.

[359] Youngjo Kim et al., "Macrophage Lamin A/C Regulates Inflammation and the Development of Obesity-Induced Insulin Resistance," *Frontiers in Immunology* 9 (2018): 696, https://doi.org/10.3389/fimmu.2018.00696.

[360] Niina Dubik and Sabine Mai, "Lamin A/C: Function in Normal and Tumor Cells," *Cancers* 12, no. 12 (December 9, 2020): 3688, https://doi.org/10.3390/cancers12123688.

[361] Ashley J. Earle et al., "Mutant Lamins Cause Nuclear Envelope Rupture and DNA Damage in Skeletal Muscle Cells," *Nature Materials* 19, no. 4 (April 2020): 464–73, https://doi.org/10.1038/s41563-019-0563-5.

[362] Jan Vijg and Yousin Suh, "Genome Instability and Aging," *Annual Review of Physiology* 75 (2013): 645–68, https://doi.org/10.1146/annurev-physiol-030212-183715.

[363] "Lamin A Buffers CK2 Kinase Activity to Modulate Aging in a Progeria Mouse Model. | Science Advances," accessed December 5, 2024, https://www.science.org/doi/10.1126/sciadv.aav5078.

[364] Min-Ho Yoon et al., "P53 Induces Senescence through Lamin A/C Stabilization-Mediated Nuclear Deformation," *Cell Death & Disease* 10, no. 2 (February 6, 2019): 1–18, https://doi.org/10.1038/s41419-019-1378-7.

[365] Atsuki En et al., "Pervasive Nuclear Envelope Ruptures Precede ECM Signaling and Disease Onset without Activating cGAS-STING in Lamin-Cardiomyopathy Mice," *bioRxiv*, April 18, 2024, 2023.08.28.555134, https://doi.org/10.1101/2023.08.28.555134.

[366] Tuo Li and Zhijian J. Chen, "The cGAS–cGAMP–STING Pathway Connects DNA Damage to Inflammation, Senescence, and Cancer," *The Journal of Experimental Medicine* 215, no. 5 (May 7, 2018): 1287–99, https://doi.org/10.1084/jem.20180139.